Tag-free semisynthetic tau proteins and novel antibodies targeted against phospho-tau

Dissertation zur Erlangung des akademischen Grades des

Doktors der Naturwissenschaften (Dr. rer. nat.)

Eingereicht im Fachbereich Biologie, Chemie, Pharmazie

der Freien Universität Berlin

Vorgelegt von

Oliver Reimann

aus Berlin

2016

Erklärung des Autors

Die Arbeit wurde zwischen dem 01. Oktober 2011 und dem 12.06.2016 unter der Leitung von Prof. Dr. Christian P. R. Hackenberger am Institut für Chemie und Biochemie der Freien Universität Berlin sowie am Leibniz-Institut für Molekulare Pharmakologie angefertigt.

Erklärung des Autors

1. Gutachter: Prof. Dr. Christian P. R. Hackenberger

2. Gutachter: Prof. Dr. Beate Koksch

Disputation am: 15.11.2016

Declaration

I herewith confirm that I have prepared this dissertation without the help of any impermissible resources. All citations are marked as such. The present thesis has neither been accepted in any previous doctorate degree procedure nor has it been evaluated as insufficient.

Berlin, 9th of June, 2016

Oliver Reimann

Publication list

The work on this dissertation resulted so far in the following publications:

1a.   O. Reimann, C. Smet-Nocca, C. P. R. Hackenberger,

        Angew. Chem. Int. Ed. **2015**, *54*, 306-310.

        Traceless purification and desulfurization of tau protein ligation products.

        DOI: 10.1002/anie.201408674

1b.   O. Reimann, C. Smet-Nocca, C. P. R. Hackenberger,

        Angew. Chem. **2015**, *127*, 311-315.

        Spurlose Aufreinigung und Desulfurierung von Ligationsprodukten des Tau-Proteins.

        DOI: 10.1002/ange.201408674

2.   O. Reimann, M. Glanz, C. P. R. Hackenberger,

        Bioorg. Med. Chem. **2015**, *23*, 2890-2894.

        Native chemical ligation between asparagine and valine: Application and limitations for

        the synthesis of tri-phosphorylated C-terminal tau.

        DOI: 10.1016/j.bmc.2015.03.028

Publication list

3. M. Kuhlmann, <u>O. Reimann</u>, C. P. R. Hackenberger, J. Groll,

   Macromol. Rapid Commun. **2015**, *36*, 472-476.

   Cysteine-Functional Polymers via Thiol-ene Conjugation.

   DOI: 10.1002/marc.201400703

4. M. Schmitz, M. Kuhlmann, <u>O. Reimann</u>, C. P. R. Hackenberger, J. Groll,

   Biomacromolecules **2015**, *16*, 1088-1094.

   Side-Chain Cysteine-Functionalized Poly(2-oxazoline)s for Multiple Peptide conjugation by Native Chemical Ligation.

   DOI: 10.1021/bm501697t

5. S. Schwagerus*, <u>O. Reimann</u>*, C. Despres, C. Smet-Nocca, C. P. R. Hackenberger,

   J. Pept. Sci. **2016**, *22*, 327-333.

   Semisynthesis of a tag-free *O*-GlcNAcylated tau protein by sequential chemoselective ligation.

   DOI: 10.1002/psc.2870

   *equal contribution

Talks

1. <u>Oliver Reimann</u>, Christian P. R. Hackenberger, Fonds der Chemischen Industrie (FCI) scholarship meeting, Berlin (Germany), 21st of February, **2014**.

    Semisynthetic access to post-translationally modified variants of the Tau protein.

2. <u>Oliver Reimann</u>, Christian P. R. Hackenberger, Biochemistry meeting of the Gesellschaft Deutscher Chemiker (GDCh), Berlin (Germany), 16th of July, **2014**.

    Traceless purification tags to streamline protein semi-synthesis.

3. <u>Oliver Reimann</u>, Christian P. R. Hackenberger, 2015 International Chemical Congress of Pacific Basin Societies (Pacifichem), Honululu (USA), 15th – 20th of December, **2015**.

    Post-translationally modified tau proteins accessed by a novel purification tag.

Posters

1. Malgorzata Broncel, <u>Oliver Reimann</u>, Christian P. R. Hackenberger, SPP1623 Meeting, Berlin (Germany), 20th of October, **2011**.

    Cracking the phospho- and the glycocode of Tau.

2. Malgorzata Broncel, <u>Oliver Reimann</u>, Christian P. R. Hackenberger, Molecular Interactions, Berlin (Germany), 12th of September, **2012**.

    Understanding Tau phosphorylation and glycosylation and their impact on each other.

3. <u>Oliver Reimann</u>, Malgorzata Broncel, Christian P. R. Hackenberger, 1st combined external doctoral students workshop Graduate Schools SFB 765 and 858, Rheinsberg (Germany), 6th – 9th of March, **2013**.

    Phosphorylation as a key modification of tau.

4. <u>Oliver Reimann</u>, Christian P. R. Hackenberger, CPS meeting, Vienna (Austria), 3rd – 6th of April, **2013**.

    Semisynthetic approach toward C-terminally phosphorylated tau.

Posters

5.   Oliver Reimann, Maria Glanz, Caroline Smet-Nocca, Christian P. R. Hackenberger,

Advances in Research on Neurodegenerative Disease with a Focus on Dementias, Halle

(Germany), 4th – 5th of May, **2015**.

Synthetic access to post-translationally modified tau proteins by a novel purification

tag.

6.   Kristina Siebertz, Oliver Reimann, Patrick Becker, Caroline-Smet-Nocca, Christian P.

R. Hackenberger, 1st ECBS & ICBS joint meeting 2015, Berlin (Germany), 7th – 9th of

October, **2015**.

On the road to new semisynthetic tau proteins.

Other contributions

1. Christian P. R. Hackenberger, <u>Oliver Reimann,</u>

    Nachrichten aus der Chemie **2013**, *61*, 298–312.

    Synthetische Todesküsse: Chemischer Zugang zu ubiquitinierten Proteinen.

    DOI: 10.1002/nadc.201390088

2. Unpublished manuscript for methods in molecular biology:

    <u>Oliver Reimann</u>, Caroline Smet-Nocca, Christian P. R. Hackenberger
    "Tag-free semisynthesis of the tau protein"

3. Online article published in q&more:

    Kristina Siebertz, <u>Oliver Reimann</u>, Christian P. R. Hackenberger
    "Alzheimer: die Suche nach einem Ausweg" or "Alzheimer's: searching for a way out"
    Available under:
    http://q-more.chemie.de/q-more-artikel/206/alzheimer-die-suche-nach-einem-ausweg.html - German language
    and
    http://q-more.chemeurope.com/q-more-articles/206/alzheimer-s-searching-for-a-way-out.html - English language

Acknowledgement

I would like to thank my supervisor and mentor Prof. Dr. Christian Hackenberger for his trust, encouragement and guidance during my Ph.D. I highly appreciated his open-door policy, thereby permitting numerous discussions about projects in the dynamic and exciting field of Alzheimer's research that I was allowed to work in. In this multidisciplinary field, I was able to learn techniques of chemistry, biochemistry and medicinal research. I would also like to thank Prof. Hackenberger for warranting me a high degree of freedom, allowing me to pursue my own ideas in research and also develop my career aside the lab.

I thank also my Bachelor and Master thesis supervisor Prof. Dr. Beate Koksch for her support during my studies and for being my second supervisor for this Ph.D. thesis.

Moreover, my thanks belongs to Prof. Dr. Nedjeko Budisa for being my supervisor in the graduate school SFB765.

I further thank all my great collaborators that I had worked with during my Ph.D. A very close collaboration was closed down with Dr. Caroline Smet-Nocca from the university of Lille and her Ph.D. student Clement Déspres. I experienced great hospitality during my research stay in Lille and had many fruitful discussions with them about the semisynthesis of tau. I thank also Dr. Dmytro Puchkov for the TEM recordings and great discussions. I appreciate further the work, explanations and discussions of Christine Koehler from the lab of Prof. Dr. Edward Lemke from the EMBL in Heidelberg; the group of Elisabeth Kremmer and especially her coworker Andrew Flatley from the Helmholz Center in Munich, Andrea Rottach and Klaus Goeber from the group of Prof. Dr. Heinrich Leonhardt from the LMU Munich; Dr. Stefan Prokop and Prof. Dr. Frank Heppner from the Charité; Kristin Arnsburg and Manuel Iburg from the group of Dr. Janine Kirstein at the FMP; Julia Abele and Prof. Dr. Daniela Dieterich from the Otto von Guericke University of Magdeburg; Dr. Michael Schuemann and Heike Stephanowitz from the lab of Dr. Eberhard Krause at the FMP. I would like to thank further my collaborators Dr. Carola Schipke and Bianca Kochnowsky from the group of Prof. Dr. Oliver Peters from the Charité Berlin for introducing me to the topic of ELISA development. I would also like to thank Matthias Kuhlmann and Michael Schmitz from the group of Juergen Groll from the university of Wuerzburg for great discussions in the polymer projects.

Acknowledgement

I would like to express my gratitude to the great students that I supervised during my Ph.D. I would like to thank especially Maria Glanz and Sergej Schwagerus, who are both now Ph.D. students themselves in the Hackenberger lab.

In general, I experienced a very productive and open working atmosphere at the Free University and the Leibniz-Institute of Molecular Pharmacology, for which I would like to thank my entire work-group, including many former members. Especially Jordi Bertran, Lukas Artner, Nicole Nischan and Simon Reiske were important figures during my Ph.D. They were there from the beginnings at the FU and with them I share many great memories inside and outside the lab. I would like to thank Olaia for her help in questions of organic chemistry and for being a great office mate. I always had very good times with my FMP lab-mate Dominik Schumacher and the other current group members Kristina Siebertz, Simon Klenk, Marc-André Kasper, Annet Hauser, Alice Baumann, Anselm Schneider and Debasish Bhowmick. They have been always very helpful and I could always rely on finding discussion partners for chemical issues. Aside that, we always had a lot of fun.

Moreover, I would like to thank our secretaries Katta Wittig, Marianne Dreissigacker and Katharina Tebel for being great support for organizational issues. I was also lucky to have our great technical assistants Dagmar Krause, Ines Kretschmar and Kristin Kemnitz-Hassanin, who were always very helpful.

At all times, my family was a great support for me and helped me with many things that were not chemistry related. My father Johannfried Seitz-Reimann, my brother Philipp Reimann, my grandmother Karin Regierer, my aunts and uncles Babette Regierer, Christoph Regierer, Anne Roever and Knut Miehe were always at my side with advise and support. Moreover, I would like to thank Minh-Chanh Pham, Lien Tran-Thi and Linh Pham for being there for me as well.

A very special thank you goes of course to my girlfriend Thien-Kim Pham for countless strategic discussions, support and love, who made the years of my Ph.D. a great time.

Abstract

The work of this Ph.D. puts the focus on tau, a key protein in Alzheimer's Disease (AD). During progression of AD, tau becomes abnormally phosphorylated. This high degree of phosphorylation is associated to key events in the disease, such as protein aggregation and destabilization of the neuronal integrity. A natural regulator of tau phosphorylation is *O*-GlcNAcylation, a post-translational modification, placed on the same residues as phosphate. Here, new synthetic pathways to generate homogeneously phosphorylated or *O*-GlcNAcylated tau proteins are presented, which are accomplished by combined approaches of native chemical ligation (NCL) and expressed protein ligation (EPL). A new method was established, in which purification was achieved after ligation and desulfurization by means of a traceless photocleavable biotin tag that was installed during solid phase peptide synthesis (SPPS) in synthetic tau fragments. This protocol allowed access to tag-free tau peptides and proteins, which were conveniently desulfurized post-ligation during peptide immobilization, if required. The molecular targets were either phosphorylated or *O*-GlcNAcylated tau proteins, carrying these post-translational modifications in the AD relevant paired helical filament 1 (PHF-1) epitope (Ser396/400/404). To get more insights into the impact of tau phosphorylation in PHF-1 *in cellulo* and *in vivo*, monoclonal antibodies against tau were generated, tri-phosphorylated in this particular epitope. The antibodies were characterized by several experimental settings and enabled the generation of new insights into cellular tau localization. Moreover, the exploration of the diagnostic potential of these new antibody clones was started.

Kurzzusammenfassung

Der Fokus dieser Dissertation liegt auf Tau, einem Schlüsselprotein in der Alzheimer Erkrankung. Im Fortlauf von Alzheimer wird Tau hyperphosphoryliert, wobei der hohe Grad der Phosphorylierung mit Schlüsselereignissen der Krankheit wie der Aggregation von Tau oder dem Verlust der neuronalen Integrität in Verbindung gebracht wird. Die post-translationale Modifizierung der *O*-GlcNAcylierung wird ebenfalls an Tau beobachtet und gilt als natürlicher Regulator der Phosphorylierung. Hier werden neue Syntheserouten präsentiert, die den Zugang zu homogen-phosphorylierten und *O*-GlcNAcylierten Tau Derivaten durch kombinatorische Ansätze aus nativer chemischer Ligation (NCL) und exprimierter Protein Ligation (EPL) ermöglichen. Es wurde eine neue Methode entwickelt, die eine Reinigung von Ligationsprodukten durch einen spurlos photospaltbaren Biotin-Tag ermöglichten, der während der Festphasen Peptid Synthese in die synthetischen Peptid-Fragmente eingeführt werden kann. Dieses neuartige Protokoll ermöglichte den synthetischen Zugang zu Tag-freien Tau Proteinen, die ohne großen experimentellen Aufwand während ihrer Immobilisierung entschwefelt werden konnten.

Die molekularen Ziele dieser Arbeit waren phosphorylierte oder *O*-GlcNAcylierte Tau Proteine, die diese post-translationalen Modifikationen im sog. „paired helical filament" 1 (PHF-1) Epitop (Ser396/400/404) enthalten. Um weiteres Wissen über den Einfluss starker Tau Phosphorylierung in PHF-1 *in cellulo* und *in vivo* zu erhalten wurden monoklonale Antikörper gegen dreifach phosphoryliertes Tau entwickelt und diese dann in unterschiedlichen Experimenten charakterisiert. So konnten neue Einsichten über die zelluläre Lokalisation von Tau in Abhängigkeit von der PHF-1 Phosphorylierung gesammelt werden. Darüber hinaus wurde begonnen, das diagnostische Potential der neuen Antikörper Klone zu erforschen.

Abbreviations

ABPP	activity based protein profiling
AD	Alzheimer's disease
ADAM	a disintegrin and metalloproteinase
AFM	atomic force microscopy
AGD	agyrophylic grain disease
AMP	adenosine monophosphate
AMPK	AMP activated protein kinase
APP	amyloid precursor protein
APRIL	a proliferation-inducing ligand
ATP	adenosine triphosphate
BCIP	5-bromo-4-chloro-3'-indolyphosphate p-toluidine salt
beta-Me	beta-mercaptoethanol
Boc	tert-butoxycarbonyl
BSA	bovine serum albumin
BuOx	2-butenyl-2-oxazoline
CA	California
CaMK	calmodulin-dependent kinase II
CBD	Chitin binding domain
CBDD	corticobasal degeneration disease
CBP	calmodulin-binding peptide
CDK	cyclin dependent kinase
CE	Conformité Européenne
C.elegans	Caenorhabditis elegans

CJD	Creutzfeldt-Jacobs disease
CK1	casein kinase 1
CMA	carboxylmethylaspartate
CNS	central nervous system
CPP	cell-penetrating peptides
CPT	camptothecin
CSF	cerebrospinal fluid
Csk	C-terminal Src kinase
CuAAc	Cu(I)-catalyzed azide-alkyne cycloaddition
Da	Dalton
DAPI	4',6-diamidino-2-phenylindole
DBU	1,8-Diazabicyclo[5.4.0]undec-7-en
Dbz	3-(Fmoc-amino)-4-aminobenzoyl
Dde	1-(4,4-dimethyl-2,6-dioxocyclohex-1-ylidene)ethyl
DecOx	2-decenyl-2-oxazoline
DHB	2,5-dihydroxybenzoic acid
DIC	N,N-diisopropylcarbodiimide
DIPEA	N,N-diisopropylethylamine
DMF	N,N-dimethylformamide
Dmnb	4,5-dimethoxy-2-nitrobenzyl carbonyl
DMPA	dimethoxyphenylacetophenone
DNA	deoxyribonucleic acid
DTT	dithiotreitol
EcLeuRS	Leucyl-tRNA synthetase

Abbreviations

E.coli	Escherichia coli
ECS	extracellular space
EcTyrRS	tyrosyl-tRNA synthetase
EDTA	ethylenediaminetetraacetic acid
EEGE	ethoxy ethyl glycidol ether
EF-Tu	elongation factor thermos unstable
EGTA	ethylene glycol- bis(2-aminoethylether)N,N,N',N'-tetraacetic acid
ELISA	enzyme-linked immunosorbent assay
ELP	elastin-like polypeptides
EntK	enterokinase
EPL	expressed protein ligation
ER	endoplasmatic reticulum
ESI	electrospray ionization
Exp	experimental
FCM	flow cytometry
FCS	fetal calf serum
FDA	US Food and Drug Administration
Fmoc	fluorenylmethyloxycarbonyl
FMP	Forschungsinstitut für Molekulare Pharmakologie
FTDP-17	frontotemporal dementia with parkinsonism-17
FTLD	frontotemporal lobe dementia
GDP	global gross domestic product
GFP	green fluorescent protein
GmbH	Gesellschaft mit beschränkter Haftung

Abbreviations

Gn	guanidine
GSK-3β	glycogen synthase kinase 3β
GST	glutathion-S-transferase
HA-tag	human influenza hemagglutinin tag
HATU	N-{(dimethylamino)-1H-1,2,3-triazolo [4,5-b]-pyridino-1-ylmethylene}-N-methylmethan-aminium hexa-fluorophosphate
HAZA	2-(2-alkoxy-4-hydroxy-phenylazo) benzoic acid
HBTU	N-[(1H-benzotriazol-1-yl)(dimethylamino)-methyleneb-N-methylmethanaminiumhexafluorophosphate N-oxide
HCTU	2-(6-Chlor-1H-benzotriazol-1-yl)-1,1,3,3-tetramethylaminium-hexafluorophosphate
HD	Huntington disease
HMPB	4-hydroxymethyl-3-methoxyphenoxy)butanoic acid
HOBt	1-hydroxybenzotriazole
HPLC	high performance liquid chromatography
HRP	horseradish peroxidase
HRV	human rhinovirus
HSPG	heparan sulfate proteoglycans
ICC	immunocytochemistry
IHC	immunohistochemistry
IMAC	immobilized metal affinity columns
IP	immunoprecipitation
IPTG	isopropyl-β-D-thiogalactopyranosid
ITC	inverse transition cycling

Abbreviations

KAHA	α-ketoacid-hydroxylamine
K_d	dissociation constant
L	Liter
LBD	Lewy body dementia
LC	liquid chromatography
LCV	luminescent cell viability
LLS	laser light scattering
LMTX	leucomethylthioninium.2HX
LR	low resolution
m	milli
M	molar
MAG2	Magainin-2
MALDI	*matrix*-assisted laser desorption/ionization
MAPT	microtubule-associated protein tau
MARK	microtubule affinity-regulating kinases
MBD	microtubule binding domain
MBD-tag	maltose binding domain tag
MBHA	**4-methylbenzhydrylamine**
MCI	mild cognitive impairment
MeCN	acetonitrile
MEF	mouse embryonic fibroblast
MeOH	methanol
MeOx	2-methyl-2-oxazoline
MESNa	sodium methanethiolate

MMBA	4-(mercaptomethyl)benzoic acid
MPAA	4-mercaptophenlyacetic acid
MRI	magnetic resonance imaging
mRNA	messenger ribonucleic acid
MS	mass spectrometry
MS/MS	tandem mass spectrometry
MT	microtubule
MUC	mucin
Nbz	*N*-acyl-benzimidazolinone
NCL	native chemical ligation
NGF	nerve growth factor
NFT	neurofibrillary tangle
NIA	National institute of Aging
NIH	National institute of Health
NMDAR	*N*-methyl-D-aspartate receptor
NMR	nuclear magnetic resonance
NTA	nitrilotriacetic acid
O-GlcNAc	*O*-linked β-*N*-acetyl glucosamine
OGT	*O*-glycosyltransferase
Opr	5-oxaproline
PBS	phosphate buffered saline
PC	photocleavable
PCB	photocleavable biotin
Pen	penicillamine

Abbreviations

PET   positron emission tomography

PG   protecting group

pg   picogram

PHB   polyhydroxybutyrate

Ph.D   doctor pf philosophy

PHF   paired helical filaments

PHP   pseudo-phosphorylated

PhRMA   pharmaceutical research and manufacturing association

PiD   Pick disease

PKA   cyclic AMP-dependent protein kinase

PKN   protein kinase

PNA   peptide nucleic acid

POI   protein of interest

POx   poly(2-oxazoline)

PrK N-propargyl-Lysine

Prof.   professor

PS   polystyrene

PSD   postsynaptic density protein

PSP   progressive supranuclear palsy

PTM   post-translational modification

PTS   Protein trans-splicing

PyBOP   benzotriazol- 1-yl-N-oxy-tris(pyrrolidino)phosphonium
                   hexafluorophosphate

PylRS   pyrrolysyl-tRNA synthetase

Abbreviations

RNA	ribonucleic acid
RP	reversed-phase
rt	room temperature
SBD	starch binding domain
SDS-PAGE	sodium dodecyl sulfate polyacrylamide gel electrophoresis
SEA	bis(2-sulfanylethyl)amino
SH3	SRC homology 3
SICLOPPS	split-intein circular ligation of peptides and proteins
SPPS	solid phase peptide synthesis
SRC	sarcoma
STEP	striatal-enriched protein tyrosine phosphatase
STEPL	sortase-tag expressed protein ligation
T	Tween
TBS	tris buffered saline
t-BuSH	*tert*-butylthiol
TCEP	tris(2-carboxyethyl)phosphine
TEM	transmission electron microscopy
TEV	tobacco etch virus
TFA	trifluoroacetic acid
TFET	trifluoroethanethiol
Thz	thiazolidine
TIS	triisopropylsilane
T_M	melting temperature
TMB	3,3',5,5'-tetramethylbenzidine

Abbreviations

TNBS	2,4,6-trinitrobenzenesulfonic acid
ToF	time of flight
TRAIL	tumor necrosis factor-related apoptosis-inducing ligand
TRIS	tris(hydroxymethyl)aminomethane
TTL6	tubulin tyrosine ligase 6
UAA	unnatural amino acid
UDP	uridine diphosphate
UPLC	ultra-high performance liquid chromatography
USA	United States of America
UV	ultraviolet
VA-044	2,2'-azobis[2-(2-imidazolin-2-yl)propane] dihydrochloride
VaD	vascular dementia
vMRI	volumetric magnetic resonance imaging
WB	western blot
WHO	world health organization
WT	wild type
YFP	yellow flourescent protein

Table of contents

Table of contents

1. MOTIVATION

In times of demographic change observed nowadays, Alzheimer's Disease (AD) becomes one of the biggest challenges of society concerning health and economy. Researchers found the proteins amyloid-β and tau to be key factors to disease pathways, as they undergo modifications, possibly triggering pathogenic aggregation.

In the 1980's, a certain awareness of the disease started growing and more efforts were put into the development of a potential cure, but up to this day, all attempts of scientists and clinicians to cure the disease had failed. To pave the way for a future treatment, the underlying molecular mechanisms have to be discovered that drive the progression of the disease. Therefore, effective molecular tools must be developed, enabling the researchers to study crucial events of AD.

In the past, most of the research was centered around the amyloid-β protein and the so called amyloid hypothesis of AD, but the theory that amyloid pathology alone is responsible for AD did not prove sufficient in reality.[1] Today, the tau protein has gained more attention in the Alzheimer's society.[2]

One key observation was a high degree of phosphorylation of tau proteins found in brains of AD patients.[3] The sites of phosphorylation that most likely occur in the course of AD were identified mainly by techniques of mass spectrometry, but the impact of distinct phosphorylation events on the behavior of the total protein remained unknown.[4, 5] Many phospho-specific tau antibodies have been generated in the past that helped to get new insights on the impact of tau phosphorylation, but many questions remain unanswered. Alternatively, molecular biologists and biochemists have tried to apply kinases on recombinant tau protein.[6] This technique is certainly easy to perform, but the obtained results are barely suitable to explain the impact of distinct phosphorylation events, due to the big heterogeneity of phosphorylations on tau, which are generated by this approach. In order to get higher site-specificity, other scientists have genetically introduced negatively charged amino acids into tau to mimic the desired positions of phosphorylation. In the following sections, examples will be provided that show the validity of this approach.[7] Nevertheless, this technology still remains only an approximation to reality.

1. MOTIVATION

We believe that studies on homogeneously phosphorylated protein structures themselves are required to obtain more insights on the impact of tau phosphorylation in pathology. This goal can be achieved through techniques derived from chemical biology, where full-length proteins can be generated by the so called protein semisynthesis.[8] Here, peptides can be chemically synthesized in a defined step-by-step fashion, which allows for the site-specific incorporation of any natural or unnatural functional group on peptide level. The resulting synthetic portion can then be ligated to a desired expressed portion of a protein by a chemoselective reaction. We see great potential in this technology to generate phosphorylated tau proteins, which may enable their investigation and thus pave the way to novel insights on AD.

2. INTRODUCTION & BACKGROUND

The World Alzheimer Report 2015 summarizes alarming circumstances that the world is facing due to higher life expectancies and the resulting demographic change.[9] Today, there are 46 million people worldwide affected by dementia, a number higher than the whole population of Spain. The progression of the disease in a worldwide scope is alarming. There were 36 million people suffering from dementia in 2010, whereas the amount of patients will more than double to 74.7 million only 20 years later in 2030. The predicted number of people with dementia for the year 2050 is 131.5 million. Dementia does not only affect the patients, but has also great impact on families and care-givers, as a large portion of nursing service is provided by family members at the homes of the patients. Despite humane concerns, this development has a tremendous impact on the world's economy. In 2018, costs associated with dementia will supersede the trillion US dollar benchmark and thus make more than 1.1% of the global gross domestic product (GDP), which will double until 2030, as stated in the Alzheimer Report 2015.

It is thus a logical consequence that governments worldwide make strong commitments to investments and advancements in dementia research and care. This commitment was recently demonstrated at the WHO-hosted ministerial conference on global action against dementia in March 2015, where more than 80 countries joined experts to the event. The Director-General of the WHO, Dr. Margaret Chan, said at this conference: "There is a tidal wave of dementia coming our way worldwide. We need to see greater investments in research to develop a cure, but also to improve the quality of life of people living with dementia and the support given to their caregivers".[10]

This statement reflects the need for an effective cure of Alzheimer's disease, which is not available up to now. Despite a considerable increase in understanding AD, the development of a drug to delay, slow down or even cure it is exceptionally difficult. The Pharmaceutical Research and Manufacturing association (PhRMA) found out that between 1998 and 2014 the failure rate has been immense in developing AD treatments. A total of 30 drug failures in clinical trials came on one approved drug, resulting in an incredibly low success rate of about 3%,[11] whereas in average 1 out of 10 drugs in clinical phases gets approved by the FDA.[12] All of these failed drugs have passed animal testing and were willingly transferred to clinical trials by pharma companies.

2. INTRODUCTION & BACKGROUND
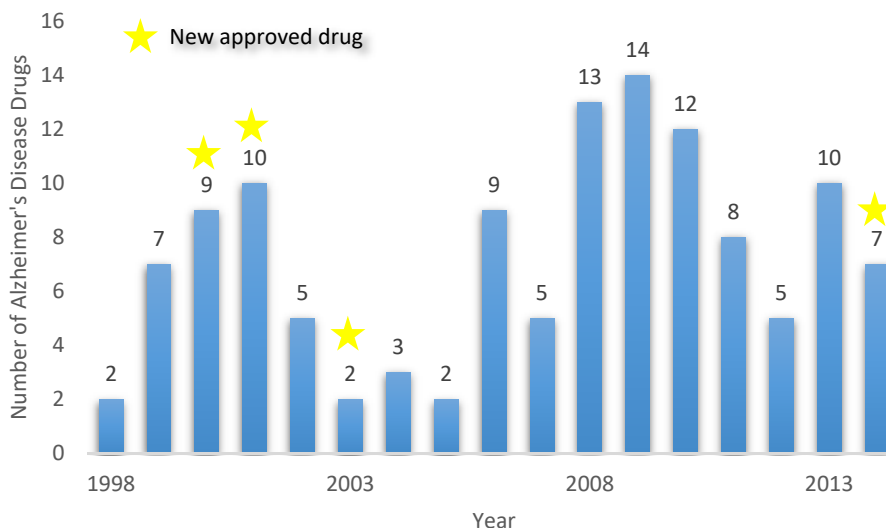
Figure 1: Number of drugs against Alzheimer's disease that have failed during clinical trials between 1998 and 2013. Yellow stars symbolize the development of a new drug, approved by the US Food and Drug Administration (FDA).

There are five medications available on the market that are approved by the FDA to treat symptoms of Alzheimer's disease in all diagnosed stages of the disease, ranging from mild forms of dementia to full-blown AD cases (severe).[13]

Table 1: FDA drugs to treat Alzheimer's disease.[13]

drug name	brand name	approved for	FDA approved
donepezil	Aricept	all stages	1996
rivastigmine	Exelon	all stages	2000
galantamine	Razadyne	mild to moderate	2001
memantine	Namenda	moderate to severe	2003
donepezil and memantine	Namzaric	moderate to severe	2014

In general, the five FDA approved drugs can be categorized in a function-dependent manner:

- Cholinesterase inhibitors (donepezil, galantamine, rivastigmine)
- *N*-methyl-D-aspartate receptor antagonist (memantine)

All of these drugs regulate neurotransmitters in the neuronal network and thus target mainly the symptoms of the disease. This in turn may help patients to carry out daily activities or

maintain their thinking or speaking skills. However, these drugs were not designed to stop or reverse the underlying progression of the disease.

In contrast, many disease-modifying drugs are currently under development. A large portion of the efforts centered around amyloid modulation, more in detail γ-secretase inhibition, passive vaccination or amyloid immunotherapy.[14] However, despite the high number of 60 potential Alzheimer medicines currently tested in clinical trials or under revision by the FDA, so far no disease-modifying drug against AD made it to the market.[15, 16] Possible reasons for these high failure rates can be traced back various reasons such as active metabolites, differences between the human target and the previous animal model, the incompleteness of AD pathology of transgenic animal models, or the choice of an adequate patient population for the trial design.[16] An overall reason for this lack of success in developing drugs for AD can be simply summarized as a lack of knowledge about this disease on a molecular basis.

Even though pathological alterations in the brain of a female patient suffering from dementia were described by Alois Alzheimer already more than a century ago,[17, 18] the molecular mechanisms of AD remain still largely unknown. Alois Alzheimer described two lesions, which are still the two most prominent hallmarks of AD today, which were finally assigned in the mid-1980s. Those were on the one hand amyloid plaques that consist of a small peptide called amyloid-β,[19, 20] and on the other hand NFTs consisting of hyperphosphorylated tau proteins.[3, 21, 22] Although the occurrence of these two lesions in brains of patients are highly indicative for AD, there are numerous other structural and functional alterations associated with the disease, such as e.g. inflammatory responses or oxidative stress.[23-26] In the end, the combined consequences from the described factors may be hold responsible for people dying of AD. Self-evidently, this introduction will be centered around the two most prominent examples of amyloid-β and the tau protein due to the immense complexity of the topic, whereas the focus will be on tau, being the major target of this Ph.D thesis.

2.1   Amyloid-β, its role in AD and the amyloid cascade hypothesis

Amyloid-β peptides are generated by endoproteolysis of the parental amyloid precursor protein (APP). This in turn is achieved by the sequential cleavage of APP by a group of enzymes or enzyme complexes termed α-, β- and γ-secretases.[27] APP is a type 1 transmembrane protein consisting of 695-770 amino acids and can undergo processing by two different pathways (Figure 2). Most of the APP is processed by the non-amyloidogenic pathway, which will not lead to the formation of amyloid-β. The enzymatic cleavage occurring first is induced by α-secretases belonging to the family of disintigrin and metalloprotease (ADAM) proteins, namely ADAM9, 10 or 17. ADAM induced cleavage occurs within the amyloid-β domain and thus prevents the release of the amyloid-β peptide and leads to the generation of the larger ectodomain sAPPα and the smaller C-terminal fragment C83. The amyloidogenic pathway involves the APP cleavage by the β-secretase BACE, releasing an ectodomain (sAPP-β), leaving the last 99 amino acids of APP (known as C99) within the membrane. The fragment C99 gets subsequently cleaved by the γ-secretase complex, which is made up of presenilin1 or 2, nicastrin, anterior phyranx defective and presenilin enhancer 2. This cleavage leads to the formation of free amyloid-β[1-40] and amyloid-β[1-42] in a ratio of about 10:1, whereas the amyloid-β[1-42] shows amyloidogenic properties due to higher hydrophobicity and thus higher fibril forming propensity.[28] It is this longer form that is also found predominantly in the cerebral plaques that are characteristic to AD.[29]
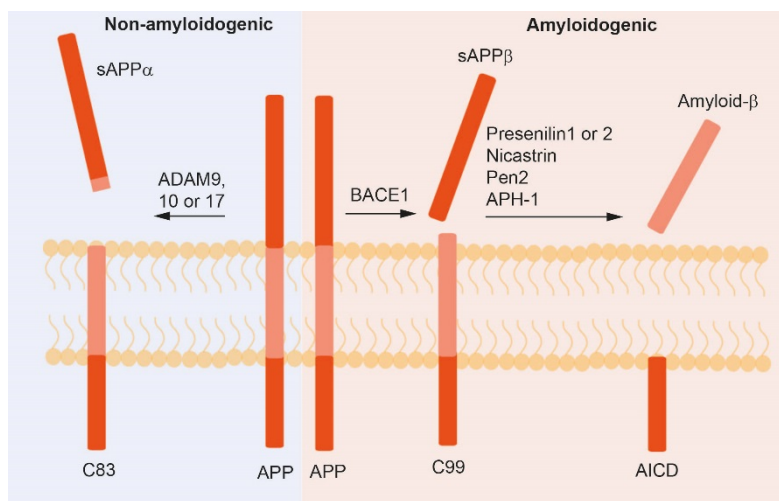
Figure 2: Proteolysis of APP.[27]

2. INTRODUCTION & BACKGROUND

The development of a disease stage classification has been a very challenging task and created a highly controversial debate. A major drawback is that the staging system can only be approximated in living humans and not definitively assigned.[30] Clinicians, neuropsychologists and pathologists agree that amyloid-β pathology is necessary to diagnose AD, but a straightforward correlation between amyloid-β deposition and disease progression cannot be made.[31] In fact, amyloid-β deposition and distribution in the brain can only be poorly correlated with the disease. Individuals can present few if any clinical symptoms of dementia, but show considerable amyloid deposits in their brains.[31] Further support of this observation was provided by the human amyloid-β immunization trial (AN-1792). Patients were injected with the full-length amyloid-β[1-42] peptide together with an adjuvant. Treated patients in these trials showed much lower amyloid-β depositions in brains after their autopsy and death as might have been expected based on historical levels for a given clinical stage. However, despite the remarkably lower levels of amyloid-β deposits presumably caused by the immunotherapy, the patients showed cognitive decline to an end-stage and finally died of AD, undistinguishable from untreated AD patients.[32]

Many efforts have been directed against insoluble aggregates of human amyloid-β – so called senile plaques. This was a result of the so called amyloid "cascade hypothesis", related to a hierarchical scheme, in which amyloid-β deposits are the driving force in both sporadic and familial AD.[33] In a more recent description by Lemere *et al.* in 2010, the following statement has been made, describing the amyloid-β hypothesis:[34]

"Over time, an imbalance in amyloid-β production and/or clearance leads to gradual accumulation and aggregation of the peptide in the brain, initiating a neurodegenerative cascade that involves amyloid deposition, inflammation, oxidative stress, and neuronal injury and loss. ... Oligomeric and fibrillar forms of amyloid-β cause long-term potentiation impairment and synaptic dysfunction, and accelerate the formation of neurofibrillary tangles that eventually cause synaptic failure and neuronal death."

As many details of this theory were slightly varied over time, the core massage remained the same throughout the literature and suggests a linear pathway that begins with the formation of amyloid-β aggregates and results finally in dementia and AD.

Another theory states a contrary to the amyloid cascade hypothesis. Here, rather the soluble monomers and oligomers than insoluble neuritic plaques are described as the toxic amyloid-β species.[35, 36] Franz Hefti *et al.* support the view that amyloid plaques may serve rather as a sort of sink for toxic soluble amyloid-β species such as monomers and oligomers.[37] This theory is nowadays shared by many[38] and gains support by for instance by the preliminary results from the clinical trial of the antibody Solanezumab, owned by the company Eli Lilly. In result, the application of Solanezumab slowed down cognitive decline in patients with mild AD, but failed to do so for patients showing symptoms of moderate AD. Further results of this clinical study are to be expected by the end of the year 2020.[39] Among different factors, the fact that amyloid-β in neuritic plaques and free oligomeric forms are in an equilibrium make the development of a general strategy to prevent amyloid-derived pathology very difficult. If indeed plaque removal results in the release and deposition of soluble amyloid-β from the plaques and if some soluble species are neurotoxic, then this would explain the failures of attempts to stop neurodegeneration by such attempts.

How could a successful amyloid-based therapy look like? The preceding observations suggest that a multi-drug therapy could have an impact on cognitive decline of patients with amyloid-β pathology. The therapy should prevent the synthesis, remove the reservoir by removing the plaques and reduce the concentration of soluble oligomers of amyloid-β in the extracellular space (ECS). This goal can possibly be achieved by a combinatorial approach of administering drugs against the APP cleaving enzyme BACE1, while directing immunologic attacks toward amyloid-β in neuritic plaques and the soluble oligomers.[38] Nevertheless, treatments may only be successful if they can prevent the formation of both, the extra- and intracellular soluble amyloid-β.

2.2 The tau protein

2.2.1 Description of the tau protein

The microtubule-associated protein tau (MAPT) was discovered in the year 1975, where it was identified as a key protein in microtubule assembly and stabilization.[40] Tau can modulate the transport of vesicles and organelles along the microtubules (MTs), serve as an anchor for enzymes or regulate the dynamics of the MTs.[41, 42] The MAPT is intrinsically unstructured and in its unmodified state the protein shows low tendency to aggregate into paired helical filaments (PHFs, observed by Kidd[43]) or NFTs, which are both characterized in many diseases comprised as tauopathies. Among those diseases are AD, Down's Syndrome, progressive supranuclear palsy (PSP), corticobasal degeneration disease (CBDD), agyrophylic grain disease (AGD), Pick disease (PiD), Huntington disease (HD) and frontotemporal dementia with parkinsonism-17 (FTDP-17).[44]

The human tau protein is encoded by the gene called *MAPT*, which comprises 16 exons on chromosome 17q21.[45] In the human brain, tau is mainly found in the neurons, but there is also precedence of tau in glia and outside cells.[46, 47] There are six tau isoforms present in adult human brain that are generated by alternative splicing of exons E2, E3 and E10. The exons E2 and E3 encode each for a 29-residue insert near the N-terminus of the protein. Isoforms containing either 0, 1 or 2 inserts are thus found. The resulting isoforms are known as 0N, 1N or 2N, respectively. The exon E10 encodes a C-terminal repeat domain, which will ultimately create tau carrying either 3 or 4 of these C-terminal domains (3R or 4R) and is associated to many tauopathies (**Figure 3**).[48]

Figure 3: The different isoforms of the tau protein, generated by alternative splicing. The exons E2 and E3 are subject to alternative splicing and thus lead to expression of tau containing either 2, 1 or 0 N-terminal inserts marked as N1 or N2. The exon E10 encodes for the C-terminal repeat domain R2 and is equally regulated by alternative splicing.[45]

Tau is a highly water-soluble protein. Its longest isoform (2N4R) contains 80 Ser or Thr residues, 56 negatively charged residues (Asp, Glu), 58 positively charged residues (Lys, Arg) and 8 aromatic residues (5 Tyr, 3 Phe). It is remarkably stable under high temperatures and acidic conditions. The protein tau is overall basic, whereas the N-terminal portion is rather acidic and C-terminal portion more neutral.

In general, tau can bind to the outside and possibly also to the inside of microtubules, whereas the N-terminal and C-terminal regions project outwards (**Figure 4**).[49, 50] The ability of the tau protein to bind microtubules depends on the microtubule binding domain (MBD) comprising the 3 or 4 tandem repeats on adjacent regions.[51] The tandem repeats are thought to bind the MTs directly through their positive net charge that can interact with negative charges distributed on the MTs.[49, 52] As only approx. 130 amino acids are involved in MT binding, the about 240 amino acid long N-terminal and the 70 amino acid long C-terminal portion of the protein, which make up around 70% of the protein in the longest tau isoform 2N4R, are not directly involved in this binding process.[53]
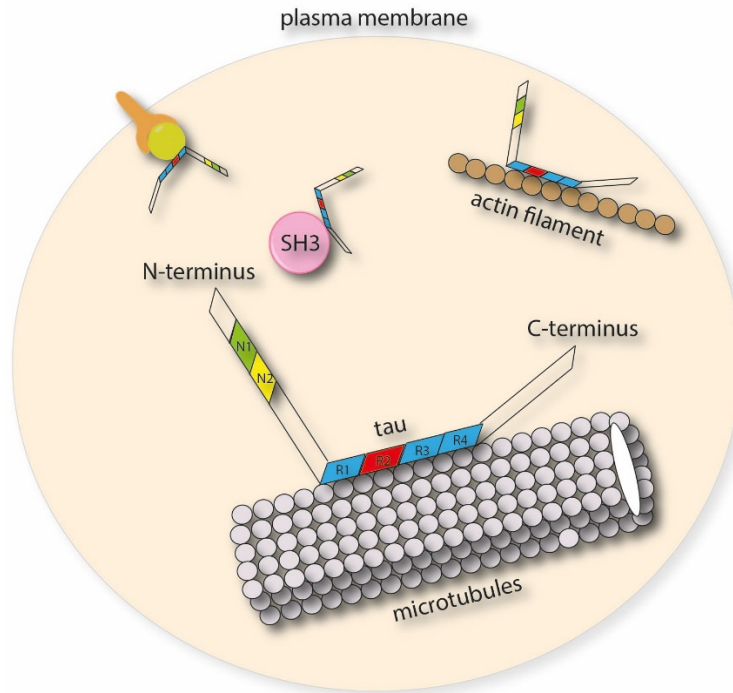
Figure 4: The intrinsically unstructured protein tau binds divers types of molecules such as lipid carriers, SH3 domains, kinases and others. This suggests a central role of the tau protein in signaling pathways and cytoskeletal organization. The N-terminal and C-terminal portions of the protein are pointing outwards from the MT binding tandem repeats.[54]

Isoforms containing the R2 repeat domain have been shown to bind more tightly to microtubules than isoforms with only 3 C-terminal repeats and furthermore assemble microtubules more efficiently.[55]

The N-terminal projection domain could influence the attachment or spacing between cell components and microtubules.[56, 57] The inserts in the N-terminal region may further influence the subcellular localization of the tau protein, depending on the presence of the N0, N1 or N2 isoform.[58] There is a Pro-rich region in the N-terminal portion of tau (approx. 100 amino acids from residue 150 to 250) containing seven PXXP motifs, which can serve as binding sites for signaling proteins with SRC homology 3 (SH3) domains, like the Tyr kinase FYN.[59]

The C- and N-terminal domains were shown to adapt a paperclip like conformation, where they fold on top of the repeat domain and thus protect tau from aggregation.[60] Especially, the C-terminal region is supposed to play a crucial role in the prevention of aggregation, as was demonstrated by L. I. Binder *et al.*[7] This theory was tested by investigating tau with pseudo-phosphorylation in the C-terminal region. For this purpose a double mutant was created, where

the residues Ser396 und Ser404 were replaced by Glu residues using site-directed mutagenesis. The aggregation propensity of the resulting double mutant $[396/404]_{S \to E}$ was assayed by right angle laser light scattering (LLS) and showed to be greatly accelerated when compared to wildtype (WT) tau. The polymerization rate of tau was even further increased when tau truncated after Glu391 was investigated by LLS. The results suggested that tau phosphorylation and truncation both potentiate the rate of filament formation *in vitro*, whereas strikingly deletions from the tandem repeat domains did not lead to tau polymerization. Binder *et al.* suggest that phosphorylation occurs as an early event in the course of AD development, which leads to "unfolding" or "straightening" of the C-terminal tail of tau. This in turn would prevent its inhibitory interaction with the MBD and ultimately constitutes the onset of functional problems for the affected neurons. They further reasoned that in the course of these neuronal difficulties in AD resulting from these early events, the release of proteases such as m-calpain,[61] cathepsins[62] or caspase-3[63] is triggered. If this protease dysregulation occurs when the C-terminus of tau is phosphorylated and thus bent outwards or unfolded, several sites of the protein may be exposed to these proteases and truncation events can occur.

Once tau has formed pathological PHFs, the C-terminal and the N-terminal domains form a "fuzzy coat" that surrounds the core, which is built up by the repeat domains.[64] The fuzzy-coat of PHF shows a remarkable flexibility and is very difficult to image, which is why its structure remains largely obscure.[47] In the literature, it has been described as a two-layered polyetrectrolyte brush, which represents a structure that may contribute to the stabilization of tau fibrils.[53] The characterization of the fuzzy coat was achieved by applying techniques of transmission electron microscopy (TEM) and atomic force micrsocopy (AFM), which allowed for monitoring of the mechanical and adhesive properties of the fuzzy coat by their modulation by electrolytes or pH variations.

2.2.2 Functions of axonal tau

In adults brains tau mainly distributes into axons, where it interacts with MTs through the repeat domains and flanking regions. Tau stabilizes MTs and thus initializes the polymerization of tubulin. This regulates the instability of the MTs and thus allows for reorganization of the

cytoskeleton in neurons.[65, 66] The residues 224-237, 245-253, 275-284 and 300-317 are involved in the binding of tau to the interface between α-tubulin-β-tubulin heterodimers, whereas in contrast residues between the MT-binding domains remain flexible.[67] When tau is bound to MTs, it is further stabilized and more resistant to aggregation, since it can form a local hairpin conformation through the residues 269-284 (especially the hexapeptide ^{275}VQIINK^{280}) and 300-310 (especially the hexapeptide ^{306}VQIVYK^{311}), residues usually thought to be involved in the aggregation of tau.[67]

Besides the regulatory function of tau on MTs, axonal transport is further regulated by tau through influencing the functions of the motor proteins dynein and kinesin, which transport cargos towards the minus ends (cell body) and plus ends (axonal terminus) of microtubules.[68] Although there are studies suggesting that tau plays an important role in axonal transport *in vitro* or *in cellulo*, the deletion or overexpression of tau in mice was shown to have only little impact on axonal transport, which implies that different and yet unknown *in vivo* mechanisms may exist and counteract the effect of tau on axonal transport.[69] Moreover, tau is thought to be essential for axonal elongation and maturation. This was shown in experiments where tau was knocked down in rat neurons, which inhibited neurite formation, whereas in contrast the overexpression of tau promotes the formation of neurites even in cells of non-neuronal descent.[70, 71]

2.2.3 Cellular localization of tau and its function assignments

Usually, tau becomes enriched in the cytosol and is distributed within the somatodendritic compartment. Its predominant occurrence is manifested in axons. There are numerous studies that have identified tau in different subcellular compartments. Tau was localized in microtubules of growth cones[72, 73] and in mitotic spindle,[74] which rose the question, whether tau has functions that exceed tubulin polymerization and MT stabilization. Non-phosphorylated tau protein has been localized in the plasma membrane of different cell lines,[75] where the N-terminal domain of tau mediates the interaction to the plasma membrane.[76] The described translocation to the membrane is highly dependent on phosphorylation. This was demonstrated through the inhibition of Casein kinase 1 (CK1) and Glycogen synthase kinase

3β (GSK-3β), which significantly increased tau translocation to the membrane. Moreover, inhibiting phosphorylation on the N-terminal portion of tau prevented the tau localization at the plasma membrane.[77] In addition to its localization at plasma membranes, tau was identified in the lipid rafts of mouse brain, AD affected brain and lipid rafts of primary neurons, where it is regulated by amyloid-β oligomers.[78, 79] In neurons, tau localizes also in synapses, indicating the involvement of tau in signal transduction.[76, 80, 81] In this context, researchers have found out that tau also localizes in dendrites, which mediates amyloid-β toxicity by targeting the sarcoma (Src) kinase FYN to postsynaptic NMDA receptors in mouse brains.[82] The observation that tau is localized in small amounts in dendrites is further discussed to occur also in synaptic spines.[82] However, the function of dendritic tau is not well understood and only poorly characterized. It was suggested that tau hyperphosphorylation is closely connected to the mislocalization of tau to the dendrites, where it changes synaptic function by affecting glutamate receptor trafficking.[83]

These results collectively suggest that factors such as hyperphosphorylation can change the localization and the function of the tau protein. This in turn could lead to events such as somatodendritic accumulation, axonal MT disassembly, PHF or NFT formation and finally neurodegeneration.[84] Tau appears to be an ubiquitous protein and fulfills many functions. Regarding the importance of the nucleus in homeostasis, the localization of tau to the nucleus may be of particular interest.

2.2.4 Nuclear tau

In the year 1988 tau-derived PHFs were identified in nuclei obtained by biopsies from AD brain.[85] Tau has been later assigned to be present in the nucleus first by visualization through the dephosphorylation-dependant antibody Tau-1.[86] Later, tau was also found to be present in the nucleolus.[87, 88] Liu *et al.* observed that the 1N4R isoform in the murine brain was mainly localized in the nucleus and to a small extent also in soma and dendrites, but not in axons.[58] But also other isoforms (e.g. 2N4R) can localize with small quantities in the nucleus.[58, 89] It remains not clear, whether the nuclear compartment could also harbor an abnormal tau, but

it is widely implied, that the bulk of nuclear tau may arise from a distinct transcript and is comprised of a dominant isoform.[58, 89]

Phosphorylation of tau is suggested to be an important modifier of tau function and thus it is very important to know if phosphorylation also triggers nuclear localization of tau. Researchers have indeed found phosphorylated and non-phosphorylated tau in LAN-5 neuroblastoma cells in a similar pool as in the cytoplasm.[87] In an experimental set-up, an intact isolated cell nucleus was incubated with ATP Gamma ^{32}P, which revealed that the nuclear tau was likely dephosphorylated in the nucleus, but phosphorylated in the cytoplasm before its translocation, whereas other studies led to the conclusion that tau can be phosphorylated in the nucleus, seen in normal cell lines, mouse brain and human brain.[90-93] Generally, the results presented in this section suggest the existence of both phosphorylated and non-phosphorylated nuclear tau, which may be dependent from the cell type and the intranuclear localization, whereas tau found in the nucleolus seems to be restricted to non-phosphorylated tau.

The function of tau in the nucleus is assumed to be protective against DNA damage, which can be induced e.g. by hydroxyl free radicals (-OH), which are known to induce breakage of double-stranded DNA.[94-97] Some researchers found that the addition of tau to Calf Thymus DNA (CTDNA) increased the melting temperature (T_M) of the DNA from 67° to 81°C in a concentration-dependent manner.[98] Along those lines, the ability of tau phosphorylated by GSK-3β (phosphorylation site at Ser396 was confirmed by western blotting) to bind DNA was investigated. It was found that the binding of tau to DNA and its resulting protection against thermal denaturation was diminished or completely inhibited through this phosphorylation.[94] According to these observations it was postulated that tau phosphorylation e.g. by GSK-3β and the resulting dysfunctions as occurring in AD may compromise MT formation and stabilization and additionally hamper DNA stabilization.[95]

There is not yet a clear explanation on the mechanism of tau interaction to DNA and thus its protective role *in vivo* remains unclear, but its dynamic on- and off-binding suggests that tau may shuttle between cytosol and the nucleus in analogy to heat-shock proteins.[95, 99] However, there are many indications that the involvement of nuclear tau in neurodegenerative diseases is at least partially caused by hyperphosphorylation.[100] There has been further evidence of this

theory, when human neuroblastoma cells were infected with the Herpes simplex virus type 1 (HSV-1), which led to an increase of phosphorylation and interestingly also to an accumulation of tau in the nucleus, which was monitored by immunoblot and immunofluorescence analysis using antibodies targeted against C-terminal tau phosphorylations.[101] There is further *in vitro* evidence that phosphorylated tau can bind and alter the conformational integrity of DNA, by which the nucleosomal organization can be altered and thus has an impact on the gene expression.[102] In a recent work, the depletion of nuclear tau into neurons during AD progression was shown, thus providing an attractive link to the role of tau in the neurodegenerative process of AD.[103] These results lead to the conclusion that AD related modifications on tau such as hyperphosphorlyation cause the gradual depletion of tau from the nucleus even before NFT formation. Further investigations may be required, to identify the exact role of nuclear tau in normal and disease state, before efficient therapies can evolve.

2.2.5 Tau phosphorylation and aggregation

During development, the human tau phosphorylation pattern undergoes changes over time. In this course, fetal tau carries an average of 7 residues of phosphate, whereas adult tau bears merely two residues of phosphate.[104] In AD, tau becomes decorated by approx. 8 phosphate residues, known from mass spectrometry analysis of brain material.[105] The protein harbors as much as 85 potential phosphorylation sites in the 2N4R isoform, whereas most of them are actually accessible due to the unfolded nature of the tau protein. There are about 45 phosphorylation sites observed experimentally,[106] whereas most of the potential phosphorylation sites are accumulated in the flanking regions of tau (most are shown in **Figure 5**). Among those sites are 17 Thr-Pro or Ser-Pro motifs, which are of particular interest, since they are hyperphosphorylated in AD and other tauopathies. These motifs can be subject to signal-transducing proline-directed Ser/Thr-kinases. Other phosphorylation sites located within or nearby the repeat domains (R1-R4) are for instance decorated by microtubule affinity-regulating kinases (MARK, also known as PAR1 kinases), cyclic AMP-dependent protein kinase (PKA) and Ca^{2+} - or calmodulin-dependent kinase II (CaMK).[106]
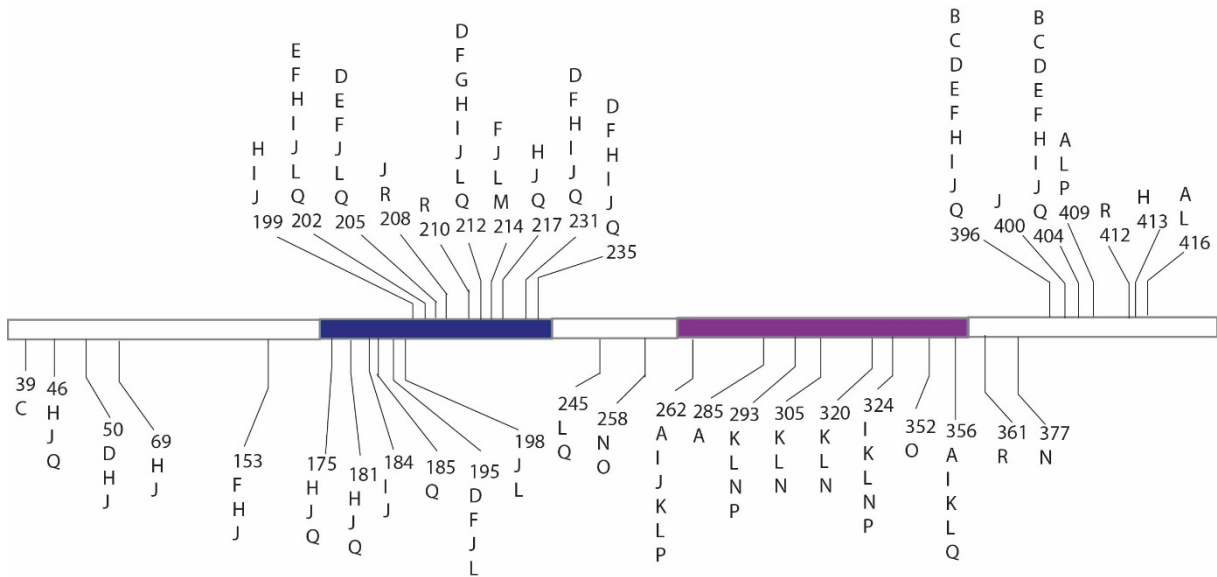
Figure 5: Phosphorylation sites of tau identified *in vitro*. The proline rich region is blue and the repeat region is purple. The phosphorylation sites are clustered around the proline rich region flanking the tandem repeats on the N-terminal site and the very C-terminal portion. The letters mark the identified kinases: **A)** Ca^{2+} -calmodulin-dependent protein kinase II; **B)** casein kinase I; **C)** casein kinase II; **D)** cdc2 protein kinase; **E)** cyclin-dependent kinase 2; **F)** cyclin-dependent kinase 5; **G)** dual-specificity tyrosine phosphorylated and regulated kinase; **H)** mitogen-activated protein kinase; **I)** glycogen synthase kinase 3α; **J)** glycogen synthase kinase 3β; **K)** microtubule-affinity-regulating kinase; **L)** protein kinase A; **M)** protein kinase B/Akt; **N)** protein kinase C; **O)** PKN; **P)** 35/41-kDa protein kinase; **Q)** stress-activated proteinkinase; **R)** tau tubulin kinase.[107]

It is worth mentioning that phosphatases are much more sensitive to temperature changes than kinases.[108] This could be an explanation for the observation that tau phosphorylation occurs during hibernation and in anesthesia-induced hypothermia.[109, 110]

The regulating function of phosphorylation to physiological functions of tau has been in the focus of investigation, including the regulation of microtubule assembly and stabilization. It was for instance shown that phosphorylation of KXGS motifs located within the repeat domains of tau by MARK, PKA or CaMKII (especially of Ser262) can reduce the binding capacity of tau to microtubules.[106] It was additionally shown that phosphorylation on residues Ser214 and Thr231 located in the flanking regions of tau destabilize MTs, whereas phosphorylations on other Thr-Pro or Ser-Pro sites in the flanking regions have only weak influence on the binding of tau and MTs. It was demonstrated that a phosphorylation on the Thr231 site leads to a *trans*-to-*cis* isomerization. The resulting conformational change is the reason for the inability of tau to bind MTs.[111]

Hyperphosphorylation of tau is possibly inducing pathological features through other mechanisms, for instance the induction of tau missorting from axons to the somatondritic compartment, which can cause synaptic dysfunction.[83, 112, 113] Furthermore, tau hyperphosphorylation may alter its degradation through the proteasome or autophagy and its truncation. Phosphorylation of Ser422 for instance can inhibit the cleavage of tau by caspase 3 at Asp421.[114] Another explanation for tau pathology induced by hyperphosphorylation is provided by the fact that highly phosphorylated tau reveals impairment of association to binding partners. For instance, only phosphorylated tau can interact with the kinesin-associated protein JUN N-terminal kinase-interacting protein 1 (JIP1), which in turn compromises the formation of the kinesin complex, which mediates axonal transport.[115]

Thirdly, tau hyperphosphorylation is closely related to tau aggregation into PHFs or NFTs as tau hyperphosphorylation and aggregation are both observed at elevated levels in AD (**Figure 6**).[3]
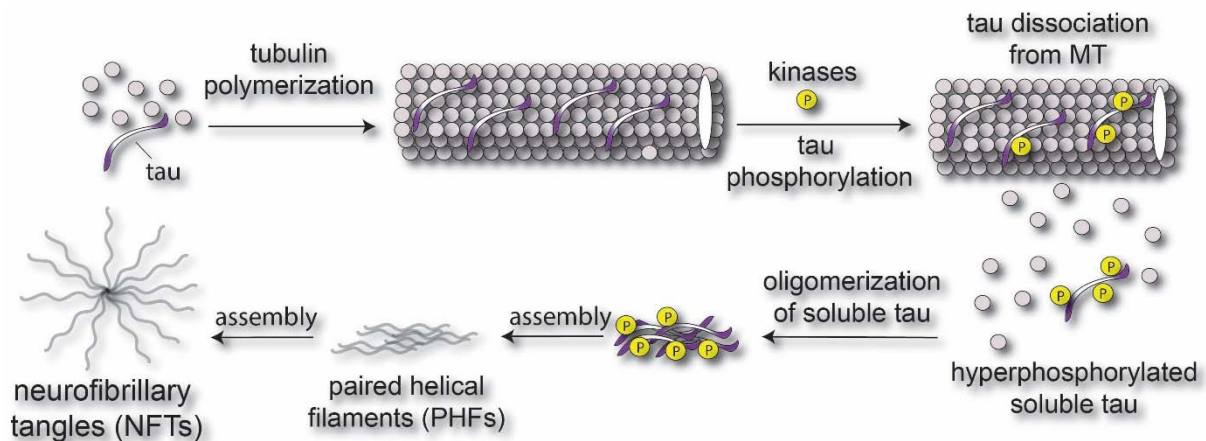
Figure 6: Hypothesis of tau dissociation from MTs induced by hyperphosphorylation, leading to higher amounts of MT disassembly and clustering of phosphorylated tau to oligomers, followed by further aggregation to paired helical filaments (PHFs) and neurofibrillary tangles (NFTs).

The aggregation of tau is a characteristic hallmark for many diseases comprised as tauopathies. Reasons for enhanced tau aggregation can be divers and are subject to intensive research. For instance tau mutations in or near the microtubule-binding domain (e.g. G272V, N279K, ΔK280, P301L, V337M or R406W) are not only associated with alterations in alternative splicing, but also to higher aggregation propensity along with reduced MT binding capacity.[47, 116, 117] It was shown that the sequence VQIVYK is sufficient for the formation of

fibrils composed of steric "zippers". Those are build up by two tightly integrated β-sheets. It is thus not surprising that disruption of this motif by mutations weakens the β-sheet forming propensity, whereas a mutation from Pro to Leu for instance strengthens this propensity and leads to enhanced tau aggregation *in vitro* and *in vivo*.[118] Further acceleration of tau aggregation can be achieved by polyanionic cofactors that can interact with the positively charged surface of tau. *In vitro*, aggregation can be provoked through the addition of sulfated glycosaminoglycans (e.g. heparin), nucleic acids, arachidonic acid micelles, acidic peptides or even carboxylated microbeads.[119-121] When polyanions are added, tau aggregates regardless of its phosphorylation state, which raises the question if phosphorylation is really a driving force for tau aggregation or whether the addition of polyanionic reagents gives rise to realistic aggregation scenarios.[119, 120]

It is thought that tau hyperphosphorylation precedes tau aggregation.[122] The influence of tau phosphorylation on aggregation is subject to a controversial debate, which is partially owed to the great heterogeneity of phosphorylation sites on tau. In an attempt to shed light onto the role of specific phosphorylations on tau aggregation, Broncel *et al*. were able to install a single phosphate residue at Ser404 by a technique called expressed protein ligation (EPL; see section 2.3.7), which was later shown to have no influence on the aggregation behavior, as in comparison to wild type tau no significant changes were marked.[123]

It was demonstrated experimentally that hyperphosphorylated tau isolated from AD patients brains can self-assemble into PHFs *in vitro*,[5] but the responsible phospho-sites remain unknown. It might be further questionable, whether cofactors are required for tau aggregation. Furthermore, tau phosphorylation on certain sites may also prevent aggregation[124] and some phospho-species of tau derived from insect Sf9 (ovarian) cells form oligomers instead of aggregated fibres.[125] When looking at tau phosphorylation it should be also considered that possibly phosphorylation drives aggregation indirectly through detaching tau from the MTs[126] or through mechanisms described in section 2.2.1. There it is described that C-terminal tau phosphorylation may disturb the inhibitory function of C-terminal tau, thus exposing the interior portion of the protein to further kinases or proteases, which can lead to the formation of truncated tau with enhanced aggregation potential.[7]

Tau versions that are truncated and contain the repeat domain have a higher tendency for aggregation probably due to the disruption of the usual paperclip formation that tau usually adapts. PHFs isolated from human brains from AD patients were treated with pronase (protease mixture) to remove the fuzzy coat. After further investigation, two tau fragments terminated at Glu391 were identified.[64] Further evidence for enhanced aggregation propensity of truncated fragments can be found when looking at tau cleaved behind Asp421, which usually takes place via protease activity of caspase 3.[127] Another example is truncation of tau by asparagine endopeptidase, which cleaves tau after Asn255 and Asn368 under *in vitro* conditions,[128] an AD-specific truncation associated with neurodegeneration. In this assay, tau was cotransfected with a glutathion-S-transferase (GST) tag for purification and expressed in mice. Subsequently, asparagine endopeptidase, a lysosomal Cys peptidase, was added to kidney lysate from these transfected mice and tau proteins were pulled-out from the lysate mixture and then analyzed by SDS-PAGE, where their truncation became obvious through the presence of shorter protein fragments containing the GST-tag.

Tau aggregation can also be triggered by implanting nucleation seeds from preformed PHFs, whereas the aggregation process follows then a nucleation-elongation process.[129] In this work, fibrils were observed by TEM and the aggregation monitored with thioflavin T (ThT, **Figure 7**), a β-sheet intercalating agent that is used to visualize the presence of fibrillization of misfolded proteins.
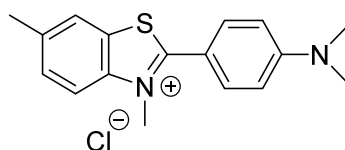
4-(3,6-dimethyl-1,3-benzothiazol-3-ium-2-yl)-*N,N*-dimethylaniline chloride

Thioflavin T (ThT)

Figure 7: The chemical structure of Thioflavin T.

But there is also evidence that tau aggregation may be triggered in the same way *in vivo*. Strikingly, when tau seeds are injected into WT mouse brains, they induce a time-dependent tau pathology from the injection site to synaptically connected brain regions.[130] As tau can

convert to conformationally stable strains, tau pathology is discussed in the context of prion diseases (**Figure 8**).[131, 132]
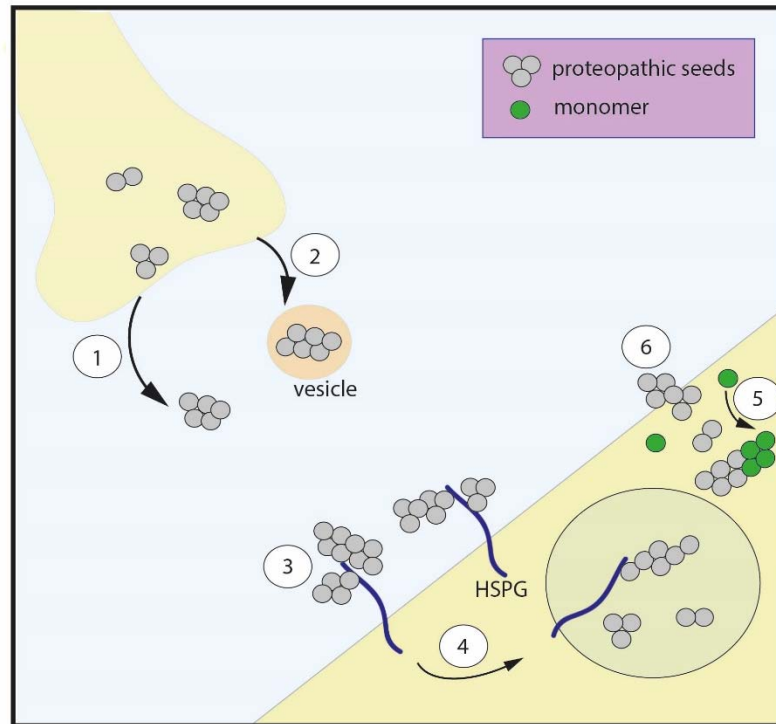
Figure 8: Shown are mechanic deatails about the prion-like transcellular propagation of tau: 1) proteopathic seeds accumulate inside the neurons, from which they can be released, or 2) can exit the neuron via vesicles, such as exosomes; 3) extracellular proteopathic seeds can bind cell-surface heparan sulfate proteoglycans (HSPGs); 4) the binding of aggregated species can trigger micropinocytosis, which constitutes an actin-driven uptake process, which leads to the internalization of tau seeds; 5) proteopathic tau seeds escape the lumen of the macropinosome via an unknown mechanism, whereas free-floating inside the cell cytoplasm they can convert monomers into aggregates via a templated conformational change; 6) in same cases, tau aggregates can pass the plasma membrane.[133]

2.2.6 Hypotheses of tau-related toxicity

The so called "loss of function hypothesis" states that tau is necessary for the integrity of the neuronal network and thus reduction of the tau level caused by aggregation may cause MT disassembly, which leads to deficits in axonal transport. In favor of this theory speaks the observation that tau knock-out mice showed indeed behavioural impairment, which indicates the necessity of tau for normal brain functions.[134] Loss of tau function is closely related to hyperphosphorylation, which causes tau detachment from MTs and thus their destabilization. However, as tau is a multifunctional protein, the toxicity due to loss-of-function can be also

traced back to impairments of these functions. For instance, compromised neuronal protection induced by oxidative stress can be a factor leading ultimately to neurodegeneration.

Moreover, the occurrence of NFTs in brains and their spatial distribution correlates with the severity of AD. It was thus assumed that NFTs themselves contribute to toxicity, which led to the formulation of the so called "neurotoxic gain of tau function" hypothesis. However, the solemn existence of NFTs was shown not to be sufficient for neurodegeneration. It was demonstrated in the superior temporal sulcus brain region that neuronal loss exceeds sevenfold the number of neurons that formed NFTs, which implied that the majority of neurons dies without prior NFT formation.[135] A study showed further that NFT bearing neurons could survive up to 20 years.[136] It may thus be seen very critical, whether NFTs themselves cause toxicity in neurons. This observation suggest that rather soluble tau species are the culprit in AD. It is further discussed, whether PHF and NFT formation can be rather seen as a rescue mechanism and protects neurons from being damaged by soluble tau species. Thus, an indirect protection mechanism would prevail, by which neurons are protected from direct assaults, such as e.g. attacks by reactive oxygen species that can be generated through mitochondrial dysfunction, which could possibly result from toxic tau species.[137] Despite the present facts, aggregates of tau can sequester other cell compartments on the long term and thus compromising neuronal function on the long term. Moreover, axonal transport could be hampered through the presence of bulky aggregates.

The main focus of researchers has nowadays centered on the identification of neurotoxic soluble tau species, as levels of soluble oligomeric tau are elevated in AD.[138] These oligomeric tau species are not very well characterized today, owing to experimental difficulties, but it was demonstrated in cell toxicity assays that tau oligomers made from pro-aggregant recombinant tau were toxic to cultured cells.[139, 140] There were other studies conducted where the exposure of neurons to tau oligomers induced local neurotoxicity, shown by the loss of spines.[125]

The group of Eckhard Mandelkow addressed the question whether tau aggregates are essential for neurodegeneration or not by generating two mouse models, either expressing full-length human tau with an anti-aggregant mutation (Pro substitutions, that break β-sheets) or human tau with a pro-aggregant mutation (ΔK280 truncated tau, known for enhancing the tendency

of tau to form β-sheets).[141-143] As a result, the mice expressing anti-aggregant tau showed almost no pathology, whereas mice expressing the pro-aggregant tau species developed AD-like features such as missorting of tau to the somatodendritic compartment, tau conformational changes, tau hyperphosphorylation, NFTs and cognitive deficits. In consequence, the ability of tau to aggregate seems to be crucial for pathologic features of tau. However, one has to view this mouse model with caution, since an artificial construct was created and since tau also interacts with many different other proteins, the outcome of such mutations is unpredictable.

Another prevalent hypothesis of tau induced toxicity is its mislocalization. Usually, only small amounts of tau localize in the dendritic compartment, whereas the dendritic localization of tau is significantly higher in individuals with AD.[47] Hyperphosphorylation is also a crucial mechanism in missorting of tau, as it drives tau into postsynaptic spines, which results in synaptic dysfunction.[83, 112, 144] In cultured neurons, tau seems to mediate toxicity that is induced by amyloid-β by promoting the translocation of tyrosine-ligase enzyme 6 (TTL6) into dendrites and further the destabilization of MTs by spastin.[145]

In conclusion, the reason why tau aggregation is toxic to neurons is not clear. The contribution of monomeric, hyperphosphorylated or truncated tau variant to neurotoxicity in AD have to be further investigated. Especially hyperphosphorylation has been assigned to toxic gains of function, which could be independent of aggregation, as molecular interactions to other binding partners can be compromised or enhanced. It was for instance shown in a *Drosophila melanogaster* model of tauopathy that tau hyperphosphorylation had unusual F-actin alignment and accumulation as a consequence, ultimately leading to neurodegeneration.[146]

2.2.7 *O*-GlcNAcylation of tau

The post-translational modification (PTM) of *O*-GlcNAcylation was discovered by Torres and Hart in the year 1984 and has ever since been found in all multicellular eukaryotes.[147] In the past, *O*-GlcNAcylation was mainly determined by mass-spectrometry based methods on brain tissue of humans and mice, which has helped to identify *O*-GlcNAc on more than 1000 proteins, including tau and APP, as well as low-abundant transcription factors.[148-150] This PTM is installed onto Ser and Thr residues by the glycosyltransferase called *O*-GlcNAc transferase

(OGT). As substrate for this enzyme serves uridine diphosphate (UDP)-GlcNAc,[151, 152] whereas there is no known consensus sequence, which governs the attachment of *O*-GlcNAc residues, although most *O*-GlcNAcylation sites are disordered.[149] *O*-GlcNAcylation is a reversible PTM, since its detachment is carried out by glycoside hydrolase *O*-GlcNAcase (OGA). The half-life of an *O*-GlcNAc modification can be as low as just several hours.[153, 154] The role of *O*-GlcNAcylation is particularly important in neurons, since the expression of OGT and OGA are there the highest and about tenfold higher than in the peripheral tissue.[155-157]

The ability of *O*-GlcNAc levels to change in dependence to variations in cellular glucose availability displays its nutrient responsiveness. This happens both, *in cellulo* and *in vivo*, where reduced glucose levels induced by fasting were observed to correlate with decreased brain *O*-GlcNAcylation.[158] This described nutrient responsiveness stems from the low UDP-GlcNAc levels in flux provided by the hexosamine biosynthetic pathway. This pathway consumes about 2-5% of the available glucose taken up by cellular glucose transporters.[159]

On tau, *O*-GlcNAcylation was first observed in bovine samples and was argued to be present with four *O*-GlcNAc units per tau molecule.[160] Ever since, several studies have shown that tau phosphorylation and *O*-GlcNAcylation are reciprocal and thus have a regulating function on each other, as e.g. *O*-GlcNAc can antagonize tau phosphorylation at various sites in tissue culture cells and rat brain slices.[161] The role of tau *O*-GlcNAcylation is vividly discussed in the context of AD, as tau derived from NFTs bear no *O*-GlcNAc PTMs.[156] The hypothesis of reciprocal regulation between tau phosphorylation and *O*-GlcNAcylation was further supported by the observation that fasted mice showed increased tau phosphorylation[158] and another study, which revealed that blocking phosphatase action resulted in less tau *O*-GlcNAcylation. Moreover, it was shown that the application of the OGA inhibitor Thiamet-G increased brain *O*-GlcNAcylation,[162] and OGA inhibition decreases tau phosphorylation at several pathological sites.[163]

There have been several *O*-GlcNAc sites mapped onto human tau protein located at Thr123, Ser208, Ser400, Ser409/Ser412/Ser413.[164, 165] *O*-GlcNAcylation on Ser400 was further identified on human tau expressed in mice and on rat tau.[164, 166] A recent, very exhaustive mass spectrometry study on tau PTMs in a transgenic mouse model revealed the *O*-GlcNAcylation

site at Ser400 as the only undoubted decoration on tau found.[4] In the findings of Morris *et al*, OGA inhibition increased *O*-GlcNAcylation without changing tau phosphorylation, indicating that these PTMs are not necessarily reciprocal and rather suggest an unknown mechanism of inhibiting tau aggregation by extensive *O*-GlcNAcylation, independent of tau phosphorylation.[4]

On the peptide level, Smet-Nocca *et al*. have depicted this reciprocal relationship of tau *O*-GlcNAcylation and phosphorylation at high resolution.[167] In their experiments, they probed *O*-GlcNAcylation sites of tau by probing *in vitro* activity of OGT on recombinant tau and on synthetic peptides of the MAP. Generated *O*-GlcNAc sites were then analyzed either by per residue resolution of NMR spectroscopy or mass spectrometry. There have been already previous studies that showed the applicability of this concept when phosphorylation sites on tau were investigated.[168-171] By applying purified kinases such as PKA, CDK2/cyclinA3 or GSK-3β to tau, patterns of phosphorylation similar to those identified by phospho-tau specific antibodies, mass spectrometry analysis or peptide sequencing were generated.[172-176] The combination of their phosphorylation approach with OGT provided a valuable tool to study tau *O*-GlcNAcylation. In result of their analysis of tau exposed to OGT by NMR spectroscopy, *O*-GlcNAcylation did not occur in detectable levels. On the peptide level, the researchers were able to confirm the previously identified *O*-GlcNAcylation site Ser400 and were further able to identify two novel *O*-GlcNAcylation site located in the proline rich domain of tau at residues Ser208 and Ser238. Furthermore, Smet-Nocca *et al*. have demonstrated the impact of *O*-GlcNAcylation on phosphorylation events. The installation of *O*-GlcNAc at the Ser400 site by OGT was shown to downregulate phosphorylation at position Ser404 and even completely abolish the phosphorylation on Ser396. This study impressively showed the regulatory potential of *O*-GlcNAcylation on tau phosphorylation in this AD-relevant site, termed PHF-1 epitope (Ser396/400/404).
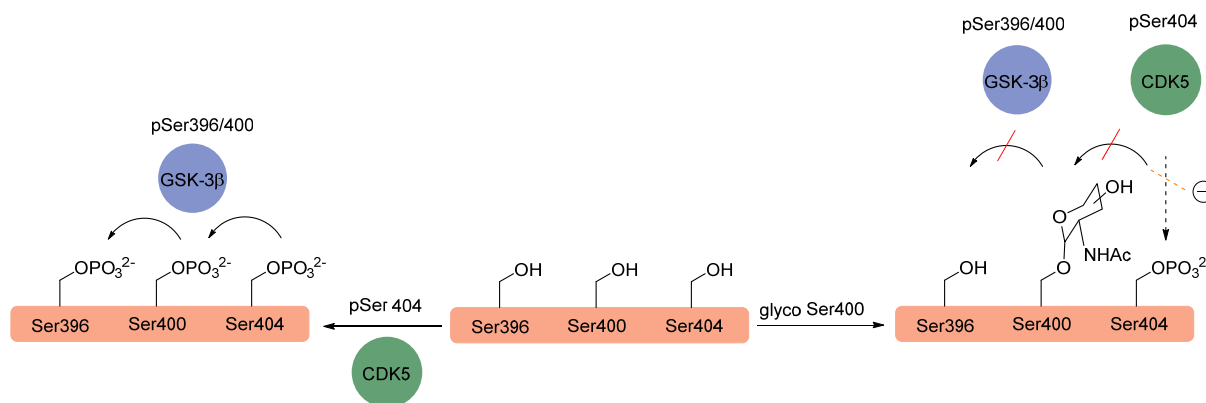
Scheme 1: Reciprocal relationship between tau phosphorylation and O-GlcNAcylation at the PHF-1 epitope of tau comprised of the three serine residues at 396, 400 and 404. Phosphorylation on Ser404 is carried out by CDK5 as a primary event, followed by phosphorylation by GSK-3β of residues 400 and 396. On the synthetic peptide tau[392-411], it was shown that O-GlcNAcylation of Ser400 downregulates phosphorylation of Ser404 by CDK5 and further inhibits phosphorylation at position 396.[167]

2.2.8 Interplay between β-amyloid and tau

It is widely assumed that tau and amyloid-β do not act in isolation, but that there is rather an intensive cross-talk between the two proteins.[177-179] It is worth mentioning that tau pathology is assumed as a downstream event of amyloid-β pathology, which provides evidence for the amyloid cascade theory.[180, 181]
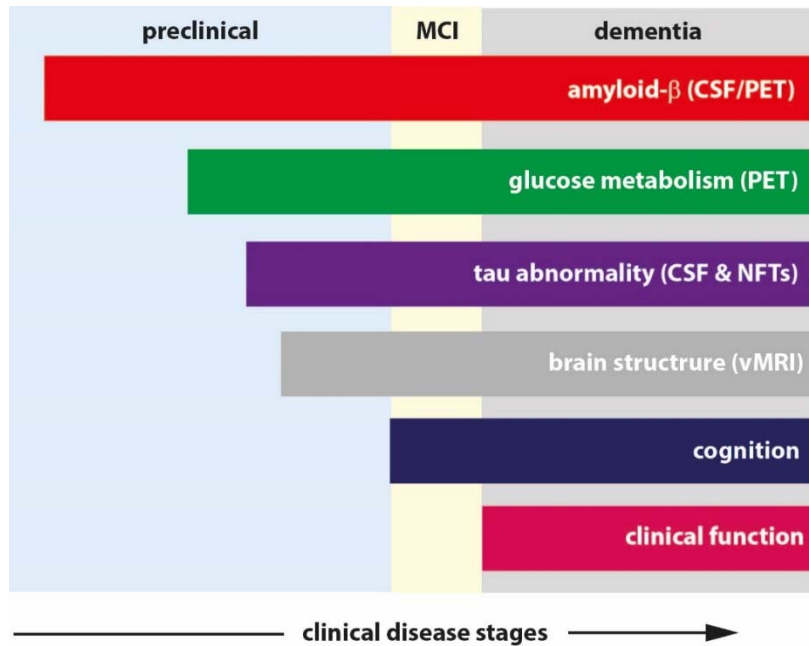
Figure 9: A model for changes of biomarkers and their association with AD progression. The earliest biomarker during the course of AD is amyloid-β, which can be found in cerebrospinal fluid (CSF) or assessed by positron emission tomography (PET) amyloid imaging. Subsequent to preclinical changes of amyloid-β, the glucose metabolism becomes impaired and increased tau levels are measured in CSF due to pronounced tau abnormalities. When the disease becomes more severe and first clinical symptoms are observed as in mild cognitive impairment (MCI) stage, there are differences in brain structures measurable by volumetric MRI (vMRI). As disease progression continues, the diseases state of dementia is finally reached.[156]

It was shown that the reduction of tau levels in APP transgenic mice can reverse memory impairment, reduce susceptibility to experimentally induced excitotoxic seizures and decrease early mortality, all without altering amyloid-β levels or plaque load.[182] This rather crucial role of tau was further supported by the finding that hyperphosphorylated tau accumulates in dendritic spines of cultured CA3 hippocampal neurons.[83] Further evidence of an interplay between tau and amyloid-β delivered a study, in which human APP transgenic mice were crossed with human tau transgenic mice, which led to an enhanced aggregation of tau with concomitant dendritic spine loss, resulting in strong cognitive impairment of these mice.[183]

The causality of this observed enhanced tau induced toxicity upon elevated amyloid-β levels is under debate, but one crucial aspect could be associated to the *N*-methyl-D-aspartate receptors (NMDARs). Under physiological conditions, tau has a critical role in targeting the Fyn kinase to spines, where it phosphorylates the NMDAR subunit of NR2b and recruits PSD-95 into a protein complex to mediate excitotoxicity.[184] The Fyn-tau interaction was confirmed by

experiments, where Fyn was targeted against post-synaptic sites in the presence of tau *in vivo*, which did not take place in tau knock-out mice, where Fyn accumulated in the soma.

If elevated amyloid-β levels are present and phosphorylated tau, more Fyn is targeted to the spine and toxicity is enhanced.[82] This assumption gets support by the observation that crossing human APP transgenic mice with mice expressing the aggregation prone tau mutant P301L leads to 100% death of the mice after only four months.[185] Furthermore, an increased level of intracellular calcium induced by amyloid-β-mediated overexcitement of extrasynaptic NMDARs has been proven to activate the tau modifying kinases AMPK and PAR-1/MARK. In more detail, the kinase AMPK phosphorylates tau at position Ser422 in the presence of amyloid-β,[186] an AD relevant epitope.[187] During the progression of AD pathology, amyloid-β has been proposed to further activate the Fyn phosphatase striatal-enriched protein tyrosine phosphatase (STEP), eventually inactivating Fyn. This in turn can lead to the loss of synapses and dendritic spine collapse.[186, 188] It was thus suggested by G. S. Bloom that amyloid-β may be the trigger and tau the bullet of AD pathology.[189]

2.2.9 Diagnosis of Alzheimer's disease with focus on tau

The diagnosis of AD is based on guidelines established by an expert committee composed of the Alzheimer's Association, the National institute of Aging (NIA) and the National Institute of Health (NIH). Until recently, AD was merely diagnosed using clinical assessments during the dementia stage or post mortem by neuropathology. Nowadays, it is widely accepted that key biological changes occur in the body already in a preclinical disease stage years or even decades before symptoms such as confusion or loss of memory are visible. The guidelines that have been developed to diagnose AD are not an immediate call for a final diagnosis, but rather an agenda to identify biomarkers that may signal when presymptomatic brain changes begin. This is hoped to help target these changes in early stage and thus enable the best possible treatment.

In contrast to previous efforts focusing on diagnosing at the dementia stage of disease, clinical trials have moved to earlier stages of AD,[190-192] before extensive neurodegeneration has occurred and even to prevention trials that set in before symptom onset, when disease-modifying

approaches are thought to have a maximal effect.[193-195] Moreover, biomarkers aid to identify pathological hints in AD patients on the one hand and on the other hand may help to track biological effects of drugs. Today, a probable diagnosis of AD can be established with a confidence of >90%, based on clinical criteria, which include medicinal history, physical examination, laboratory tests, neuroimaging and neuropsychological evaluation.[196] An early and accurate diagnosis is very important, but remains a challenging task, since early symptoms of the disease are shared with a variety of disorders, which may be assigned to other types of dementia than AD, such as MCI, vascular dementia (VaD), frontotemporal lobe dementia (FTLD), or Lewy body dementia (LBD). This aspect is actually important, since the different types of dementia may actually require different types of treatments.

In particular, three different types of biomarkers have been well-established and validated internationally to aid the diagnosis of AD in CSF with enzyme-linked immunosorbent assays (ELISAs): amyloid-β[1-42], total tau and phospho-tau181, some of which have Conformité Européenne (CE)-marking in Europe, but none of them has a clearance by the FDA. The consensus nowadays is the testing of all three biomarkers in CSF is necessary, which increases the diagnostic validity for sporadic AD. In total, the combined assays yield a sensitivity of >95% and a specificity of >85%.[197-200]

Biomarkers in general have certain requirements, which have been established in several publications and that are summarized in **Table 2**.[201-204]

2. INTRODUCTION & BACKGROUND

Table 2: Criteria for the establishment of a good biomarker for the diagnosis of dementia.[196]

entry	criteria
1	reflect physiological aging process
2	reflect basic pathophysiological processes of the brain
3	react upon pharmacological intervention
4	display high sensitivity
5	display high specificity for the disease as compared to related disorders
6	allow measurements repeatedly over time
7	allow reproducibility in laboratories worldwide
8	should be measurable in non-invasive easy-to-perform tests
9	should not cause harm to the individuals being assessed
10	tests should be inexpensive and rapid
11	samples should be stable to allow easy and cheap transport
12	easy collection of fluids not only in hospitals
13	changes should be at least twofold to allow differentiation of controls
14	define good cut-off values to distinguish diseases
15	data published in peer-reviewed journals
16	data reproduced by at least two independent researchers

Total-tau levels in CSF increase with age in healthy controls: <300 pg/mL (21-50 years); <450 pg/mL (51-70 years); <500 pg/mL (>70 years).[205] In tested individuals, total-tau levels are significantly increased in AD patients as compared with age-matched controls (**Table 3**).

Table 3: Internationally established biomarkers found in CSF and used to diagnose AD. The shown data was obtained from the manuals of the 96-well ELISA kits of the company innogenetics.

biomarker	controls (pg/mL)	AD (pg/mL)
amyloid-β 1-42	794±20	<500
total tau	136±89 (21-50 years)	not relevant for sporadic AD
	243±127 (51-70 years)	>450
	341±171 (>71 years)	>600
phospho-tau-181	23±2	>60

Despite the significant increase of total tau during the course of AD, the reason for the found elevated levels can also be traced back to other diseases such as Creutzfeldt-Jacobs disease (CJD) (>3000 pg/mL). **Table 4** gives an overview on changes of total tau in different conditions and disease states.

Table 4: Observed changes of biomarkers in CSF in different diseases associated to the nervous system.[196, 206] The symbol – stands for no change, ↑ for an increase and ↓ for decrease.

disease	amyloid-β	total-tau	phospho-tau-181
acute stroke	-	↑(↑)	-
alcohol dementia	-	-	-
AD	↓	↑	↑
CJD	↓↓	↑↑↑	-
depression	-	-	-
FTLD	↓	↑	-
LBD	↓	↑	↑
neuroinflammation	↓	-	-
normal aging	-	-	-
Parkinson's disease	-	-	-
VaD	↓(↓)	↑	-

Despite the non-specificity of total-tau as a biomarker for AD, it may still be regarded as a valuable tool at the transition between MCI and AD, since high CSF tau level are found in 90% of MCI cases that later progress to AD, but not in cases of stable MCI.[197] However, more specificity toward AD is evident for the recognition of phosphorylated tau, as can be seen for phospho-tau-181 in **Table 4**. Moreover, K. Blennow *et al.* suggest that the recognition of other phospho-epitopes through antibodies that recognize tau phosphorylation in positions 199, 231, 235, 396 and 404 might offer significant improvements towards early diagnosis of AD.[198] It has been shown that phospho-tau-231 and phospho-tau-181 are suitable to distinguish AD from controls and FTLD, VaD, LBD and depression.[207, 208] In another study, phospho-tau-231 detection was shown to help monitoring the longitudinal decline from mild to moderate AD.[208]

In routine diagnostic procedures, there are no tests for other CSF biomarkers in use today, which is owed to the high heterogeneity of measured probes. Several other molecules are differing in CSF between AD patients and age-matched controls. In this context, cognitive decline is correlated with loss of the neurotransmitter acetylcholine. This loss is counteracted by the nerve growth factor (NGF), which is reproducibly increased in CSF of AD patients.[209-211] However, the changes are too low to establish NGF as a viable biomarker usable for diagnosis of AD.

Biomarkers derived from fluids other than CSF such as blood, saliva or urine are desperately pursued since CSF requires a lumbar puncture of a patient with potential side effects, which makes follow-up experiments of the same patient difficult. Moreover, analysis of CSF is limited by costs, as commercial ELISA assays for the three common biomarker amyloid-β, total-tau and phsopho-tau-181 (e.g. by the provider innogenetics, www.innogenetics.be) are cost intensive. According to calculations of Humpel, a 96-well plate for an ELISA costs approx. 900 €, which has to be tripled since all three biomarkers have to be tested usually. Furthermore, analysis is performed usually as duplicate and includes a standard curve, which finally leads to costs of 68 € per patient, excluding costs for personnel and laboratory expenses.[196] It is thus a goal to get the costs down to about 10 € per patient. Cheaper versions of the diagnostic kits are meanwhile provided through the INNO-BIA AlzBio3 (innogenetics), which allows the simultaneous detection of all three biomarkers.[212] It is thus the reduction of costs on the one hand, and the identification or validation of new specific and sensitive biomarkers on the other hand that is in the focus of finding tools suitable for AD diagnosis.

2.2.10 Therapeutic strategies targeting tau pathology

Since hyperphosphorylation is closely related to tau pathology, the blocking of extensive tau phosphorylation is one valid strategy to fight AD. Hyperphosphorylation may ultimately be traced back to an imbalance of phosphatases and kinases. It is thus not surprising that there is an increase of expression of active forms of various kinases crucial to AD, such as CDK5, GSK-3β, Fyn, JNK, p38, ERK1 and ERK2.[213] Owed to the connection of these kinases to AD,

there have been multiple efforts to develop kinase inhibitors as a possible treatment strategy for AD.

There is e.g. the compound SP600125 (**Figure 10**), a widely used pan-JNK, which has beneficial features and effects on cognition and reduces neurodegeneration in an APP/PS1 transgenic mouse model of AD.[214] Also CDK5 is a possible target to treat AD. Alzheimer patients have increased levels of calcium in their brains, which activates CDK5 and results in pathological hyperphosphorylation in neuronal cells and ultimately to cell death.[215, 216] Another potential drug target is the kinase GSK-3β. Among various drugs targeting this particular kinase, tideglusib (**Figure 10**) has recently completed phase II clinical trials without any significant results upon administration over 26 weeks to patients with mild to moderate AD (NCT01350362). However, when administered to patients with progressive supranuclear palsy (PSP), the compound had considerable effects on the progression of brain atrophy.[217] Another approach to target tau phosphorylation is the activation of phosphatases, but today there is merely one compound tested in this course. This phosphatase 2 agonist Vel015 (**Figure 10**) is undergoing phase II clinical trials, after animal experiments were positively evaluated.[218, 219]

Researchers have also discovered organic compounds that break up aggregates of tau. Strikingly, the compound methylene blue and some derivatives have this ability and were shown to improve the efficacy of mitochondrial electron transport, reduce oxidative stress, prevent mitochondrial damage and are further modulators of autophagy.[213, 220] The next-generation derivative of methylene blue, leucomethylthioninium.2HX (LMTX, **Figure 10**), appeared to have preventive properties and further has the ability to break up aggregates of clustered tau. The compound is undergoing phase III clinical trials. Moreover, some hexapeptides consisting of D-amino acids that selectively interact with the steric zippers that are build up by the hexapeptide VQIVYK were shown to suppress tau aggregation *in vitro* and are thus potential candidates for clinical trials.[221]

Other studies pointed towards another direction of tau-based therapy against AD. Instead of breaking-up tau aggregates or preventing tau aggregation, microtubule stabilization was desired. For instance TPI 287 (**Figure 10**) is microtubule stabilization agent, just like Paclitaxel, a well-known cancer agent. TPI 287 stabilizes microtubules by binding to tubulin

like tau and is currently evaluated in clinical trials (NCT01966666). The short peptide NAPVSIPQ (known as NAP) made it to phase II clinical trials, but was shown to exhibit improvements to patients.[222] Another microtubule stabilizer is called epothilone D (also known as BMS-241027, **Figure 10**). This compound showed therapeutic effect in preclinical studies in transgenic mouse models of tauopathy.[223]
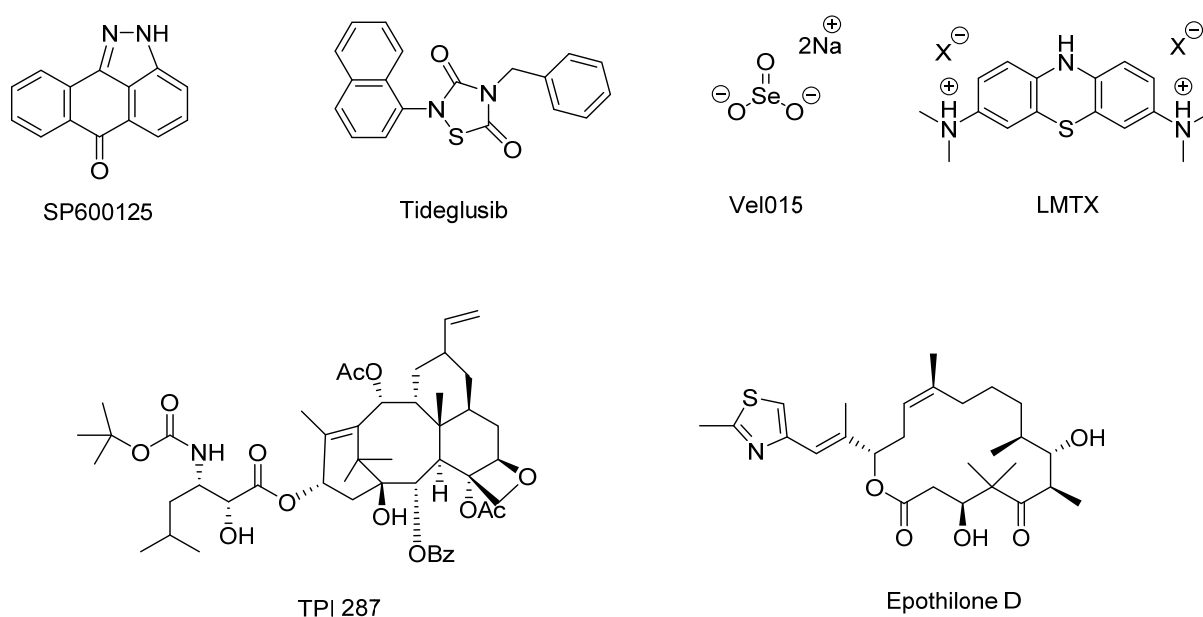

Figure 10: Chemical structures of selected potential drugs for AD therapy that are tested in clinical trials.

Active and passive immunotherapy are also considered to have some potential in treating AD symptoms. Application of antibody-based therapy led the reduction of tau aggregates and improved clearance of tau oligomers was achieved by this immunotherapy.[224-226] It is widely accepted that the cycling of antibodies between plasma compartments and the central nervous system (CNS) leads to descent exposure of the antibodies. Once the antibody reaches a neuron, it may enter it via a clathrin-mediated endocytosis, which follows binding to low affinity FcγII or FcγIII receptors on neurons,[227] but other mechanisms are discussed in addition,[228] by which the antibodies reach neuronal tau and thus prevent its aggregation.

Ser/Thr-Pro motifs exist in two distinct conformations, namely *cis* or *trans*. Pin1 prolyl izomeraze is able to regulate the function of phosphorylation or dephosphorylation of some phospho-proteins, including some Ser/Thr sites on tau through the restoration of the original trans conformation and further aids the dephosphorylation of such sites.[229] A related study showed that a *cis* tau specific antibody was able to prevent tauopathy in a model, which

displayed tau pathology after brain injury.[230] As pathological tau is able to exit neuronal cells, some antibodies have also therapeutic effects in extracellular environment.[231] Along those lines, there was evidence that some antibodies target extracellular tau seeds, thus preventing the seeding and propagation of tau related pathology in transgenic mice.[232]

2.3 Peptides and proteins

The so called "central dogma of molecular biology" states that DNA makes RNA and RNA makes proteins, first formulated by Francis Crick in 1958.[233] This general rule emphasizes the order of events starting from transcription and ending in translation. Protein biosynthesis follows the principle steps of initiation, elongation and termination. The assembly of amino acids in nature takes place *via* templated amidation of amines from unprotected amino acids and RNA (**Figure 11 A**). Post-translational processing of the completed polypeptide further plays a particularly important role for assuring fidelity of synthesis and the proper function of the protein product. It is nowadays known that PTMs can alter the function, localization, stability towards degradation by the proteasome and influence the targeting of proteins.[234] Moreover, unusual PTM modifications are associated with numerous diseases such as cancer or Alzheimer's disease. The study of PTMs is a complex field of research, as access to homogeneously modified proteins is limited by methods of expression and application of enzymes.[235] Therefore, many synthetic efforts were undertaken to produce and purify peptides and proteins, homogeneously modified by PTMs at only one or more amino acid positions, which can be introduced during solid phase peptide synthesis (**Figure 11 B**). As misregulation of PTMs are associated to many diseases, these constructs can help to understand the structural or functional impact of these PTMs on the proteins of interest. Some of the most influential advancements in the synthesis of functional peptides and proteins were made by developments of chemoselective ligation protocols (**Figure 11 C**).[236] The fields of chemical peptide and protein synthesis are subject to the following section. The focus here are modern concepts of native chemical ligation and expressed protein ligation, two techniques that have revolutionized the field of chemical protein synthesis (semisynthesis).
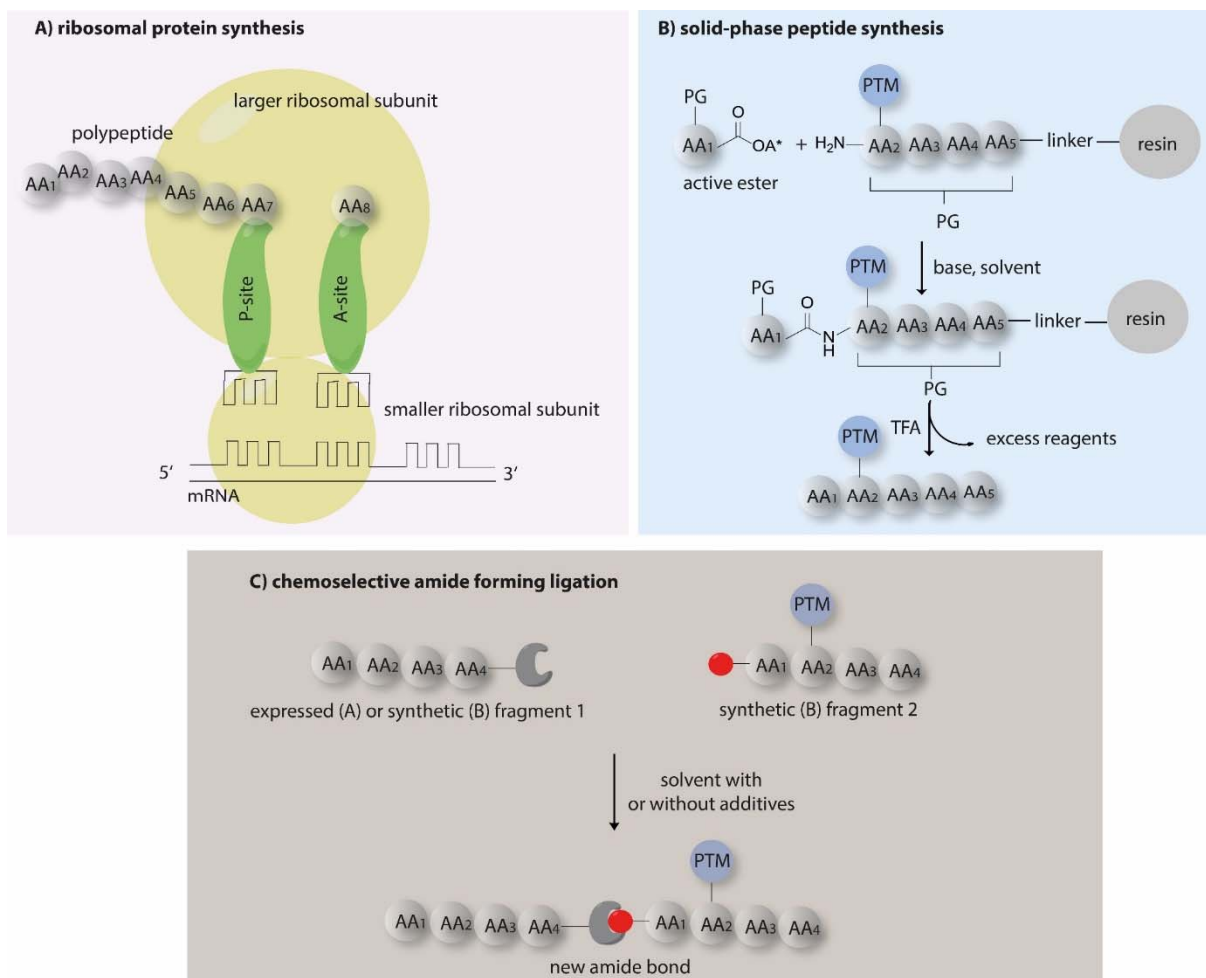
Figure 11:[237] Shown are biochemical and chemical methods on how peptide or protein synthesis are carried out and how post-translational modifications can be installed site-specifically. **A**) Simplified scheme of ribosomal protein synthesis. Templated amidation with unprotected amino acid building blocks serve for protein assembly. The A-site serves as the entry point for aminoacyl transfer RNA and elongation of the polypeptide occurs along the P-site. By this cascade of reactions, an amide bond is formed between two amino acids. By this process, high molecular weight proteins are formed; mRNA: messenger RNA. **B**) Schematic illustration of solid phase peptide synthesis. Peptides are generated on solid support by coupling of protected amino acid (PG = protecting group) bearing a C-terminal active ester and amino acids with free amines on solid support in the presence of solvent and base. On a routine basis, peptides of 30-50 amino acids can be produced at sufficient quantities. **C**) Chemoselective amide forming ligation for the synthesis of complex peptides or proteins. Two functional groups (red circle and grey fitting shape) can react chemoselectively in the presence of all other naturally occurring functionalities of peptides and proteins.

## 2.3.1 Solid phase peptide synthesis (SPPS)

Peptides are formed through repetitive amide bond forming reactions between the 20 natural L-amino acids that finally form functional peptides or proteins. A milestone for the chemical

synthesis of peptides was achieved through the development of the so called solid phase peptide synthesis (SPPS), which was discovered by the pioneer Bruce Merriefield.[238] This discovery led to the Nobel Prize in 1984.[239] The SPPS technology enabled researchers to recover their desired peptides by one single cleavage step from the resin. By means of SPPS, major improvements over previous peptide synthesis attempts were achieved, given through simplicity, speed and efficiency, since all reactions can be effectively carried out in a single reaction flask.[240] Moreover, excess reagents can be washed away from the solid support during synthesis by a simple filtration step. In contrast to protein biosynthesis, SPPS is carried out from the C-terminus to the N-terminal end, whereas the α-amino group of each added amino acid and the side chain functionalities are shielded by protecting groups. The corresponding C-terminal carboxyl-group has to be activated to couple successfully to the resin. After the coupling reaction, the resin is washed to remove all by-products and the temporary protecting group on the α-amino end is deprotected. After a subsequent washing step, the next coupling can take place with the described synthetic steps in a repetitive way. In a final step, the permanent side-chain protecting groups are removed in the same way as the peptide is cleaved off the solid support.

The feature that defines the chemistry of SPPS is the temporary protecting group at the N-terminus of each amino acid, whereas the two most widely applied strategies involve either the *tert*-butoxy-carbonyl (Boc) group (sensitive to acids such as trifluoroacetic acid, TFA) (**Scheme 2 A**),[238, 241] or the fluoren-9-ylmethyloxycarbonyl (Fmoc) group (sensitive to bases such as piperidine) (**Scheme 2 B**).[242]

A)

B)
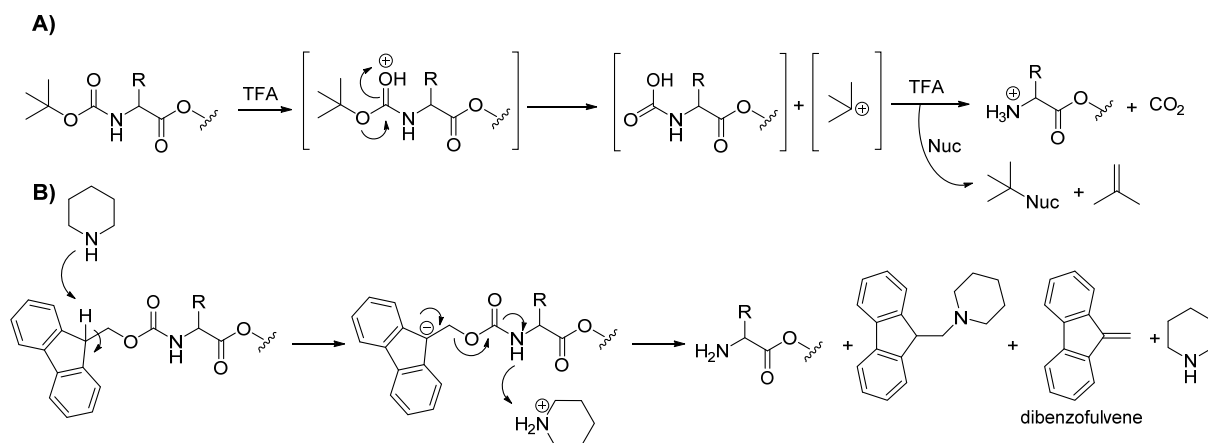
Scheme 2: Deprotection scheme of the two most popular α-amino protecting groups. **A)** Deprotection scheme of the Boc group; **B)** mechanism of deprotecting Fmoc.

The progression of amino acid coupling reactions is often achieved by the so called Kaiser Test.[243] This test provides qualitative evidence for the presence or absence of free primary amino groups and is thus a useful indicator for the completeness of a coupling step. The chemistry behind this test is based on the reaction of ninhydrin with primary amines, which yields a dark blue color (**Scheme 3**).
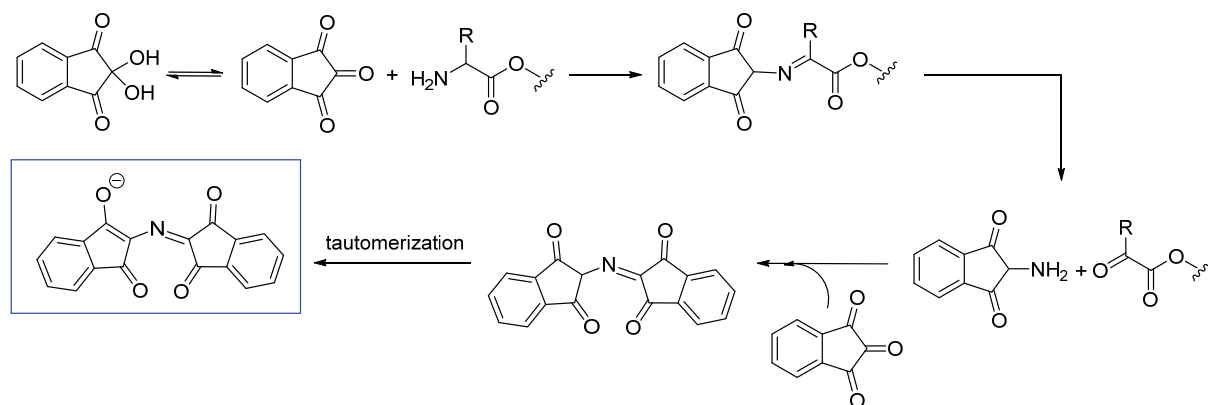
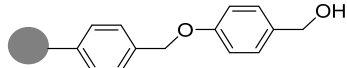**Scheme 3**: Reaction mechanism of the Kaiser Test with ninhydrin.
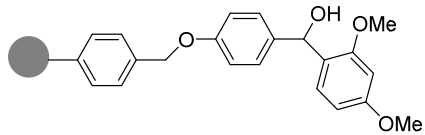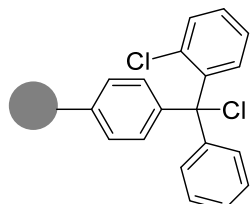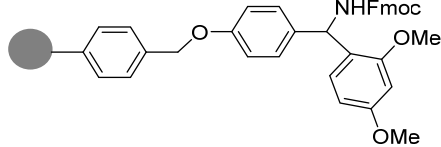
As solid phase, polystyrene containing 1% or 2% divinylbenzene is the most common core resin in solid-phase chemistry.[240] The resin particles are usually spherical beads of two different sizes of either 100-200 mesh (75-150 microns) or 200-400 mesh (35-75 microns). Nowadays, very versatile resins such as the ChemMatrix® resin is available, which has been recently proven useful for the synthesis of long and challenging peptides,[244] owed to its high loading (0.2-0.7 mmol/g) and to its good swelling capacity, even in water. The swelling of most resins is working best with CH_2Cl_2, superior to *N,N*-dimethylformamid (DMF). However, this swelling factor

gradually decreases in CH_2Cl_2 as the chain length of the peptide increases. In contrast, the swelling capacity of resin materials often increases for DMF treated resin upon chain elongation. In addition, CH_2Cl_2 is not compatible with Fmoc-SPPS, due to the formation of piperidine hydrochloride and it is further usually not a good solvent for Fmoc-amino acids and some coupling reagents.

In SPPS, linkers are attached to the resin that allow for amino acid coupling and chain elongation on the solid phase. The linker fused to the resin defines the chemistry, under which the final peptide cleavage from the resin is performed. A large number of linkers were developed in the past years,[241] whereas the most popular commercially available ones are cleaved under acidic conditions, yielding C-terminal carboxylic acid (e.g. Wang resin) or an amide (e.g. MBHA resin) (**Table 5**).

Table 5: Selection of popular resins used for SPPS.

resin name	resin structure	cleavage conditions	peptide product
Wang resin		90-95% TFA in CH_2Cl_2, 1-2 h	acid
HMPB resin		1-5% TFA in CH_2Cl_2, 5-10 min	acid
2-Chlorotrityl chloride resin		1-5% TFA in CH_2Cl_2, 1 min	acid
Rink amide resin		50% TFA in CH_2Cl_2	amide

The addition of coupling reagents is crucial to achieve activation of the α-carboxyl group of the amino acid in order to form an amide bond in the course of SPPS. *N,N'*-diisopropylcarbodiimide (DIC, **Scheme 4 A**) is often used as a coupling reagent, whereas partial racemization of the coupling product was observed with this agent. This happens if the formed *O*-acylisourea is cleaved off due to its high reactivity by two possible paths (**Scheme 4 B**). The mechanism involves the abstraction of the α-hydrogen from the α-carbon of the activated amino acid either by the formation of an enolic intermediate (path a) or via the formation of a 5-membered oxazolinone ring (path b). This problem is mainly solved by the addition of 1-hydroxybenzotriazole (HOBt), since the corresponding benzotriazolylester is more stable and less prone to racemization than the *O*-acylisourea. In order to further improve strategies to circumvent racemization during peptide synthesis, onium (aminium/uranium and phosphonium) salts were developed.[245] Widely used onium salts are *N*-[(1*H*-benzotriazol-1-yl)(dimethylamino)-methyleneb-*N*-methylmethanaminiumhexafluorophosphate *N*-oxide (HBTU), benzotriazol- 1-yl-*N*-oxy-tris(pyrrolidino)phosphonium hexafluorophosphate (PyBOP) and *N*-{(dimethylamino)-1H-1,2,3-triazolo [4,5-b]-pyridino-1-ylmethylene}-*N*-methylmethan-aminium hexa-fluorophosphate (HATU) (**Scheme 4 A**). The use of these agents goes hand in hand with application of HBTU in the presence of base, usually *N,N*-diisopropylethylamine (DIPEA) (**Scheme 4 C**).

A)

B)

C)
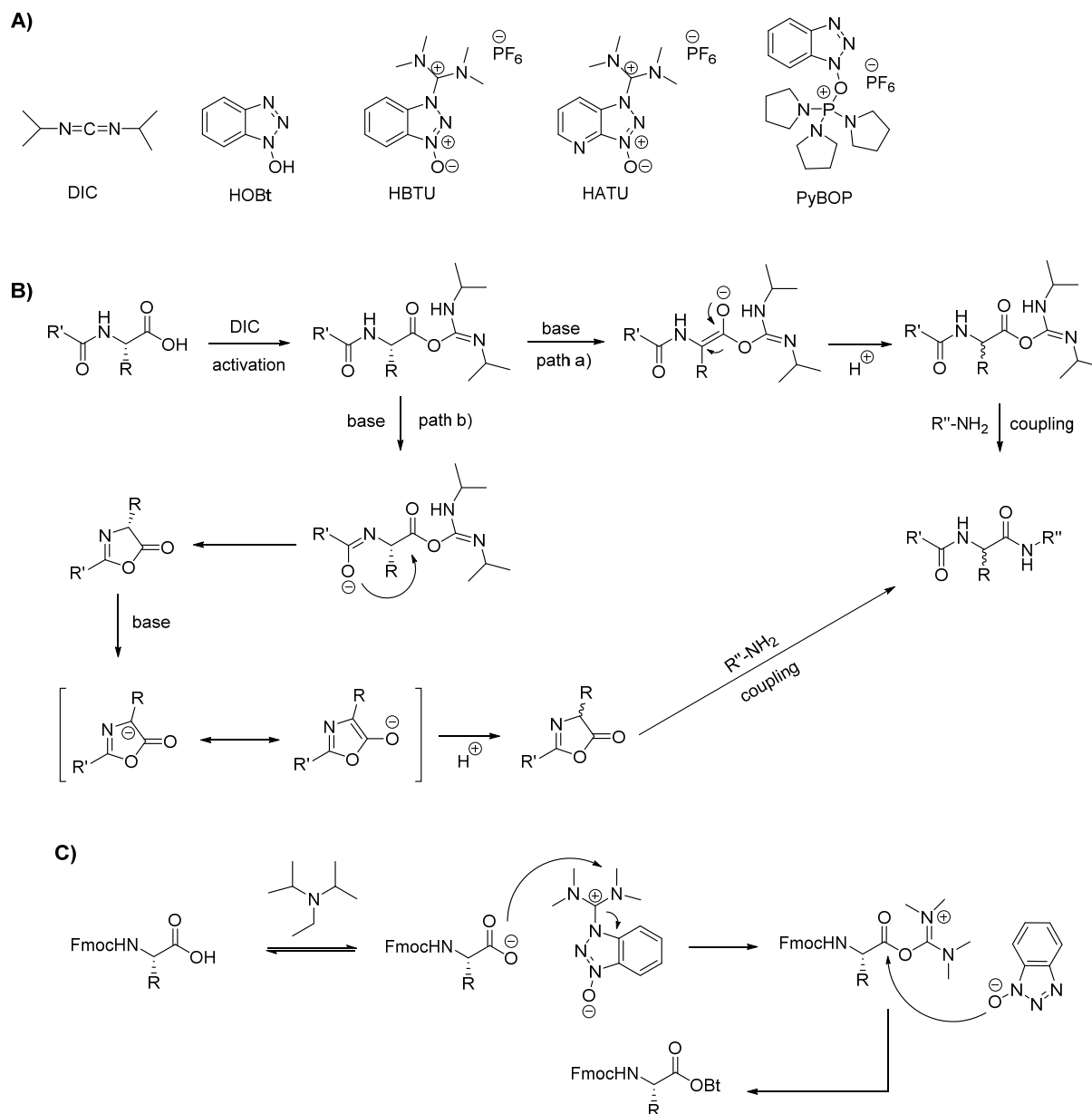
Scheme 4: **A**) Common coupling reagents applied in SPPS; **B**) reacemization pathways during SPPS coupling with DIC; **C**) mechanism of amino acid activation by HBTU.

2.3.2 Introduction of post-translationally modified amino acids by SPPS

PTMs describe covalent modifications of proteins, which occur during or after protein biosynthesis. The decoration of a protein by PTMs may have high impact on the protein function or the interaction between different proteins. For instance lipidation (palmitoylation, myristoylation) and prenylation (farnesylation, geranylation) induce membrane anchoring of proteins and thus contribute to vesicular transport and cell signaling, growth and differentiation.[246] Glycosylation is another important class of PTMs, which is involved in

extending protein half-life, targeting and cell-interactions. Phosphorylation is thought to be the most relevant PTM in nature, since it is by far the most abundant. It is for instance relevant for signal transduction.[240]

2.3.2.1 Phosphopeptides

Phosphorylation occurs on Thr, Tyr and Ser residues in proteins. In general, there are two different approaches to introduce phosphorylation to peptides during SPPS.[247]

(i)   Direct phosphorylation of the corresponding amino acids on the resin, after the synthesis is finished and the corresponding amino acid side chains are removed. In this course, orthogonal protecting groups are usually applied to selectively deprotect the residue of interest, leaving the remaining side chains of the other amino acids protected. Those orthogonal protecting groups for Thr, Ser and Tyr can be for instance the trityl group (deprotection with 1% TFA in CH_2Cl_2) or groups that can be for instance cleaved off by photolysis, such as the 4,5-dimethoxy-2-nitrobenzyl carbonyl group (Dmnb).

(ii) Introduction of phosphorylated amino acids by SPPS, which is often preferred over the firstly described method (i), since side-reactions such as Cys or Met oxidation can be avoided. Phosphorylated amino acids are usually provided as monobenzyl protected derivatives. This modification further enhances the feasibility of this approach due to higher acid and base stability of the incorporated phospho-amino acids. It is important to note that upon direct incorporation of phosphorylated amino acids, basic reaction conditions and thus side-reactions through $N{\rightarrow}O$ acyl migration can be avoided (**Scheme 5**).
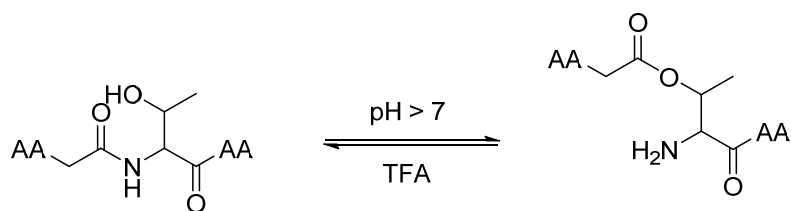
Scheme 5: Side-reaction that possibly occurs during the direct phosphorylation approach (i) upon an $N{\rightarrow}O$ acyl shift at elevated pH.

The minimal β-elemination of phosphate in Fmoc-SPPS makes strategy (ii) usually the method of choice. Also very recently, Lys phosphorylation, a rare post-translational modification, was achieved synthetically.[248] Special considerations are to be made in this case, due to the acid labile P-N bond. During SPPS, the Lys residue is introduced as an azide building block, which is converted to the corresponding phospho-Lys after the cleavage of the peptide from the resin by the Staudinger phosphite reaction. The phosphites applied were either protected by base-labile or photocleavable protecting groups and were thus compatible with the maintenance of the *P-N* bond (**Scheme 6 B**).
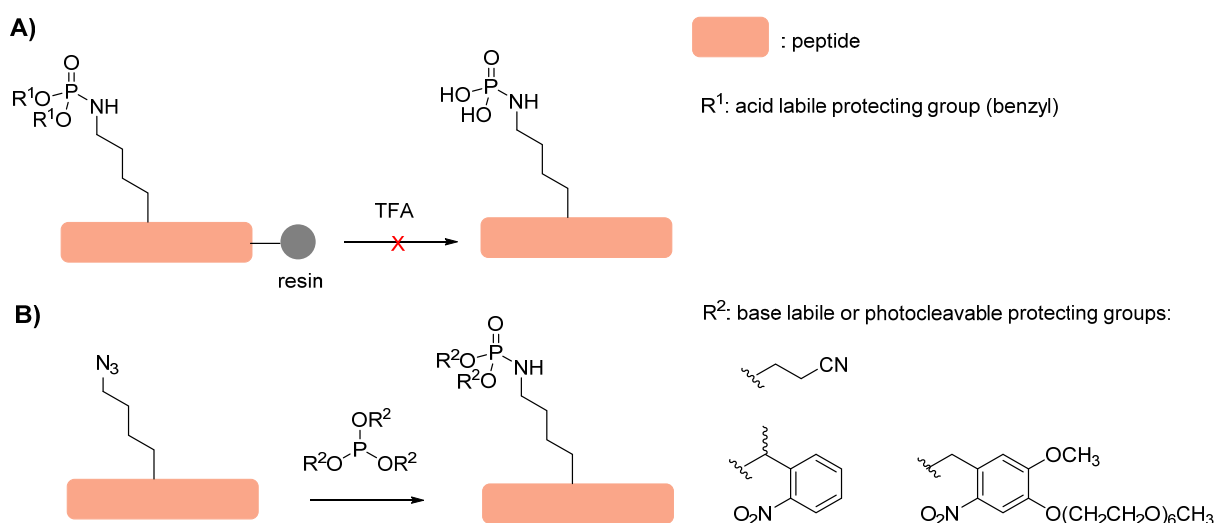
Scheme 6: **A**) Scheme of direct incorporation of phospho-Lys to peptides and subsequent acidic cleavage as a strategy not feasible to obtain the product; **B**) Staudinger Phosphite reaction between the azide of an ε-azido Lys and a substituted phosphite, protected by either base-labile protecting groups or by groups cleavable by photolysis.

While protein phosphorylation can occur on nine amino acids (Ser, Thr, Tyr, His, Lys, Arg, Asp, Glu, Cys), one has to say that by far the most discussed types of phosphorylation in literature are on Ser, Thr and Tyr residues.[249]

2.3.2.2 Glycopeptides

Glycosylation occurs on Asn (*N*-glycosylation), Ser or Thr (*O*-glycosylation), which can be performed on synthetic peptides after SPPS or by the introduction of glycosylated building blocks during SPPS.[250-252] On-resin glycosylation is often unfavorable owed to the fact that the glycosyl-moiety is attached to impure starting material. Convergent Ser or Thr glycosylation approaches require the use of activated sugars due to the rather low reactivity of the selectively deprotected side-chain hydroxyls. In case of direct peptide *N*-glycosylation, intramolecular aspartimide formation severely hampers the success of the reaction. To address this problem, a protocol was developed, which involved the emplacement of a pseudoproline motif, derived from Ser/Thr at the *n*+2 position relative to the Asn position (Lansbury aspartylation) (**Scheme 7 A**).[253, 254] The most commonly applied method, however, is the incorporation of glycosylated building blocks during SPPS (**Scheme 7 B**).[252] As the glycosidic bond of saccharides is acid labile and the sugars are also prone for β-elimination through basic treatment, the hydroxyl-groups are usually protected as esters, which minimizes the possible side-reaction occurring upon acidic treatment. The protected sugars are further stable to bases, which are usually applied to remove the Fmoc-group during SPPS (piperidine or 1,8-diazabicyclo[5.4.0]undec-7-en (DBU)). Usually, glycosylated building blocks are introduced to peptides during the chain elongation process with acetyl protection, which avoids side reactions on the free hydroxyl groups of the sugar and stabilizing it.
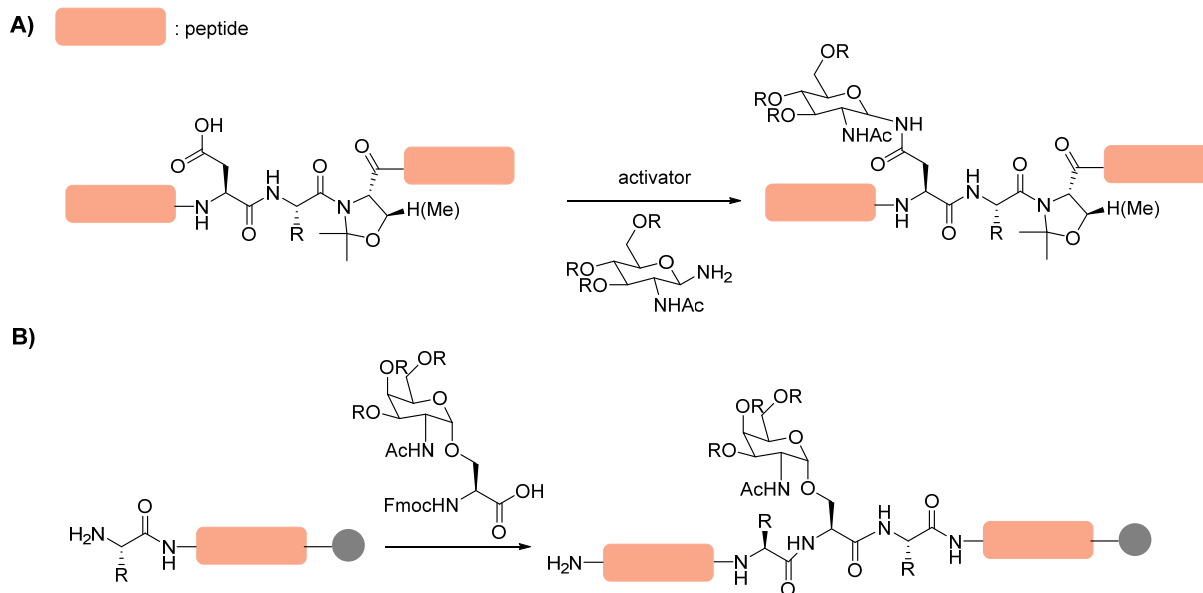
Scheme 7: **A**) Landsbury aspartylation facilitated by a pseudoproline motif for the convergent synthesis of *N*-linked glycopeptides; **B**) linear „cassette"-based approach to synthesize *O*-linked glycopeptides.

2.3.3 Native chemical ligation (NCL)

A common feature of most ligation strategies is that two molecules undergo a capture step that links two peptides with one another, which is followed by an irreversible intramolecular rearrangement.[8] This mechanism also takes place in a reaction termed native chemical ligation (NCL). A reversible thiol-thioester exchange between an electrophilic thioester at the C-terminus of the N-peptide and the nucleophilic thiol of a Cys residue located at the N-terminus of the C-peptide mediate this chemoselective capture step (**Scheme 8 A**). Noteworthy, internal Cys residues located in the interior of the peptide sequences do not interfere with the NCL reaction. This owes to the irreversible intramolecular *S,N*-acyl shift, which is favored due to a five-membered transition state (**Scheme 8 B**). The full-potential of this reaction was discovered by Stephen Kent and his coworkers in 1994, where the synthesis of interleukin 8 (IL-8) from two synthetic peptide fragments was reported.[255]
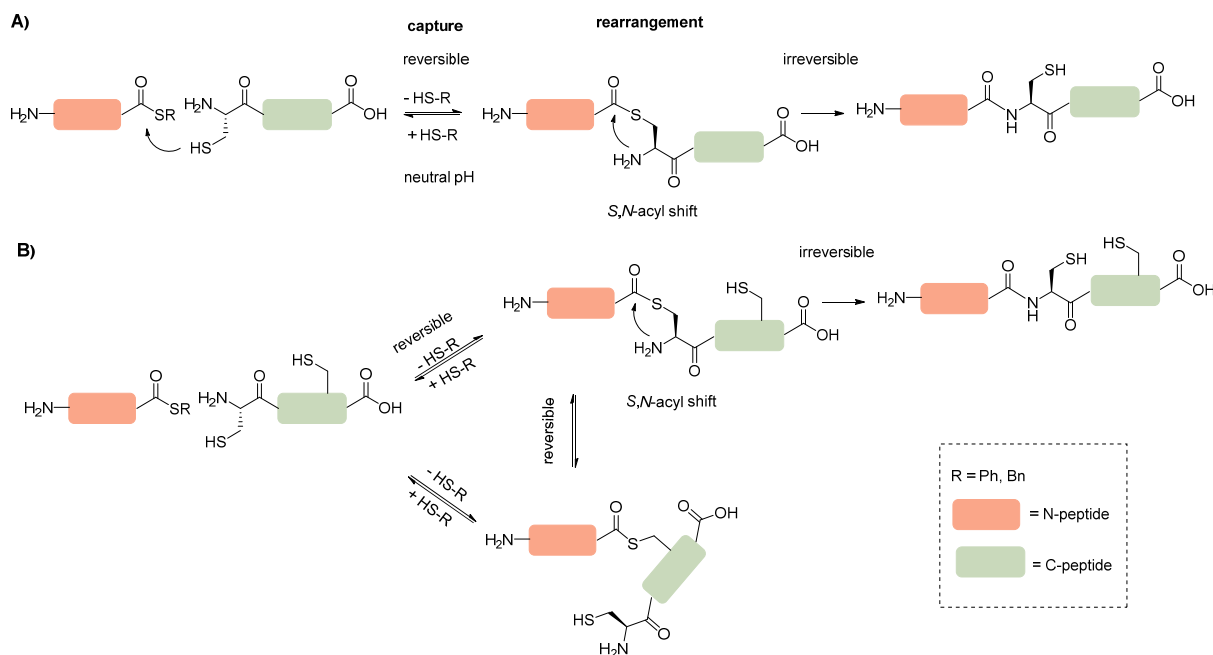
Scheme 8: The reaction of a native chemical ligation: **A)** mechanistic details; **B)** explanation for selectivity of C-terminal Cys peptides that undergo NCL reactions.
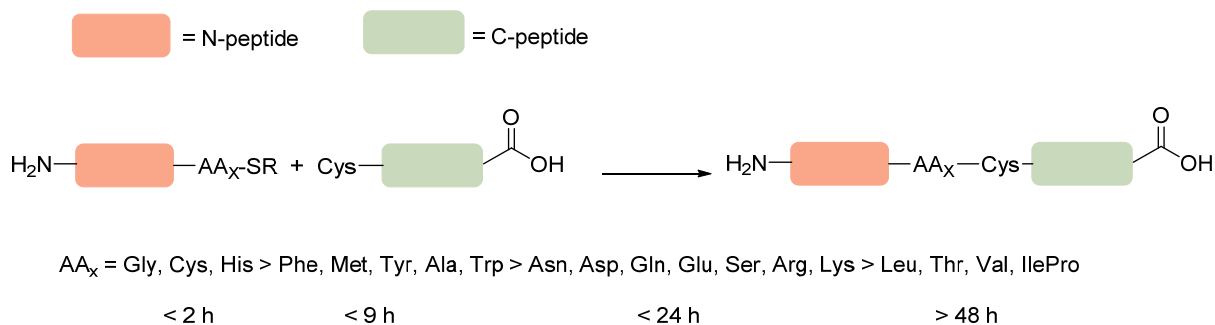
Up to this day, NCL derived peptides and proteins were successfully used in many different fields and helped to solve problems in the determination of structure-function relationships,[256] allowed novel protein design,[257] enabled NMR spectroscopy[258] and X-ray crystallography[259] of complex protein structures and helped to assign functions of post-translational modifications of proteins in dynamic biological processes.[260] Additionally, the ligation of peptides or proteins to other biomolecules such as peptide nucleic acid (PNA) or DNA is feasible by NCL. One major advantage of NCL reactions over other technologies are the mild reaction conditions, as they proceed at rather neutral pH in aqueous buffers. This is of outmost importance, as basic conditions would render residues containing amines such as Lys nucleophilic enough to attack thioesters and thus hamper NCL reactions with N-terminal Cys peptides. Moreover, thioesters are not stable under basic conditions. Also acidic conditions are unfavorable for NCL reactions, since the nucleophilicity of Cys is diminished and thioesters are stabilized to a higher extent as at neutral pH.[261, 262] The kinetics of NCL reactions are influenced by the C-terminal amino acid of the N-peptide bearing the thioester group, as Dawson and his co-workers have impressively demonstrated by a systematic study on a cassette of model peptides carrying each of the natural amino acids at this position (**Scheme 9**).[263]

= N-peptide   = C-peptide

H_2N—[N-peptide]—AA_X-SR + Cys—[C-peptide]—COOH $\longrightarrow$ H_2N—[N-peptide]—AA_X—Cys—[C-peptide]—COOH

AA_X = Gly, Cys, His > Phe, Met, Tyr, Ala, Trp > Asn, Asp, Gln, Glu, Ser, Arg, Lys > Leu, Thr, Val, IlePro

< 2 h   < 9 h   < 24 h   > 48 h

Scheme 9: Influence of C-terminal amino acids of the N-peptide on kinetics of NCL reactions.[263]

Their study impressively demonstrated the tremendous influence of the C-terminal amino acid of the N-peptide on the kinetics of the NCL reaction. The fastest NCL reaction was reported to occur when Gly is the thioester bearing amino acid, whereas the NCL does not reach completion when β-branched amino acids or proline was present in this position, even after 48 h. Other difficulties have been reported for Glu, Gln, Asp and Asn, if positioned at the C-terminus of the N-peptide.[264] The side-reactions reported were either thioester hydrolysis or β- and γ-linked ligation products, respectively (**Scheme 10**).[264]
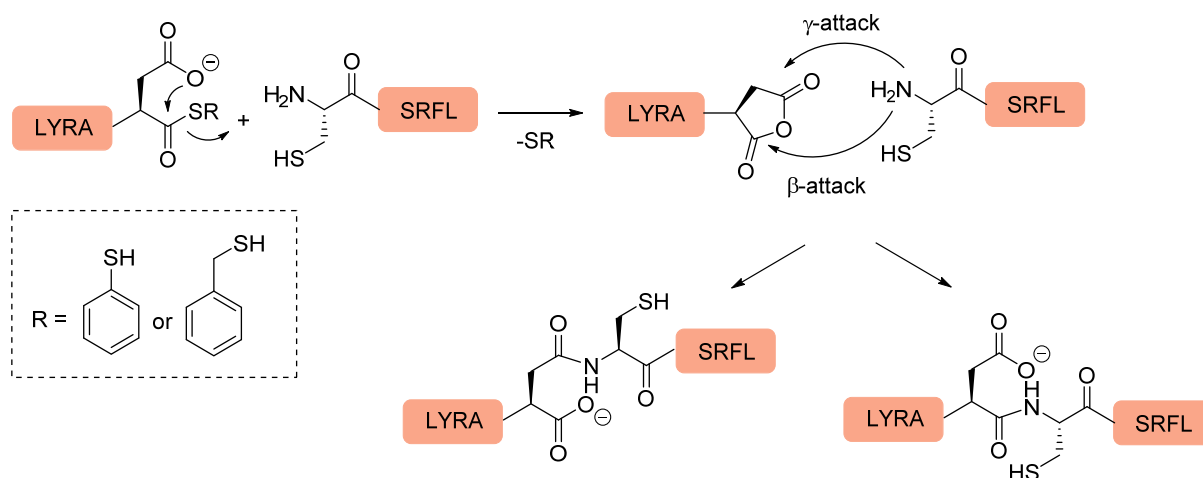
Scheme 10: Reaction scheme of the formation of a cyclized by-product derived from Asp thioesters. The five-membered ring can be opened again by nucleophiles such as amines, present at the N-terminus of peptides.[265]

Since these studies were published, a new thiol additive was discovered that seemed to solve many issues connected to this problem: 4-mercaptophenlyacetic acid (MPAA). This thiol additive was highly water-soluble, odorless and showed to significantly enhance the rate of NCL reactions and drive them toward completion within short times.[266] There has been a thorough investigation about the impact of MPAA on the formation of by-products during the course of NCL at Gln/Glu- or Asp/Asn-Cys junctions.[267] In the end of this study by Dang *et*

al, MPAA was able to sufficiently trigger NCL reactions for Gln, Glu and Asn thioester, but failed to do so for Asp thioesters due to high by-product formation (**Scheme 10**).

2.3.4 Methods to produce C-terminal thioester peptides for linear and convergent peptide and protein synthesis by NCL reactions

As C-peptides for NCL reactions merely require a N-terminal Cys, no further processing is needed. On the other hand, the synthesis of C-terminal thioester peptides of the NCL N-peptides requires special considerations, which led to the development of several protocols applicable in Fmoc- and Boc-based SPPS. The Boc-strategy requires HF to cleave peptides from the resin and is thus difficult and dangerous in handling, whereas high yielding procedures are reported (**Scheme 11 A**).[268] Moreover, Fmoc-based strategies are usually preferred, when glycol- or phosphopeptides are generated.

The application of Fmoc-strategies is more complicated due to the electrophilicity of the thioester functions, but due to the convenience of Fmoc-based SPPS, several strategies were developed that deliver C-terminal thioester peptides by this way (**Scheme 11 B-E**). For instance, the so called alkanesulfonamide "safety-catch" resin approach, in which the peptides are activated by diazomethane,[269] palladium-catalyzed allylation,[270] or by iodoaceto-nitrile[271, 272] to yield a secondary sulfonamide and further converted to thioesters by the addition of nucleophilic thiols (**Scheme 11 B**).[269, 273] In a final step, TFA treatment renders peptides ready for NCL reaction. Another common approach for the synthesis of thioesters makes use of the TGT[274] resin or the 2-chlorotritylresin,[275] which both are highly acid sensitive and allow cleavage of globally protected peptides from the resin by mild acid treatment (**Scheme 11 C**). The thioester is then generated in a subsequent step through C-terminal activation of the protected peptide in solution and coupling to a thiol. A final TFA treatment would also in this case generate thioester peptides.[276] A drawback of the method is the epimerization that can occur during the in-solution activation and thioesterification, which limits this approach mainly to peptides with a C-terminal Gly residue.[277] Another strategy to generate C-terminal peptide thioesters works by an ester-thioester rearrangement and employs a carboxy ethyl ester, which is equipped with a disulfide protected thiol in the β-position

(**Scheme 11 D**).[278] The synthesis of the peptide is carried out on the resin-bound S-protected β-mercapto-α-hydroxypropionic acid. Thiophenol is then added after cleavage, which deprotects the disulfide and triggers an intramolecular *O,S*-shift to render a thioester peptide. Further efforts toward thioester peptide synthesis were made by using a disulfide protected thiol in the β-position on phenylesters (**Scheme 11 E**). The reaction itself is performed in solution and starts with the corresponding ester, which is coupled to a protected peptide. Finally, a thiol is added in excess after the global deprotection by TFA, which induces an *O,S*-shift and thus the thiol thioester exchange.[279]
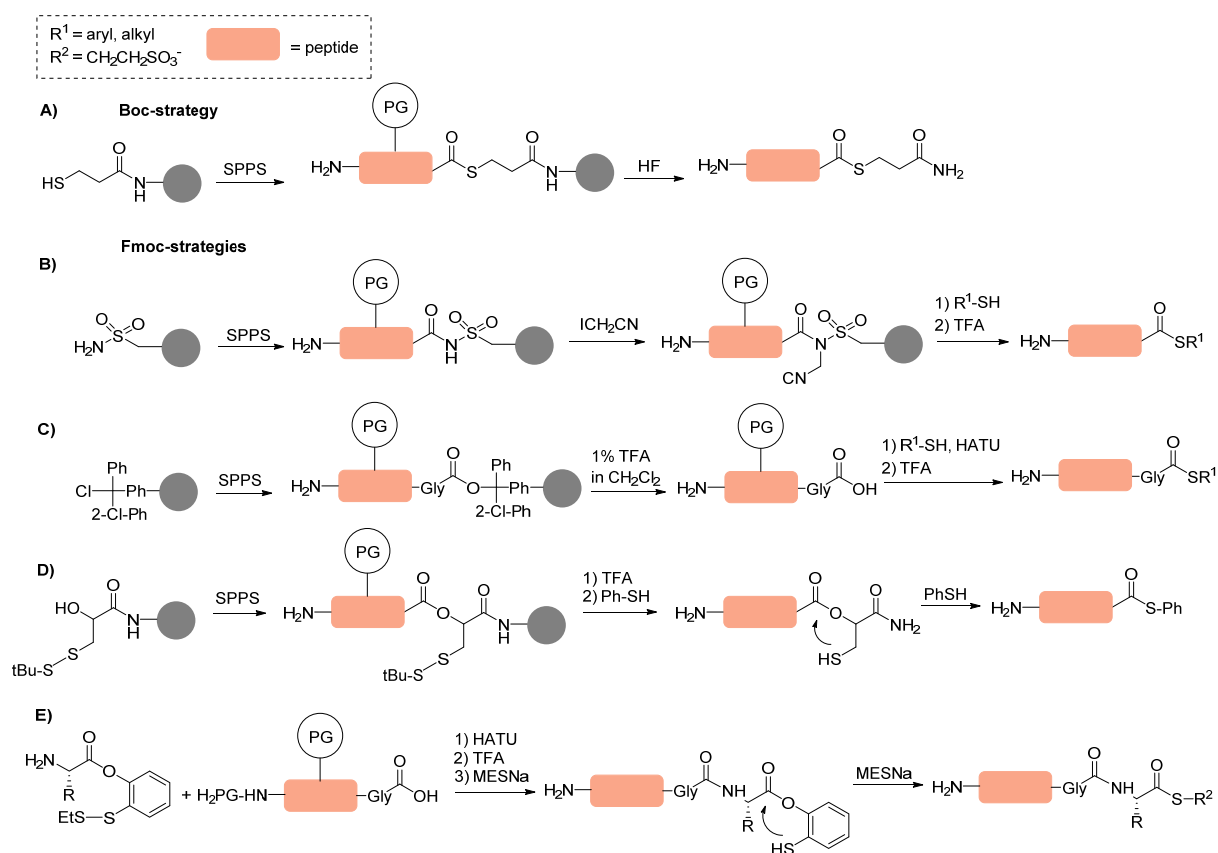
Scheme 11: Selected strategies for generating peptide thioesters.

Despite these efforts to facilitate synthesis of C-terminal peptide thioesters, their Fmoc-SPPS remains considerably more challenging than regular SPPS of the corresponding C-terminal acids or amides. Blanco-Canosa *et al.* have tackled this problem and developed an alternative approach for the Fmoc-synthesis of peptides for use in NCLs.[280] Their approach is based on the formation of a C-terminal *N*-acylurea functionality, which is a mild acylating agent that was already previously used in SPPS.[281, 282] Blanco-Canosa and Phil Dawson have found that *o*-aminoanilides are stable synthetic intermediates that are sufficiently transformed into

51

aromatic *N*-acylurea groups by *p*-nitrophenylchloroformate and treatment with DIPEA base, following chain assembly (**Scheme 12**). The *N*-acyl-benzimidazolinone (Nbz) moiety functions in their proposed reaction scheme as a leaving group. The resulting resin-bound acylurea peptide can be deprotected and cleaved from the resin using TFA from acid labile linkers under standard conditions. The resulting mildly activated Nbz-peptide can be easily handled under acidic conditions and HPLC purification. However, despite their relative stability under acidic pH, these thioester precursors can undergo thioesterification under neutral pH by the addition of thiols and be used for *in situ* NCL, being compatible with all other peptide side-chain functionalities.
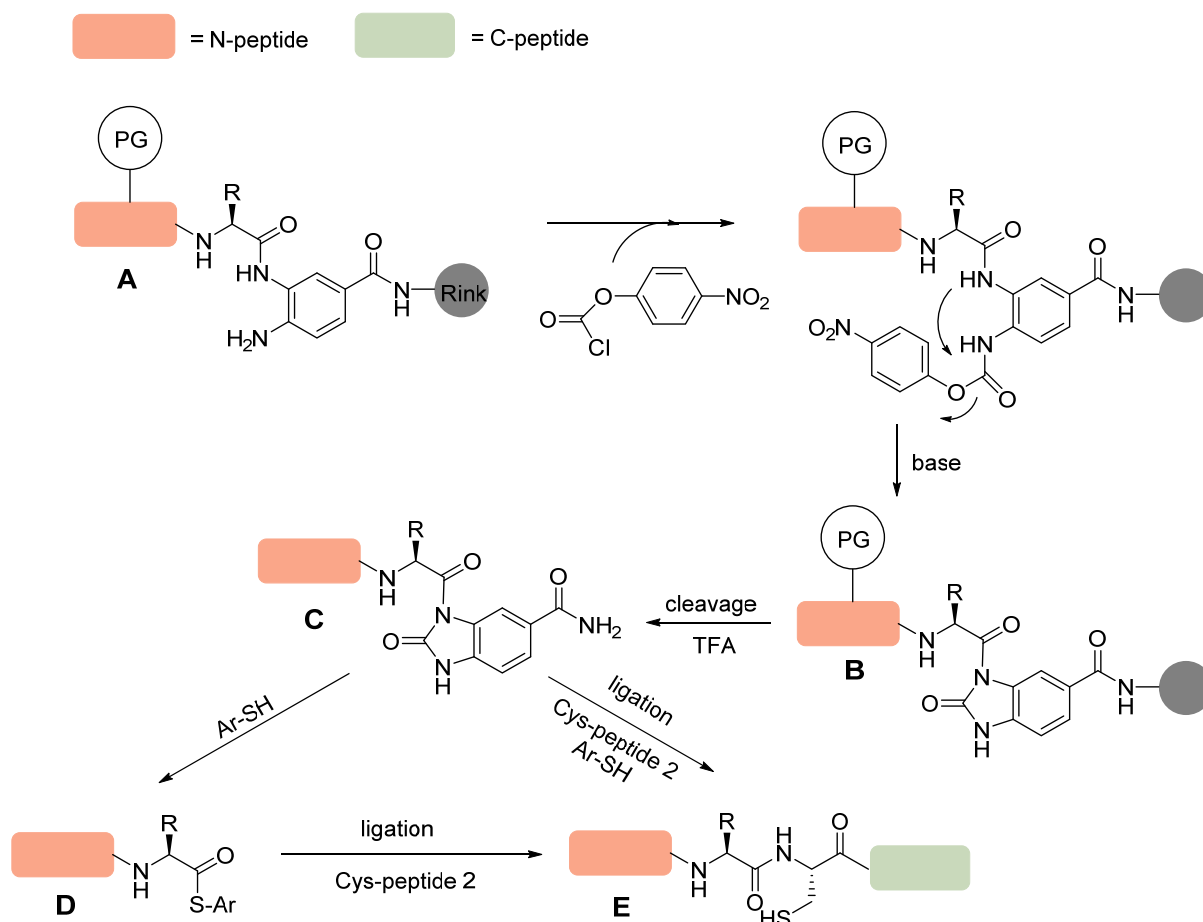
Scheme 12: Scheme of synthetic thioester precursor peptides according to Blanco-Canosa *et al.*[280] After Fmoc-SPPS, the aminoanilide **A** gets acylated and cylized by the addition of *p*-nitrohenylchloroformate and base to yield the resin-bound acylurea peptide **B**. Afterward, the peptide is deprotected and cleaved off the resin by TFA, providing free peptide **C**, which can be further transformed to the thioester peptide **D** upon thiol addition and used for NCL. Peptide **C** can also directly get exposed to Cys-peptide in the presence of aryl thiol (Ar-SH) to undergo *in situ* NCL to form the ligation product **E**.

Despite this great effort, researchers encountered problems when using this strategy, if strong coupling conditions were applied such as extended coupling times and strong coupling reagents such as HATU. Moreover, if Gly was the first amino acid coupled, double coupling to both free amine groups of compound **A** (**Scheme 12**) was observed. Thus, Hamentha *et al.* have developed an orthogonal protection strategy to protect one of the two accessible amines, thereby avoiding side-reactions through double modification (**Scheme 13**).[283]
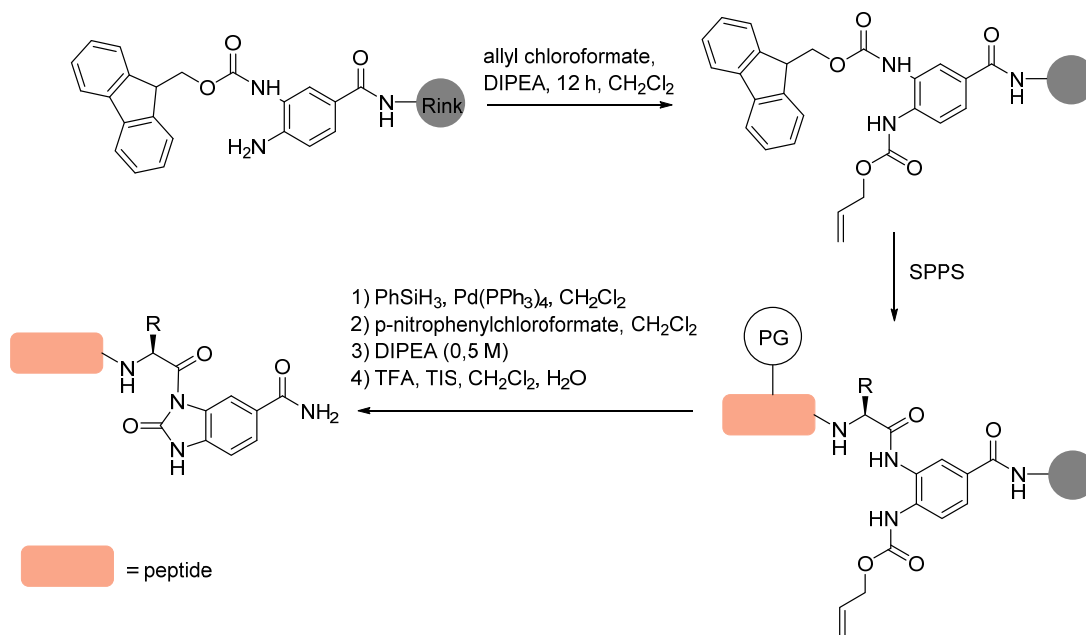
Scheme 13: Synthesis of a Nbz-activated peptide by orthogonal allyl protection of an amino-group, thus preventing double modification. A final allyl deprotection, activation and TFA treatment renders the activated peptide for further use in NCL.[283]

Another facile route was recently introduced by Blanco-Canosa *et al*, in which limitations, such as diacylated products that cannot be cylized into *N*-acylurea peptides, are also abolished. They have introduced a novel *N*-acylurea linker equipped with an *o*-amino(methyl)aniline (MeDbz) moiety, thus enabling a more robust peptide assembly.[284] They have demonstrated the generality of their approach by synthesizing a penta-Gly peptide under different SPPS conditions including microwave assisted SPPS and heating up to 90°C, which yielded the desired *N*-acyl-*N'*-methylacylurea (MeNbz) product (**Scheme 14**).
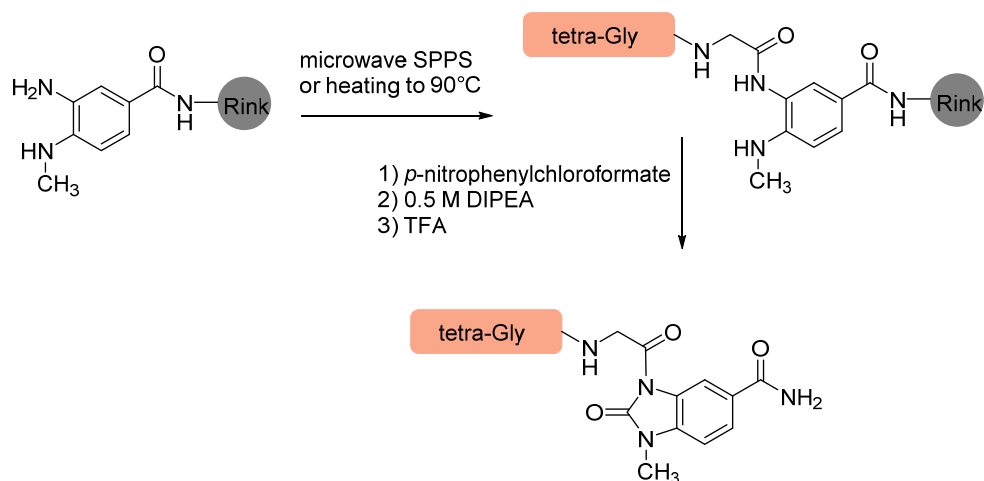
Scheme 14: Improved synthesis of thioester precursor protein by using *o*-amino(methyl)aniline (MeDbz).[284]

This approach (**Scheme 14**) has the advantage over the previously decribed technique (**Scheme 13**) that no Alloc-deprotection has to be performed, thus saving an additional step in the synthesis pathway.

Another ground-laying work was introduced by Fang *et al*, in which they describe the ligation of peptide hydrazides as a complementary method to NCL.[285] In their method, a chemoselective reaction between a C-terminal peptide hydrazide and a N-terminal Cys-peptide is described. It is noteworthy that peptide hydrazides can be readily prepared by Fmoc-SPPS and upon oxidation transformed to azides to undergo thiolysis (**Scheme 15**).
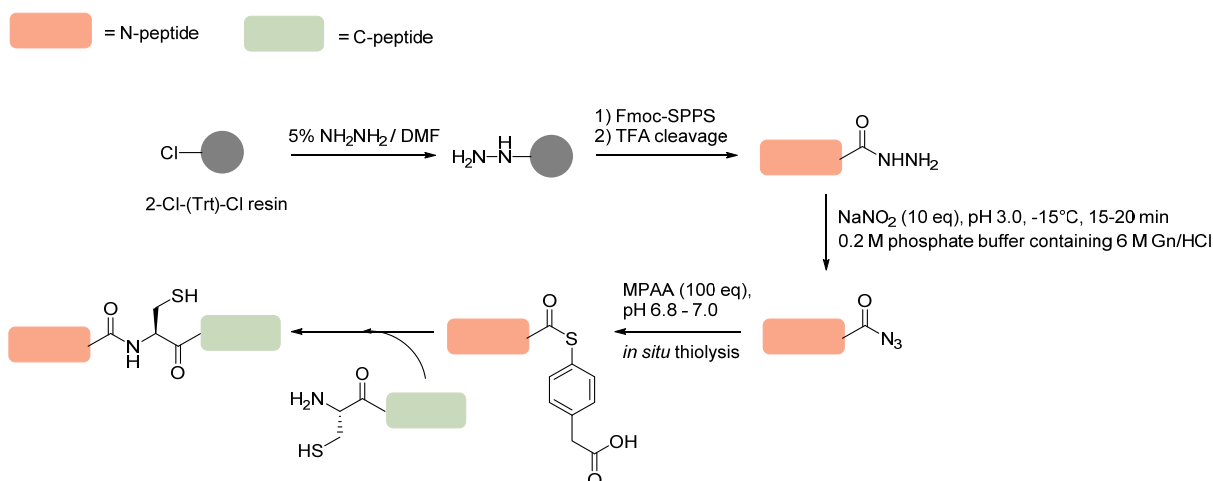
Scheme 15: General scheme for the ligation between a Cys-peptide and peptide hydrazides, starting from the preparation of hydrazide resin from commercially available 2-Cl-(Trt)-Cl resin, followed by standard SPPS, hydrazide oxidation to an azide by the addition of sodium nitrite and *in situ* thiolysis.

This so called "Liu protocol" is nowadays widely applied, especially since it allows for convenient sequential ligations of many peptide fragments by the same method (**Scheme 16**).
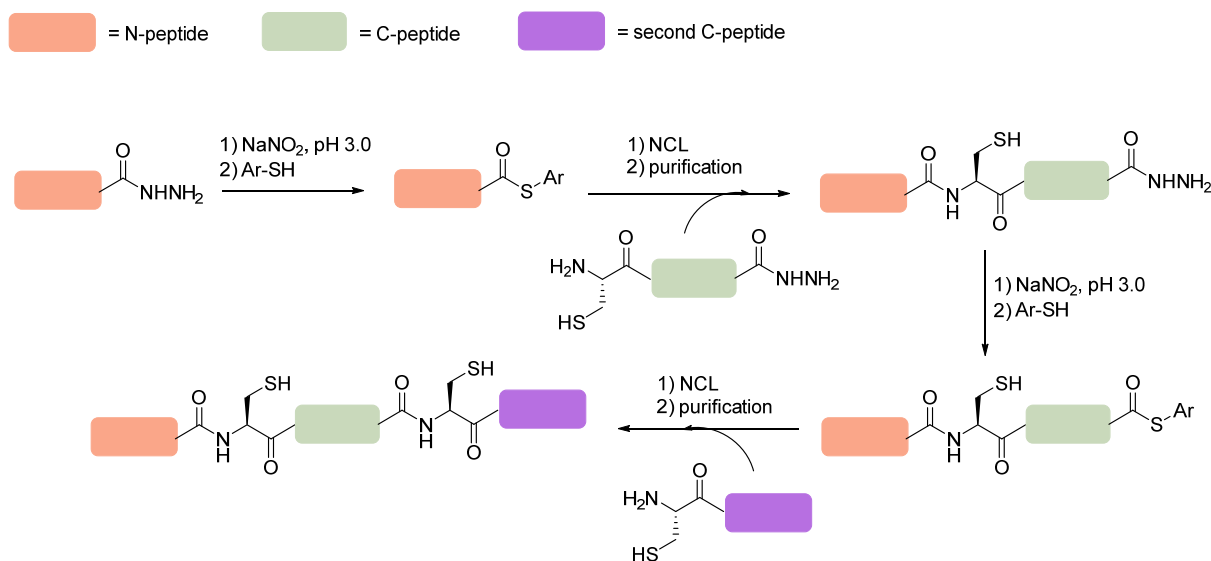
Scheme 16: Synthetic route to prepare peptides by sequential ligations according to the previously established hydrazide protocol.[286]

The method has also certain disadvantages, as oxidation of methionine may occur if the cooling is not carried out properly. Moreover, the "Liu protocol" is not applicable with thiazolidine protected Cys, which makes an additional Thz-protection necessary (**Scheme 17**).[287] Here, the 2-(tertbutyldisulfanyl)ethyloxycarbonyl (Tbeoc) has to be used to protect the amine function of the Thz group.
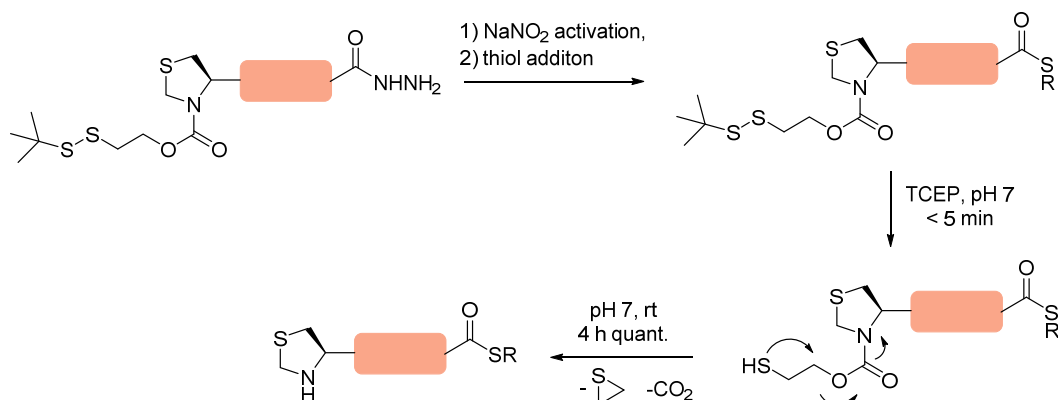
Scheme 17: Application of the Liu protocol with Tbeoc protection of the thiazolidine group.

In "convergent synthesis of proteins", two halves of the target sequence are prepared from multiple peptide segments and become ligated in a final step to yield the full-length peptide chain. This strategy was first applied by coworkers of the Kent lab, where they introduced the

so called "kinetically controlled ligation".[288] In their approach, Cys residues that are not supposed to react, were temporarily protected as thiazoline, which can be deprotected if required to Cys by the addition of 0.2 M methoxyamine hydrochloride at pH 4, thus not influencing other functional groups.[289] In their study, Bang *et al.* took advantage of the fact that aryl-thioesters are much more reactive than alkyl-thioesters, thus allowing a stepwise ligation process in the absence of excess thiols.

They have impressively demonstrated the strength of their approach by the fully convergent synthesis of crambin from six peptide fragments.
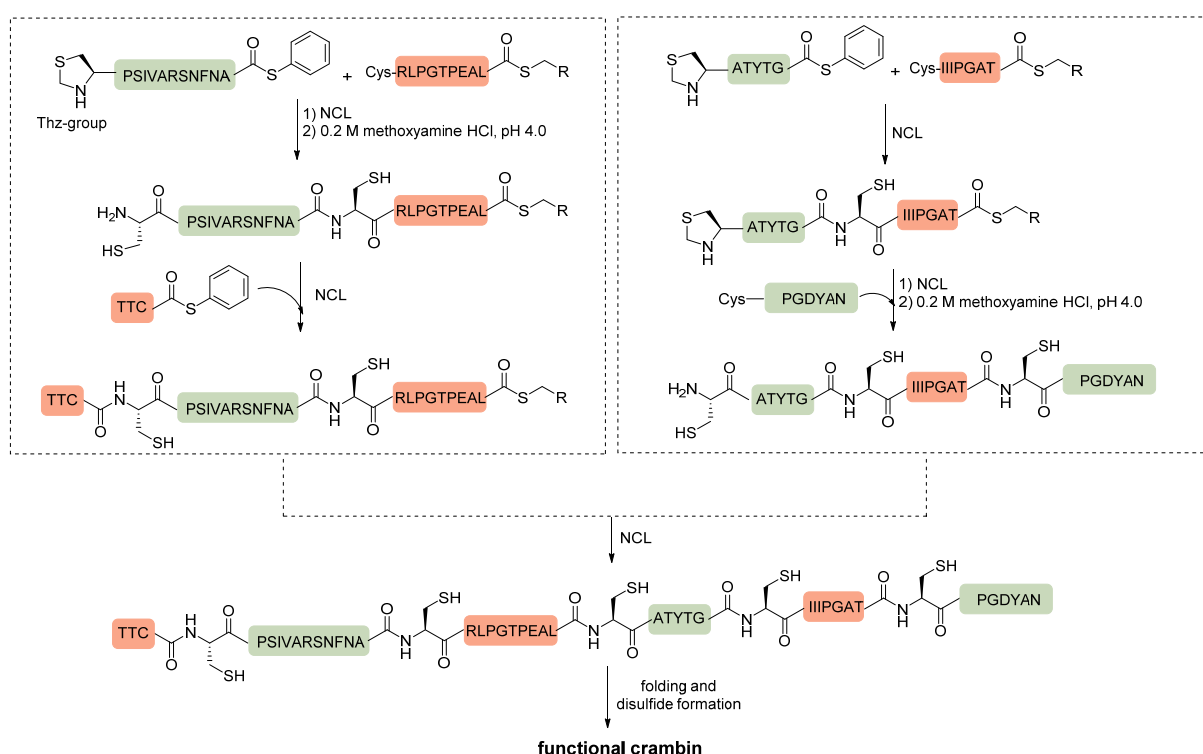
Scheme 18: Convergent synthesis of the protein crambin from six peptide fragments. The box on the left shows the kinetically controlled synthesis of the N-terminal portion of crambin through NCLs from C- to N-direction. The box on the right shows the kinetically controlled ligation of the C-terminal portion of the protein in N- to C-direction.

The described method has the drawback that isolated aryl-thioesters are required, which are difficult in handling due to their ability to hydrolyze. Therefore, so called latent thioesters or stable thioester precursors as described in the Liu protocol are often preferred over isolated aryl-thiols.

Another prominent method to produce such stable thioester surrogates was provided by Melnyk and his coworkers, introducing their bis(2-sulfanylethyl)amino (SEA) ligation.[290] They

demonstrated that the SEA group can be either provided as SEA[off] as an oxidized form, not directly reacting in NCL reactions, or as SEA[on] in the reduced form, forming a thioester, which can participate under NCL conditions (**Scheme 19**).
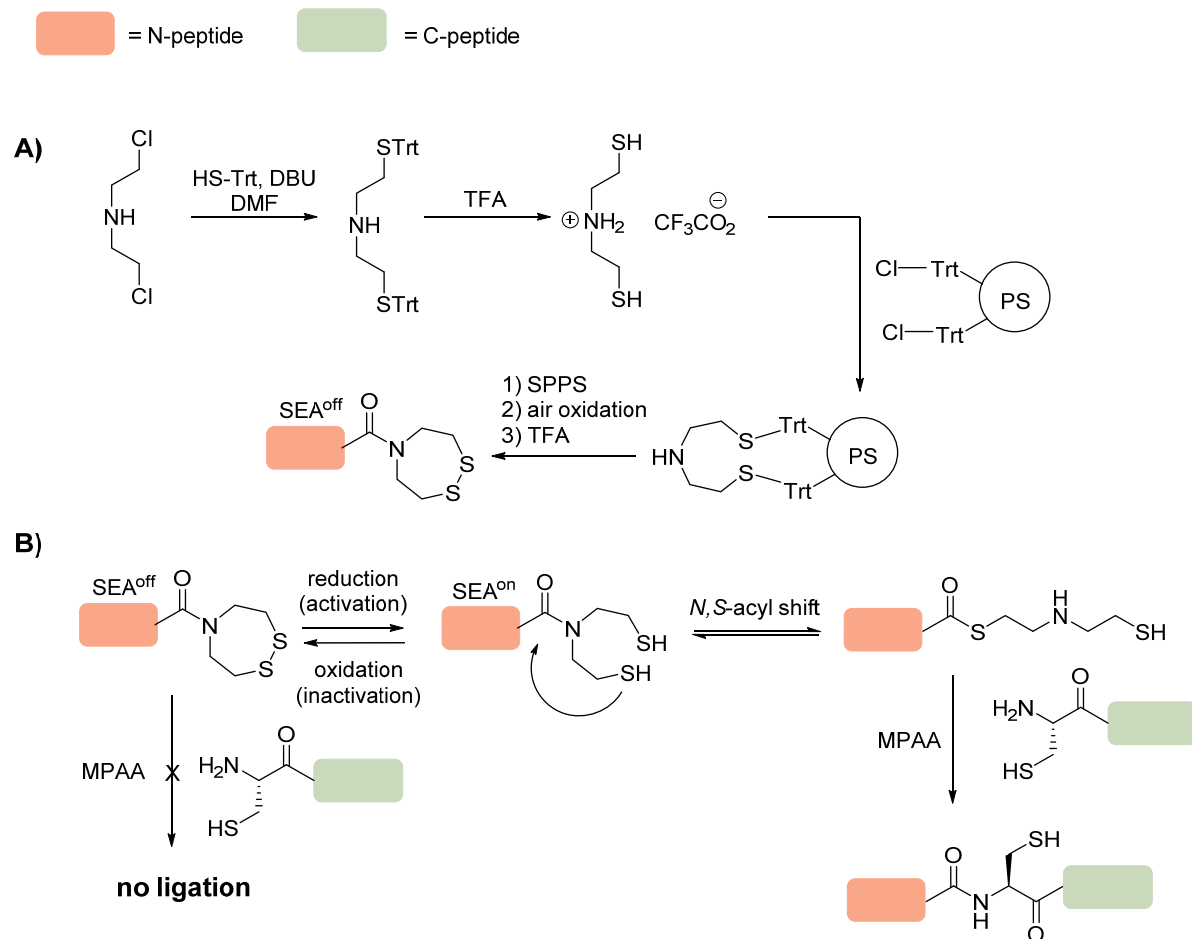
Scheme 19: **A)** Synthesis of the peptide thioester precursor SEA[off]; **B)** representation of the bis(2-sulfanylethyl)amido native chemical ligation (SEA ligation) and the SEA[on/off] concept.[290, 291]

2.3.5 N-terminal Cys surrogates and post ligation desulfurization chemistry

Originally, NCL reactions rely on a peptide bearing an N-terminal Cys residue. However, Cys is an amino acid with a relatively low abundance (1.1%) in naturally occurring proteins, strongly hampering the generality of the approach when it comes to spotting disconnections in a certain protein target. In consequence, researchers put considerable efforts into the development of N-terminal Cys surrogates that can extend the applicability of the NCL approach, whereas native amino acids are to remain at the ligation junction after the NCL reaction. Thus, in the early 2000's there have been several examples of removable auxiliaries

in the ligation process of assembling peptides and proteins.[292] Here, a thiol containing auxiliary is placed in proximity to the N-terminus of a C-peptide, which reacts with a thioester in a rearrangement similar to Cys residues in NCL. A final chemical transformation furnishes the desired native peptide or protein (**Scheme 20 A**). In a subsequent step, the auxiliary can be removed under conditions that vary with the auxiliary used (**Scheme 20 B**).
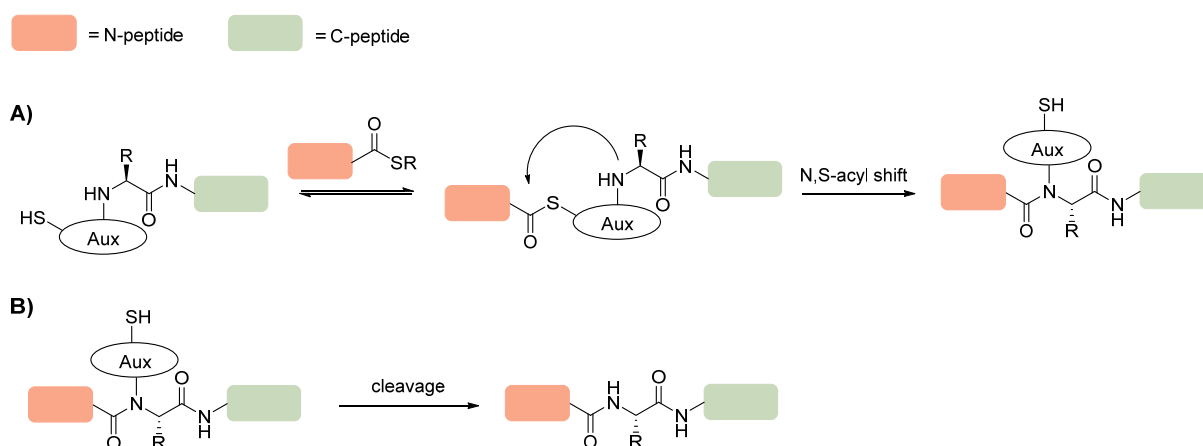
Scheme 20; **A)** General scheme of auxiliary mediated ligation of two peptides; **B)** removal of the auxiliary based on reducing conditions with Zn,[293] HF or TFA/TMSBr,[294] by light cleavage[295, 296] or by the addition of TCEP (morpholine and 40°C),[297] depending on the auxiliary used.[298]

Nevertheless, challenges concerning auxiliary directed NCL reactions remained due to high synthetic efforts, harsh auxiliary cleavage conditions and often low yields.[236]

Therefore, alternative approaches evolved that made use of ligation-desulfurization chemistry, which was first demonstrated by Yan and Dawson through a reductive desulfurization of Cys rendering native Ala at the ligation site.[299] As this method relies on the presence of Raney Nickel, unspecific adsorption to the catalyst appeared problematic and side-reactions such as thioether desulfurizations were observed. Thus, another homogeneous method was developed, which relied on a radical-initiated mechanism.[300] The latter method was developed by Wan and Danishefsky and employed a metal-free radical desulfurization protocol using the water soluble radical initiator 2,2'-azobis[2-(2-imidazolin-2-yl)propane]dihydrochloride (VA-044) in the presence of tris(2-carboxyethyl)phosphine (TCEP) and t-BuSH (**Scheme 21**).

A)

B)

(n = 1 or 2, R^1SH = Cys, R^2SH = t-BuSH
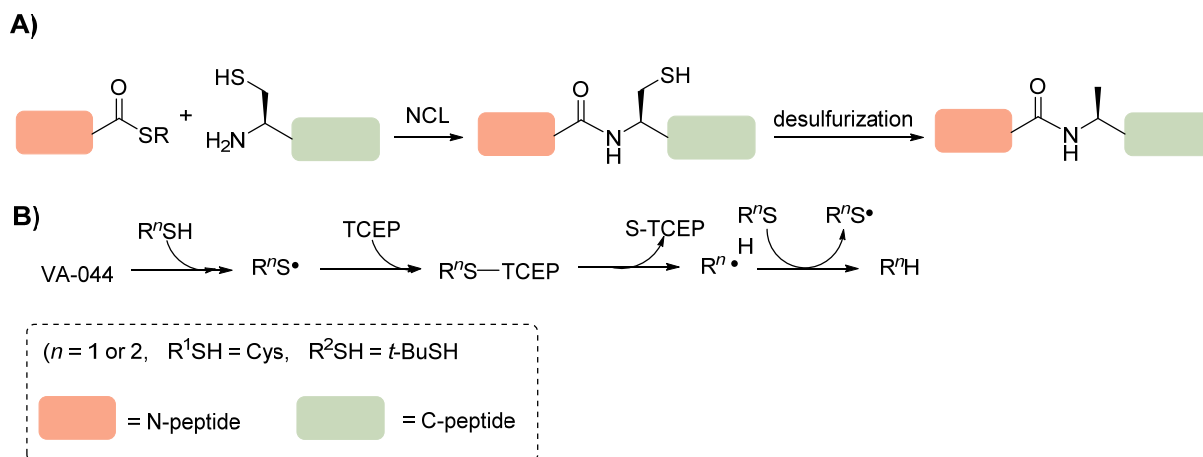
■ = N-peptide   ■ = C-peptide

Scheme 21: **A)** NCL reaction between a thioester peptide and a peptide bearing an N-terminal Cys residue, followed by desulfurization, furnishing an Ala residue at the ligation junction; **B)** proposed mechanism for the radical initiated homogeneous desulfurization.[301]

These desulfurization protocols enabled scientists to carry out ligations at Ala junctions by replacing a natural Ala residue by Cys, whereas a final chemical work-up delivered the native Ala. This discovery has fueled a whole new field of employing unnatural amino acid derivatives bearing suitable thiol auxiliaries in ligation-desulfurization chemistry.[299] A first example was provided by the preparation of β-thiol Phe, which was used for NCL and underwent a post ligation desulfurization.[302] Herein after, a whole toolbox of different thiolated amino acids was developed that can be used in NCL reactions and yield natural amino acids upon desulfurization, reviewed by Malins and Payne (**Figure 12**).[236]

A)

| Phe | Val | Arg | Leu | Asp |

B)

| Val | Lys | Thr | Gln | Glu |

C)

| Lys | Pro | Trp |
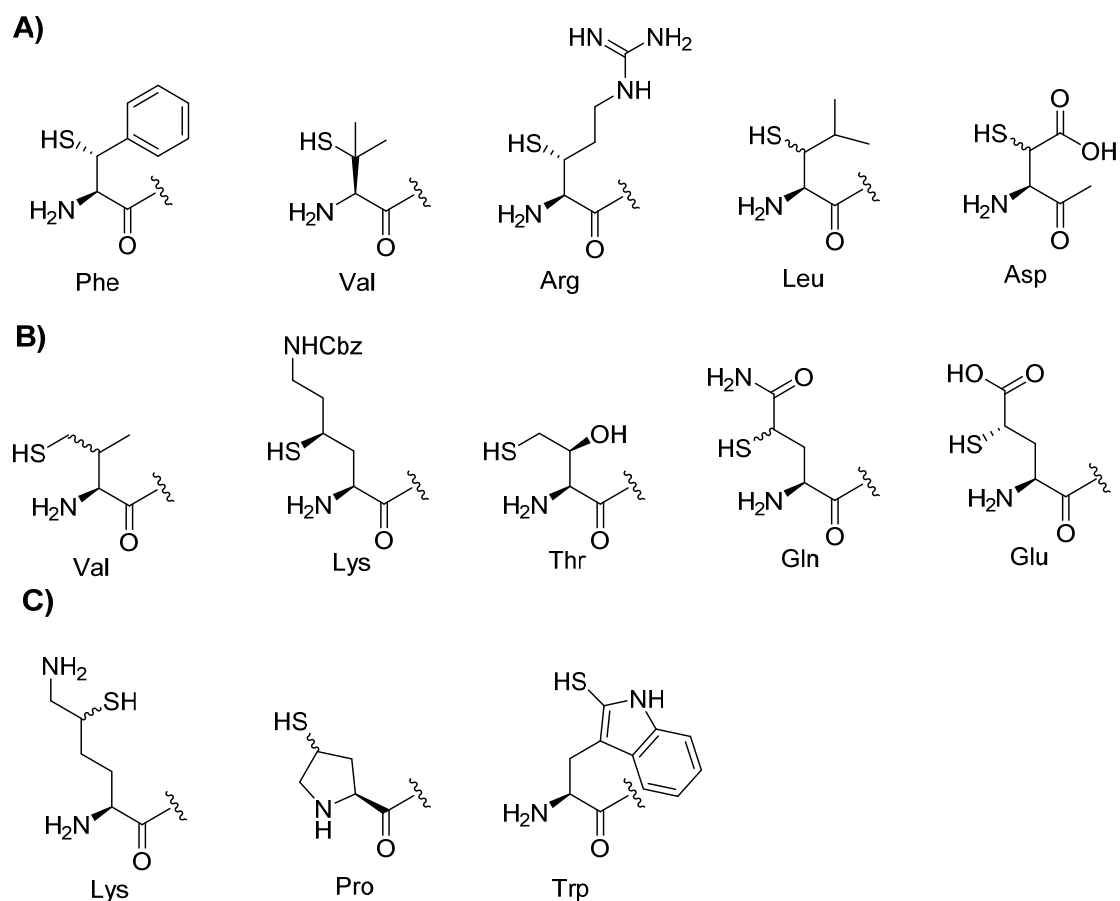
Figure 12: Cys surrogates that have been developed and employed in NCL reactions. **A)** β-thiol amino acids; **B)** γ-thiol amino acids; **C)** other thiol derived amino acids.

Noteworthy, such thiolated amino acids exhibit increased rates of reaction in comparison to NCLs mediated by auxiliaries, owing in part to decreased steric bulk at the ligation junction and the ability to proceed primarily through 5-membered (for β-thiol derivatives) or 6-membered (for γ-thiol derivatives) ring intermediates in the S,N-acyl transfer step. Such surrogates have enabled researchers to generate complex peptide and protein targets such as human parathyroid hormone,[303] a mucin 1 (MUC1) glycopeptide oligomere[304] and ubiquitination of Lys side-chains.[305] But on the downside, these surrogates cannot be conveniently incorporated into expressed sequences, thus limiting their application.

One major drawback of desulfurization chemistry is the lack for selectivity, as the employment of this reaction will desulfurize all unprotected Cys or Cys-surrogate residues. In consequence, those native inner-sequence Cys residues that are not wanted to be converted to Ala need to be protected, as they are often crucial for protein folding and function. A possible protecting group for Cys residues that withstand desulfurization conditions is the acetamidomethyl (Acm)

group, as demonstrated by Kent *et al.*[306] This Acm protecting group is removed after SPPS through treatment with I_2 or Hg (II).

Another possible solution to the problem of unselective desulfurization is offered by the use of selenocysteine (Sec), which is able to participate in NCLs and can be chemoselectively deselenized in the presence of unprotected Cys residues.[307] The deselenization takes place at room temperature in the presence of TCEP and dithiotreitol (DTT) and is thought to proceed comparable to the radical initiated desulfurization of Cys in the presence of the radical initiator VA-044 and TCEP (**Scheme 22 A**). The reason for the selectivity of Sec deselenization over Cys desulfurization may be attributed to the preferential formation of selenium-centered radicals and the weakness of the selenium-carbon bond, but a detailed mechanism has not been reported yet. This precedence led to the development of two additional selenol-derived amino acid derivatives, namely γ-selenoproline[308] and β-selenolphenylalanine (**Scheme 22 B**).[309]

A)

B)
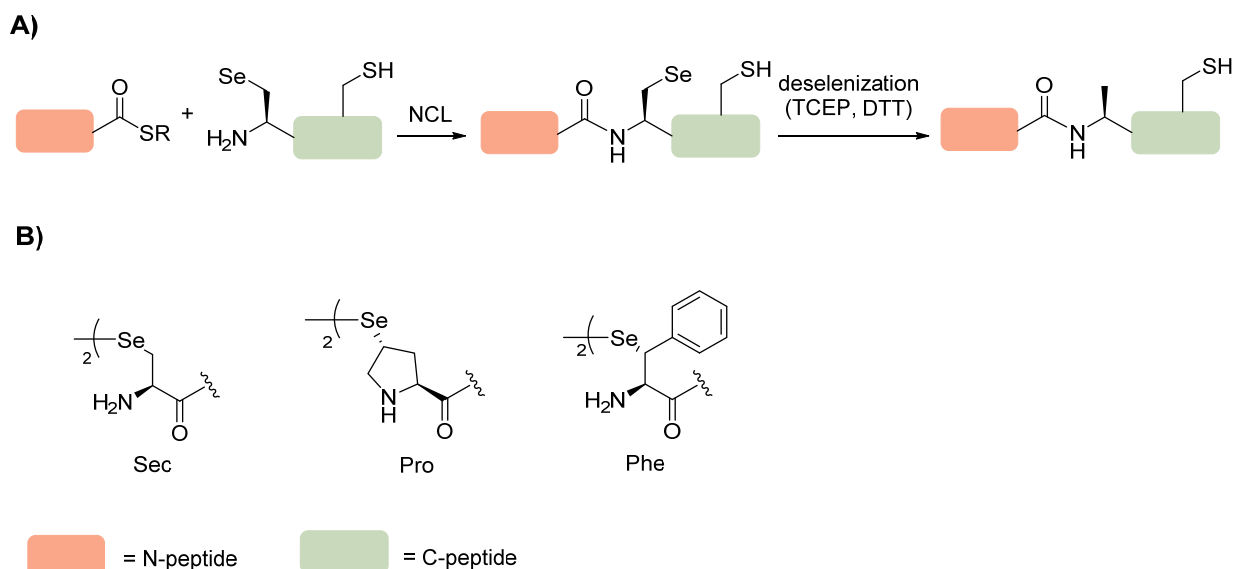
Scheme 22: **A)** Chemoselective ligation between a peptide bearing a C-terminal thioester and another peptide equipped with an N-terminal Sec residue; **B)** other selenol-derived amino acids in their protected form as diselenide, as such they can be used in SPPS.

Additionally, Sec ligations can also be carried out at Ser ligation sites, as Sec can be converted post-ligation to Ser through the addition of potassium peroxymonosulfate (oxone), as demonstrated by Malins *et al.*[310] In disfavor of the use of selenium amino acids is the difficulty to incorporate them conveniently by expression into proteins and that they are time-intensive to produce. Moreover, owing to the low redox potential of SEC (-381 mV), selenopeptides exist

as the corresponding diselenide dimers under standard conditions, which do not participate in NCL reactions in the absence of an external reductant such as additional aryl-thiol additives, which serve to generate reactive selenol compounds.[311] A possible solution to this problem was recently presented by Mitchell *et al*, where selenocysteine-selenoester ligations were probed and found to work highly efficient, even at sterically hindered ligation junctions without need of any further reductive additives.[311] They were able to obtain ligation yields ranging between 53% and 93%, depending on the C-terminal amino acid of the N-peptide within minutes of reaction time, thus paving the way for further applications of selenocysteine in NCL reactions. The mechanism by which the ligation takes place is yet not certainly clarified, but when using Sec instead of Cys or Cys-surrogates, one faces the challenge of diselenide formation. In addition, inter- or intramolecular mixed forms of oxidized forms between Sec and Cys can occur, possibly lowering the available effective concentration of selenocysteine ready for ligations. Moreover, the generation of selenoesters at the C-terminal site of the N-peptide is carried out through off-resin activation and selenoesterification, which may lead to racemization through mechanisms described in **Scheme 4 B**.

2.3.6 The application of new thiol derivatives in NCL reactions – toward one-pot procedures of NCL and desulfurization

On a regular basis, thioester peptides are prepared as alkyl thioesters, since they are relatively stable and they can be easily stored for longer times. Alkyl thioesters are quite unreactive in NCLs and require treatment with an excess exogenous aryl thiol, generating a more reactive aryl thioester *in situ*. In this context, thiol additives enable fine-tuning of thioester reactivity, thus influencing the reaction rate and scope. This observation lays the fundament of kinetically controlled ligations, described in section **2.3.4**.[288]

In the course of an extensive screening for thiol additives suitable for NCL reactions, Johnson and Kent identified the water-soluble aryl thiol 4-mercaptopehnylacetic acid (MPAA), which provides for enhanced reactivity over other thiols usually employed in NCL reactions.[312] Despite the improvements for NCL reactions reported for MPAA, aryl thiol additives hamper one-pot procedures for NCL and desulfurization due to competitive desulfurization of aryl thiols

over alkyl-Cys thiols. In other words, the ability of aryl thiols to function as a radical scavenger complicates the homogeneous radical initiated desulfurization procedure, making an additional purification step necessary, in which excess aryl thiols are removed. There has been a number of attempts to avoid this problem through new and innovative protocols, such as e.g. liquid/liquid extraction, which helped to extract excess thiophenol from NCL reaction mixtures.[313] In another protocol developed by Ashraf Brik and coworkers, a bifunctional aryl thiol catalyst was used, which enables the researcher to pull out excess thiol at a hydrazide moiety on aldehyde functionalized resin by the formation of a hydrazone bond.[314] In another work by Payne and coworkers, trifluoroethanethiol (TFET) was introduced as a novel thiol additive, not interfering with the desulfurization reaction.[315] The utility of the TFET reagent in one-pot NCL, desulfurization reactions was demonstrated by the total synthesis of madanin-1 and chimadanin, two tick-derived proteins. A different protocol described successive on-resin ligations and desulfurizations, whereas the final product was released by treatment with TFA.[316]

2.3.7 Expressed protein ligation (EPL)

If one fragment of the two portions combined in a NCL reaction is of recombinant origin, one generally speaks from expressed protein ligation (EPL) or the semisynthesis of proteins, by which strengths of biochemical engineering are combined with organic synthesis. This methodology allows for the site-specific introduction of protein modifications, such as post-translational modifications or the attachment of fluorophores. The EPL strategy was introduced by Muir, Sondhi and Cole,[317] whereas the underlying method bases on the naturally occurring process of protein splicing. In this process, an internal protein domain excises itself out of a precursor peptide, thus creating a native peptide bond between the flanking N- and C-terminal portions of a protein. The first step of this well understood process is the transfer of the N-terminal extein unit to the side-chain -SH or -OH group of a Cys/Ser residue located at the N-terminus of the intein (*N,S*-acyl shift). The next step is a further transfer of the N-terminal extein to the Cys/Ser/Thr at the +1 position of the C-extein. This in turn leads to the formation of a branched intermediate. A concerted mechanism makes the last step of

protein splicing, where a conserved Asp residue at the C-terminus of the intein cyclizes and a peptide bond is formed between the two exteins through an *S,N*-acyl shift (**Scheme 23**).[318, 319]
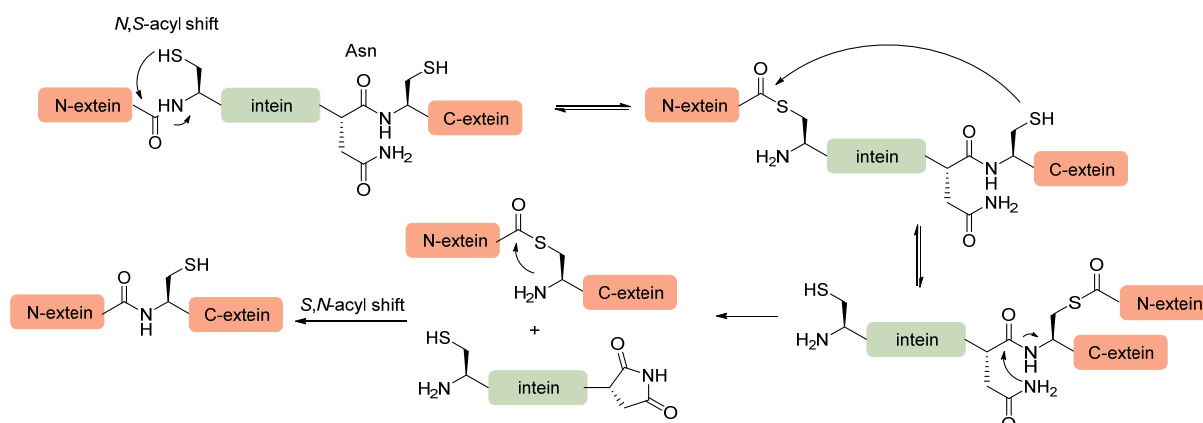
Scheme 23: Mechanistic details about intein mediated splicing of proteins.

In order to carry out NCL reactions, a thioester protein needs to be generated in order to react with a synthetic peptide equipped with a N-terminal Cys residue or a Cys surrogate. To further the process suitable for semisynthesis of proteins, the target protein sequence can be genetically fused with an intein. Then, an affinity tag is also fused to the construct and replaces the C-extein for purification purpose. An often used system is the IMPACT® system, commercially available from New England Biolabs.[320] In this system, a chitin binding domain (CBD) is fused to the target protein-intein fusion protein at the C-terminal end, allowing for convenient purification on chitin resin. As the intein catalyzes the reversible *N,S*-acyl shift, mutations in the intein prohibit further processing of the splicing process (usually an Asn/Ala mutation). After all contaminants from the expression are washed off, the protein thioester can be prepared by the addition of excess thiols such as sodium methanethiolate (MESNa) via a transthioesterification reaction. The resulting thioester protein can be either eluted from the column and be stored until further use or can be reacted *in situ* with a synthetic Cys peptide on the column.
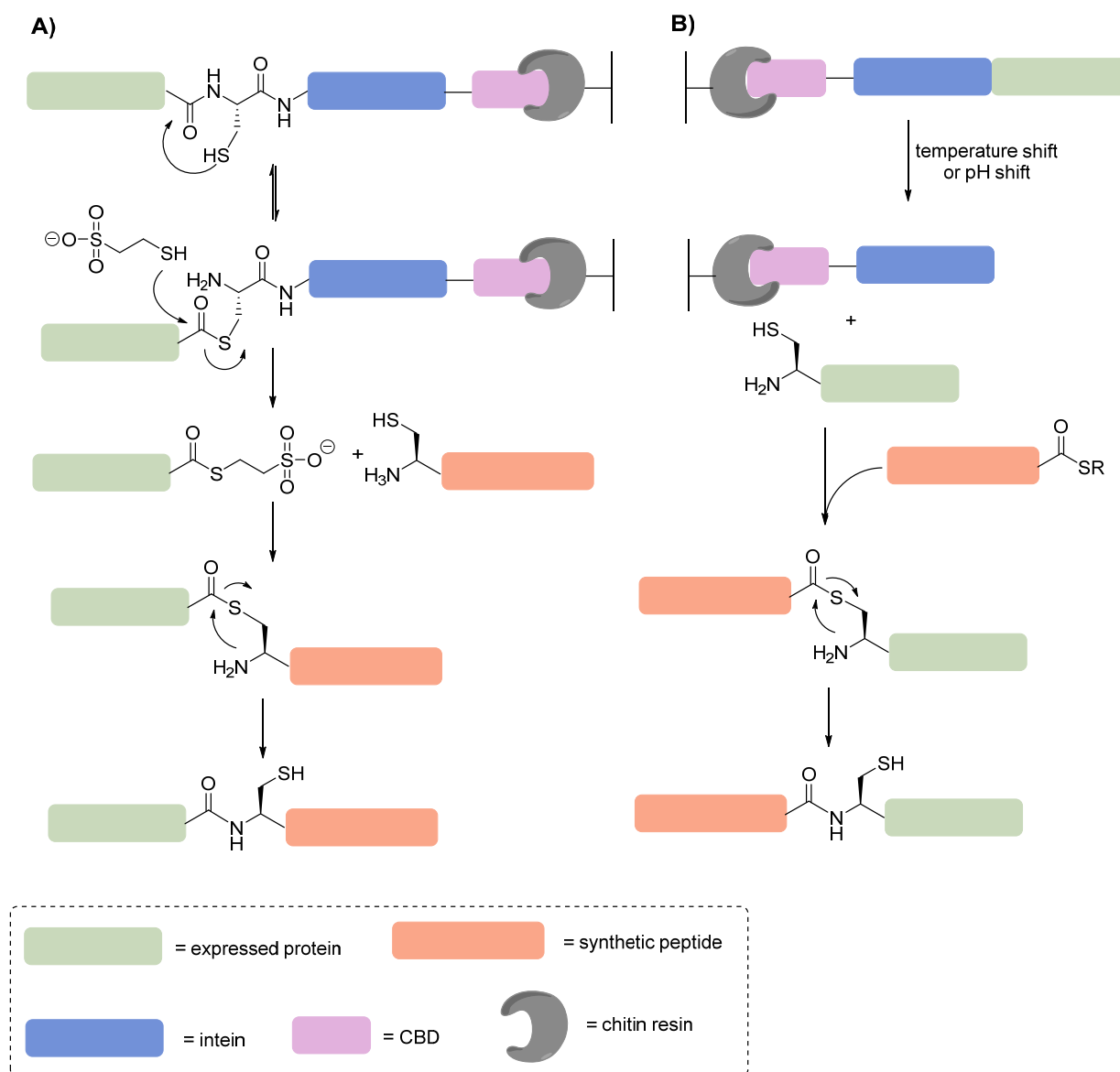
Scheme 24: **A)** Semisynthesis of a protein through the generation of a C-terminal thioester protein by the IMPACT system, followed by a NCL to a synthetic peptide; **B)** generation of a semisynthetic protein through a NCL between a synthetic peptide and a protein bearing an N-terminal Cys-residue, generated by the IMPACT system; CBD = chitin-binding domain.[8, 319]

Tom Muir and his co-workers have proposed another method, by which protein semisynthesis is feasible by protein trans-splicing (PTS). In nature, protein splicing typically occurs spontaneously, but some inteins exist naturally in a split form.[321] Here, the two split inteins are separately expressed and and remain inactive until they encounter their complementary partner and undergo cooperative folding and thus splice. PTS by naturally occurring split inteins is facilitated by protein-protein interaction and exhibits thus low concentration dependence.[322] The technology of split-inteins in protein semisynthesis is thus for challenging

substrates advantageous, when protein concentration, solubility and the ability to refold the ligation product are critical issues.[323] Muir and his coworkers have recently discovered and designed novel split-inteins that exhibit exceptional protein splicing activity and moreover, show increased expression levels when fused to proteins, including heavy chains of antibodies relative to other N-intein fusions.[324]
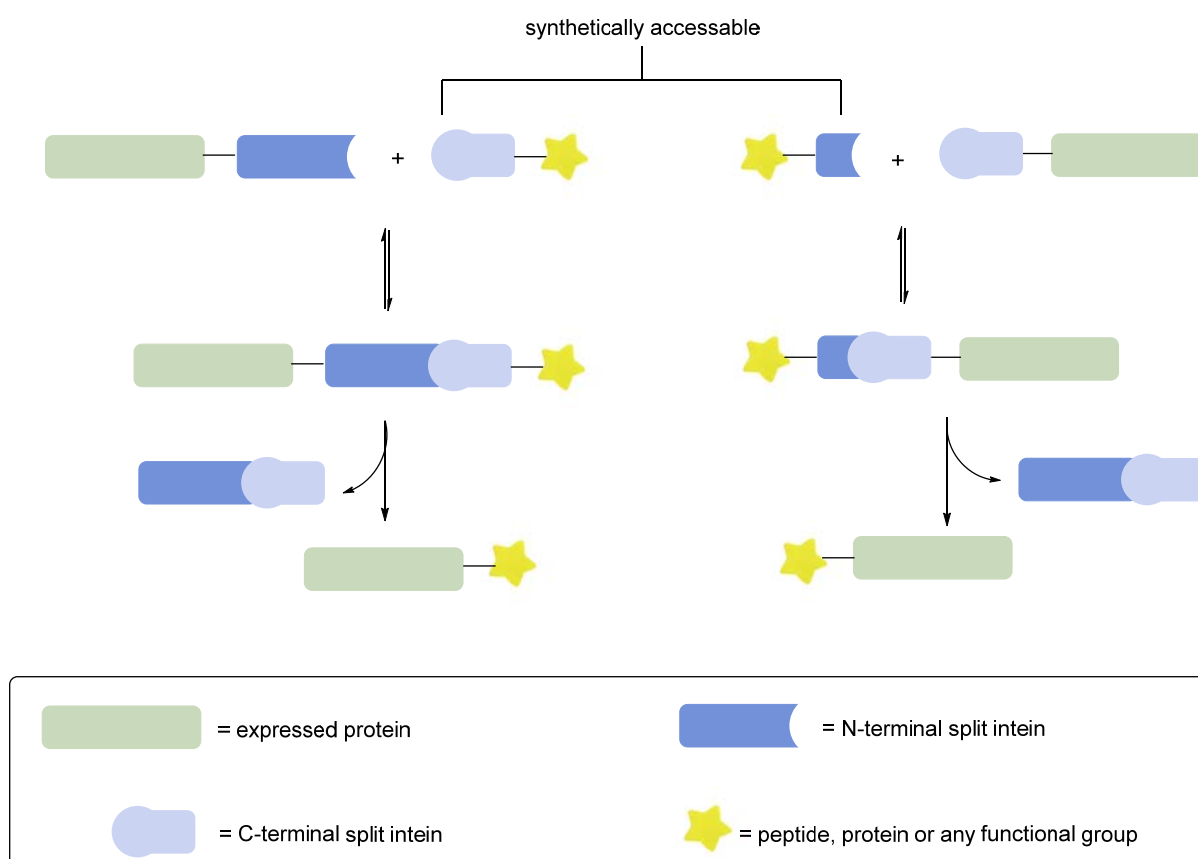
Scheme 25: Semisynthesis through protein *trans*-splicing (PTS) with synthetically accessable C-intein (left) or N-intein (right).[321]

Another technique was presented by the group of Derek Macmillan, where they observed thioester formation of expressed proteins carrying an C-terminal Cys residue under heating at 50°-60°C at pH 5 in the presence of excess MESNa.[325, 326] The thioester formation worked especially fine, when three amino acids toward the N-terminus (XaaCys) either His, Cys or Gly were present, but isolated yields are usually between 30% and 60% and moreover, heating between 50°C and 60°C can be problematic in terms of racemization.
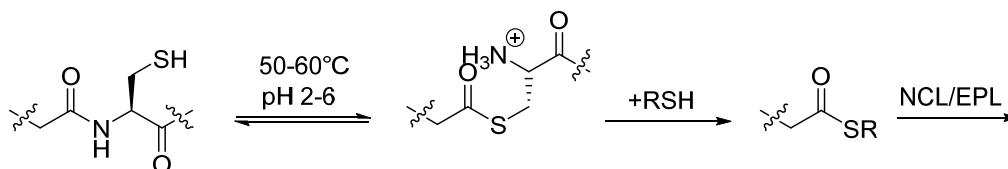
Scheme 26: Thioester formation through *N,S*-acyl shift.

The EPL technology is applied in many different fields, including research on proteins bearing homogeneous post-translational modifications, such as phosphorylation and *O*-GlcNacylation, two modifications that can be readily introduced to synthetic peptides by a building block approach (section **2.3.2**).[327] Especially the most common post-translational modification, namely phosphorylation, is often studied by means of EPL,[328] for instance for the kinase Csk.[317] In the previously mentioned study, the authors were able to show that phosphorylation of a tyrosine residue in the C-terminal region of Csk resulted in enhanced activity toward its substrate protein binding partners compared to unmodified protein. Annother example is provided by Broncel *et al*, generating a homogeneously phosphorylated Alzheimer relevant tau protein, which was further investigated for its aggregation potential.[123] But also the PTM of ubiqutination is accessible by EPL, which was for instance impressively demonstrated in the lab of Ashraf Brik, where the ability to prepare a homogeneously polyubiquitinylated α-globulin protein in a proof-of-principle study was demonstrated.[283]

2.3.8 Prominent examples of chemoselective ligations between peptides and proteins other than NCL and EPL

Despite the tremendous impact of NCL and EPL in the field of chemical protein semisynthesis, other ligations were developed that also allow for the formation of native peptide bonds at the ligation site. One example is the so called His-ligation, developed by Zhang and Tam in 1997 (**Scheme 27 A**).[329] In their approach they were able to generate His containing peptides in yields up to 70%, whereas the peptides cannot bear additional nucleophilic functional groups in side-chains of other amino acids.

Another method was also introduced by Tam *et al*, where a chemoselective ligation is reported based on the reaction of a N-peptide bearing a C-terminal aldehyde ester and a C-terminal peptide equipped with a N-terminal Cys residue.[330] The desired peptide bond is formed by an

O,*N*-acyl shift, which yielded the desired peptide with a thiazolidine group in the backbone. In a work-up reaction, this thiazolidine group can be converted to Cys (**Scheme 27 B**).

A different and relatively new chemoselective ligation method was introduced by Zhang *et al.* in 2013,[331] which bases on the previously described method by Tam and coworkers. They were able to show that peptides with C-terminal salicylaldehyde esters react with N-terminal Ser or Thr residues, which in turn yield cyclic *N*,*O*-benzylidene acetal intermediates, which can be directly cleaved and yield a native peptide bond after the reaction at the ligation junction (**Scheme 27 C**). This method has some limitations, such as difficult synthetic access to peptides with C-terminal salicylaldehyde esters, the requirement of relatively high substrate concentrations and the use of organic solvents, thus limiting the biocompatibility of this reaction.[332]
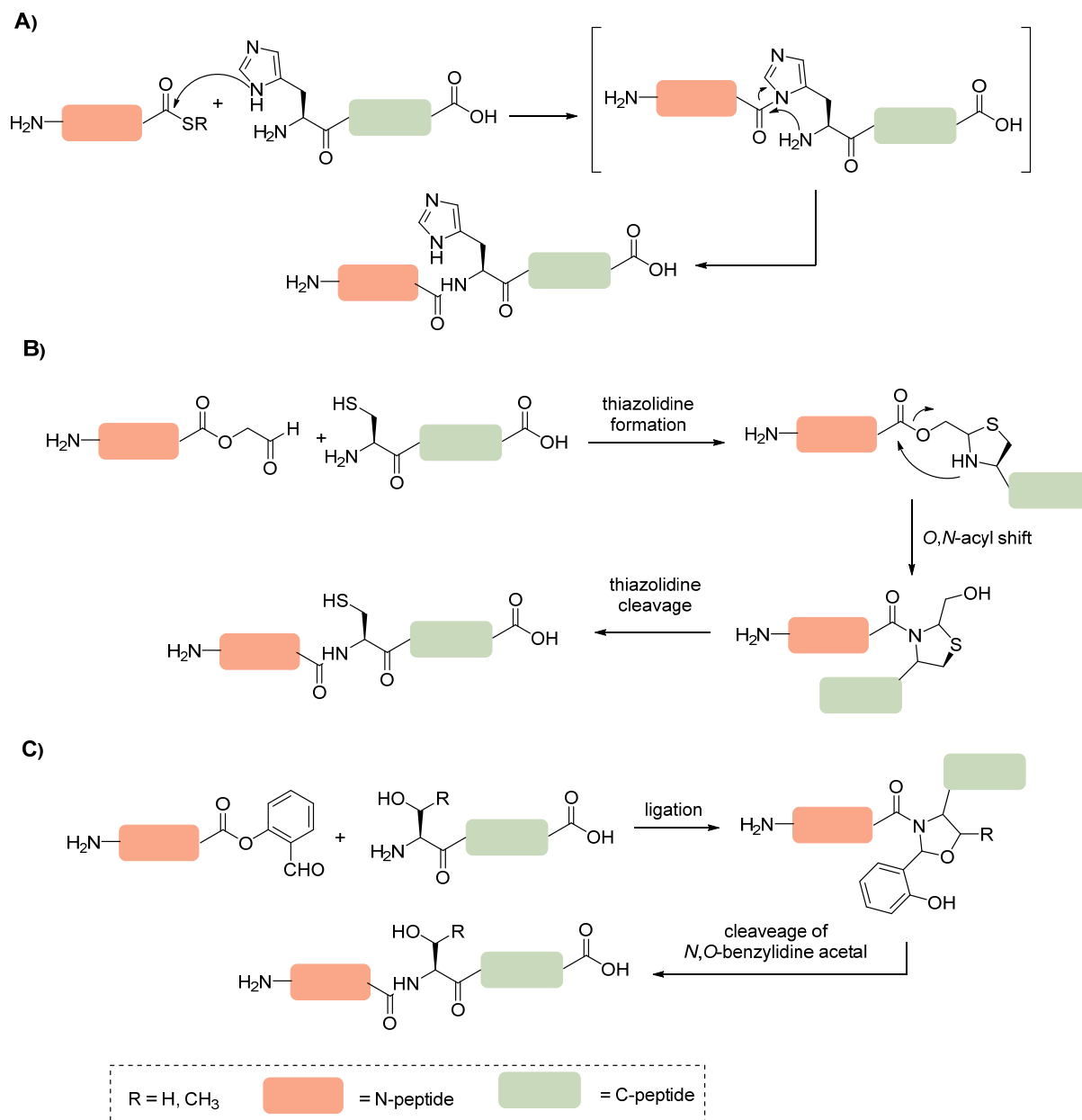
Scheme 27: A) His-ligation; **B)** ligation by Tam *et al*; **C)** ligation at Ser or Thr.

Bode and his coworkers developed another chemoselective ligation method in 2006, yielding a native peptide bond, termed the KAHA ligation (**Scheme 28 B**).[333] The substrates of their ligation are α-ketoacids and N-terminal peptide hydroxylamines. As this reaction does not require any catalysts or additives, it proceeds at slightly elevated temperatures in mixtures of water and organic solvents without the formation of by-products. The slightly acidic conditions even further enhance the outcome of the reaction and prohibit the hydrolysis of other functional group prone to undergo hydrolysis. The α-ketoacids are generated via a sulfur ylide resin (**Scheme 28 A**). The mechanism of the KAHA ligation is shown in **Scheme 28 C**.
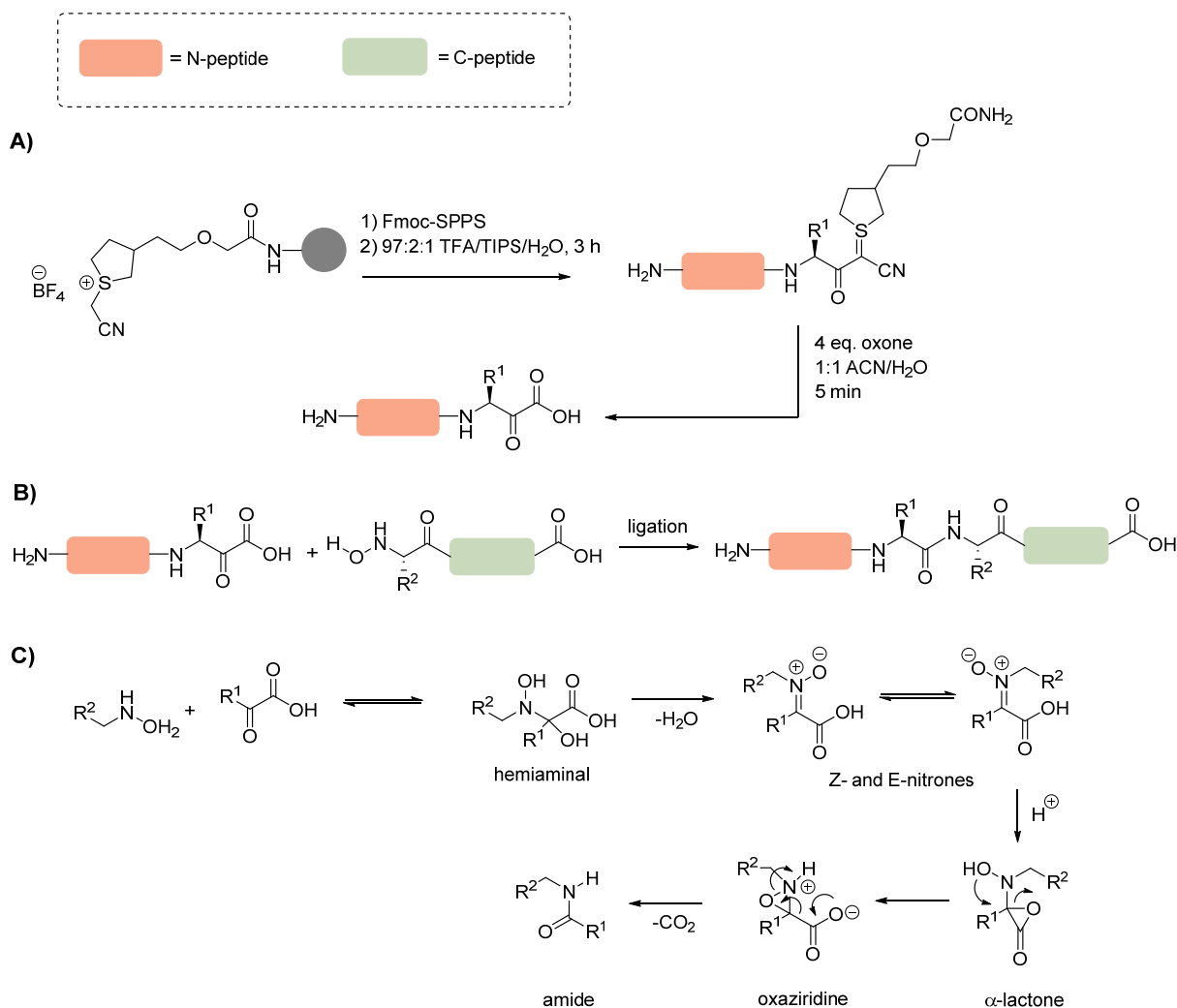
Scheme 28: **A)** Synthesis of a peptide with a C-terminal α-ketoacid on a sulfur ylide resin; **B)** KAHA ligation between two peptides; **C)** proposed mechanism for the KAHA ligation.

More recently, the repertoire of KAHA-ligations was further expanded by ligations with 5-oxaproline (Opr), which is easy to prepare and to incorporate into synthetic peptides.[334] In their approach, homoserine residues are generated at the ligation site (**Scheme 29**). The KAHA ligation with 5-oxaproline requires elevated temperatures and basic pH for the *O,N* acyl shift to take place and is thus susceptible to racemization.
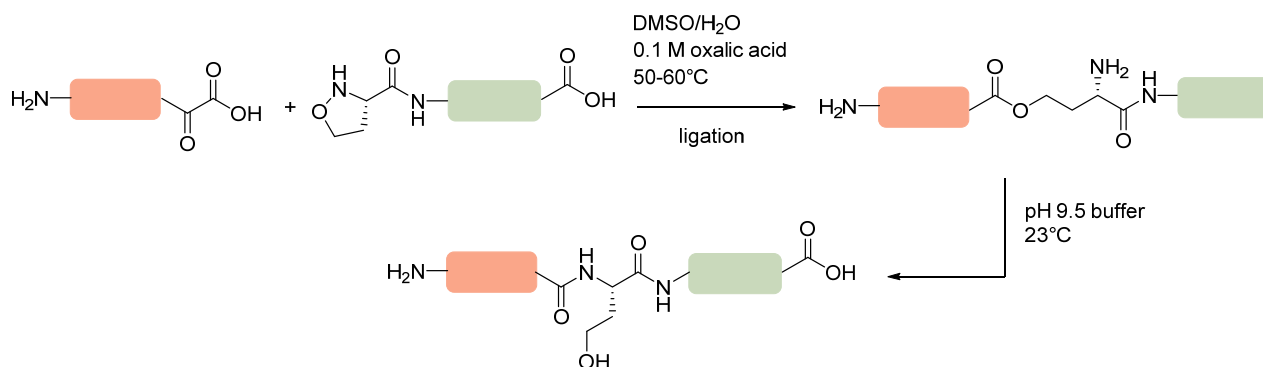
Scheme 29: KAHA ligation with 5-oxaproline modified peptides form amide bonds via an *O,N*-acyl shift.

Another method to produce naturally elongated peptides is the traceless Staudinger ligation, which was introduced by Bertozzi and Raines already in the year 2000.[335, 336] In the traceless Staudinger ligation, an α-amino acid or peptide bearing an azide react in a chemoselective fashion with a phosphinothioester to an iminophosphorane, which can undergo an intramolecular attack with an internal thioester to yield native peptide bonds at Gly-Gly-Ala or Ala-Ala junctions.[337] The reaction proceeds via a 5- or 6-membered ring intermediate, depending on the alkyl or aryl thiol or alcohol used (**Scheme 30**).[338] The Traceless Staudinger Ligation has ever since its discovery served in many different applications, such as cyclization of proteins,[339] peptide fragment coupling on solid-support[340] and the site-specific modification of a gold surface with proteins.[341]
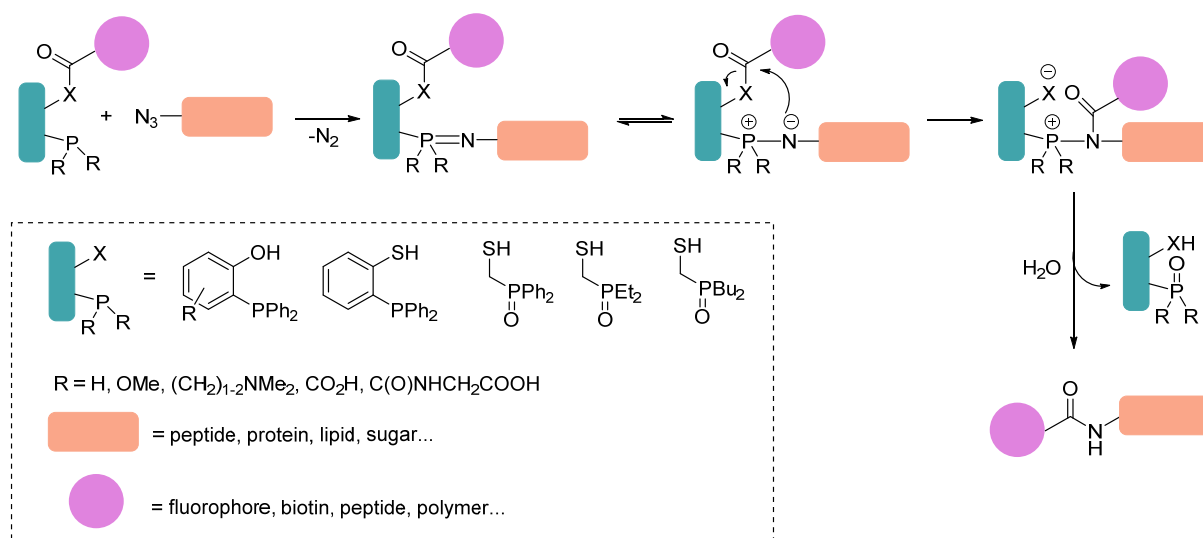
Scheme 30: Mechanistic representation of the Traceless Staudinger Ligation.[342]

Another alternative for the generation of forming a native peptide bond between two entities applicable to SPPS or generally to peptide and protein synthesis is the thioacid-azide reaction.[343-345] In this chemoselective ligation peptides with a C-terminal thioacid react with

other azide-containing molecules, thus creating a native peptide bond at the ligation junction. The mechanism of the thioacid-azide ligation proceeds via the formation of a thiatriazoline intermediate, which further undergoes a retro[3+2]-cycloaddition. This creates an amide bond under the release of N_2S under two possible pathways (**Scheme 31**).
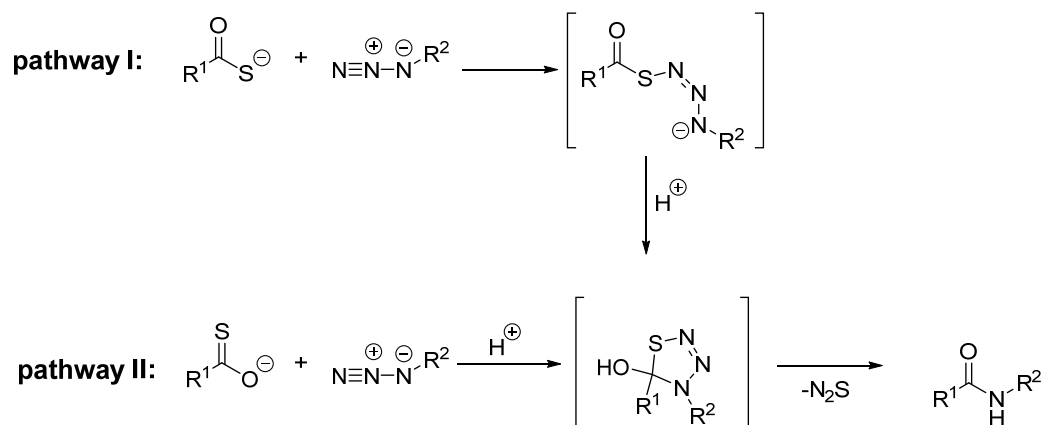
Scheme 31: Mechanism of the thioacid-azide ligation. Shown are the two possible pathways the reaction can proceed depicted in pathways I and II.

The thioacid-azide ligation has been so far successfully applied in e.g. sulfonamide resin loading,[346] protein biotinylation,[347] glycopeptide synthesis[348] or peptide ligations.[349]

2.3.9 Post-translational modifications introduced by protein engineering

Another, very powerful approach to site-specifically incorporate amino acids modified with PTMs into proteins is provided by so called "genetic code expansion". In this approach, an aminoacyl-tRNA synthetase and a tRNA are used during mRNA translation to insert a specific residue at a site, where an amber stop-codon (UAG) is placed in a gene of interest. Each mRNA codon is recognized by a specific tRNA anticodon. The tRNA is aminoacylated with an appropriate amino acid by the enzyme aminoacyl tRNA synthetase. The ribosome moves along the mRNA and forms a polypeptide or protein chain, until a stop codon, which is not recognized by any tRNA, is encountered, which in the end allows for the peptide release (**Figure 13**). The term "genetic code expansion" describes a technology, where an "orthogonal" aminoacyl tRNA synthetase-tRNA pair is used. This orthogonal pair does not aminoacylate the normal tRNAs of a cell, whereas it is able to direct the incorporation of an unnatural amino acid in response to an amber stop codon at a site of interest.[350, 351] The modified amino acid is usually added to

the medium, in which the cells are grown. Nearly all approaches of genetic code expansion utilize one of the four synthetase-tRNA pairs, which will be described herewith. The *Methanococcus jannaschii* Tyrosyl-tRNA synthestase (MjTyrRS)-tRNA$_{CUA}$ pair was the first pair that was employed to incorporate unnatural amino acids. This particular pair is orthogonal to tRNAs in *Escherichia coli* (*E.coli*), but not to tRNAs in eukaryotic cells.[352] The *E.coli* Tyrosyl-tRNA synthetase (EcTyrRS)-tRNA$_{CUA}$ and *E.coli* Leucyl-tRNA synthetase (EcLeuRS)-tRNA$_{CUA}$ pairs are orthogonal to tRNAs and synthetases in yeast and mammalian cells, but not to those in bacteria.[353, 354] Another very popular example is the pyrrolysyl-tRNA synthetase (PylRS)-tRNA$_{CUA}$ pair from *Methanosarcina*, which is orthogonal to synthetases and tRNA in *E.coli*, yeast, mammalian cells and *C.elegans*.[355-358] The latter pair has two distinct advantages over the previous three, as this synthetase does not use one of the 20 canonical amino acids, which makes it unnecessary to destroy natural synthetase activity before specificity for a new amino acid is created. Secondly, PylRS variants can be applied in *E.coli*, in which selections are the most straightforward and then unnatural amino acids can be incorporated in yeast, mammalian cells or *C.elegans*.
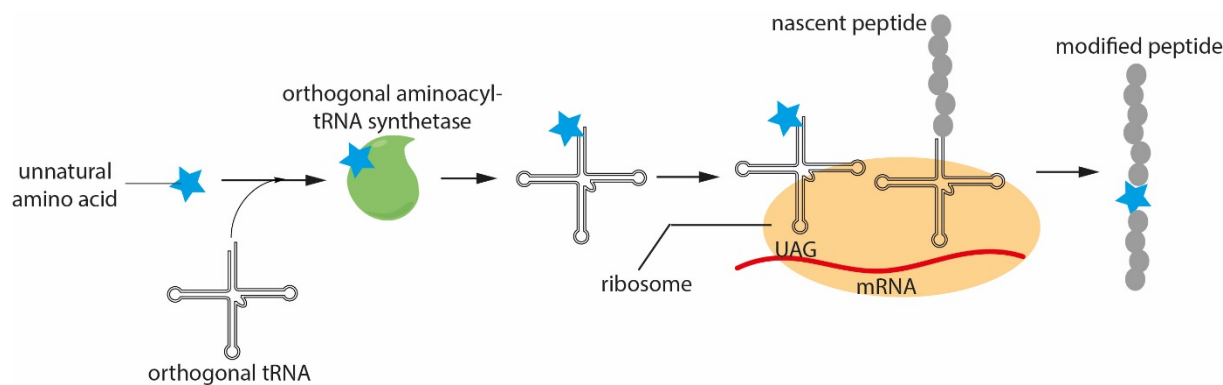
Figure 13: In the process of incorporating unnatural amino acids into proteins, the unnatural amino acid is added to the cell-growth medium and is then taken up by the cell. A specific recognition by an orthogonal aminoacyl-tRNA synthetase takes place, which then attaches the unnatural amino acid to an orthogonal amber suppressor tRNA, which is decoded on the ribosome during translation in response to an introduced amber codon (UAG). This allows for the site-specific incorporation of the unnatural amino acid into a peptide, otherwise consisting of natural amino acids.

Thus far, genetic code expansion methods have been reported for the incorporation of Tyr nitration,[359] Tyr sulphation,[360] phosphorylated Ser (pSer),[361] Lys mono- and dimethylation,[362, 363] and Lys acetylation.[357] For instance the incorporation of pSer into

histones was recently reported to work efficiently to produce mg-quantities of the phosphorylated target protein by molecular evolution of phosphoseryl-tRNA synthetase and redesign of elongation factor (EF-Tu) and expression in the *E.coli* strain BL21 (DE3).[364] However, the potential of genetic code expansion has been limited to often low efficiency incorporation of a single type of amino acid at a certain time, since each triplet codon in the genetic code is already occupied for the synthesis of natural proteins. Chin and his coworkers tackled this problem, as they reported the application of synthetically evolved orthogonal ribosome that decodes for a series of quadruplet codons and the amber codon.[365] Thus, several blank codons on an orthogonal messenger RNA are introduced, thus providing a template for the direct incorporation of distinct unnatural amino acids. This technology might help in the future to overcome limitations of amber stop codon suppression and enable scientists to incorporate multiple PTMs into proteins in acceptable yields.

2.4 Tags and cleavable linkers for purification strategies in chemical biology

The raising importance of cleavable linkers in combination with purification tags is a consequence of the fast developments in the field of chemical biology in the last few years. Since protocols with biological samples require mild reaction conditions, chemists are not able to apply protocols established in organic chemistry. In this section, an overview of different purification tags used in chemical biology together with their characteristics will be presented. Moreover, a short overview on cleavable linkers with focus on light cleavable systems will be provided, which allow for a time-resolved release of a target molecule under mild conditions. Finally, recent examples of probe enrichment in combination with cleavable linkers will be outlined in this section, including applications in the fields of purification, analytics, protein enrichment, immobilization and assay development.

2.4.1 Introduction

Chemoselective bioconjugation has an enormous impact on the field of life sciences and thus created a vastly growing industry, serving research, or the development of diagnostics and therapeutics, reviewed in several articles.[366, 367] Within the context of chemical biology, these technologies are used in numerous applications, such as in targeted drug therapy,[368] molecular imaging[369] and DNA sequencing.[370] Moreover, bioorthogonal conjugation became of outmost importance in proteomic research and is frequently used today in the fields of activity-based protein profiling[371] and protein enrichment and purification,[372] whereas the latter two will be mainly addressed in this section. Purification tags for protein purification have been reviewed extensively in the past.[373, 374]

Two molecules are often bridged through a linker, which may impose new structural or functional features on the molecule of interest.[375] Therefore, researchers thrive to apply chemical groups that allow the selective cleavage of these linkers and thus enable the liberation of the unmodified target molecule. The need to produce such unmodified molecules becomes even more prevalent, when applications for human use are foreseen.[376] Selective disconnection of chemical bonds is an omnipresent task in organic synthesis and had profound influence on the fields of solid-phase synthesis and combinatorial chemistry.[377, 378] Using cleavable linkers in chemical biology demanded conceptual rethinking, since chemists were not able to resort to harsh cleavage conditions usually applied in organic synthesis due to often fragile biological

targets such as DNA or proteins. Thus, new linker types had to be developed that allowed for mild and biocompatible cleavage conditions. Ideally, they can be installed by bioorthogonal reactions,[379] deliver high yields at low concentrations and don't require an excess of reagents.[380] In order to provide appropriate linker cleavage conditions for biological setups, many different linker types were developed, some of which have been reviewed previously e.g. by Rudolf *et al.* and Leriche *et al.*[381, 382]

This section will focus on applications of cleavable linkers for protein enrichment and purification, major tasks in chemical biology. Often, an enrichment of a probe up to a certain degree is sufficient for the intentional outcome of an experiment, but for simplification and due to blurry differentiation, the term purification will be used throughout this section for both, enrichment and purification if not explicitly mentioned otherwise. Choosing an efficient synthetic design of a purification route can be tedious, time consuming and challenging. It is therefore the intention of the author to provide the reader with a state of the art overview on modern concepts of protein purification by tags with focus on their combination with cleavable linkers. Different types of purification tags and cleavable linkers will be described and characterized. Finally, recent applications of cleavable linkers in combination with purification tags will be provided.

2.4.2 Purification tags in chemical biology

Affinity tagging was discovered in the 1960s by R. Axén *et al.*[383] and became very popular during the 1980s and 1990s. Over time, affinity chromatography (AC) became highly efficient and has ever since immensely helped to determine the structure of thousands of proteins. The mechanistic fundament of AC is formed by reversible interactions between a specific ligand that is attached to a target protein and a chromatography matrix. It is a powerful method, where one single pass through an affinity column can achieve a 1.000 to a 10.000-fold purification of a certain product from other components in a crude mixture. This allows for the use of purified proteins e.g. in functional and structural studies (95-99% purity) or their application as therapeutic agents (>99% purity). Moreover, affinity tags are nowadays also used for immunohistochemistry (IHC), immunoprecipitation (IP), flow cytometry (FCM),

protein localization and western blots.[384] In this section, different classes of AC and the corresponding purification tags will be categorized according to the matrix, where the purification is carried out on (**Figure 14**). The first type of matrix is based on small molecules, onto which certain purification tags can bind. If the matrix is made from protein, it will be termed type two and if the protein is an antibody, it will be referred to as type three.
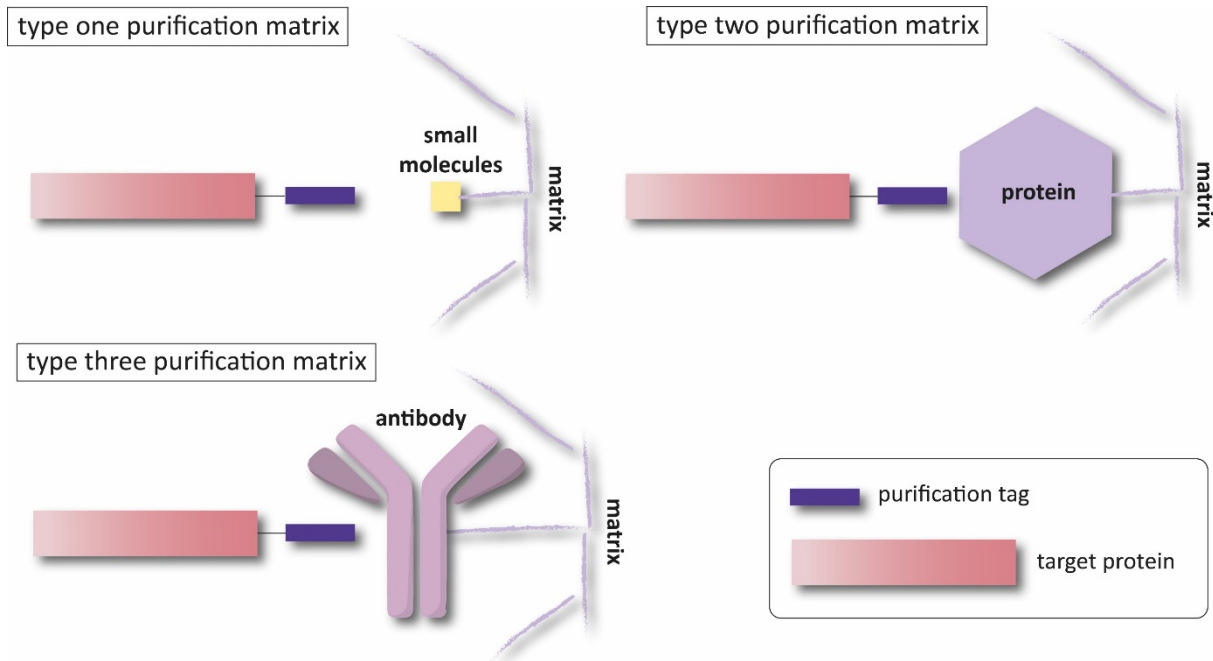
Figure 14: Types of purification matrix.

2.4.2.1 Tags for type one purification matrix

The most frequently applied tag for protein purification is without doubt the polyhistidine-tag or His-tag. Usually, 4-10 His residues are expressed at the N- or C-terminus of a protein that enable purification on immobilized metal affinity columns (IMAC) through a chelating effect of the aromatic His residues on metal ions such as Ni^{2+}, Co^{2+}, Zn^{2+} and Cu^{2+}. The most widespread IMAC support is nitrilotriacetic acid (NTA) in combination with immobilized Ni^{2+} ions. Elution of IMAC bound proteins is usually carried out with solutions containing 150-300 mM imidazole. The reason for the frequent use of the His-tag is its small size, low costs and straightforward implementation. It is a very reliable tag, since it doesn't require a certain fold and thus works under denaturing conditions. The His-tag is easily accessible, since there are several expression vectors commercially available for protein-fusion. His-tagged proteins can be

recognized by specific anti-His antibodies in immunoassay detection. Furthermore, this tag has typically low impact on the protein function or structure.[385] Due to these strengths, the His-tag is widely applied in chemical biology, but it does also suffer from several limitations. The most evident constraint is the co-purification of impurities that contain naturally occurring His-rich regions.[386] In order to counteract on this issue, the optimized *E. coli* expression strain *LOBSTR* was developed that eliminates common contaminants, which occur often during His-tag expression.[387] But there are exceptions, where a His-tag was shown to alter protein properties, despite its relatively small size. This was e.g. reported by Charbonneau *et al*,[388] who showed the impact of a His-tag on the refolding of the carboxylesterase EstGtA2. This in turn led to altered thermal stability of this enzyme. The His-tag was later developed further to the Hat-tag, where His residues are separated by other amino acids. This allowed the loading and elution of Hat-tagged proteins from IMAC resins under physiological conditions and decreased the induced protein-instability.[389] Evenly small tags are the polyarginine- and polylysine-tag, consisting of 5-6 Arg or Lys residues. Those are usually fused to the C-terminus of a protein and allow for purification by cation-exchange chromatography. The use of such tags may in some cases have positive effects on the expression and purification yields,[390] but in other cases influence the tertiary structure of proteins (see also section **2.4.4.5**).[391]

The maltose-binding domain (MBD-tag) and the glutathion-S-transferase (GST) are two prominent examples of purification tags, where a large protein is fused to the target and then immobilized on a solid support, coated with a specific small molecule ligand. The expression of MBD or GST fusion proteins cannot only enhance the solubility of their fusion partners, but can also enhance the expression in bacterial hosts.[392] However, in some cases they may also decrease the expression yield due to their high metabolic demands. When such big purification tags are used, they need to be removed in the end to avoid structural or functional implications. The chitin-binding domain (CBD) consists of just 51 amino acids and is usually applied for the affinity purification of recombinant proteins, where it is combined with an intein tag.[393] The fusion proteins are captured on a chitin-matrix and are then released upon the addition of thiol reagents or pH and temperature shifts. Such tags that bind to very cheap and ubiquitous material such as carbohydrates are of high relevance for large scaled purifications in the

industry. Along those lines, the so called starch-binding domain (SBD)[394] and the cellulose-binding domain[395] tags were developed.

An extraordinary example for affinity purification is certainly the intein-mediated *in vivo* purification by polyhydroxybutyrate (PHB) matrix association.[396] A protein of interest (POI) is expressed as a fusion protein with an intein and the PHB-binding protein in *E. coli*. The same *E.coli* cells produce intracellular PHB granules. Upon binding of the target protein to these granules by the PHB-tag, mechanic separation can be accomplished by centrifugation. In a final step, the target protein is cleaved at the intein site.

Table 6: Summary of tags binding type one matrices, their binding entities and elution conditions.

ligand	binding entity	elution conditions
His-tag	Ni^{2+}-NTA, Co^{2+}-NTA	150-300 mM imidazole or low pH
Hat-tag	Co^{2+}- carboxylmethylaspartate (CMA)	150 mM imidazole or low pH
Arg-tag	cation exchange resin	linear gradient of NaCl from 0 to 400 mM at alkaline pH>8.0
MBD-tag	cross-linked amylose	10 mM maltose
GST	glutathion	5-10 mM reduced glutathion
CBD	chitin	chitin fused to intein is cleaved with 30-50 mM dithiotreitol (DTT) or other thiols
SBD	β-cyclodextrin– epoxy-activated Sepharose	8 mM cyclodextrin
cellulose binding domain	cellulose	0-6 M Gn · HCl in Tris buffer at pH 7.2, cellulose
PHB binding protein	PHB-matrix	PHB binding protein is fused to inteins and cleaved with 30-50 mM thiol addition

2.4.2.2 Tags for type two purification matrices

A very prominent example for a tag that binds type two purification matrix is biotin. The high affinity and specificity of biotin to the bacterial protein streptavidin or the egg-white

glycoprotein avidin makes it an extremely valuable tool in chemical biology. Proteins, DNA or RNA can be efficiently captured on streptavidin coated solid supports such as resins, microtiter plates, chips or magnetic beads.[397] As biotin/streptavidin or tetrameric avidin binding is the strongest non-covalent interaction known in nature ($K_d = 10^{-15}$ M),[398] denaturing conditions like 8 M guanidine hydrochloride (Gn · HCl) at pH 1.5 or boiling in sodium dodecyl sulphate (SDS) containing buffer are necessary to elute biotinylated bound proteins from streptavidin or avidin. Approaches to allow mild elution of biotin from solid supports involved the development of nitrated streptavidin[399] or monomeric avidin proteins ($K_d = 10^{-7}$ M),[400] which in turn compromised the extraordinary high affinity of biotin.

The Strep-tag is also a widely used system. A simple octapeptide is genetically fused to the target protein that binds to streptavidin.[401] Optimization of the tag resulted in the development of the Strep II and Strep III tags and a Strep-Tactin matrix, thereby avoiding interference with folding or bioactivity and preventing aggregation of the fusion partner.[402-404] The Strep-tag or its successors are usually stripped off from affinity columns by the addition of biotin or desthiobiotin.

The calmodulin-binding peptide (CBP) binds with nanomolar affinity at physiological conditions, if calcium is present and is therefore also an attractive affinity tag.[405] The amino acid sequence of CBP is derived from human muscle myosin light-chain kinase and has also negligible impact on protein structure and functions. It is eluted after affinity purification by the removal of calcium from the buffer through the addition of the calcium chelator ethylene glycol- bis(2-aminoethylether)N,N,N',N'-tetraacetic acid (EGTA).[406]

The S-tag bases on the specific interactions between the 15 amino acid long S-tag and the S-protein, both derived from the pancreatic ribonuclease A (RNase A).[407] A major drawback of this tag is connected to the harsh elution conditions (3 M NaSCN, 3 M MgCl$_2$, or 0.2 M citrate at pH 2.0).

Elastin-like polypeptides (ELPs) don't fall into the category of affinity tags since they don't require an affinity matrix, but can be used as tools for tedious protein purifications (see also section **2.4.4.5**).[408] ELPs consist of numerous repeats of peptide motifs that can reversibly precipitate the fusion protein upon temperature upshift. Purification of the fusion protein is

thus achieved by temperature induced aggregation, separation through centrifugation and resolubilization.[409] This process is also termed inverse transition cycling (ITC).

Table 7: Summary of tags binding type two matrices, their binding entities and elution conditions.

ligand	binding entity	elution
biotin	streptavidin/avidin	8 M Gn · HCl at pH 1.5 or boiling in SDS containing buffer
	nitrated streptavidin	buffer at pH 10
	monomeric avidin	2 mM biotin in PBS buffer
strep-tag (AWRHPQFGG)	streptavidin	biotin, iminobiotin, lipoic acid, diaminobiotin
strep-tag II (WSHPQFEK)	streptavidin, strep-tactin resin	biotin, desthiobiotin
strep-tag III (WSHPQFEKGGGS GGGSGGGSWSHPQFEK)	streptavidn, strep-tactin resin	biotin, desthiobiotin
CBP (KRRWKKNFIAVSA ANRFKKISSSGAL)	calmodulin	EGTA or EGTA with 1 mM NaCl
S-tag (KETAAAKFERQHMDS)	S-fragment of RNaseA	3 M sodium thiocyanate, 0.2 M citrate at pH 2, 3 M $MgCl_2$
ELP-tag (e.g. $(VPGXG)_n$; X is any amino acid except proline)	inverse transition cycling (temperature enhancement)	temperature lowering

2.4.2.3 Tags for purification on type three matrices

A short hydrophilic octapeptide tag is termed FLAG and relies on purification by monoclonal antibodies M1, M2 and M5, each displaying different binding characteristics.[410] It should be located on the surface of a target protein in order to be accessible for the antibody, whereas the recognition can be calcium dependent or independent, which relies on the antibody.[411] Elution of captured proteins is achieved with excess FLAG peptides. Other immunoreactive polypeptides are the human influenza hemagglutinin (HA) tag[412] and the c-Myc tag[413] that

are generally used for separation. The HA tag is only 9 amino acids long and can be eluted after binding either by HA epitopes provided in TBS (1 mg/mL) or by chemical cleavage through 0.1 M glycine (pH 2-2.8), 3 M NaSCN or 50 mM NaOH.[414]

Table 8: Summary of tags binding type three matrices, their binding entities and elution conditions.

ligand	binding entity	elution
FLAG-tag (DYKDDDDK)	anti-FLAG antibody	excess of FLAG peptides, pH 3.0 or 2-5 mM ethylenediaminetetraacetic acid (EDTA)
HA-tag (YPYDVPDYA)	anti-HA antibody	excess of HA peptides, 0.1 M glycine (pH 2-2.8), 3 M NaSCN or 50 mM NaOH
c-myc (EQKLISEEDL)	anti-c-myc antibody	low pH, 0.1 M glycine (pH 2.0-2.8), 3 M NaSCN or 50 mM NaOH

2.4.3 Cleavable linker types

2.4.3.1 Overview on different linker types and concepts of their cleavage

Purification tags are usually connected to POIs by different linkers that are optimized for particular applications. Very often, the tag has to be removed from the POI post-purification to maintain the structural and functional integrity of the protein, which renders cleavable linkers indispensable tools for such purposes.[415]

There are many different systems available, such as linkers that are cleaved by enzymes, where site-specific protease cleavage is carried out under often physiological conditions. To this goal, special enzyme recognition sequences can be incorporated between an affinity tag and the POI,[416] whereas the efficiency of the linker cleavage can drastically differ, depending on the protein.[373, 416-418] The used enzymes can either be endo- or exoproteases, whereas their strengths and weaknesses were reviewed in different overview articles.[419-421]

Alternatively, linkers with self-splicing characteristics can be introduced between POI and affinity tag. Those linkers are intein-based and may reassemble in a site-specific fashion, rendering two independent protein products (see section **2.3.7**).[422, 423] In general, intein cleavage can be induced by either pH change or by thiolysis.[424] They thus provide means for a mild cleavage of the corresponding POI, applicable to various scenarios of enrichment and

purification. A summary for the use of inteins or split inteins was provided by Tom Muir and his coworkers.[321]

There are also linkers available that are sensitive to proton sources and are thus acid sensitive. There, *tert*-butyl carbamates were shown to work for protein pull-down experiments, which are cleaved by TFA, as demonstrated by Trung *et al*.[425] Treatment with strong acids like TFA leads to protein degradation, making it rarely applicable if folded proteins are required after the purification. Another acid sensitive linker was shown to be cleaved by treatment with formic acid as a milder proton source,[426] but protein degradation remained a problem. A milder cleavage is possible, if reduction sensitive linkers are applied. There are two main linker-systems available that are cleaved under reductive conditions, namely azo derivatives and disulfide bridges. Azo linkers are usually cleaved by the salt sodium dithionite ($Na_2S_2O_4$), which enables cleavage under mild, physiological conditions.**[427]** This selectivity for sodium dithionite even allows for the use of other reducing agents such as TCEP or DTT that are frequently applied in chemical biology protocols. Linkers that are based on disulfide bridges are sensitive toward reducing agents like DTT, TCEP or β-ME.[428, 429] The main disadvantage in disulfide-based systems is that often, the POIs also contain disulfide bridges, which would be thus also reduced by such agents.

Other linkers can be cleaved by oxidation agents. For instance 1,2-diol-based linkers are effectively oxidized and thus cleaved by sodium periodate ($NaIO_4$), releasing aldehydes at the cleavage sites. A vicinal linker by Yang *et al*. was used in combination with biotin for purification, whereas the generated aldehyde after the oxidative cleavage was then addressed for further functionalization.[430] Nucleophiles and bases can also be used, to selectively break bonnds in linkers and thus release an immobilized target protein from a resin. Many different systems were reviewed by Leriche *et al*, providing an extensive overview on the field.[382]

Photolabile linker systems offer a special feature: They don't require any reagent, necessary for linker cleavage. The irradiation of a probe with light is sufficient for the release of a probe that is otherwise sensitive to acids, bases or other agents presented in this section. There are general reviews available that depict the concept of photolytic cleavage of molecules.[431, 432]

2.4.3.2 Photocleavable linkers

Ortho-nitrobenzyl derivates are nowadays frequently used for amino acid protection and for linkers applied in processes of protein enrichment and purification.[431] The cleavage proceeds via a mechanism in accordance to a Norrish type II reaction on ketones and aldehydes, in which highly reactive 1,4-biradical species are formed as intermediates upon cleavage of a proton in γ-position to the nitro group (**Scheme 32**).
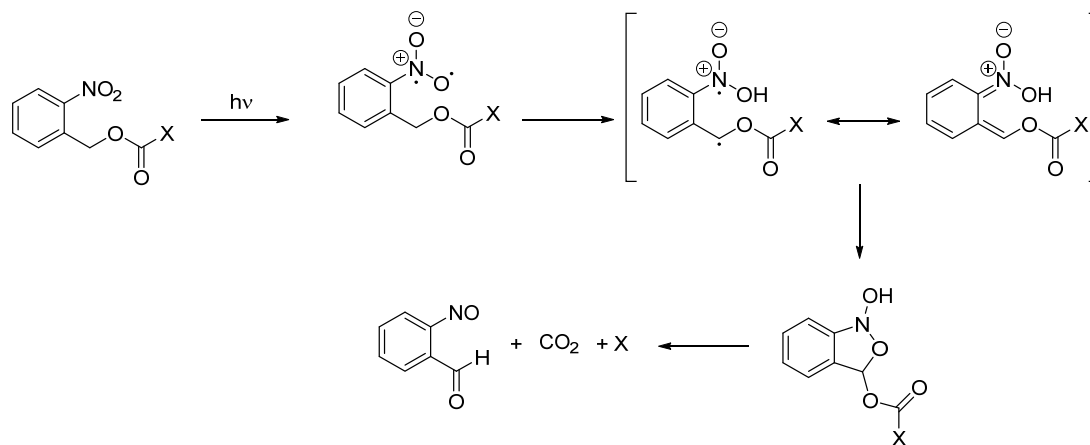
Scheme 32: Photochemically-induced photoisomerization of *o*-nitrobenzyl alcohol derivatives into *o*- nitrosobenzaldehyde via a mechanism, similar to Norrish type II reactions.

A possible side-reaction is the formation of an imine through the condensation of a primary amine and the corresponding aldehyde, generated upon photolytic cleavage. This side-reaction can be circumvented by the use of carbonyl scavangers, such as semicarbazide hydrochloride.[431] In case a ketone is released after photolysis instead of an aldehyde, no additives are required, since the ketone moiety is much less prone to imine formation.

In organic chemistry, photocleavable linkers have been widely used ever since for temporal protection of functional groups[433] or for immobilization of molecules on solid-supports.[434-436] The application of photocleavable linkers in combination with purification tags has been pioneered e.g. by Kenneth J. Rothschild and coworkers, who developed a photocleavable biotin that can be reacted with primary amines in aqueous solution, thus allowing researchers to conjugate the group to biomolecules (**Figure 15**).[437]
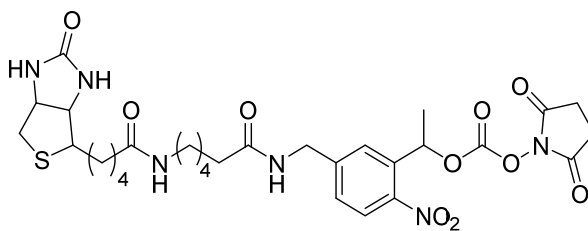
Figure 15: Photocleavable biotin compound connected to a NHS-ester for conjugation to primary amine containing biomolecules.

2.4.4 Different applications of cleavable linkers with purification tags

Cleavable affinity tags are used in diverse fields of life sciences. They are handles for protein purification and enrichment and are found in applications of different research areas, such as in enrichment studies of target proteins in complex mixtures or assay development processes. It is the goal to supply the reader in the following section with recent examples of how cleavable tags have been applied in the recent past. This is just a selection and not a complete coverage of recent developments in the field.

2.4.4.1 Hit identification in proteomic research

Single-stranded DNA serves as a first example for the use of a cleavable linker applied for proteomic research.[438] In their experimental set-up, Wu *et al.* have cultured HL60 cells in media supplemented with peracetylated *N*-(4-pentynoyl) mannosamine (Ac₄ManAl), an alkyne-tagged metabolic precursor of sialic acid,[439] which allowed for the incorporation of such tagged molecules to membrane sialylated glycoproteins (**Scheme 33 A**).

To enrich the target molecule, a compound was designed, in which a biotin is connected to DNA via a linker equipped with an azide at the 3' end (biotin-DNA-N₃). This probe was used to enrich alkyne-tagged glycoproteins from mammalian cell lysates. They performed Cu(I)-catalyzed azide-alkyne cycloadditions (CuAAC)[440, 441] as reported previously.[442] It was shown that about 90% of their biotinylated compounds were immobilized on streptavidin coated resin. The linker applied in this study is labile to the DNA cleaving enzyme benzonase and yielded comparable amounts of target proteins upon release by linker cleavage when compared to harsh boiling of the beads in SDS-buffer. Thus, the use of this DNA linker allowed for the elution of

enriched proteins under mild conditions (Tris buffer, pH 7.5, 37°C, 8 h). Upon cell lysis, enrichment on streptavidin coated beads and elution by benzonase cleavage of the DNA linker they were able to identify 36 hits from lysates obtained from the cells treated with Ac₄ManNAl, whereas no enrichment was observed in lysate from untreated cells.

As most linker systems require neutral to basic pH, mildly oxidative linker cleavage allows for product elution at pH values that are mildly acidic. Periodate-mediated diol cleavage is a well characterized reaction and applied in the field of protein chemistry such as for antibody labelling.[443-447]

An example for the utility of this reaction was provided when a building block applicable for SPPS was applied for the specific enrichment of intracellular pepstatin-sensitive aspartic proteases from primary human samples (**Scheme 33 B**).[448] Aspartic proteases of the pepsin family form a group of enzymes (cathepsin D and E, napsin A) that contain a signal sequence for translocation to the endoplasmatic reticulum (ER).[449, 450] Remarkably, they have pH optima ranging from 3 to 6,[451] while cathepsin E is assumed to have also activity at neutral pH with differing substrate specificity.[452, 453] For the enrichment of all three proteases from primary human samples, Kalbacher *et al.* used the periodate linker, which can be cleaved in the same buffer used for binding and washing to avoid pH-dependent release. As preliminary mass spectrometry data showed higher protein identification scores and sequence coverage of specifically eluted samples in comparison to non-cleaved samples, which in addition contained higher amounts of contaminants, the value of this oxidative cleavage strategy applicable at slightly acidic pH was highlighted.
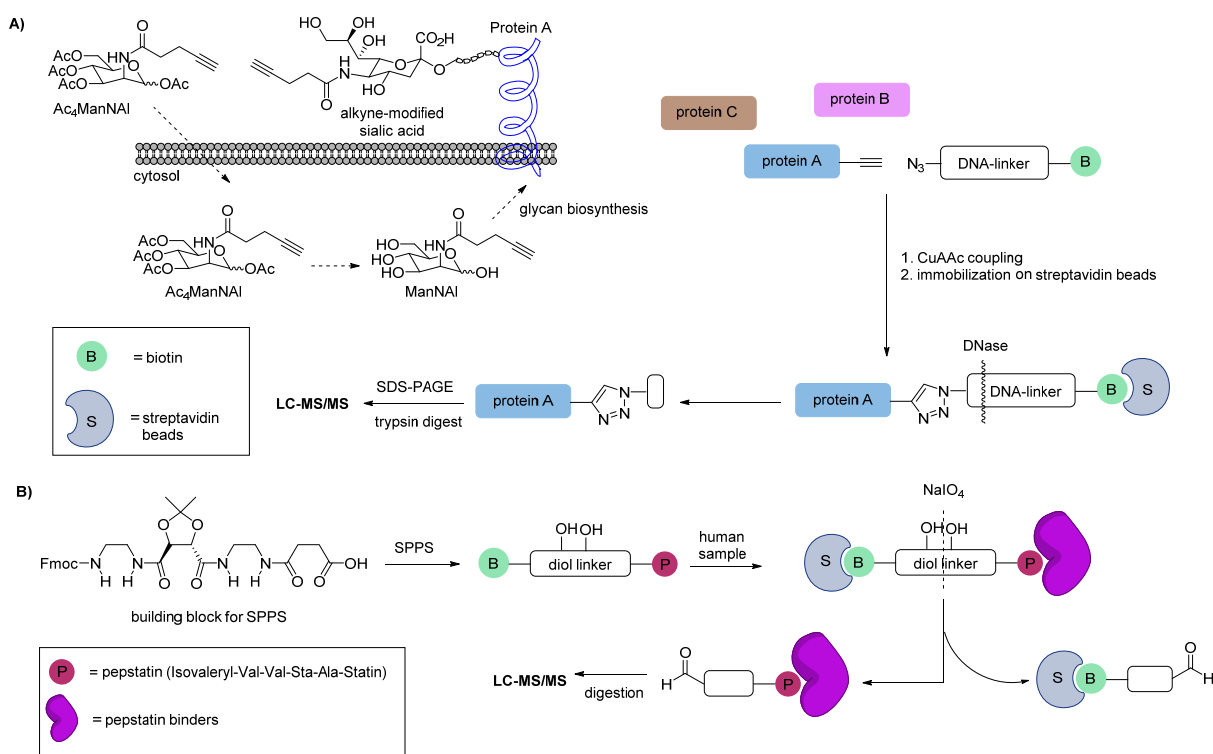
Scheme 33: **A)** Identification of sialylated glycoproteins by MS/MS from lysates of HL60 cells. Purification of sialylated proteins was accomplished with a DNA-linked biotin tag that was cleaved off by DNase;[438] **B)** application of a cleavable diol linker for the identification of pepstatin binders.[448]

2.4.4.2 Quantitative chemical proteomics

In addition to hit identification in proteomic research, a TEV protease recognition domain was used as cleavage site for quantitative proteomics of pro-labeled peptides in a platform termed isotopic tandem orthogonal proteolysis activity based protein profiling (isoTOP ABPP).[454] E. Weerapana *et al.* have recently explored the use of a dithionite cleavable azobenzene linker in place of the TEV-protease recognition site (Azo light and Azo heavy, **Figure 16**).[455] They argued that a chemically cleavable analogue could offer certain advantages, such as inexpensive materials, reduced cleavage times and increased robustness to variations in cleavage conditions. In their approach, Weerapana and co-workers created a system that allowed cleavage of isotopically tagged proteins in just 2 h at room temperature compared to 30°C overnight required for TEV cleavage. The used tag contained an azide for click chemistry conjugation to alkyne-functionalized proteins, an isotopically light or heavy valine for quantification by mass spectrometry, a dithionite-cleavable azobenzene linker and a biotin for enrichment on streptavidin coated beads. Thus, they were able to demonstrate a decrease of background noise

of probes that were cleaved with sodium dithionite compared to samples that were directly subjected to tryptic digest for quantitative mass spectrometry analysis during immobilization on streptavidin coated beads.

Azobenzene linkers were initially used for protease-directed activity-based probes,[456, 457] and where then further developed to click-chemistry-compatible compounds that were used to identify lipoproteins,[458] *S*-palmitoylated,[459] acetylated[460] and newly synthesized proteins.[461]
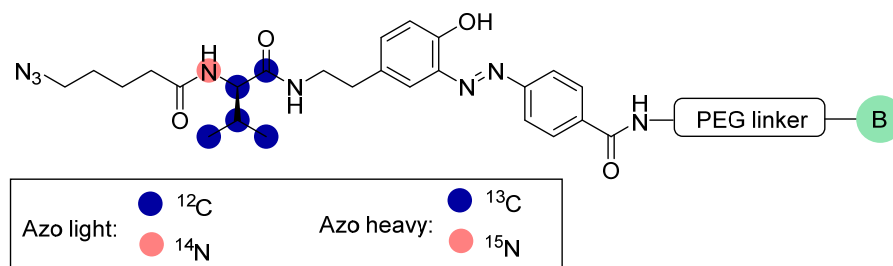

Figure 16: Structure of the azobenzene linker used for quantitative proteomics.[455]

2.4.4.3 Chemical processing of peptides and proteins

An example of peptide processing by means of a traceless linker is given by Mootz *et al.* providing a genetically encoded, photoactivatable intein for the controlled production of cyclic peptides.[462] The approach they followed is termed split-intein circular ligation of peptides and proteins (SICLOPPS), which is used to produce large cyclic peptide libraries. But the method suffers from the limitation of spontaneous protein splicing, which leads to product formation inside cells, rendering peptide isolation inconvenient and precluding traditional *in vitro* assays. Mootz *et al.* improved this method by installing the photocaged tyrosine derivative ortho-nitrobenzyltyrosine at an internal non-catalytic position of the intein, which allowed the isolation of stable intein constructs (**Scheme 34 A**). After the expression, the target protein was isolated on streptavidin beads by means of a streptavidin-binding peptide or a His-Tag and cyclization was induced by the irradiation with UV-light (366 nm) for four minutes. Thus, they have created a traceless linker that serves as a cyclization inducer.

Other scientists have also used inteins as traceless linkers, such as in the work by Petersson *et al*, in which unnatural amino acids were introduced to the C-terminus of proteins by stop codon suppression.[463] This leads sometimes to the formation of truncated side products. To efficiently separate their desired protein from unwanted material, they co-expressed their POIs with a

His-tagged intein, which did not disrupt the native fold of the POI. When they purified their His-tagged target proteins on Ni-NTA columns, they were able to create the corresponding thioester by the addition of β-mercaptoethanol either on or off column. Hydrolysis of the thioester yielded finally the purified product with a C-terminal carboxylic acid (**Scheme 34 B**).
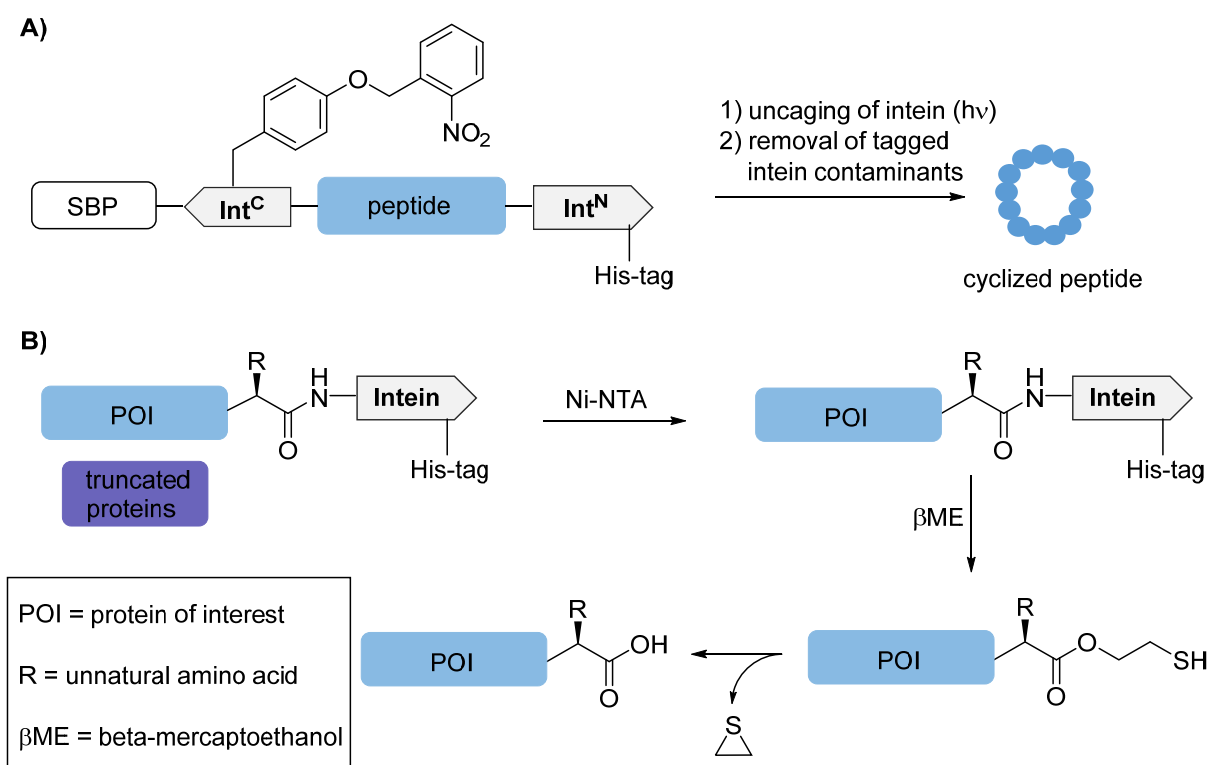
Scheme 34: **A)** Isolation of a peptide containing caged C- and N-terminal inteins.[462] Upon UV-light irradiation, a circular antimicrobial peptide is formed. **B)** Expression of proteins containing unnatural amino acids in the C-terminal region as intein fusions. Thioester formation with β-mercaptoethanol was followed hydrolysis, which yielded the POI with a C-terminal acid.[463]

2.4.4.4 Purification and concomitant labeling of proteins

Tsourkas *et al*. have recently introduced the so called sortase-tag expressed protein ligation (STEPL, **Scheme 35 A**).[464] They expressed a single construct with the amino acid sequence LPXTG (X can be any amino acid except proline), (GGS)$_5$ linker, sortase A and a His-tag respectevily to the C-terminus of a given POI. The flexible (GGS)$_5$ linker gives the sortase domain the conformational freedom to recognize the LPXTG sequence.[465] Upon the addition of calcium, any given cargo (drugs, imaging agents, nanoparticles, etc.) that bears an

N-terminal glycine is ligated to the POI, while simultaneously, the rest of the sortase chimera is cleaved off and can be pulled out by Ni-NTA. Thus Tsourkas *et al.* have created a method that works site-specifically and stoichiometrically as purification and conjugation are co-dependent. They demonstrated the systems flexibility and utility by conjugating *Her2/neu* and *EGFR*-targeting affibodies to fluorophores for imaging or an azide for subsequent copper-free click chemistry reactions with azadibenzocyclooctyne (ADIBO)-functionalized superparamagnetic iron oxide nanoparticles.

Another elegant one-step site-specific labelling strategy was developed by Chilkoti *et al.*[466] As in the previous study they used a sortase tag, this time in tandem with ELPs (see section 2.3), which in turn enabled them to obtain recombinant fusion protein without chromatography or affinity purification (**Scheme 35 B**). The sortase allowed the covalent coupling of an extrinsic moiety to the purified target protein and was removed post purification by ITC.

It is further stated that this method provides means to obtain pure recombinant and labelled proteins in a simple, robust and scalable fashion. To demonstrate the flexibility of their system, the chemotherapeutic drug camptothecin (CPT) was coupled to tumor necrosis factor-related apoptosis-inducing ligand (TRAIL; amino acids 114-281), which generated a hybrid anticancer agent. Despite the observation that no beneficial effects were achieved by TRAIL co-treatment with CPT, the method still provides a state of the art example of protein purification with concomitant labelling.
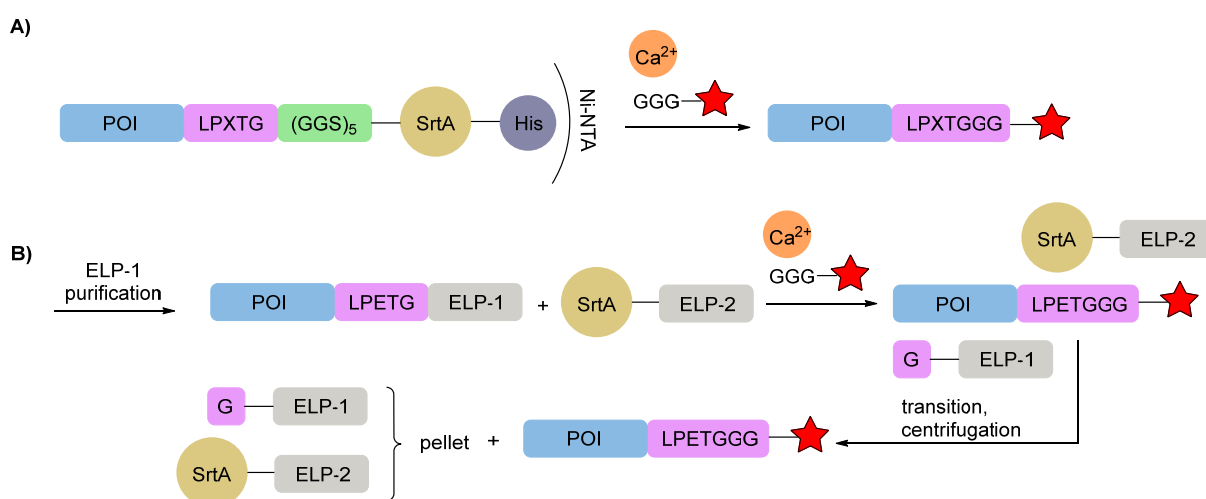
Scheme 35: **A)** Sortase-tag expressed protein ligation (STEPL);[464] **B)** reaction catalyzed by SrtA-ELP for recovery and labeling of POIs from binary ELP fusions.[466]

Verhelst *et al.* have synthesized a set of trifunctional biotin reagents for protein labelling, capture and release.[467] They explored linkers that can be cleaved by tartrate (vicinal diol), sodium dithionite (diazobenzene), hydroxylamine (bisaryl hydrazone) or reductive conditions (disulfides). In addition they established a novel linker, based on the 1-(4,4-dimethyl-2,6-dioxocyclohex-1-ylidene)ethyl (Dde) group (**Scheme 36 A**). This particular group is normally used for the protection of ε-amines of lysine in SPPS and can be cleaved with 2% hydrazine or 0.05% SDS in buffer. Their linker systems contained also azides that can be addressed for click chemistry labelling. When fluorophores were attached to the POIs, they were able to monitor the depletion of labelled cathepsins from a proteome by using immobilized streptavidin.

Otaka *et al.* have worked on a related concept using a linker containing a thiol cleavable *p*-nitrobenzenesulfonyl group (*p*Ns) (**Scheme 36 B**).[468] In combination with biotin they were able to enrich their target proteins in a similar manner as with conventional cleavable purification tags, but could moreover selectively label their target so that it could be distinguished from contaminated non-target proteins. Remarkably, their system can be switched on by thiol additives through deprotection of the *p*Ns-group, leading to a chemical reaction cleaving the linker and rendering an aminooxy group on the target, available for chemoselective labelling with aldehyde derivatives. In this study, an alkynylated enolase was used as the target protein.
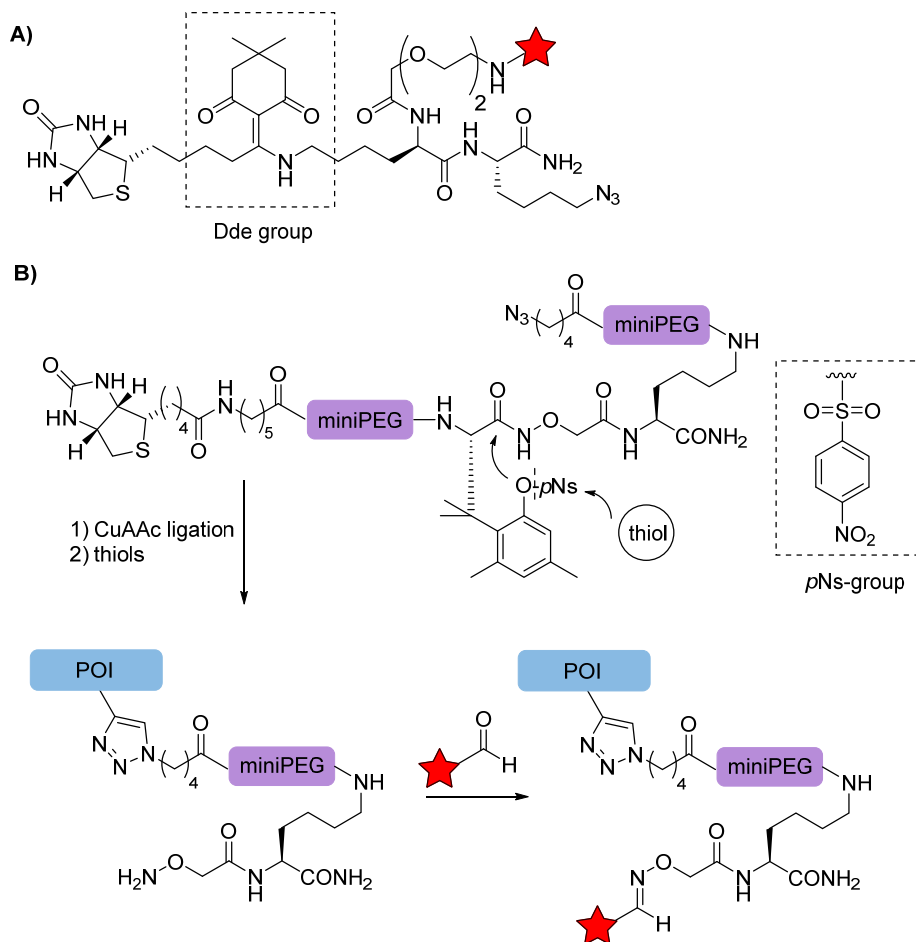
Scheme 36: **A)** Trifunctional linker with cleavable Dde group bearing a fluorophore, a biotin for purification and an azide available for click-chemistry based conjugation to a target protein;[467] **B)** ligation, purification and cleavage of the linker renders an accessible hydroxylamine, which can react with molecules bearing aldehydes.[468]

2.4.4.5 Solubility of proteins after expression and purification

Cleavable linkers and purification tags can be used to alter the solubility of a certain target protein. In this context Zhang *et al.* have found a straightforward way to produce the protein APRIL, a proliferation-inducing ligand.[408] Initially, APRIL was expressed as fusion protein with an ELP to allow its purification. After the expression, the scientists were not able to separate APRIL after ITC (see section **2.4.2.2**) from the cleaved ELP tag. To overcome this obstacle, they inserted a small ubiquitin-related modifier protein (SUMO) linker in between the ELP and the protein APRIL, which facilitated the separation of ELP-SUMO and APRIL immensely due to enhanced solubility. SUMO was cleaved off by SUMO protease and rendered biologically active human APRIL with normal biological activity on Jurkat cells.

This principle was reversed by Lin *et al*, who were interested in the production of the antimicrobial peptide (AMP) histatin 1.[469] Histatins and their derivatives have been commonly recombinantly expressed in *E. coli* by fusion technology and purified by a conventional GST-tag.[470-472] Peptide fusions were purified by traditional affinity chromatography, followed by cleavage using cyanogen bromide or thrombin and further purified by reversed phase HPLC.[471-474] In contrast, they have used a cleavable self-aggregating tag consisting of a self-cleavable intein and a self-assembling peptide ELK16 (I-ELK16). At first, the insoluble aggregate histatin1-I-ELK16 was produced and separated from all soluble material. Upon intein cleavage with dithiotreitol (DTT) the peptide was solubilized with a purity of 70%. A final HPLC run rendered the peptide in high purity and with a comparable yield to attempts where the GST-tag was used. The antimicrobial activity of the peptide was retained throughout the process. This technique worked faster when compared to the GST-tag approach and is thus a useful tool for protein expression and purification.

Wu and his co-workers have used a MBD-tag to solubilize the microtubule associated protein light chain 3 (LC3).[475] They report the first synthesis of a phosphatidylethanolamine (PE) lipidated LC3 using the techniques of lipidated peptide synthesis and EPL. In many cases, lipidation renders proteins insoluble and makes their handling difficult. Wu *et al.* have used a simple TEV-cleavable MBD-tag to facilitate the handling of lipidated proteins in the absence of detergents and allows the ligation under folding conditions. The resulting MBD-LC3-PE conjugate was thus soluble in buffer without detergents and could be used for later studies.

Recently, a novel toolbox approach was published by Portal *et al*, where multifunctional probes were attached to biomolecules either by maleimide-coupling or by EPL (**Figure 17 A**). This helped to solubilize proteins with low solubility for further analysis.[476] At the C-terminal site, the reagents were equipped with a photocleavable linker attached to a purification tag, which also allowed for probe enrichment upon successful labeling (**Figure 17 B**). Thereby, Portal *et al.* were able to produce HuR protein, which was soluble enough to carry out confocal fluorescence spectroscopy.
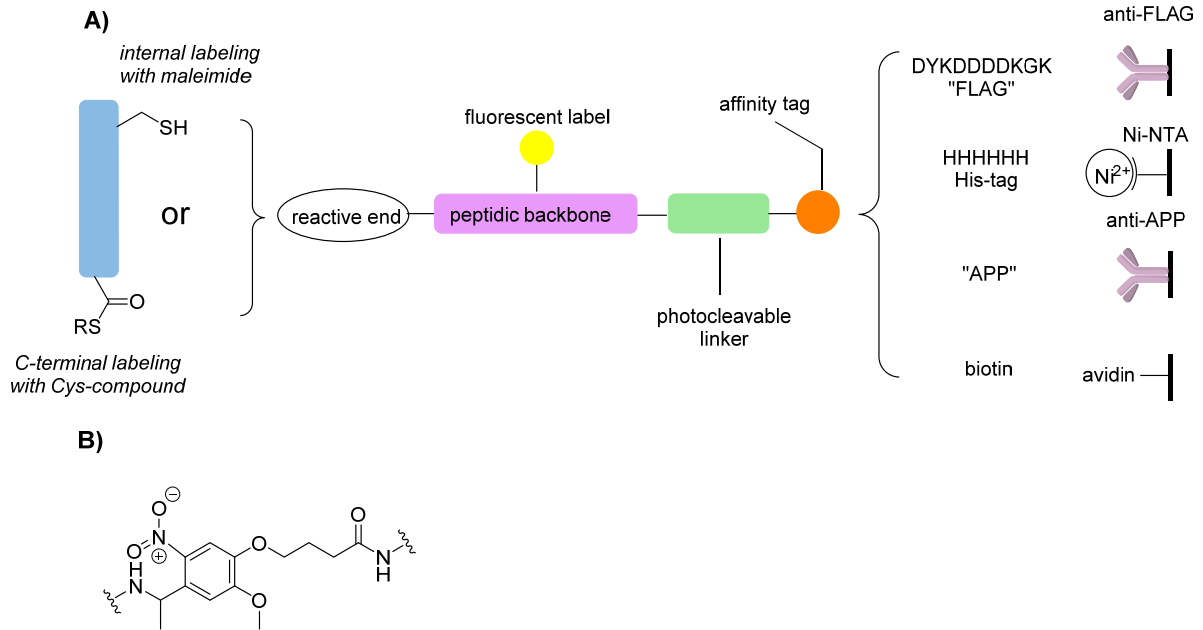
Figure 17: **A)** Protein labeling by multifunctional toolbox compounds either internal through maleimide conjugation or C-terminal through EPL. These reactive ends are connected to a peptidic backbone, which is conjugated to a fluorescent label and a photocleavable linker bound to an affinity tag (FLAG-tag, His-tag, APP-hexapeptide or biotin); **B)** chemical structure of the photocleavable linker.

2.5 Chemical access to ubiquitinylated proteins

Abstract (as published online): Synthetische Todesküsse: Chemischer Zugang zu ubiquitinierten Proteinen.

Summary of content: The article provides the reader with state-of-the-art methods on how to synthetically generate ubiquitinylated proteins by chemical means. A brief summary of the biological function of ubiquitination is given, followed my synthetic routes on how to obtain ubiquitinylated proteins. The article summarizes techniques to synthesize native ubiquitin isopeptide linkages, as well as routes for the synthesis of isopeptide-mimetics. Many different chemoselective strategies of bioconjugation are shown, highlighting the versatility of chemical approaches to obtain ubiquitinylated proteins.

Responsibility assignment: The topic of this review article was chosen by Prof. Christian P. R. Hackenberger, whereas the actual content was elaborated by Oliver Reimann.

3. OBJECTIVES

The impact of specific phosphorylation and *O*-GlcNAcylation patterns on tau protein structure and function is largely unknown.[5] In consequence, two distinct goals are defined in the context of this thesis:

(i)   development of synthetic pathways to generate homogeneously phosphorylated and *O*-GlcNAcylated versions of tau that allow for their structural and functional characterization

(ii)   generation and characterization of monoclonal antibodies targeted against AD relevant phosphorylation sites on tau to study cellular distribution and diagnostic potential

(i) The generation of homogeneously phosphorylated full-length proteins is a prevalent challenge for molecular biologists, biochemists and chemists. As short proteins up to a length of about 50 amino acids are often synthesized by SPPS, other techniques have to be applied for longer peptides. Small to middle-sized proteins can be generated by NCL, where two or more synthetic peptide fragments are ligated to yield the corresponding protein. For larger proteins, the synthetic effort becomes often too high and EPL is applied to generate proteins that can be equipped with functional groups in their synthetic parts (see chapter **2.3**).
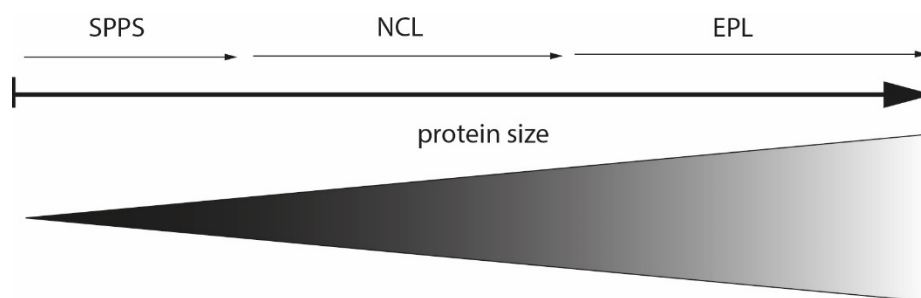
Figure 18: Techniques, usually applied for synthesis of proteins, depending on the size of the target.

The tau protein becomes highly phosphorylated in AD and further forms aggregates, finally assembling into NFTs. Up to this day, the implications of site-specific phosphorylations on the structure and function of the tau protein remain largely unknown. Moreover, tau *O*-GlcNAcylation was previously shown to have a regulatory effect on tau phosphorylation, but its role in AD is still under debate. In AD, both of these PTMs occur in the PHF-1 epitope

(Ser396/400/404) in AD diseased brains, which was shown by mass spectrometry analysis of brain material from AD patients or transgenic mouse models of AD.[4] To study the distinct impact of site-specific PTMs on tau, the generation of homogeneously phosphorylated and *O*-GlcNAcylated tau proteins is necessary. To target a larger protein like tau, which consists of 441 amino acids in its longest isoform, protein semisynthesis by EPL is the method of choice. This technology offers the unique possibility to site-specifically place PTMs like phosphorylation or *O*-GlcNAcylation onto proteins, by which the chirality of the decorated amino acid is retained (see section **2.3**). Therefore, new synthetic pathways have to be developed that allow for the generation and isolation of full-length tau bearing post-translational modifications at specific sites.

(ii) To study tau in a cellular context, antibodies are often applied, as they offer analytical, diagnostic and therapeutic potential to investigate and even fight AD on a molecular level (see sections **2.2.9** and **2.2.10**). Several antibodies targeted against phospho-tau are already available, but their great potential seems not exceeded yet (see sections **2.2.9** and **2.2.10**). Moreover, there is no antibody available addressing the tri-phosphorylated PHF-1 epitope of tau. Therefore, the generation and evaluation of antibodies, targeting tau tri-phosphorylated in PHF-1 is in the scope of this work.

GOAL (i) – NEW SYNTHETIC PATHWAYS TO GENERATE TAU PROTEINS HOMOGENEOUSLY MODIFIED BY POST-TRANSLATIONAL MODIFICATIONS

Project 1: A new synthetic route toward tri-phosphorylated C-terminal tau peptide by means of NCL

The C-terminal fraction of tau contains the AD relevant phospho-epitope PHF-1, where three phospho-Ser residues are present in close proximity to each other. Previously, the linear synthesis of the 52 amino acid long fragment for further use in EPL did not work due to low coupling efficiency, induced by bulky phosphorylated amino acids. In consequence, a synthetic route based on NCL needs to be established that provides access to this tri-phosphorylated peptide.

Project 2: Development of a traceless linker for the affinity purification of ligation products

To study subtle changes on tau induced by PTMs, any additional group, such as a purification tag, should be removed from the protein scaffold. Previously, an irreversibly attached biotin-tag was used to purify semisynthetic tau proteins.[123] This purification tag may also have an impact on structure or function of the protein, which makes a post-purification removal of the tag by a traceless linker desirable.

Project 3: Semisynthesis of phosphorylated and *O*-GlcNAcylated tau proteins and their purification by a traceless affinity tag

Building on accomplishments of projects 1 and 2, the aim is to apply the newly developed methods to generate tag-free semisynthetic post-translationally modified versions of the tau protein. The expressed protein portion of tau should be generated with isotopic labeling, using either ^{15}N- or ^{15}N-/^{13}C-labeling. The generation of these partially labeled proteins shall allow their structural investigation by NMR.

GOAL (ii) – GENERATION AND CHARACTERIZATION OF NEW MONOCLONAL ANTIBODIES TARGETED AGAINST PHOSPHO-TAU

Project 4: Generation of antibodies targeted to the tri-phosphorylated PHF-1 epitope of tau and assignment of the specificity of their binding

Monoclonal antibodies targeted against phospho-species of tau offer great potential for the investigation of this protein in pathways of AD and further offer higher specificity for AD in contrast to monoclonal antibodies targeted against total tau (**Table 4**). It thus may be assumed that the generation of monoclonal antibodies against tau phosphorylated in PHF-1 offers great potential to get new insights into AD. To ensure that the right conclusions are drawn from experimental results obtained by the new antibodies, their proper characterization is crucial and is a goal of this work.

Project 5: *In cellulo* and *in vivo* **studies with the new antibodies and evaluation of the diagnostic potential**

Tau mislocalization is often associated with its phosphorylation (see sections **2.2.3** and **2.2.4**). A goal of this work is to study these issues in a cellular context with the newly obtained antibody clones. Moreover, further insights should be obtained by the study of tau phosphorylated in PHF-1 *in vivo*, where *C.elegans* will serve as a model system. A relatively short life span of approx. 2 weeks makes these animals suitable to study age-dependent changes of tau phosphorylation, which can be detected by antibodies. Moreover, the diagnostic potential of these new antibodies will be evaluated in CSF material of AD patients.

GOAL (iii) – FUNCTIONALIZATION OF CYS-CONTAINING POLYMERS BY THE NCL REACTION

Project 6: Two different polymer backbones with Cys-functional groups modified by NCL

Polymer-peptide conjugates have been proven useful for applications in multivalent display, enhancement of solubility or the formation of gel-type structures.[477-479] Therefore, the applicability of NCL reactions to novel Cys-functionalized polymer scaffolds has great potential and will be explored in this thesis by a proof-of-principle study. It is further intended to control the degree of polymer functionalization by the addition of different equivalents of peptide.

4. RESULTS & DISCUSSION

4.1 Tri-phosphorylated C-terminal tau via a native chemical ligation at an Asn/Val junction
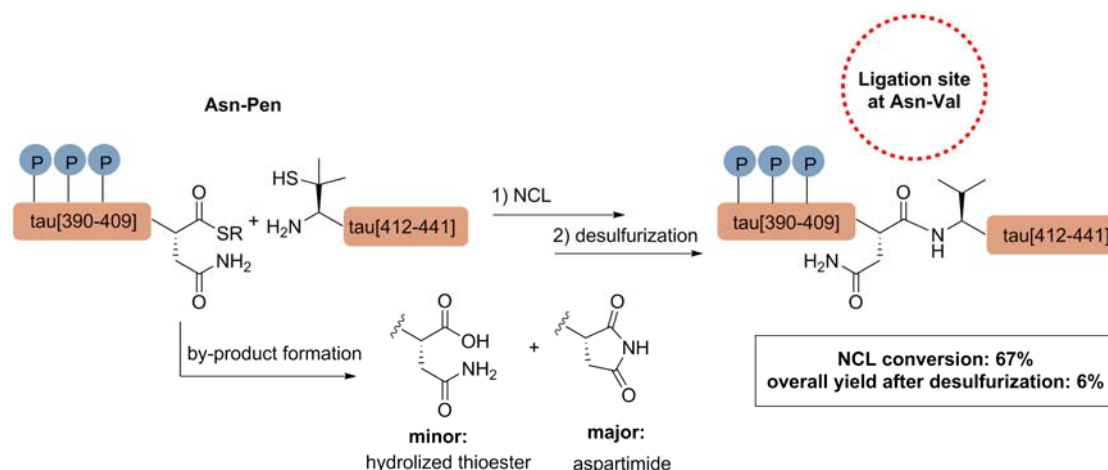
Figure 19: Native chemical ligation between Asn-thioesters and mercaptovaline, followed of radical initiated homogeneous desulfurization. The ligation works, but provides precedence of problems due to massive by-product formations, such as thioester hydrolysis and predominantly aspartimide formation.

Abstract: We present the successful native chemical ligation (NCL) at an Asn-Val site employing β-mercaptovaline and subsequent desulfurization in the synthesis of native phosphorylated C-terminal tau, relevant for Alzheimer's disease related research. Despite

recent progress in the field of NCL, we illustrate limitations of this ligation site that stem from thioester hydrolysis and predominantly aspartimide formation. We systematically investigated the influence of pH, temperature, peptide concentration and thiol additives on the outcome of this ligation and identified conditions under which the ligation can be driven toward complete conversion, which required the deployment of a high surplus of thioester. Application of the optimized conditions allowed us to gain access to challenging tri-phosphorylated C-terminal tau peptide in practical yields.

Summary of content: The C-terminus of tau harbors an epitope, which is highly phosphorylated in Alzheimer's disease. This epitope is called paired helical filament epitope 1 (PHF-1) and is comprised of three Ser residues in close proximity to each other (Ser396/400/404). As linear synthesis of the 52 amino acid long tri-phosphorylated C-terminal peptide tau[390-441] failed, it was intended to synthesize this challenging peptide by NCL. As in the C-terminal portion of the tau protein, Cys residues that enable NCL are often absent. Thus, a site needed to be identified, suitable for NCL.

An Asn/Val junction was investigated, which could be beneficial for the synthesis, since the N-peptide, bearing the three phosphorylation sites of the PHF-1 epitope, is of rather short length (21 amino acids). The synthesis of the 21 amino acid long N-peptide thioester proceeded smoothly and was high yielding. Moreover, the other C-peptide, bearing a biotinylated Lys, was efficiently synthesized in good yields. Ever since the discovery of MPAA as a thiol additive in NCL reactions, ligations at Asn/Cys junctions were reported to work well in NCLs without the occurrence of major side-products. Since no Ala was available in close proximity on the C-terminal side of the PHF-1 epitope, a ligation with a thiolated Val (commercially available β-mercaptovaline, also called penicillamine (Pen)) residue was aimed at, which would yield native Val at the ligation site upon homogeneous desulfurization.

Instead, massive aspartimide formation was observed, even if highly activating aryl thiols such as thiophenol or MPAA were used. Thus, a screening on NCL conditions was performed, varying the pH, thiol additives, reaction times, temperature and peptide concentration. After this screening, ligation conditions were identified, by which the C-peptide was fully consumed. In these optimized reaction conditions, thiophenol was used as a thiol additive and the pH was

set at 8.5. Temperature enhancement did not lead to superior ligation results and thus, the reaction was carried out at room temperature over 29 h. Despite the almost quantitative conversion of the C-peptide, the precious tri-phosphorylated N-peptide thioester had to be used in a fourfold excess to reproducibly generate conversions of around 90% of the C-peptide. This observation displayed a precedence not described in the literature and indicates that ligations with such slow kinetics as with sterically hindered Pen are unfavorable to use, when Asn thioesters are part of the ligation. This is due to the relatively high pH, required for the reaction to proceed, which further triggers the aspartimide formation and thioester hydrolysis. In summary, optimized NCL reaction conditions for Asn/Val ligations are presented, achieving conversions of over 90% of the C-peptide. Therefore, four equivalents of the Asn-thioester peptide were required. This enabled access to tri-phosphorylated C-terminal tau[390-441], but very high material expanses were required and precious peptide was sacrificed. This observation is likely to be transferred to thioesters at Asp, Gln and Glu, which are all known to form cyclized by-products. It might also be possible, that other thiolated amino acids used in NCL reactions and subsequent desulfurization have slower reaction kinetics than Cys and thus, cyclized by-products could become more prevalent.

Outlook: The optimization of this ligation site was successfully completed, but further applications with this particular NCL junction are not recommended. The use of another ligation site to obtain this particular peptide is highly recommended, due to high cost and time expenses.

Responsibility assignment: The outline of this project was provided by Prof. Christian P. R. Hackenberger. The experiments were conducted by Oliver Reimann and Maria Glanz. Oliver Reimann carried out initial ligations and established the peptide synthesis. The screening for optimal reaction conditions was performed by Maria Glanz, whereas the final application of the optimized reaction conditions to obtain tri-phosphorylated C-terminal tau was mainly performed by Oliver Reimann.

4.2 Traceless purification of ligation products with concomitant desulfurization

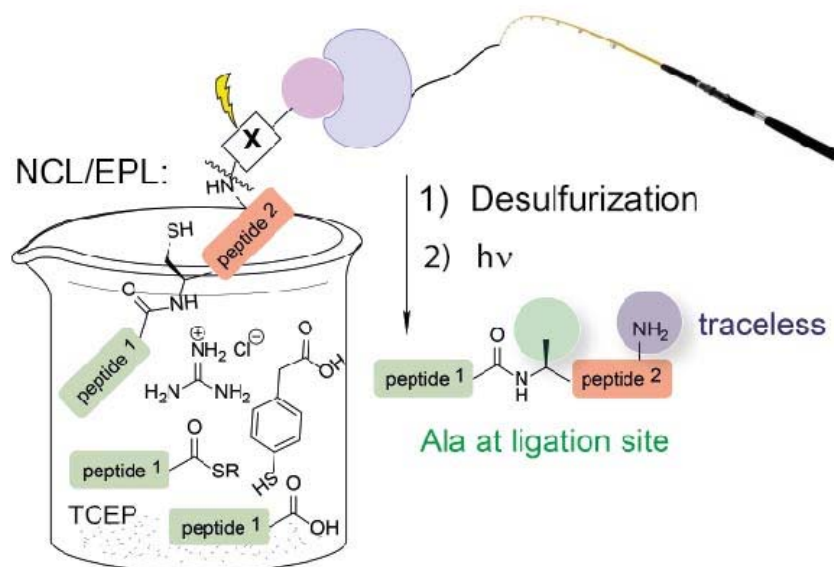This chapter was published in the following journals:

Figure 20: Traceless purification of ligation products allows for a concomitant desulfurization on resin, thus providing a facile route to obtain pure desulfurized ligation products in high purity without the need of HPLC purification.

4. RESULTS & DISCUSSION

Abstract: We present a novel strategy for the traceless purification and synthetic modification of peptides and proteins obtained by native chemical ligation. The strategy involves immobilization of a photocleavable semisynthetic biotin–protein conjugate on streptavidin-coated agarose beads, which eliminates the need for tedious rebuffering steps and allows the rapid removal of excess peptides and additives. On-bead desulfurization is followed by delivery of the final tag-free protein product. The strategy is demonstrated for the isolation of a tag-free Alzheimer's disease related human tau protein from a complex EPL mixture as well as a tri-phosphorylated peptide derived from the C-terminus of tau.

Summary of content: In this article, a new method is presented that facilitates chemical work-up and purification of NCL and EPL reactions. A bifunctional photocleavable linker is introduced to peptides during SPPS. Therefore, a Lys residue with an orthogonal Alloc-protecting group was inserted into the peptide sequence, thus allowing for the site-specific introduction of the bifunctional linker on resin via a simple incubation with base. In a next step, biotin was coupled to the linker, followed by the cleavage of the full-length peptide off the resin by standard TFA treatment. The applicability of the new tag and efficacy of its cleavage was tested by an incubation on streptavidin coated agarose beads of a test peptide, equipped with the photocleavable biotin (PCB) and a fluorophore. A highly efficient immobilization of the biotinylated peptide on the streptavidin coated agarose beads was demonstrated and a convenient cleavage of the linker at a wavelength of 297 nm and an irradiation time of only 5 min was shown, providing the tag-free peptide with an isolated yield of 82% of unbiotinylated native peptide. To further show the potential of the new linker, the full-length tau protein was generated by semisynthesis, whereas the synthetic C-terminal portion of the protein contained the photocleavable biotin group. After the expressed protein ligation, excess peptide (5.8 kDa) was removed from the reaction mixture by spin-filtration (30 kDa cutoff) and the resulting mixture of tau[1-389] and tau[1-441]-PCB were incubated on a suitable amount of streptavidin coated agarose beads. Subsequent washes and a final irradiation by UV-ight of $\lambda = 297$ nm delivered the desired protein in good yield. The procedure allowed for the release of the desired protein in a suitable buffer and made further re-buffering steps unnecessary. It was further shown by western blot experiments that the correct full-length tau

was present, which was free of biotin, thus giving proof to the reliability of the method. This was the first report of tag-free semisynthetic tau.

We reasoned further that radical initiated homogeneous desulfurization chemistry can be applied to peptides or proteins, while they are immobilized on the streptavidin coated agarose beads, as streptavidin is free of Cys. This hypothesis was tested, when two peptides with sequences of the tau protein were reacted with each other by NCL, whereas the C-peptide was equipped with a N-terminal Cys instead of a native Ala. Moreover, the C-peptide contained the PCB group, which allowed for the direct immobilization of the target ligation product on streptavidin coated agarose beads upon slight dilution. It was shown that desulfurization under homogeneous conditions was possible, while the peptide was immobilized on the beads. This procedure yielded highly pure ligated and desulfurized peptide in an extremely high yield and extremely low time expenditure, as no HPLC purification was required. This new technology enabled the generation of C-terminal tau[390-441], containing three phosphorylations on Ser residues, relevant to Alzheimer's disease in good yields.

In summary, the developed technology allows for a straightforward purification and desulfurization of ligation products. Thereby, long and challenging peptides of the tau protein can be obtained in good yields. The application of this method delivered the first tag-free semisynthetic tau protein.

Outlook: As the newly developed method provides an efficient and convenient route to obtain pure ligation products without HPLC, the semisynthesis and purification of tau peptides and proteins in larger quantities remains a challenge. However, this method should help to facilitate the process of purification and chemical work-up in future attempts to study the impact of post-translationally modified tau.

Responsibility assignment: The original design of the project was provided by Christian P. R. Hackenberger and Caroline Smet-Nocca. Moreover, Caroline Smet-Nocca has initially provided recombinant tau proteins to study and probe the EPL reaction, but the construct used in the presented work was generated by Oliver Reimann. All reported experiments were conducted by Oliver Reimann.

4.3 Incorporation of Lys equipped with a photolinker into proteins by amber suppression

4.3.1 Introduction to the incorporation of caged amino acids by amber suppression

Photocaged proteins can be used to control the temporal and spatial activity of a protein in a noninvasive manner, which can help to shed light into a variety of cellular processes.[480, 481] It was demonstrated that photocaged amino acids can be genetically encoded into *E.coli* and *S.cerevisiae* by using orthogonal nonsense suppressor tRNA/aminoacyl-tRNA synthetase pairs (see section **2.3.9**). Photocaging groups were reported for Cys,[357] Ser,[356] Lys[482] and Tyr[483] residues. An impressive example of the potential of this technology was provided by Edward Lemke and the P. G. Schulz lab, as they were able to photoinitiate the phosphorylation of Pho4 by the cyclin-CDK complex through uncaging and monitor the kinetics of protein trafficking in real time.[480]

4.3.2 Objective of the project

The goal of this project is the synthesis of a Lys derivative, functionalized with the bifunctional photolinker, which was published previously and described in section **4.2**. A Lys that is connected to this photolinker will be termed PC-Lys (**Scheme 37**), standing for photocleavable-Lys, in analogy to the previously published PCB-Lys.[484]

The introduction of a bifunctional photocaged amino acid PC-Lys would allow for a site-specific incorporation of a functional unit into a protein of choice by the so called copper catalyzed azide-alkyne cycloaddition (CuAAC) and further for the elegant traceless cleavage of this unit, if desired in a temporal resolution (**Scheme 37**). Within the timeframe of this Ph.D. thesis, the synthesis of the photocaged Lys derivative was to be established and the incorporation of the building block into a protein by amber stop codon suppression shall be demonstrated in a proof of principle experiment. Therefore, a collaboration with the group of Prof. Edward Lemke was closed down.
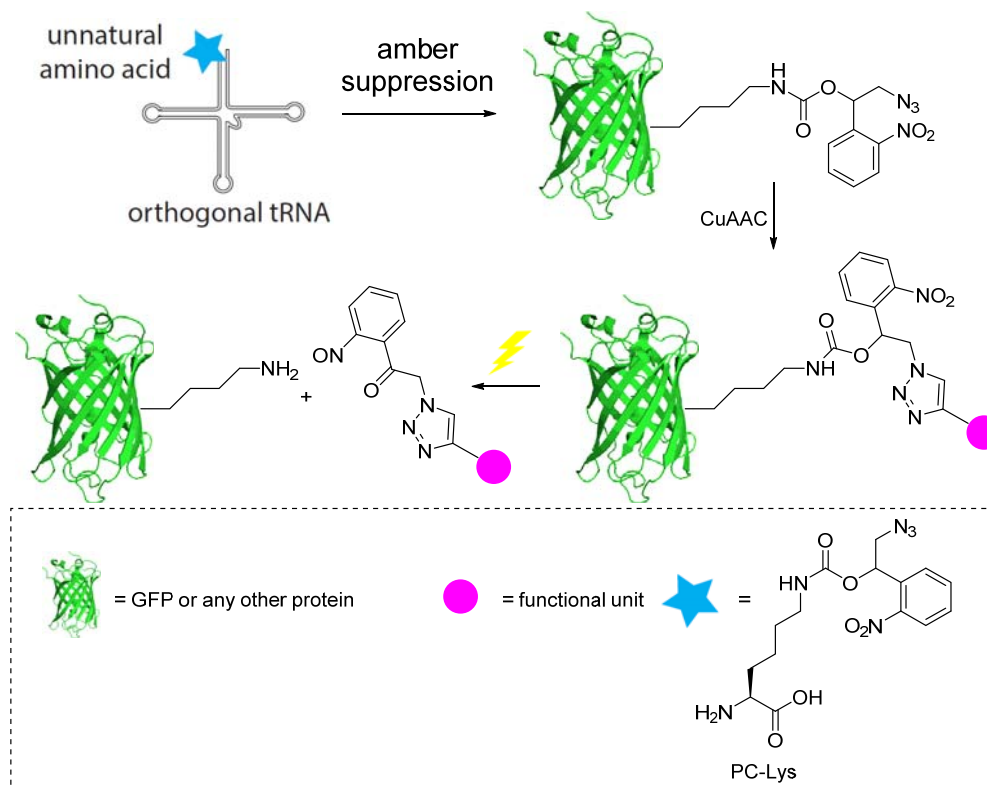
Scheme 37: Introduction of photocaged Lys (PC-Lys) with an azide function into GFP by amber suppression allows the site-specific incorporation of a functional unit (pink ball). At a given time, the group can be cleaved off the protein by UV-light irradiation. The strategy should be in principle applicable to any protein.

4.3.3 Results and discussion

The synthesis of the building block was attempted by two different synthetic routes (**Scheme 38**). At first, an on-resin approach was conducted, which should deliver the Lys derivative without the need of cumbersome purification. Therefore, Fmoc-Lys with an ε-NH$_2$-Alloc protection was coupled onto Wang resin (see section **7.2.1** for experimental details). A subsequent Pd-catalyzed cleavage of the Alloc group rendered a free ε-NH$_2$ group on the side-chain of the Lys amino acid (**1**). The activated photolinker (**2**) was subsequently coupled to this free amine by simple incubation with the resin in DMF in the presence of DIPEA as deprotonating, non-nucleophilic base. A final cleavage by TFA and a final purification by preparative HPLC yielded the desired product **3** in high purity. A total amount of only 12 mg (0,032 mmol, 32%) was obtained from a 0.1 mmol scaled reaction by the on-resin approach. In order to obtain higher amounts of about 250 mg that are required for amber stop-codon

suppression, the material expenditure would be vast and thus, another route to synthesize the desired compound was pursued.

In a publication by Peter G. Schultz and his coworkers, a nitro-benzyl chloroformic acid ester was coupled to an unprotected side-chain of Lys, while the N-terminus of the amino acid was Boc-protected.[482] Accordingly, the synthesis of the desired Lys derivative (**3**) was carried out with slight alterations, which gave the desired product in a high yield of 39% after a simple precipitation, rendering HPLC purification redundant (see section **7.2.2**).
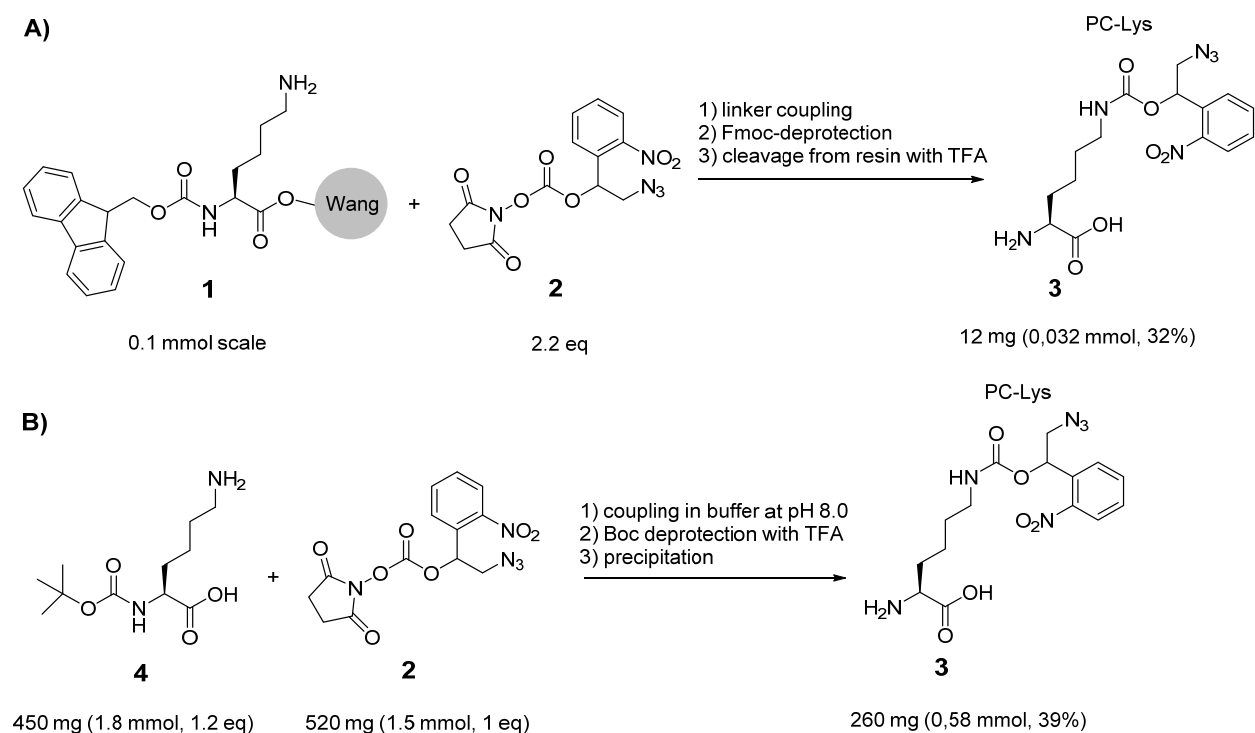
Scheme 38: Two different reaction routes to produce PC-Lys derivative **3**. **A)** On-resin approach, which shows Lys with a free ε-NH₂ group on Wang resin, the subsequent coupling of the activated linker **2** and a final cleavage off the resin by TFA, yielding the desired compound **3**; **B)** synthesis of the desired compound **3** by an in-solution approach according to Schultz and coworkers.[482]

The incorporation of the unnatural amino acid (UAA) **3** (PC-Lys) was performed in a test-scale size of 50 mL, whereas the incorporation into green fluorescent protein (GFP) was aimed at. The amber stop codon was placed in position 39, replacing a native Tyr. The GFP construct also contained a N-terminal FLAG tag and a C-terminal His-tag for purification. Two different orthogonal tRNA/tRNA synthetase pairs were tested for their ability to incorporate the UAA efficiently. Both constructs were derived from the PylRS-tRNA pair from *Methanosarcina*. For this purpose, the WT PylRS was tested, as well as a double mutant, bearing mutations

Tyr306Ala and Tyr384Phe (PylRS AF). As a control, *N*-propargyl-Lys (PrK) was tested as well, which has previously shown good incorporation by PylRS AF into GFP. The concentration of each UAA used during expression in *E.coli* were 1 mM. In result, the amber suppression and thus the incorporation of the functionalized PC-Lys building block has worked to the same extent as the incorporation of PrK, if PylRS AF was used. The incorporation of PC-Lys by PylRS WT into GFP was barely successful and yielded only very little protein (**Figure 21**).
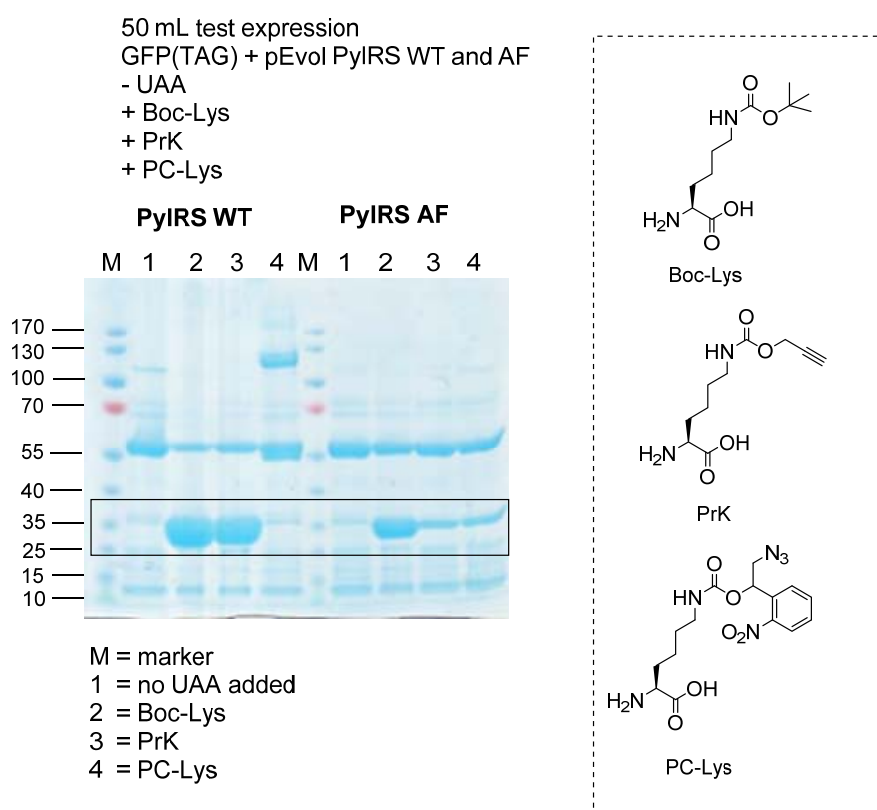
Figure 21: Incorporation of UAAs into GFP by amber suppression using PylRS WT and PylRS AF. At about 60 kDa, the PylRS is visible in SDS-PAGE, which co-purified on the Ni^{2+}-NTA beads by IMAC.

The successful incorporation of the PC-Lys amino acid into GFP was further confirmed by ESI-ToF mass spectrometry and the correct position was determined after a tryptic digest of the protein. In all measurements, smaller masses than the expected were visible to a much higher extent than the modified correct mass, pointing either to premature cleavage of the photolinker or reduction of the azide group to an amine on PC-Lys (see section **7.2.3**).

4.3.4 Summary and outlook

In summary, the synthesis of the PC-Lys amino acid was established in two different routes, leading to the convenient production of sufficient amounts of the amino acid to test amber suppression, for which 1 mM concentrations were to be achieved in expression media. It became obvious that the in-solution approach (**route B**) was superior over the on-resin approach. The successful incorporation of this bifunctional caged amino acid paves the way for further applications (**Scheme 37**), for instance for the generation of libraries of cyclic cell-penetrating peptides (CPPs). The CPPs can be separated from the cells and subsequently cleaved from GFP by light irradiation, which facilitates their analysis and thus allows for the identification of potent CPPs.

4.3.5 Responsibility assignment

The synthesis of the building block and the proper characterization (see section **7.2**) was conducted by Oliver Reimann. The incorporation of the photocaged Lys derivative by amber suppression and the characterization was executed by Christine Koehler from the group of Prof. Edward Lemke. The outline of the project was introduced by Prof. Christian P. R. Hackenberger.

4.4 Semisynthesis of tag-free *O*-GlcNAcylated full-length tau by sequential NCL and EPL reactions, desulfurization and the purification by a photocleavable biotin tag
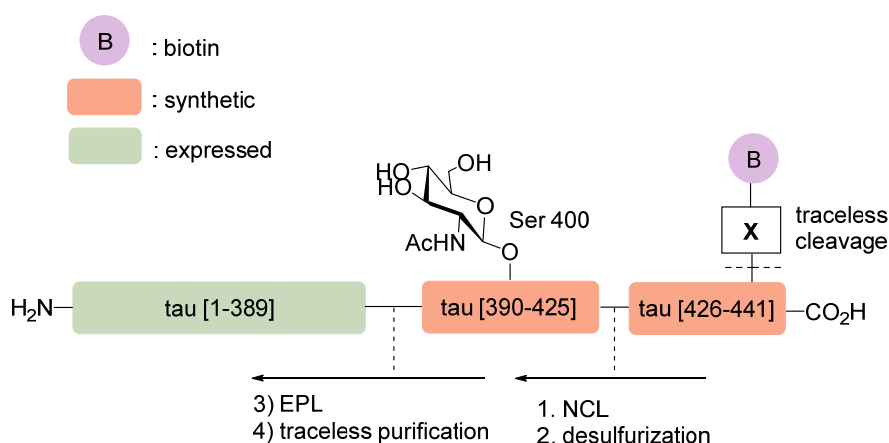
Figure 22: Tag-free semisynthetic full-length *O*-GlcNAcylated tau by NCL/desulfurization and subsequent EPL.

Abstract: In this paper we present the first semi-synthesis of the Alzheimer-relevant tau protein carrying an *O*-GlcNAcylation by using sequential chemoselective ligation. The 52-amino acid C-terminus of tau was obtained by native chemical ligation (NCL) between two synthetic peptide fragments, one carrying the *O*-GlcNAc-moiety on Ser400, which has recently

been demonstrated to inhibit tau phosphorylation and to hinder tau oligomerization, the other equipped with a photocleavable biotin handle. After desulfurization to deliver a native alanine at the ligation junction, the N-terminal cysteine was unmasked and the peptide was further used for expressed protein ligation (EPL) to generate the full-length tau protein, which was purified by a photocleavable biotin tag. We thus provide a synthetic route to obtain a homogenous tag-free *O*-GlcNAcylated tau protein that can further help to elucidate the significance of PTMs on tau and pave the way for evaluating possible drug targets in Alzheimer's disease.

Summary of content: The *O*-GlcNAcylation of tau is an important PTM, since it regulates phosphorylation. The only undoubtedly proven *O*-GlcNAcylation site with *in vivo* relevance is located at Ser400 within the PHF-1 epitope of tau, which is comprised of the three residues Ser396/400/404.[4] This particular *O*-GlcNAcylation site also serves as a phosphorylation site, which raises the question, whether these two modifications compete *in vivo* for this site Ser400. Hence, the production of tag-free *O*-GlcNAcylated tau protein was demonstrated, applying a previously developed technology for purification, described in section **4.2**. In order to obtain this semisynthetic construct, a sequential ligation strategy was applied. The 52 amino acid long C-terminal portion of the protein tau[390-441] was generated by NCL. As Cys is absent in the C-terminus of tau, an Ala residue at position 426 was changed to Cys for NCL. Therefore, the N-peptide tau[390-425](Ser-*O*-GlcNAc) with a thiazolidine (Thz) protected Cys residue in position 390 as a C-terminal Nbz-thioester precursor peptide for further ligation and the C-peptide tau[426-441], equipped with the photocleavable biotin moiety on Lys438, were synthesized. Moreover, Fmoc-Ser(β-D-GlcNAc(Ac)$_3$)-OH was produced over eight steps and used in the building block approach for the introduction during SPPS (see section **2.3.2.2**). The NCL between the two fragments was carried out under standard ligation conditions and a subsequent HPLC purification yielded the desired product in 36% yield. Hereafter, a homogeneous radical initiated desulfurization was carried out to convert the unprotected Cys in position 426 to the native Ala. An additional HPLC purification was carried out and subsequently, the deacetylation of the *O*-GlcNAc moiety was performed by treatment with base. In a next step, the N-terminal Thz group was deprotected to the Cys residue with methoxyamine hydrochloride, which was required for EPL. This protocol furnished the desired

peptide tau[390-441](Ser400-*O*-GlcNAc) (PCB-Lys438) with a free Cys residue in position 390, ready for EPL.

The N-terminal portion of tau from residue 1 to 389 was recombinantly expressed. It contained $^{13}C/^{15}N$-labeling for further NMR analysis and was expressed as an intein-GST fusion-protein in *E.coli*. The EPL reaction was carried out in the presence of 4-(mercaptomethyl)benzoic acid (MMBA). As the available amount of the C-peptide was limited, only slight excess of the peptide could be applied in the EPL reaction, which showed then an approximate conversion to the ligation product of about 50%, as analyzed by SDS-PAGE. The unreacted excess peptide was hereinafter removed by filtration. The final ligation product was isolated through loading of the mixture onto streptavidin coated agarose beads, washing and final cleavage of the tag-free full-length *O*-GlcNAcylated tau, which was achieved through irradiation by UV-light ($\lambda = 297$ nm).

In summary, the first semisynthesis of tau, homogeneously *O*-GlcNAcylated in position Ser400 was reported. A sequential ligation strategy was applied, involving NCL and EPL. Purification of the ligation product was achieved by the previously reported traceless purification strategy, thus paving the way for the generation of substrates, suitable for studies on tau and its PTMs.

Outlook: The construct that was generated by this synthetic route was the first of its kind and may thus contribute to the investigation of the influence of PTMs on the tau protein. However, the amount of generated protein was not sufficient for a proper NMR analysis, as even with labeled tau, amounts of about 2 mg of pure protein are necessary. This amount was not reached by this attempt, so that up-scaling remains a critical issue. Rebuffering and purification steps need to be reduced, as tau behaves untypical in many aspects. Considerable amounts of tau were lost, when spin-filtration was conducted with a cut-off of either 30 kDa or 10 kDa. As the molecular weight of tau is about 46 kDa, this observation was traced back to the unfolded nature of tau. At last, the formation of tau aggregates during the semisynthesis process could further hamper the yields. A description and characterization of the process is provided in section **4.5.4**.

Responsibility assignment: The synthesis of the Fmoc-Ser(β-D-GlcNAc(Ac)₃)-OH building block was conducted by Sergej Schwagerus. The suitable ligation site between Leu425 and

Ala426 was probed by Sergej Schwagerus. The desulfurization and deprotections of the acetyl-groups and the Thz group was conducted by Oliver Reimann. The EPL and purification of the semisynthetic ligation product were conducted by Oliver Reimann and Clement Despres, as well as the analysis of the product by SDS-PAGE and MALDI-ToF mass spectrometry. The project was guided by Prof. Christian P. R. Hackenberger.

4.5 Toward the semisynthesis of tri-phosphorylated tau proteins and controls

4.5.1 Introduction on previous achievements

The first semisynthesis of the tau protein was reported by Malgorzata Broncel *et al.* from the Hackenberger group in 2012.[123] In this proof of principle study, the C-terminal fragment tau[1-389] was produced recombinantly as a fusion protein with a C-terminal intein and further with a chitin binding domain for immobilization. The applied protocol was derived from an IMPACT® system, which has been previously described in this thesis (**Scheme 24**). Addition of MESNa delivered the corresponding thioester of tau[1-389] for further EPL reactions. The 52 amino acid long peptide was generated by linear SPPS and contained either no phosphate or a single phosphate in position Ser404, a site often phosphorylated in AD (section **2.2.5**). Moreover, a non-cleavable biotinylated Lys building block was introduced in position 438, where a native Lys is located. EPL delivered the desired full-length tau protein, either non-phosphorylated or mono-phosphorylated (**Scheme 39**). A subsequent spin-filtration aided the removal of unreacted excess peptide. Afterward, the ligation product was separated from the unreacted C-terminal tau portion by affinity chromatography on monomeric avidin. The unreacted and unbiotinylated protein tau[1-389] was removed through washing and the pure ligation product was eluted from the monomeric avidin beads by the addition of excess biotin, delivering the final ligation product. The presence of the phospho-Ser in position 404 was confirmed by western blot, using a specific antibody against tau, carrying phospho-Ser in position 404. It was further demonstrated that the semisynthetic mono-phosphorylated tau protein had the same ability to polymerize tubulin as WT tau.
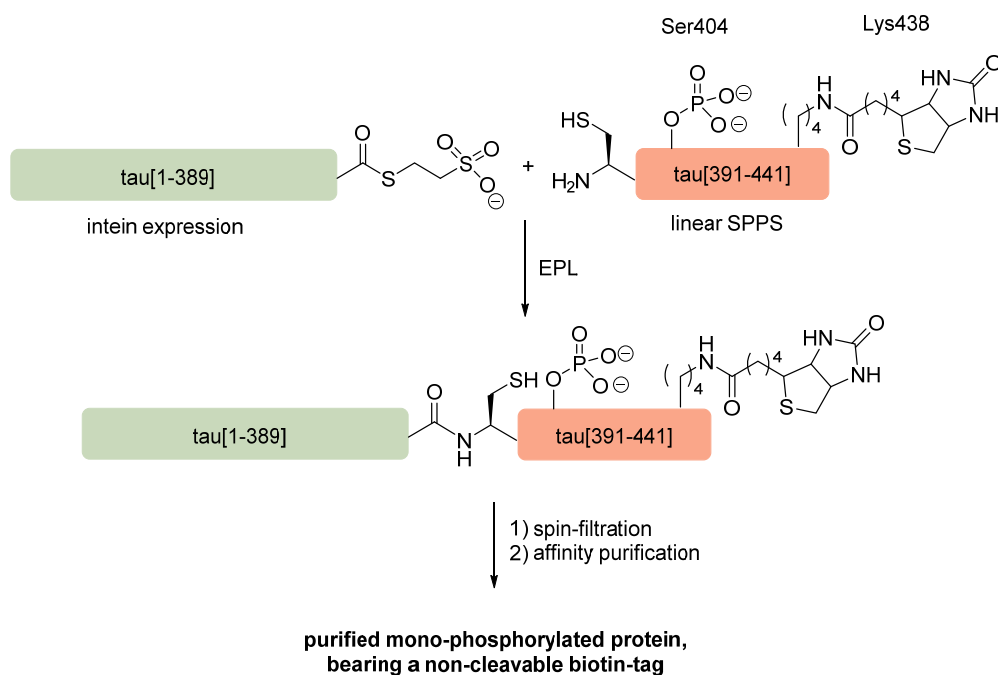
Scheme 39: Strategy to prepare semisynthetic mono-phosphorylated tau protein and its subsequent purification on a non-cleavable biotin-tag.[123]

4.5.2 Outline of this project

The aim of this project was the semisynthesis of a functional, tag-free full-length tau[1-441] (pSer396/400/404). In general, the semisynthesis of tri-phosphorylated tau should be carried out in analogy to the protocol established by Broncel *et al.*[123] Previously, it became obvious that the linear peptide synthesis of the 52 amino acid long C-terminal tau[390-441] containing three phospho-Ser residues was not feasible. This precedence was rationalized by steric demand issues, associated with benzyl-protected phospho-Ser building blocks that were used during peptide synthesis. Therefore, new synthetic routes had to be developed to gain access to this challenging peptide. During the course of finding a suitable synthetic route toward the desired peptide, two methodological papers were generated, described in sections **4.1** and **4.2**.

In short summary, a suitable ligation site was identified for the synthesis of C-terminal tau[390-441] by NCL/desulfurization and a synthetic route for the traceless purification of ligation products was established. It was intended to generate semisynthetic tri-phosphorylated tau according to the previously established protocols, enabling the investigation of structural or functional implementations that PHF-1 tri-phosphorylation has on tau. In collaboration

with the group of Caroline Smet-Nocca at the university of Lille, ^{13}C- and ^{15}N-labeled tau[1-389] thioester protein will be generated, usable for EPL with C-terminal tau peptides (**Scheme 40**). The strategy of applying heteronuclear NMR spectroscopy was previously used by Guy Lippens group to determine the full-phosphorylation pattern of ^{15}N-labeled tau after co-incubation with cAMP dependent kinase without the need of any further purification.[485] Thus, the semisynthetic strategy using labeled expressed tau[1-389] (**Scheme 40**) holds great potential for the observation of perturbations on tau structure induced by phosphorylations.
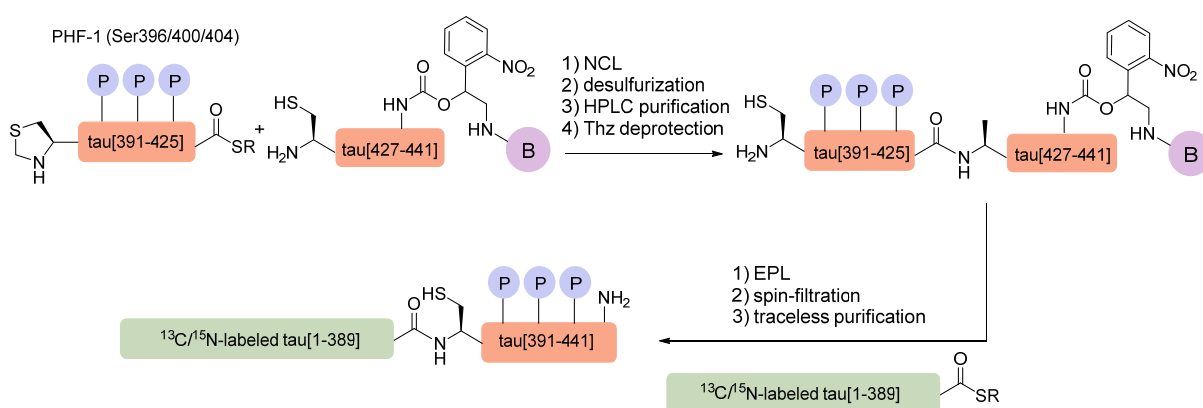
Scheme 40: Synthetic strategy to obtain semisynthetic tri-phosphorylated tau by sequential NCL/desulfurization, EPL and traceless purification.

4.5.3 Results and discussion

The N-peptide tau[390-425] and the C-peptide tau[426-441] were required for NCL reactions to obtain the C-terminal tau fragment tau[390-441]. The N-peptide **5** (**Scheme 41**) was synthesized with a C-terminal modification that enables NCL at the C-terminal Leu and contained further the phosphorylated PHF-1 epitope of Ser396/400/404. In addition, the peptide carried a N-terminal Thz-group, stable under desulfurization conditions. Upon deprotection with methoxyamine hydrochloride at pH 4, the Thz group is converted post-desulfurization to Cys, enabling further EPL with the ligation product. The peptide was synthesized on Dawson Dbz NovaSynTGR resin,[484] in analogy to our previously published protocols, whereas an Alloc protection strategy of an accessible amine on the resin was applied (see section **2.3.4**).[283] The synthesis was carried out manually, as very thorough monitoring by either test-cleavages and HPLC-MS or the Kaiser test was necessary to ensure good coupling

yields. It was discovered that the synthesis was not successful under standard FastMoc chemistry and only worked sufficiently, if 2-(6-Chlor-1*H*-benzotriazol-1-yl)-1,1,3,3-tetramethylaminiumhexafluoro-phosphate (HCTU) was used as coupling reagent in the absence of HOBt and the use of a surplus of base. Moreover, a double coupling strategy was needed, due to otherwise incomplete couplings. In addition, several pseudoprolines were used, facilitating the synthesis of this challenging peptide (**Scheme 41**).
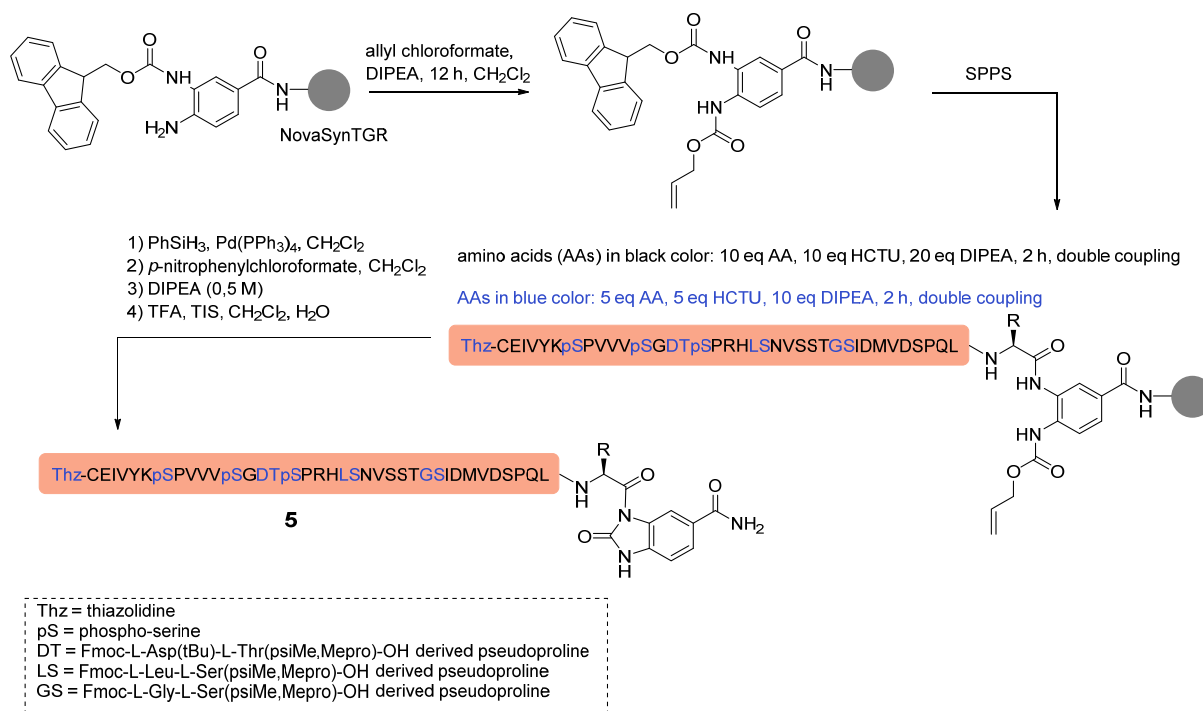
Scheme 41: Synthesis of the N-fragment **5** for NCL toward tri-phosphorylated tau protein.

The C-peptide **6** had at its N-terminal position a Cys instead of the native Ala and was equipped with PCB-Lys438. The synthesis was carried out as published previously (see section **4.2**).[484] The native chemical ligation between the two fragments **5** and **6** was carried out with TFET as a thiol additive (see section **2.3.6**).[315] The two peptides were dissolved in ligation buffer (6 M Gn · HCl, 100 mM Na$_2$HPO$_4$, 50 mM TCEP, TFET (2% vol/vol), pH 7.6) and the reaction proceeded at 37°C under slight agitation (**Scheme 42**). After 90 min, the ligation was finished, since the TFET thioester was reacted or hydrolyzed, leaving no additional N-peptide ready for ligation. Homogeneous desulfurization was then initialized by the addition EtSH, TCEP, *t*-BuSH and VA-044 (see section **2.3.5**). The reaction was allowed to proceed for 2.5 h and subsequently, the ligation was purified by semi-preparative HPLC. The yield of the

one-pot procedure was about 10% of desulfurized ligation product **7**, which delivered 0.6 mg of isolated product in the end.
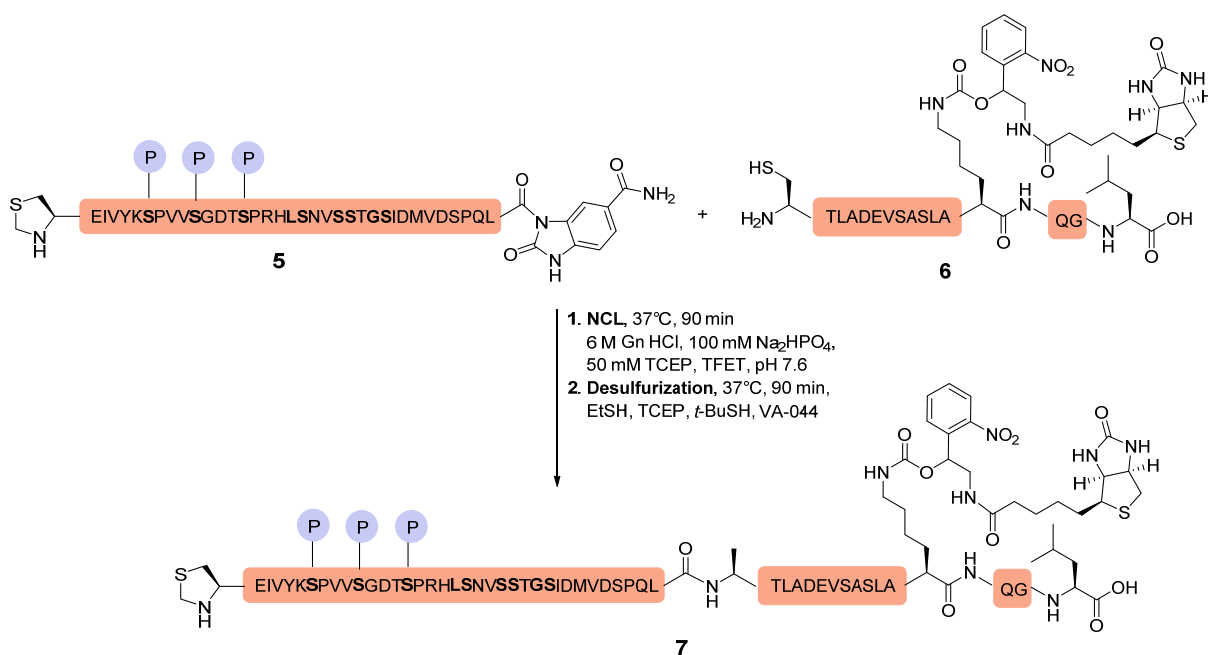
Scheme 42: One-pot NCL/desulfurization reaction between the tri-phosphorylated N-peptide tau[390-425]-Nbz (**5**) and the C-peptide **6**, which yielded the desired ligation product **7** after addition of the desulfurization agents.

This reaction was repeated in a larger scale, yielding also approx. 10% of the product, which gave in the end 2 mg of the desulfurized ligation product. Then, peptide **7** was reacted with 0.2 M methoxyamine hydrochloride solution at pH 4.0 for the deprotection of the thiazolidine group, prior to further use. In a following step, the deprotected peptide was applied in EPL with the expressed C-terminal portion of tau (**8**), which was generated as a MESNa alkyl thioester according to the IMPACT® system (New England Biolabs) (see section **2.3.7**). The product of this reaction was peptide **9**.

4. RESULTS & DISCUSSION
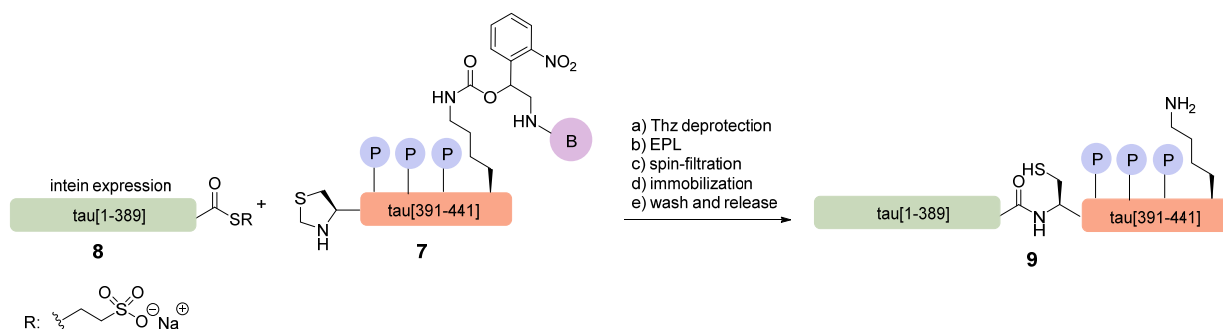
Scheme 43: Thz deprotection of **7**, followed by its EPL reaction with the C-protein thioester tau[1-389]SR (**8**) and subsequent purification, yielding the corresponding ligation product **9**.

The low conversion of **8** to **9** was problematic for the subsequent affinity enrichment on streptavidin beads, since a considerable amount of unligated compound **8** was co-purified due to unspecific binding to streptavidin (**Figure 23 A**). The final product was analyzed by SDS-PAGE, exhibiting an improvement from a 10/1 mixture to a 1/1 mixture of **8** and **9** after the elution induced by UV-light irradiation (**Figure 23 B**).
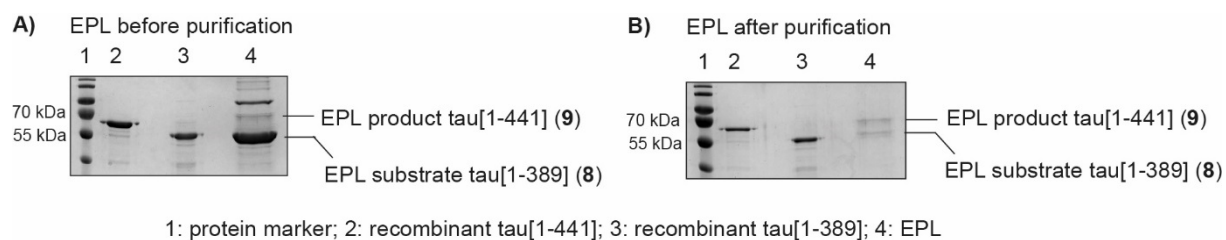
Figure 23: SDS-PAGE analysis of **A)** the crude EPL mixture and **B)** the EPL mixture after purification in comparison to recombinant tau[1-389] ligation substrate **8** (M_W calcd. 41 kDa) and full-length semisynthetic tau **9** (M_W calcd. 46 kDa).

The ligation product was further characterized by MALDI-ToF-MS (**Figure 24**).
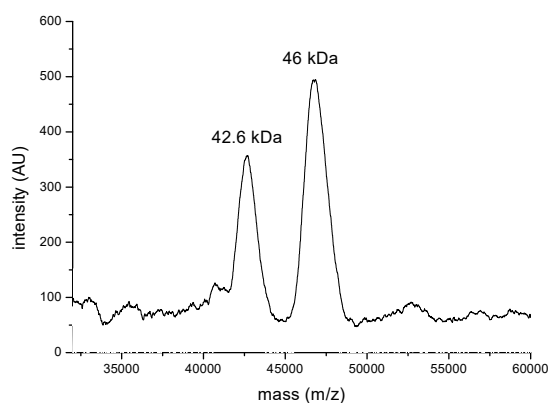
Figure 24: MALDI-ToF-MS spectrum of the purified EPL product, containing the unligated substrate tau[1-389] (**8**) (obs: 42.6; M_W calcd. 42 kDa) and full-length semisynthetic tau **9** (obs: 46 kDa; M_W calcd. 46 kDa).

The identity of the ligation product was tested by conducting a western blot experiment with the semisynthetic construct using an anti-tau antibody targeted against C-terminal tau (mouse monoclonal lgG1, Santa Cruz Biotechnology) (**Figure 25 A**). Moreover, the absence of biotin in the ligation product **9** from the same batch was demonstrated by an anti-biotin western blot (**Figure 25 B**).

A) Anti-Tau 46 antibody

Ponceau   Anti C-terminal tau

1: EPL mixture
2: recombinant tau[1-441]
3: recombinant tau[1-389]
4: protein marker

B) Anti-biotin

1: purified EPL
2: EPL mixture
3: recombinant tau[1-389]
4: recombinant tau[1-441]
5: protein marker
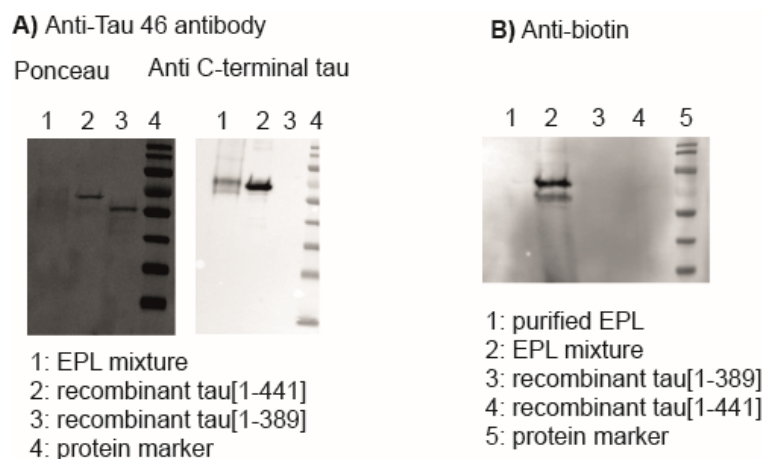
Figure 25: **A)** Ponceau staining of membrane (left) and anti-C-terminal tau western blot (right, tau 46 antibody) recognizing the EPL product in lane 1 and the recombinant tau in lane 2. **B)** The anti-biotin western blot clearly confirms the presence of biotin in the ligation product prior to purification (lane 2) and some unspecific binding to the prevalent band of unligated tau[1-389]. No biotin was detected post-purification by the PCB moiety on streptavidin coated agarose beads (lane 1).

In a next step, the semisynthesis of partially labeled protein **10** was aimed at, using unphosphorylated C-peptide **11** for EPL (**Scheme 44**). Linear SPPS of the unphosphorylated tau peptide **11** was possible due to the absence of bulky phospho-Ser residues and thus conducted as published previously.[484] The C-protein tau[1-389] was expressed in the lab of Caroline Smet-Nocca with ^{15}N-labeling, allowing for the generation of compounds suitable for later NMR analysis. The EPL reaction between the labeled tau portion **10** and the peptide **11** proceeded with an approximate efficiency of 50%, using 100 mM of the thiol additive 4-(mercaptomethyl)benzoic acid (MMBA, **Scheme 44**). The benzylic thiol MMBA was previously reported to result in fast reactions, whereas the corresponding thioesters also exhibit good stability toward a wide pH range.[486]
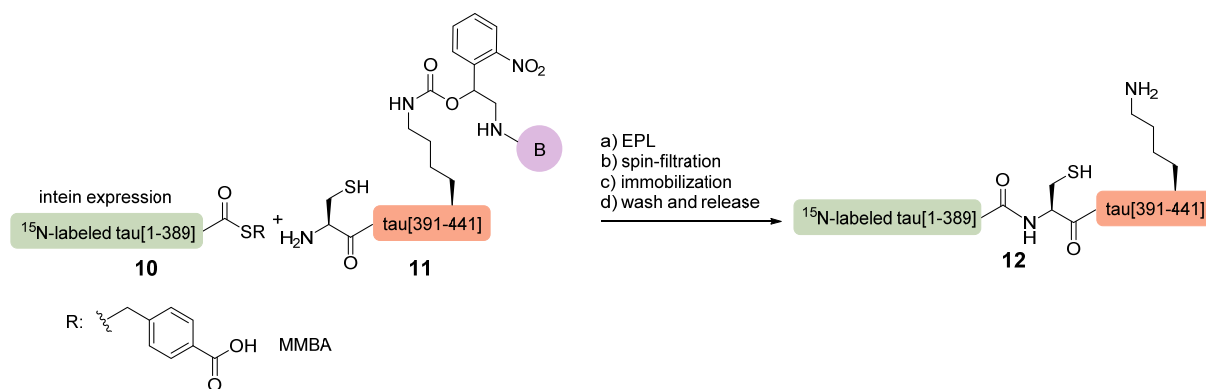
Scheme 44: Expressed protein ligation between the expressed ^{15}N-labeled N-terminal portion of the tau protein **10** and synthetic C-terminal tau peptide **11**, resulting in the partially labeled product **12**.

The ligation product was purified by a first spin-filtration step (30 kDa cut-off), which removed excess peptide from the mixture and a second purification on streptavidin coated agarose beads, but also led to the loss of a higher amount of sample, which passed the spin-filter membrane. The purified ligation product was obtained by immobilization on streptavidin coated agarose beads, washing and subsequent UV-light irradiation at 297 nm. This delivered the final tag-free product **12**, analyzed by western blot using an antibody targeted against C-terminal tau (mouse monoclonal lgG1, Santa Cruz Biotechnology) (**Figure 26**).
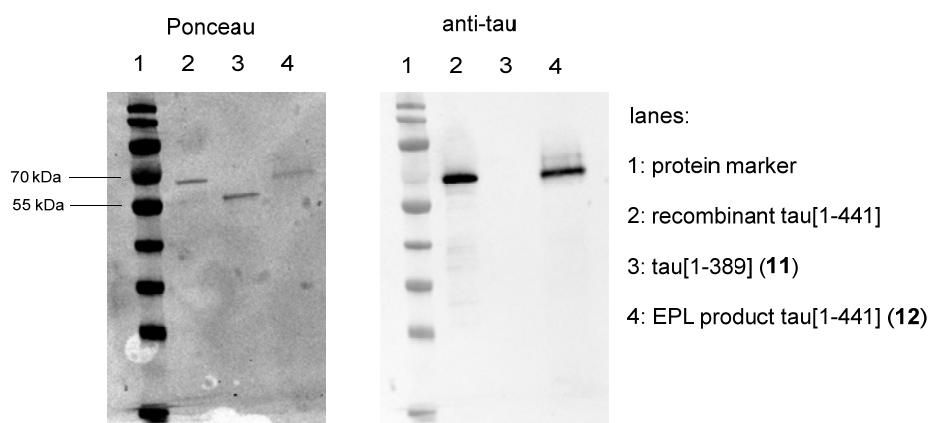
Figure 26: Coomassie stained SDS-PAGE gel (12%) showing purified ligation product **12** in lane 4.

Moreover, the absence of biotin on **12** from the same mixture was demonstrated by a western blot against biotin (**Figure 27**).

4. RESULTS & DISCUSSION

lanes:

1: protein marker

2: recombinant tau[1-441]

3: recombinant tau[1-389] (**11**)

4: EPL mixture containing biotinylated ligation product tau[1-441] and tau peptide[390-441]

5: purified EPL product (**12**)
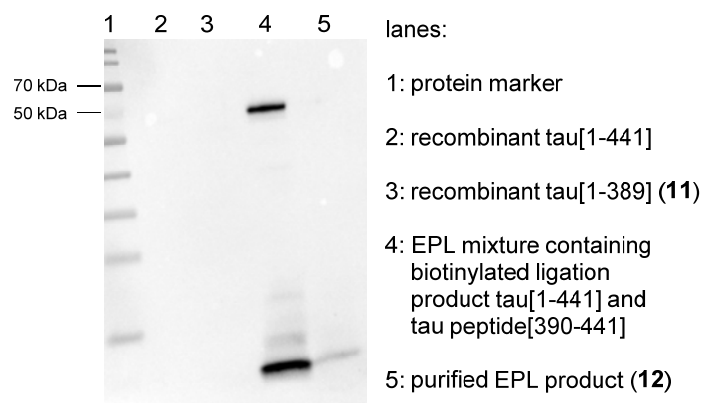
Figure 27: Anti-biotin western blot from the same batch shown in **Figure 26**.

The product was further analyzed by MALDI-ToF-MS, giving further evidence of the correctly formed product, even though **12** was measured at a quite low intensity (**Figure 28**). The yield of the reaction was estimated by optical density and determined to be about 1.5 mg. A final desalting and rebuffering to 50 mM NH_4HCO_3 delivered the product upon lyophylization.
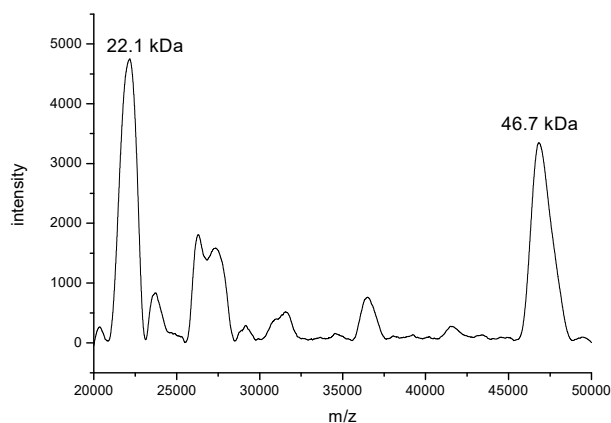
Figure 28: MALDI-ToF-MS spectrum of purified ligation product **12**. The calculated molecular weight for tau[1-441] (Ala390Cys) with ^{15}N-labeling of 46.4 kDa is in rough accordance with the observed peak of 46.7 kDa (broad peaks).

A challenging aspect in the expression of labeled proteins is the expression yield, resulting from expression conditions that are different than for unlabeled proteins. This low expression yield was also observed by coworkers of the Smet-Nocca lab. In addition, the binding capacity of chitin resin (2 mg protein/mL resin) is rather low. This in turn is unfavorable for EPL reactions, where high protein and peptide concentration are required. In contrast, GST beads are able to bind up to 10 mg of protein per mL of resin, thus giving the possibility to enhance

the effective protein concentration per mL through the use of smaller volumes of resin. In consequence, Smet-Nocca and her coworkers replaced the CBD-tag with a GST-tag (**Scheme 45 A**). The ability to carry out EPLs on GST beads was demonstrated by a test reaction at first. The expressed constructs were either derived from Origami or from the BL21 strain. For each reaction, 1 mg of peptide **11** was used and 100 mM MMBA thiol were added. The experiment showed that the expression in BL21 was favored over expression in Origami and that the ligation proceeded with an approximate conversion rate of 50% (**Scheme 45 B**).
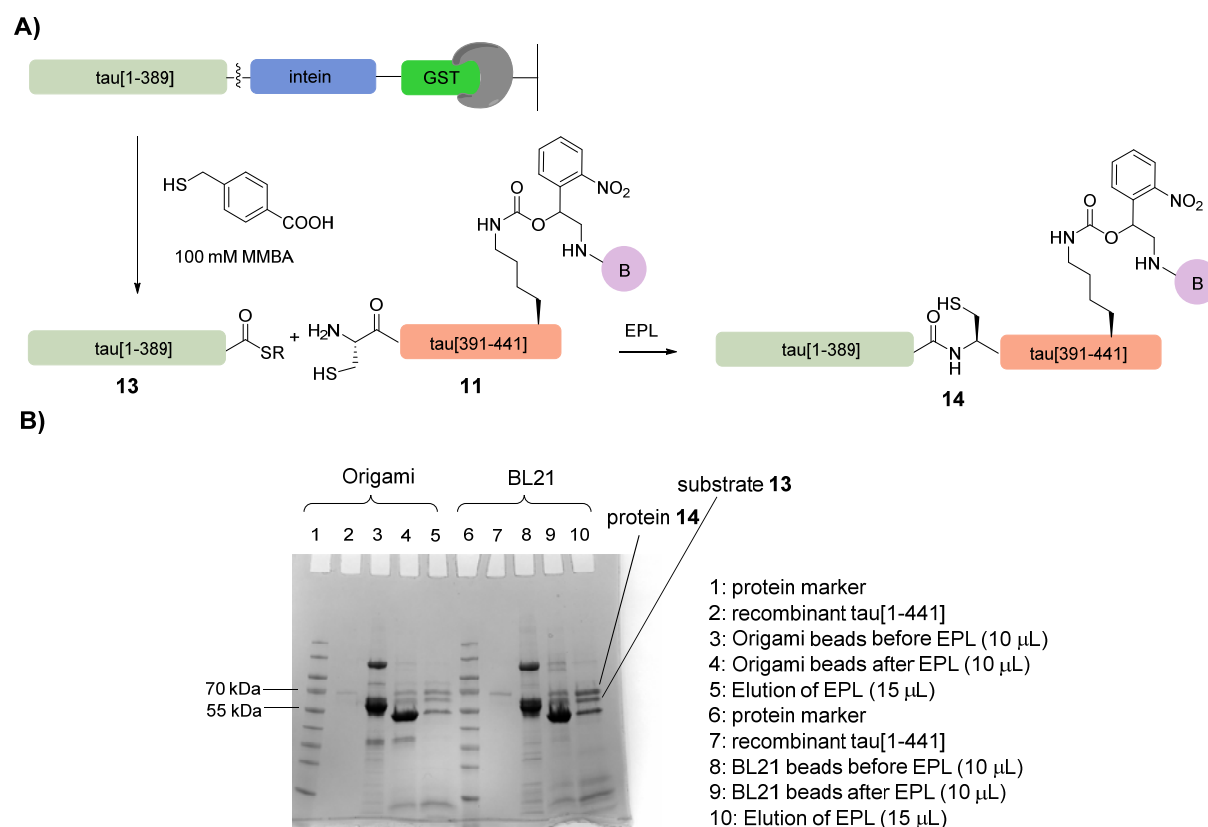
Scheme 45: **A)** Generation of the MMBA thioester **13** through elution from GST beads, followed by the EPL with peptide **11**. **B)** SDS-PAGE gel of thioester formation and on-bead EPL through the addition of peptide **11** to expressed protein portion **13** on GST-resin.

To further optimize the ligation, it was intended to replace an affinity purification step by HPLC purification. Toward this goal, the C-terminal tau peptide **15** was synthesized without any purification tag, in accordance to the previously published protocol by Broncel *et al.*[123] Moreover, the ^{15}N-labeled tau-intein-GST fusion-protein was expressed (see section **7.3.7**) and protein thioester **10** from a 2 L expression was put to EPL with peptide **15** (4 mg, 0.75 µmol) (**Scheme 46**, see also section **7.3.9**).
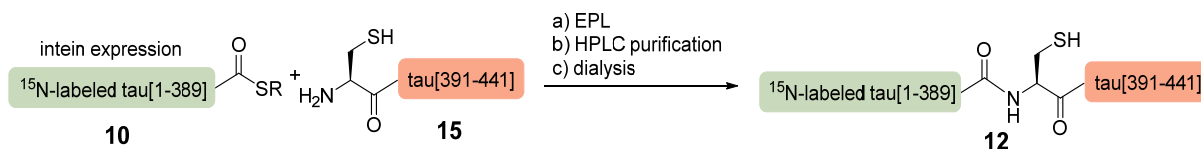
Scheme 46: EPL between peptide **15** and labeled N-terminal tau **10** in the absence of biotin, making a HPLC purification necessary.

After the ligation proceeded for two days, a conversion of about 25% was achieved and did not further improve upon longer reaction times or temperature enhancement. The progression of the reaction was monitored by SDS-PAGE. HPLC purification was conducted on a C4 column and delivered a mixture that still contained unreacted protein **10** and excess peptide **15** next to the desired ligation product **12**, as determined by gel electrophoresis and Coomassie staining (**Figure 29 A**). Dialysis (12-15 kDa M_W-cut-off) was performed separate the excess peptide, as it was found out that large portions of tau get lost during spin-filtration. A subsequent HPLC purification on a semi-preparative C18-HPLC delivered two fractions (**Figure 29 B**). Fraction 1 contained EPL product **12** with small amounts of substrate **11**, with a low overall yield of < 1 mg estimated by UV-Vis spectrophotometry. Fraction 2 contained also **12** and **11** in addition to peptide **15**, which co-eluted with the protein fraction. Fraction 2 contained 2.1 mg of this mixture, according to protein quantification by UV-Vis spectrophotometry.
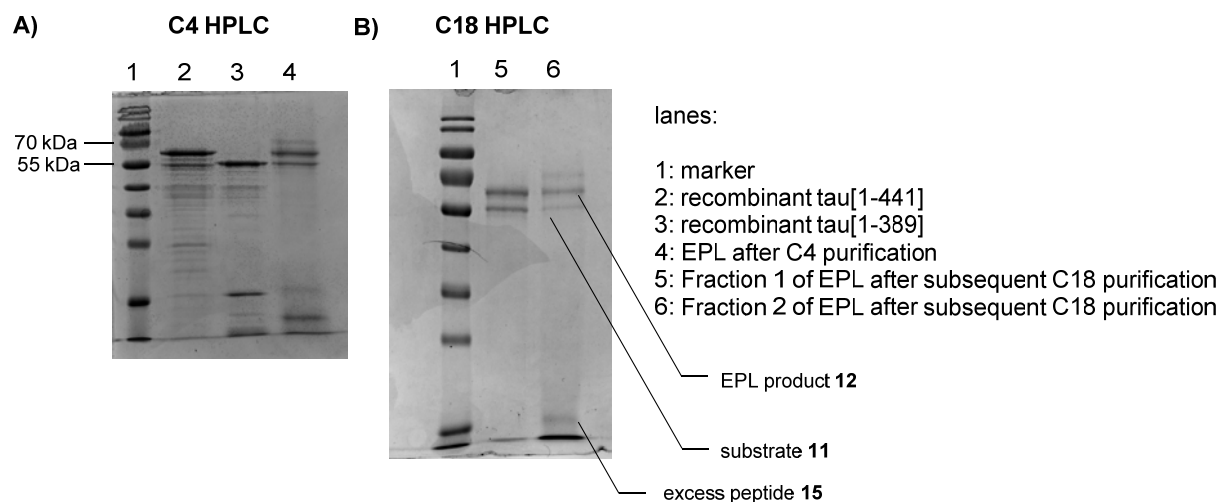
Figure 29: SDS-PAGE (12%) analysis of purified EPL product **12** after C4-HPLC purification (left) and the subsequent C18-HPLC purification, which finally yielded fractions 1 and 2, both contaminated by other species.

The ability to separate the fragment tau[1389] from full-length tau[1-441] was previously demonstrated in a test-reaction. There, 1 mg of tau[1-389] and 1 mg of tau[1-441] were solubilized and mixed together, before they were purified by C18 HPLC (**Figure 30**). In this

test-reaction, 92% of tau[1-381] and 52% of tau[1-441] were regained, as determined by weight after lyophylization.
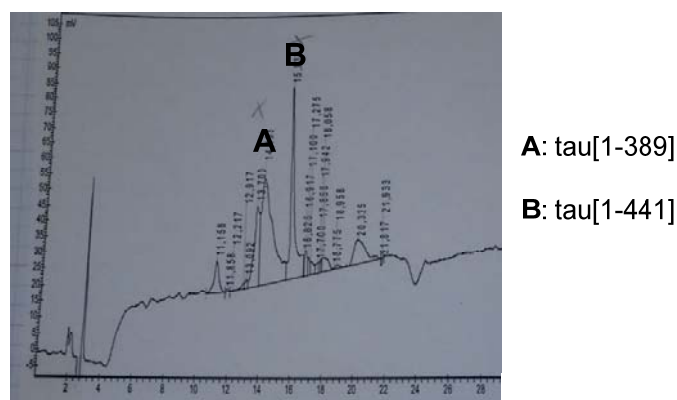
Figure 30: Test separation of the two recombinantly expressed proteins tau[1-389] and tau[1-441] by C18 semi-preparative HPLC.

Summing up, attempts to purify the EPL reaction mixture by HPLC chromatography had failed to deliver pure ligation product, which may be attributed to the large excess of peptide in the reaction mixture that possibly disturbs the proper separation on the HPLC column. In a final attempt, ^{13}C-/^{15}N-labeled tau[1-389]-intein-GST was expressed in BL21 cells from 1 L expression volume and reacted with 1.9 mg of peptide **7** (0.31 μmol) in the presence of 100 mM thiol additive MMBA (**Scheme 47**).

Scheme 47: Attempt of an EPL between double-labeled expressed tau[1-389] thioester **16** and peptide **7**.
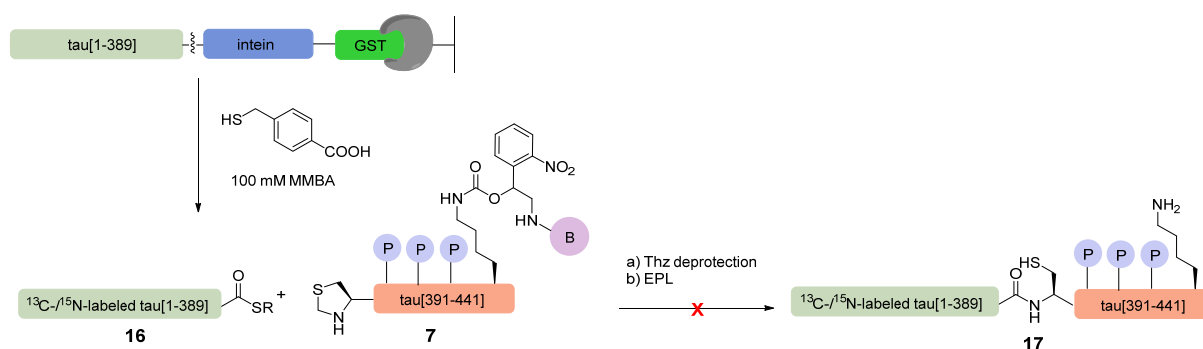
Despite the efforts to optimize the EPL by replacing the CBD-tag with a GST-tag and exchanging the thiol additive from MESNa to MMBA, no significant amounts of ligation product **17** were observed during the ligation by SDS-PAGE analysis (**Figure 31**).

4. RESULTS & DISCUSSION
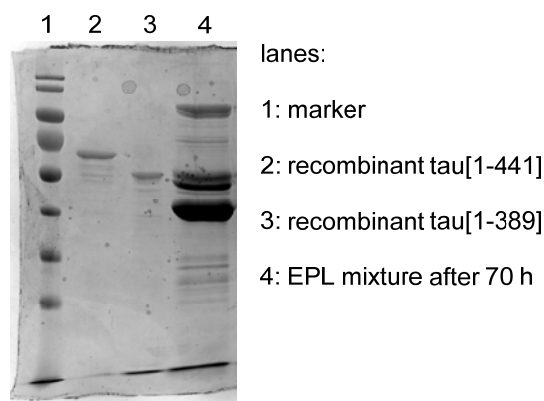
Figure 31: Outcome of the EPL reaction between tri-phosphorylated C-terminal tau (**7**) and the ^{13}C-/^{15}N-labeled protein **16** after 70 h reaction time.

A possible reason for the low conversion of the tau[1-389] fragment could be the formation of tau aggregates, which were observed during EPL and further work-up steps. All attempts to re-solubilize these aggregates failed, involving cooling to 1°C (thermodynamic equilibrium), incubation with 3 M guanidine hydrochloride, acidification to pH 2 and exposure to formic acid (up to 99%) from rt to 97°C.

Tau aggregation is occurring during the transition of random coil to β-sheet structure, which can be driven by polyanions such as heparin.[487] In EPL reactions, high concentrations of thiol additives such as MESNa are required, which might also trigger the formation of tau aggregates. In a publication by Guy Lippens *et al.* it was found that the interaction of tau and heparin takes place at several sites of the protein, which finally leads to nucleation upon unknown pathways.[488] In order to test, whether MESNa or other thiol additives for EPL reactions such as MMBA have an equal effect on tau aggregation as heparin, an experiment was conducted. The common EPL conditions were applied to either WT-tau or tau that is generated during EPL with an Ala390Cys mutation, in concentrations typically applied during EPL reactions. Moreover, pure tau-free buffer and albumin protein were used as negative controls. To obtain a positive control, tau aggregates were formed according to a published protocol by the addition of heparin, followed by a 10 day incubation of the mixture at 50°C.[487] Then, the probes were dialyzed against 50 mM ammonium bicarbonate buffer and TEM pictures of the resulting aggregates were recorded from Dr. Dmytro Puchkov. In result to the heparin-induced positive control aggregation, no fibril formation was observed and instead, amorphic aggregation was detected (**Figure 32**).
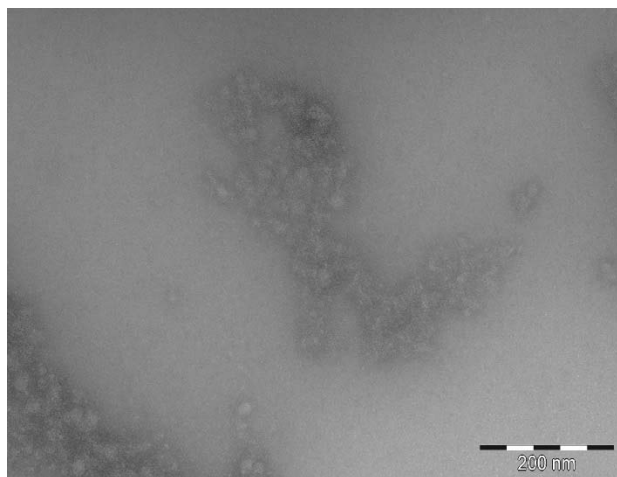
Figure 32: Control tau aggregates generated by heparin addition to tau and incubation over 10 days at 50°C.

Hereinafter, TEM pictures were recorded for samples of WT-tau, tau(Ala390Cys), albumin and pure buffer (**Table 9**). The samples were prior to their recording incubated at rt or 4°C for 72 h in EPL buffer (20 mM Tris HCl pH 8.0, 500 mM NaCl, 1 mM EDTA, 0.1% Triton-X 100, 0.1 mM TCEP, 200 mM MESNa).
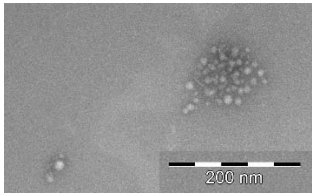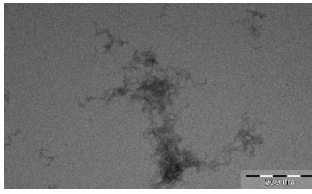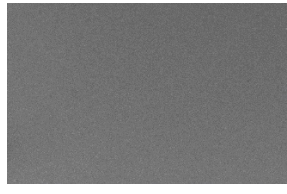
Table 9: Amorphic aggregate formation after 72 h of incubation of proteins in EPL buffer at given temperatures and subsequent dialysis.

	WT-tau	tau Ala390Cys	albumin	EPL buffer
rt	✔	✔	✘	✘
4°C	✔	✔	✘	✘

Aggregates were observed for WT-tau and tau with a Ala390Cys mutation, when samples were incubated in EPL buffer for 72 h at either rt or 4°C. The amorphic structure of the aggregates generated was comparable to the structure of the positive control (**Figure 32**), as visible in **Table 10**, whereas the quantity of the observed structures was lower in samples that were incubated under EPL conditions in comparison to the positive control experiment with heparin. The structures that were obtained by incubation of albumin in EPL conditions were not amorphic and showed intact protein in comparison to tau samples. The plain EPL buffer did not show any aggregates, as expected.

Table 10: Structures observed during conditions usually applied in EPL by TEM.

	WT-tau	albumin	EPL buffer
rt			

Tau fibrils were neither formed upon the addition of heparin (**Figure 32**) nor in EPL buffer (**Table 10**) and rather amorphic aggregation was observed. The reason for the selective aggregation in case of tau is also not clarified and needs to be further explored. In summary, the formation of these insoluble amorphic aggregates has the potential to significantly lower the yield of EPL reactions involving tau.

4.5.4 Conclusions and outlook

In conclusion, semisynthetic tri-phosphorylated tau was generated and successfully applied in EPL with unlabeled expressed tau[1-389] thioester. The enrichment of these ligation products was carried out by means of a photocleavable biotin tag. The semisynthetic protein was then characterized by MALDI-ToF MS and western blot analysis with an anti-C-terminal tau antibody. Despite this success, other attempts to generate mg quantities of either ^{15}N- or ^{13}C-/^{15}N-labeled semisynthetic tri-phosphorylated tau failed, whereas several factors were identified that hampered the outcome of these experiments. Those were for instance the low expression yields of labeled proteins and insufficient substrate concentration during EPL reactions. In order to improve the low protein concentration in EPL, the CBD-tag was replaced by GST in the lab of Smet-Nocca, which allowed for higher protein substrate concentrations in EPL reactions due to a higher binding capacity of the GST beads in comparison to chitin resin. Moreover, the thiol additive was changed from MESNa to more stable and reactive MMBA, which neither led to reproducibly higher EPL conversion rates.

Aggregation during EPL was identified as a limiting factor for isolated yield of semisynthetic tau proteins. This was demonstrated in experiments, where tau samples and the control protein albumin were incubated in EPL buffer over 72 h. This led to the formation of amorphic aggregates of tau, which were also observed for the tau incubation with heparin, whereas albumin did not show this aggregation pattern. It is possible that tau aggregation is further triggered by the presence of shortened tau[1-389] or excess peptide tau[390-441] fragments. Moreover, it may be even assumed that aggregation becomes more prevalent in other re-buffering and work-up steps, but that has to be investigated in more depth in the future. The formation of these aggregates has a negative impact on the yields obtained by EPL and thus, new pathways toward semisynthetic tau will have to be explored. The major difficulty is to maintain native tau, which precludes e.g. mutations at residues 269-284 (especially the hexapeptide ^{275}VQIINK^{280}) and 300-310 (especially the hexapeptide ^{306}VQIVYK^{311}), known to prompt tau aggregation (see section **2.2.2**). Possibly, the application of different detergents in can be beneficial for the inhibition of tau aggregation, but those have to be removed post EPL in the purification process. Moreover, there are several small-molecule aggregation inhibitors for tau described that might be also applied in EPL reactions of tau,[489] but their potential to prohibit the formation of amorphic tau aggregates in EPL reactions needs to be investigated.

4.5.5 Responsibility assignment

The peptide synthesis, NCL and EPL reactions and protein work-up was conducted by Oliver Reimann under the supervision of Prof. Christian P. R. Hackenberger, as well as the expression of unlabeled tau[1-389]-intein-CBD fusion proteins. The expression and purification of ^{13}C-/^{15}N-labeled tau proteins was carried out by Clement Després under the supervision of Dr. Smet-Nocca, as well as the replacement of the CBD-tag by a GST-tag. The transmission electron microscopy (TEM) pictures were recorded by Dr. Dmytro Puchkov (FMP).

4.6 New antibodies against the tri-phosphorylated PHF-1 epitope of tau

4.6.1 Introduction to antibodies against PHF-1 phosphorylation

Aggregation of hyperphosphorylated tau proteins is associated to neurodegenerative disorders, such as AD (see section **2.2.5**).[490] The sites Ser396/400/404 are comprised as the PHF-1 epitope, which becomes highly phosphorylated in AD and disturbs the paperclip conformation of tau, leading to higher aggregation potential.[491] Furthermore, it was demonstrated that tau phosphorylation at this epitope reduces its biological activity in promoting microtubule assembly, binding to microtubules and the ability in stabilizing microtubules against nocodazole-induced depolymerization.[492-494] Furthermore, dephosphorylation restores its biological activity and relaxes the structure of PHFs.[495, 496] All these data provide evidence for the importance of this particular epitope for AD progression.

Antibodies are valuable tools in AD research and medical diagnosis. An antibody (Ab) is a Y-shaped, large protein (usually approx. 150 kDa) produced by plasma cells. It consists of four polypeptide chains, namely two identical heavy and two identical light chains that are connected via disulfide bridges (**Figure 33**). Sugar chains are attached to conserved amino acids that are critical to the structure and function of the antibody.[497] In general, an antibody can be separated into fragment antigen-binding (Fab) and fragment crystallizable (Fc) regions. The Fab region ultimately determines the antigen specificity of an antibody, while the Fc region determines the class effect by binding specific Fc receptors.
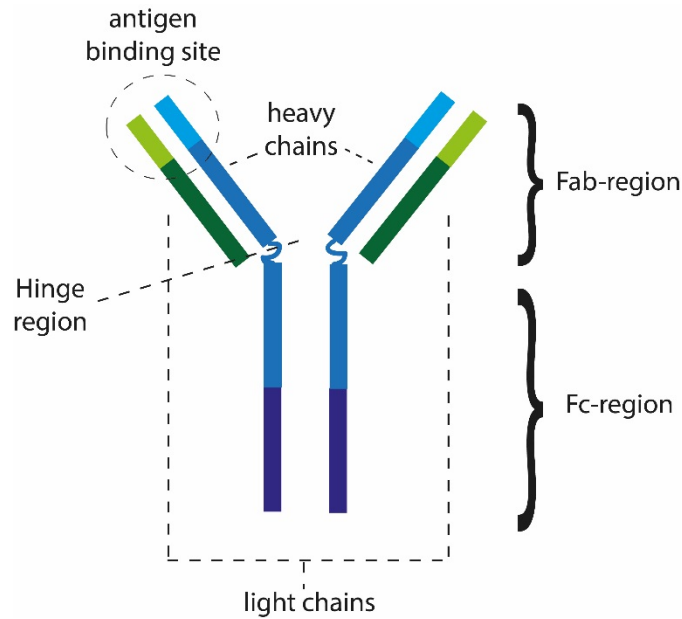
Figure 33: Major components of an antibody. The heavy and the light chain both contain a constant (darker color) and a variable region (lighter color). The Hinge region consists of approx. 15 amino acids and connects the two heavy chains by disulfide bridges. It ensures the flexibility of the antibody.

In research, specific antibodies are produced by injection of an antigen into a mammal, such as horse, sheep, rabbit, rat or mouse. Later, blood is withdrawn from the animals, which contains polyclonal antibodies in the blood serum. These polyclonal antibodies bind to the same antigen in many different versions. In order to obtain antibodies specific for a particular epitope of an antigen, lymphocytes that secrete antibodies are isolated and immortalized by fusing them with a cancer cell line. The resulting fused cells are called hybridoma cells. They continuously grow and secrete antibodies in the culture, where they are present. Hereinafter, single hybridomas are isolated to generate cell clones that all produce the exact same antibody. These clones are then called monoclonal antibodies.[498] Previously, several monoclonal antibody-based methods were developed to detect phosphorylated epitopes of the tau protein, including Thr181 & 231,[499] Thr181,[500] Thr231 & Ser235,[501] Ser199,[501] Thr231[502] and Ser396 & Ser404.[503] For phospho-Ser (pSer) located within the PHF-1 epitope, several antibodies are available, including antibodies against pSer396,[504] pSer400,[505] and pSer404.[506] But the most prominent antibody against PHF-1 phosphorylation is called PHF-1, targeted against pSer396 and pSer404. The antibody was developed by Greenberg *et al.* in 1992.[507, 508] The potential of this antibody was explored in several studies, for instance by Hu *et al*, who demonstrated a precise correlation of phospho-tau elevation detected by PHF-1 antibody and AD, in contrast

to control groups consisting of patients with non-AD dementia and vascular dementia.[503] In their study they were able to confirm 96% of cases, where AD was diagnosed *post mortem* by autopsy with specificities between 86% and 100% against controls of non-neurological, non-AD neurological, vascular dementia and all of these three control groups combined. Another example highlights the strength of the PHF-1 antibody, since Boutajangout *et al.* showed that passive immunization with PHF-1 led to a decrease of tau pathology and functional impairments in the JNPL3 mouse model of AD.[509] Moreover, Asuni *et al.* had shown that active immunization with tau[379-408](pSer396/404) peptides in P301L tangle mouse models also led to reduced aggregated tau in the mice brains and slowed progression of the tangle-related behavioral phenotype.[510]

Previously, Smet-Nocca *et al.* demonstrated that tau becomes sequentially tri-phosphorylated in Ser396, Ser400 and Ser404 by GSK-3β and CDK5 kinases.[167] These observations prompted us to generate antibodies targeted against tri-phosphorylated PHF-1 tau, to probe their performance in comparison to the established PHF-1 antibody.

4.6.2 Outline of this project

It is intended to generate monoclonal antibodies against the tau protein phosphorylated in positions 396/400/404, thereby developing a novel approach by targeting a phospho-epitope in addition to the established pSer396/404 by PHF-1 antibody. Furthermore, the evaluation of the specificity and sensitivity of the new antibody clones is aimed at. Finally, the different tau species recognized by the new antibodies are to be evaluated in a cellular context and in an animal model.

4.6.3 Results and discussion

For reasons of clarity, this project is divided into several subsections with internal responsibility assignments.

4.6.3.1 Antibody generation

Peptide **18** was required for the generation of the antibody clones and comprised the residues tau[391-410] with three phosphorylated residues pSer396/400/404. Moreover, **18** was equipped with a N-terminal Cys and two His-residues at the C-terminus. The Cys residue was needed

for conjugation of the peptide to a carrier protein, which shields the peptide and prevents it from being quickly degraded by the proteasome in order to provoke an immune reaction. Moreover, the two additional His-residues were implanted to block the correct epitope and prevent antibody generation recognizing a C-terminus. The peptide was generated partially by automated and partially by manual peptide synthesis applying a double coupling strategy. Peptide **18** was conjugated onto maleimide functionalized ovalbumin to ensure its stability and proper display, before its injection to rats, whereas the immunization with a mouse did not lead to antibody generation. The hybridoma technology was applied, allowing for the production of large quantities of identical antibodies (**Scheme 48**).
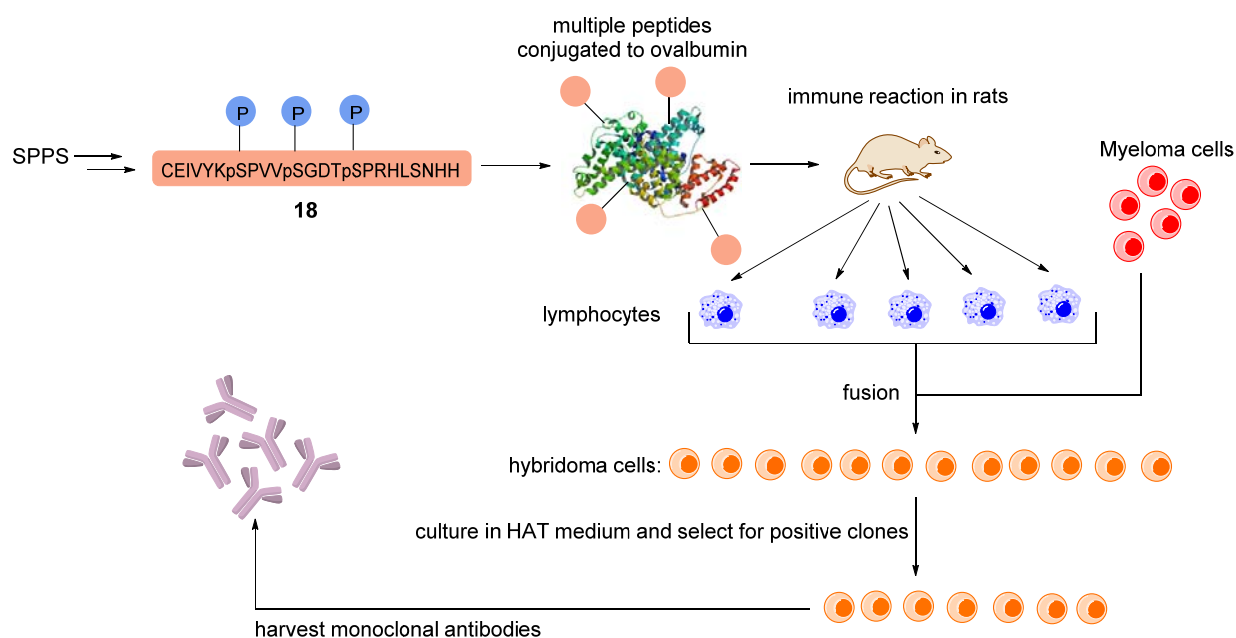
Scheme 48: Generation of monoclonal antibody clones targeted against tri-phosphorylated tau[391-410] (**18**) by the hybridoma technology.

In result, seven ppp-tau clones were generated that further be referred to as follows: 9C10, 10D5, 6F11, 15F1, 8D12, 18E5, 7F2.

Responsibility assignment: The synthesis of peptide **18** was performed by Oliver Reimann. Hereinafter, the peptide was transferred to Peps4LS, where the conjugation of the peptide to ovalbumin was carried out. The antibody generation was carried out at the Helmholtz Center in Munich in the group of Elisabeth Kremmer.

4.6.3.2 Indirect immunofluorescence experiments with ppp-tau antibodies

The seven ppp-tau clones were tested by indirect immunofluorescence assay in mouse embryonic fibroblast (MEF) cells. In this set-up, immunofluorescence staining of tau with the ppp-tau antibodies (all seven clones) and DAPIasa DNA counterstain were monitored by confocal laser scanning microscopy, as previously described by Leonhardt *et al.*[511]

In result, several clones recognized the corresponding antigen in the cytoplasm of the cells (**Figure 34**), whereas other clones specifically recognized tau in the nuclei (**Figure 35**). The control agent for nuclear recognition was 4',6-diamidino-2-phenylindole (DAPI), which selectively stains A/T-rich regions of DNA located in the nuclei of cells.

Clones with cytoplasmatic tau recognition:
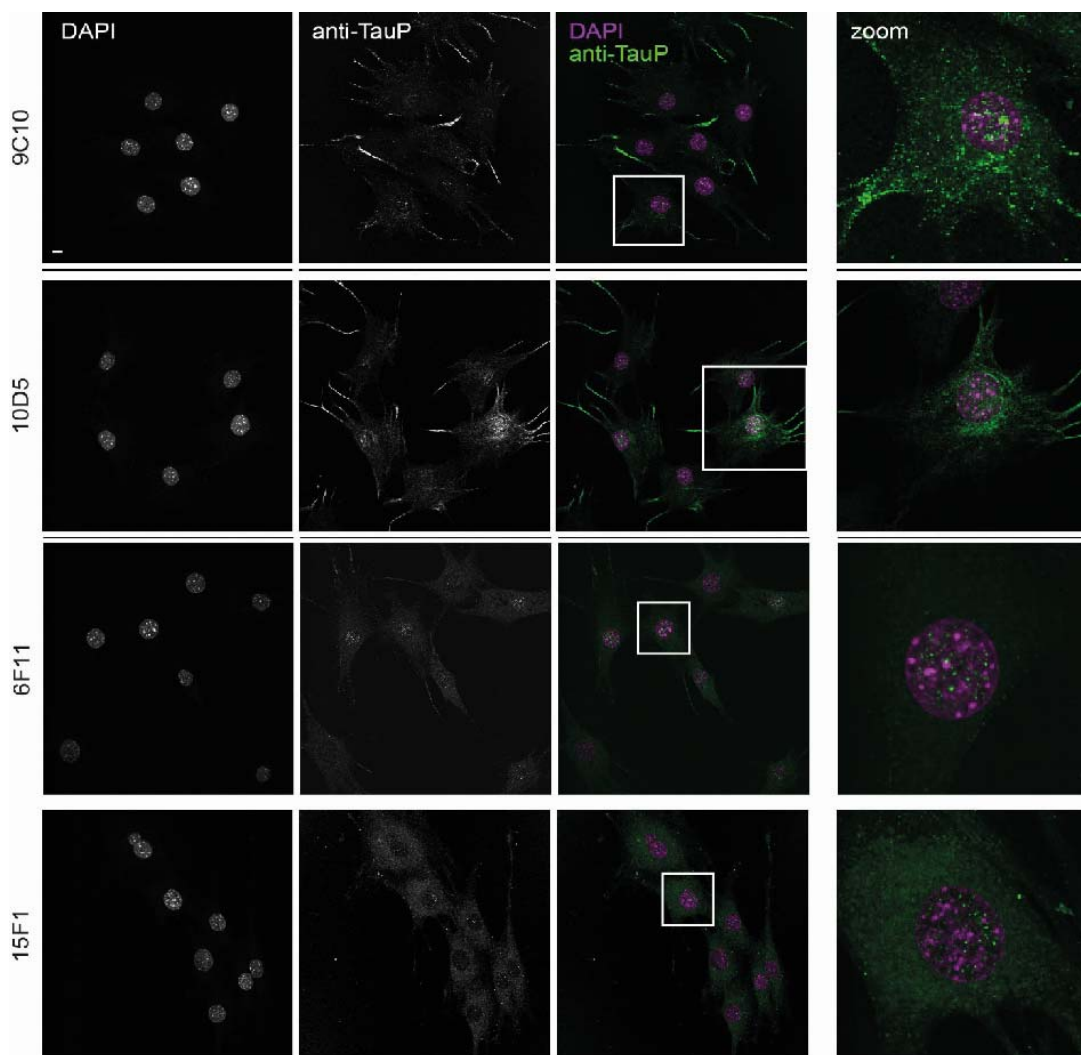
Figure 34: Clones that showed cytoplasmatic tau recognition by indirect immunofluorescence and subsequent confocal laser microscopy: 9C10, 10D5, 6F11 and 15F1.

Clones with tau recognition restricted to the nucleus:
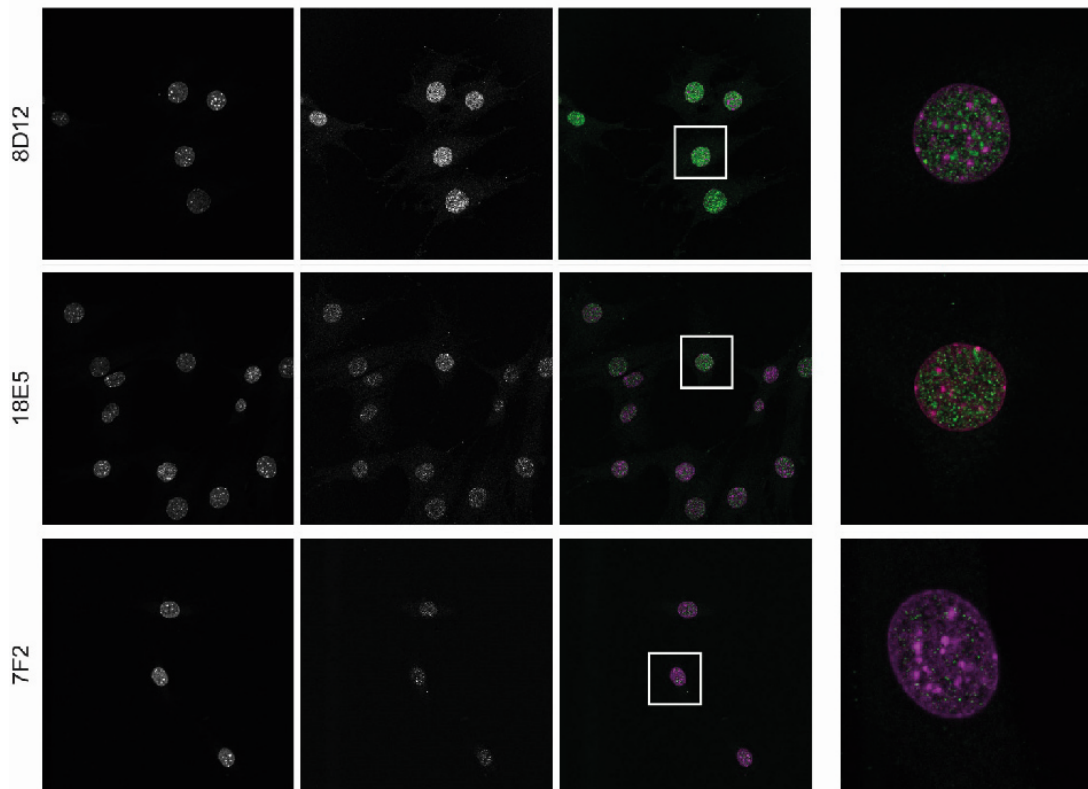
Figure 35: Clones that showed nuclear tau recognition in indirect immunofluorescence and subsequent confocal laser microscopy: 8D12, 18E5 and 7F2.

These results demonstrate to our knowledge the first phospho-dependent recognition of tau in cell nuclei. Previously, Sultan *et al.* have performed a very thorough study, in which they investigated the influence of heat stress on tau localization in cells.[512] A series of different antibodies was applied, including PHF-1. In this study, tau was detected in the nucleus, but always to a much lower extent than in the cytoplasm and recognition was never restricted to nuclei. Based on these observations, they reasoned that nuclear tau has a neuroprotective role, which becomes more prevalent in case of cellular stress. Moreover, *in vitro* studies showed that tau can bind to double- and single-stranded DNA in an aggregation-dependent, but phosphorylation independent manner.[513] These experiments showed that tau can alter the conformation of DNA at a ratio of one tau molecule on 700 base pairs of DNA. It is further stated that nuclear tau is also found in the nuclei of cells derived from AD patients and thus allows the hypothesis that nuclear tau could affect the nucleolar organization during the course of AD.

Another study suggested that only truncated tau reaches the nucleus and is independent of phosphorylation.[514] It was further argued that nuclear import and export of proteins larger than approx. 40 kDa is highly regulated and thus transport of tau to the nucleus is a consequence of passive diffusion due to small molecular weight of truncated tau versions. Additionally, N-terminal truncation could hamper the paper-clip formation of tau and thus expose residues of the protein that allow for interaction with cargo proteins that could help translocate tau to the nucleus. Tau has one so called nuclear localization signal (NLS) at residues 140-143 with no assigned functionality so far.[514]

It is intriguing that tau phosphorylation in PHF-1 leads to an exposure of a NLS sequence or allows certain protein/protein interactions that may change the localization of tau, since the paperclip conformation of tau is also hampered by PHF-1 phosphorylation.[491]

Responsibility assignment: The experiments in this chapter were conducted by Andrea Rottach under the guidance of Prof. Heinrich Leonhardt.

4.6.3.3 Epitope mapping

To further characterize the specific binding of the seven ppp-tau clones, epitope mapping was performed. This required the synthesis of a cassette of peptides with the corresponding tau sequence of tau[391-410] with iterative alterations of phosphorylations (**Table 11**). In addition, two peptides with Ser400 *O*-GlcNAcylation were generated, since this PTM also occurs in the PHF-1 epitope.

biotin-spacer-EIVYK**X$_1$**PVV**X$_2$**GDT**X$_3$**PRHLSNHH
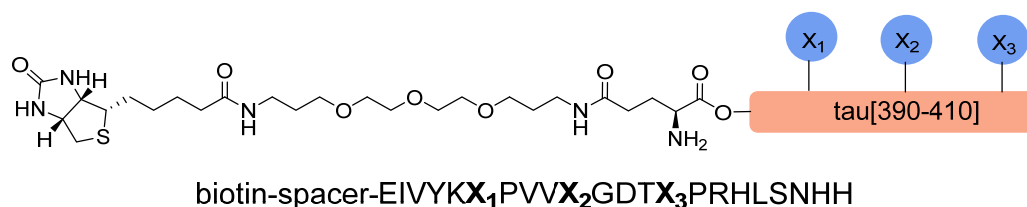
Figure 36: General structure of peptides **19-28** with **X$_1$**, **X$_2$** and **X$_3$** being the positions that are varied. Moreover, the peptides were equipped with a spacer and biotin.

The following chart (**Table 11**) shows the PTMs present in the corresponding peptides **19-28** at the positions X$_1$ (Ser396), X$_2$ (Ser400) and X$_3$ (Ser404).

Table 11: Varied positions X_1, X_2 and X_3 shown in the peptide of **Figure 36**. P = phosphate; *O*-GlcNAc implies the presence of an *O*-GlcNAcylation site.

Peptide	X_1 (Ser396)	X_2 (Ser400)	X_3 (Ser404)
19	P	P	P
20	P	P	-
21	P	-	P
22	-	P	P
23	P	-	-
24	-	P	-
25	-	-	P
26	-	-	-
27	-	*O*-GlcNAc	P
28	P	*O*-GlcNAc	P

A biotin with a spacer molecule was N-terminally introduced to immobilize the peptides on streptavidin coated well-plates for further ELISA. The peptides **19-28** were immobilized, washed with PBS and blocked with 5% milk in PBS (see section **7.4.2** for experimental details). Then, the cell-supernatants of the ppp-tau clones were pipetted into the corresponding wells. After thorough washing, the secondary sub-class specific antibody conjugated to horseradish peroxidase (HRP) was added. After the plates were washed once more, a coloring agent was added to measure the antibody binding by absorbance (**Table 12**).

4. RESULTS & DISCUSSION

Table 12: Epitope mapping results obtained from ELISA assay with the peptide cassette **19-28**. In the left column, P stands for a phosphorylation in position 396 (left), 400 (middle), or 404 (right). The letter G represents a *O*-GlcNAcylation in the corresponding position. In the top row, clones with a light blue background showed previously cytoplasmatic recognition (**Figure 34**), while clones with a light red background had shown nuclear tau recognition (**Figure 35**). Green colors mark positive recognition, whereas the darker the tone of the green color, the more intense was the positive signal.

	cytoplasmatic localization				nuclear localization		
	9C10	10D5	6F11	15F1	8D12	18E5	7F2
19 (PPP)	0.354	0.067	0.334	0.406	0.351	0.323	0.369
20 (PP-)	0.367	0.040	0.039	0.365	0.044	0.043	0.038
21 (P-P)	0.379	0.042	0.265	0.317	0.171	0.116	0.076
22 (-PP)	0.045	0.067	0.334	0.052	0.360	0.377	0.394
23 (P--)	0.371	0.049	0.106	0.183	0.049	0.042	0.038
24 (-P-)	0.048	0.051	0.041	0.050	0.041	0.048	0.038
25 (--P)	0.048	0.043	0.107	0.044	0.063	0.066	0.046
26 (---)	0.063	0.060	0.047	0.054	0.065	0.054	0.047
27 (-GP)	0.040	0.047	0.042	0.040	0.038	0.042	0.040
28 (PGP)	0.234	0.048	0.057	0.233	0.040	0.041	0.039

These results showed that the tri-phosphorylated peptide **19** was recognized by all antibody clones except 10D5, which did not show any interaction with the antigen. Moreover, *O*-GlcNacylated peptide **27** was not detected by the ppp-tau antibodies. In a previous work by Smet-Nocca *et al*, the inhibitory effect of *O*-GlcNAcylation in Ser400 on phosphorylation in position 396 was demonstrated (see section **2.2.7**).[167] Therefore, the pattern of PTM modifications on peptide **28** reassembles likely an unnatural scenario, where positions 396 and 404 are phosphorylated and position 400 is *O*-GlcNAcylated. Nevertheless, this peptide was recognized to some extent by the clones 9C10 and 15F1. The same two ppp-tau antibody clones

showed also strong recognition of tau peptides with phosphorylations in positions 396 and 404. The clone 9C10 showed in addition stronger interaction with peptide **23**, thus having possibly the 396 phosphorylation as a crucial recognition site. The clones 6F11 and 15F1 showed both a diminished affinity to peptide **23** with a single phosphorylation in Ser396, whereas single phosphorylations in positions Ser400 and Ser404 did not lead to any signals. From the obtained results, no general rules can be deduced that would link nuclear or cytoplasmatic recognition of tau antibodies to particular binding epitopes.

Responsibility assignment: Peptides **19-28** were commercially obtained, manufactured by Peps4LS (GmbH, INF 583, 69120 Heidelberg) and paid by the Hackenberger group. Peptides **27** and **28** were synthesized by Sergej Schwagerus. The epitope mapping by ELISA was carried out by Andrew Flatley in the lab of Dr. Elisabeth Kremmer at the Helmholtz Center Munich.

4.6.3.4 Evaluation of ppp-tau antibodies by western blot experiments with semisynthetic tri-phosphorylated tau

To further test the specificity of the antibody clones and exclude backbone binding, we used the semisynthetic tau construct **9** (see also section **7.3.3** for experimental details on the generation of semisynthetic protein **9**).
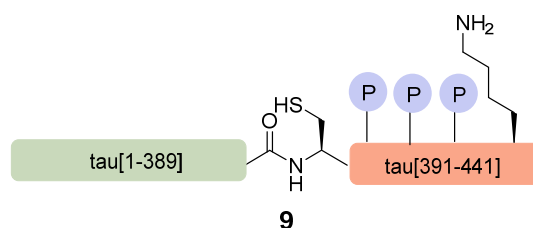
Figure 37: Semisynthetic full-length tau, homogeneously phosphorylated in PHF-1 (Ser396/400/404).

The semisynthetic product **9** and recombinant non-phosphorylated tau, which was expressed according to a previously published protocol,[123] were run by SDS-PAGE and then wet-blotted onto a nitrocellulose membrane. The different antibody clones were then tested on the two constructs and exhibited high specificity for the semisynthetic tri-phosphorylated tau (**9**) over the higher concentrated recombinantly expressed unphosphorylated tau (**Figure 38**).
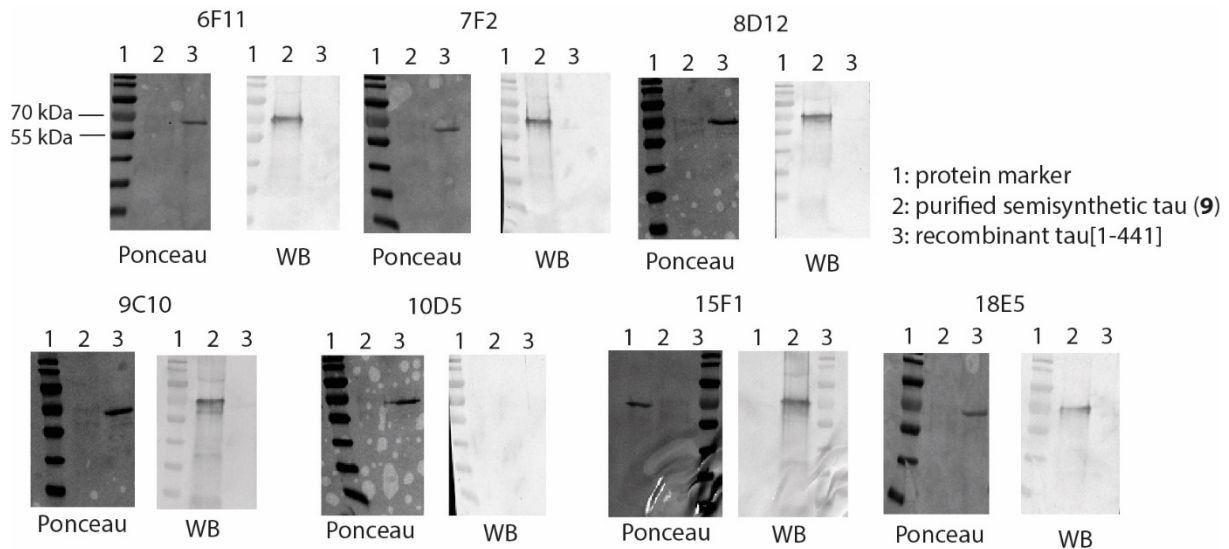
Figure 38: Ponceau stained membranes and western blots (WBs) of the seven generated antibody clones. All of them showed excellent selectivity despite 10D5, showing no recognition of either tri-phospho-tau (**9**) or unphosphorylated recombinant tau.

These results demonstrated the high specificity of the novel antibody clones for phospho-tau. The clone 10D5 did not show any interaction with the semisynthetic protein **9**, in accordance to results obtained by epitope mapping (see section **4.6.3.3**).

Responsibility assignment: These experiments were carried out by Oliver Reimann under the supervision of Prof. Dr. Christian P. R. Hackenberger.

4.6.3.5 Staining severe cases of AD and Pick's Disease

The clones 9C10 and 8D12 were tested in coloration experiments on brain tissue of deceased patients of AD and Pick's disease (frontotemporal lobe dementia - FTLD), a non-AD tauopathy. These clones were chosen, since 9C10 showed previously strong cytoplasmatic tau recognition (**Figure 34**), whereas the ppp-tau antibody 8D12 interacted with nuclear tau (**Figure 35**). Additionally, the antibody AT8 (against pThr202 and 205) was used as a comparison.

T 262-12 Alzheimer´s disease (Braak Stage VI); Hippocampus. Upper row temporal cortex; lower row Hippocampus (CA4 region)

AT8   9C10   8D12

▼ Dystrophic neurites surrounding Abeta plaques („neuritic plaques")
↖ Neurofibrillary tangles
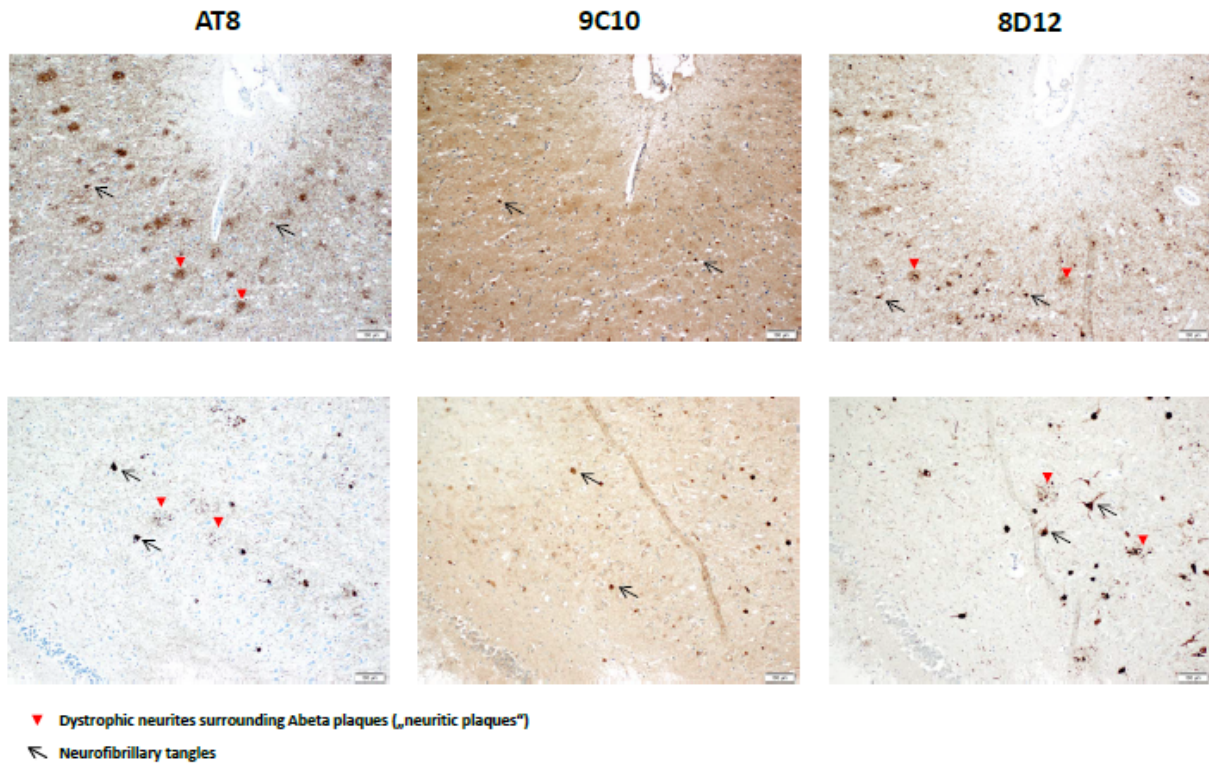
Figure 39: Staining of AD Braak Stage VI brain tissue of the temporal cortex (upper row) and the hippocampus (lower row) by antibodies AT8, 9C10 and 8D12.

Either neurofibrillary tangles (black dots marked with a black arrow) or more diffuse dots, which are dystrophic neurites made of amyloid-β and tau (marked by red triangles) were stained in this experiment. The tested clones 9C10 and 8D12 showed a comparable staining of AD pathological features to the prominent AT8 antibody in these experiments. The same experimental set-up was chosen for the severe cases of Picks disease (**Figure 40**).
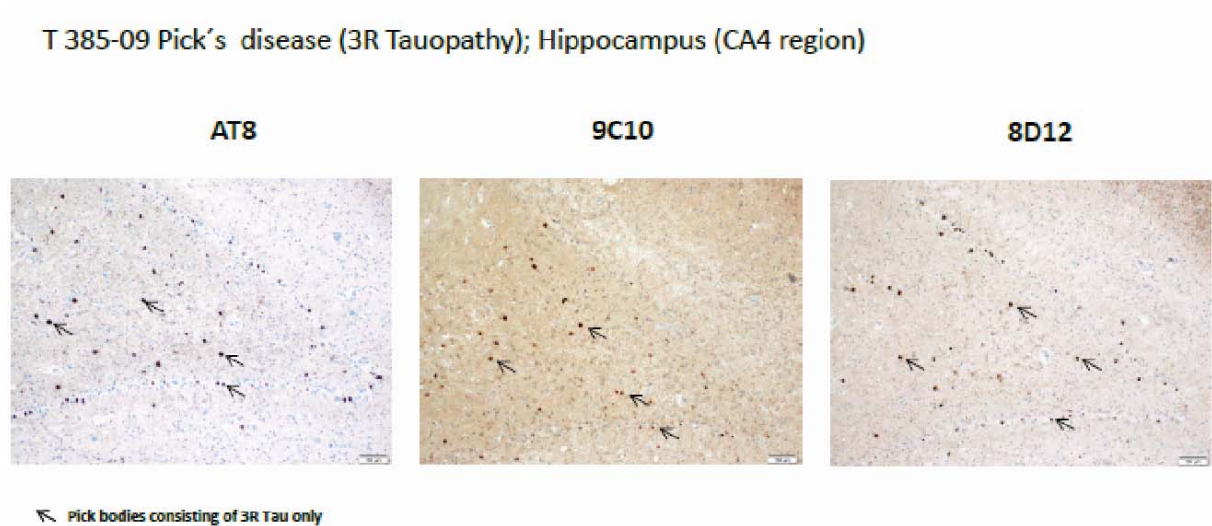
Figure 40: Staining of brain tissue of severe cases of Pick's disease by antibodies AT8, 9C10 and 8D12. The black arrows mark Pick bodies consisting of 3R tau only.

Hereinafter, multiple cell-labeling experiments were carried out and monitored by fluorescence microscopy from human cells derived from AD tissue. DAPI staining marked the nuclei of the cells. Fluorescein (FITC) labeling was carried out for AT8 staining and cyanine dye 3 (Cy3) was performed for the antibodies 9C10 or 8D12 (**Figure 41**).
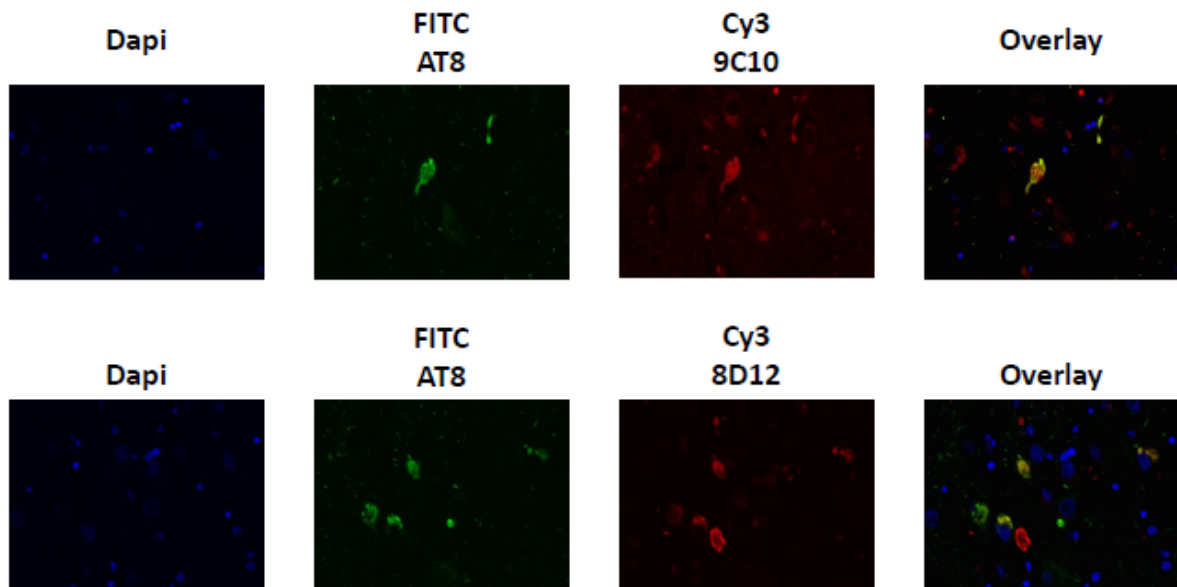
Figure 41: Multiple cell-labeling of cells derived from tissue of AD patients.

Strong labeling of the cells by 9C10 and 8D12 was observed with partial overlay with AT8 labeling, indicating that the new antibody clones provide additional information to AT8. Despite previous nuclear detection of phospho-tau by ppp-tau antibody 8D12 (see section **4.6.3.2, Figure 35**), in this experimental set-up, no nuclear tau detection was observed.

Additionally, double staining was carried out for cells derived from patients that suffered from Pick's disease (**Figure 42**).
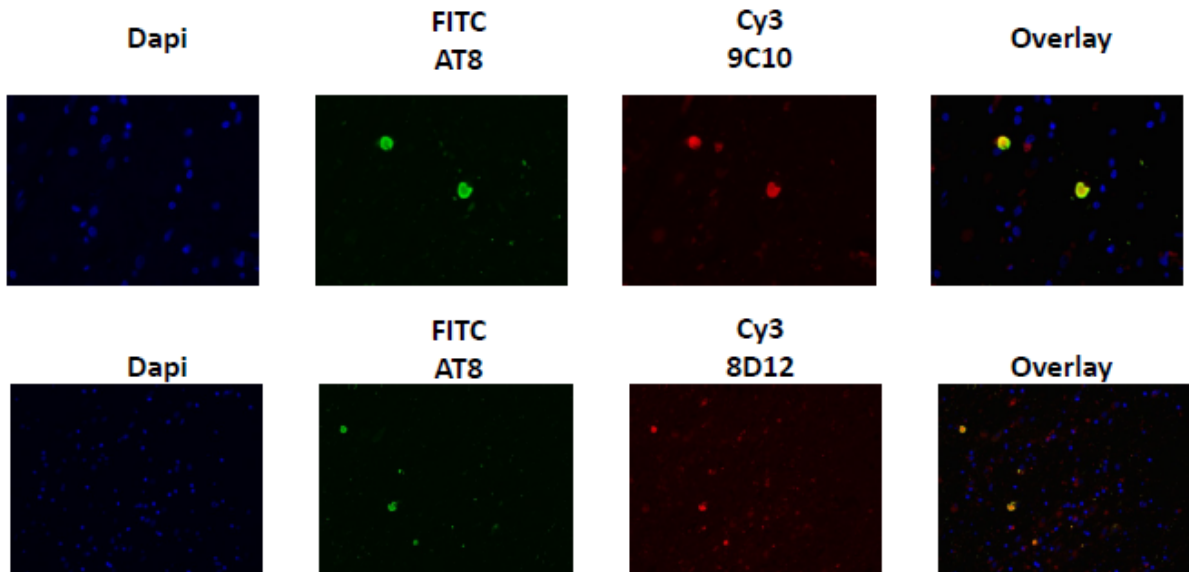
Figure 42: Multiple cell-labeling of cells derived from tissue of Pick's disease patients.

A strong labeling was also observed for Pick's disease. For the clone 8D12, some spots were detected that were not stained by AT8, but no co-localization with DAPI was observed.

In summary, these experiments showed that labeling of severe cases of AD and Pick's disease works efficiently with the two clones 9C10 and 8D12, comparable to AT8. In the future, a deeper investigation of borderline cases of AD and PD would be needed to get further insights into the ability of the antibodies to detect early changes in the course of these diseases.

Responsibility assignment: These experiments were carried out by Dr. Stefan Prokop from the group of Prof. Frank Heppner at the Charité Berlin (neuropathology).

4.6.3.6 PHF-1 phosphorylation on tau in the *C.elegans* model

The nematode *Caenorhabditis elegans* (*C.elegans*) is a invertebrate animal model that offers the possibility to unravel mechanisms of tau pathogenesis. Advantages of the *C.elegans* model over other animal models are fast aging, facile manipulability and its transparency, allowing for live-imaging of molecular changes inside the animal. Age-related changes of tau phosphorylation would be easily monitored, since a worm lives usually between 15 and 20

days.[515] In particular, such simple models can help to reveal the contribution of hyperphosphorylation, conformational changes of tau and tau aggregation to neurodegenerative disorders like AD.[516] Previously, the pan-neuronal expression of human tau in transgenic worms was shown to cause progressive uncoordinated locomotion, which is characteristic of defects in the nervous system.[517] Moreover, a *C.elegans* model was established, overexpressing human tau with a P301L mutation.[518] There, animals expressing this mutant tau showed stronger reduction of mobility and higher degree of progressive axonal degeneration. A model to study tau hyperphosphorylation was developed by Roland Brandt *et al*,[516] in which pseudo-phosphorylated (PHP) tau constructs were generated in *C.elegans*. At AD relevant phosphorylation sites including Ser396 and Ser404, the charged amino acid Glu was placed (see section **2.2.1** for more information on pseudo-phosphorylation). By comparing PHP tau with WT-tau expressed in *C.elegans* by immunofluorescence staining and western blot analysis of worm lysates, they reported that normal human tau in *C.elegans* is highly phosphorylated at many sites and exhibits conformational changes, similar to pathologic tau in AD.

In this course of the current investigation, two different models of *C.elegans* were generated, one overexpressing WT human tau-YFP fusion protein and one overexpressing human tau with P301L mutation as YFP fusion. The animals were overexpressing these two versions of tau in neuronal cells. To visualize detection of phosphorylated tau in the animals, a mixed population of nematodes was fixed by formaldehyde and stained with either 8D12 or 9C10 in a 1:100 dilution. Afterward, a secondary antibody with an AlexaFluor594 label was added, which allows for the direct visualization of bound primary antibody inside the fixed worms by fluorescence microscopy. Moreover, DAPI staining was performed to enable detection of potential nuclear localization of tau. In result, no tau detection was observed (**Figure 43**), which would be visible by an overlay of green signals obtained through YFP monitoring and red signals generated through AlexaFluor594 labeling.

Neuronal tau(P301L), 8D12 (1:100), anti-rat (1:200)   Neuronal tau(P301L), 9C10 (1:100), anti-rat (1:200)
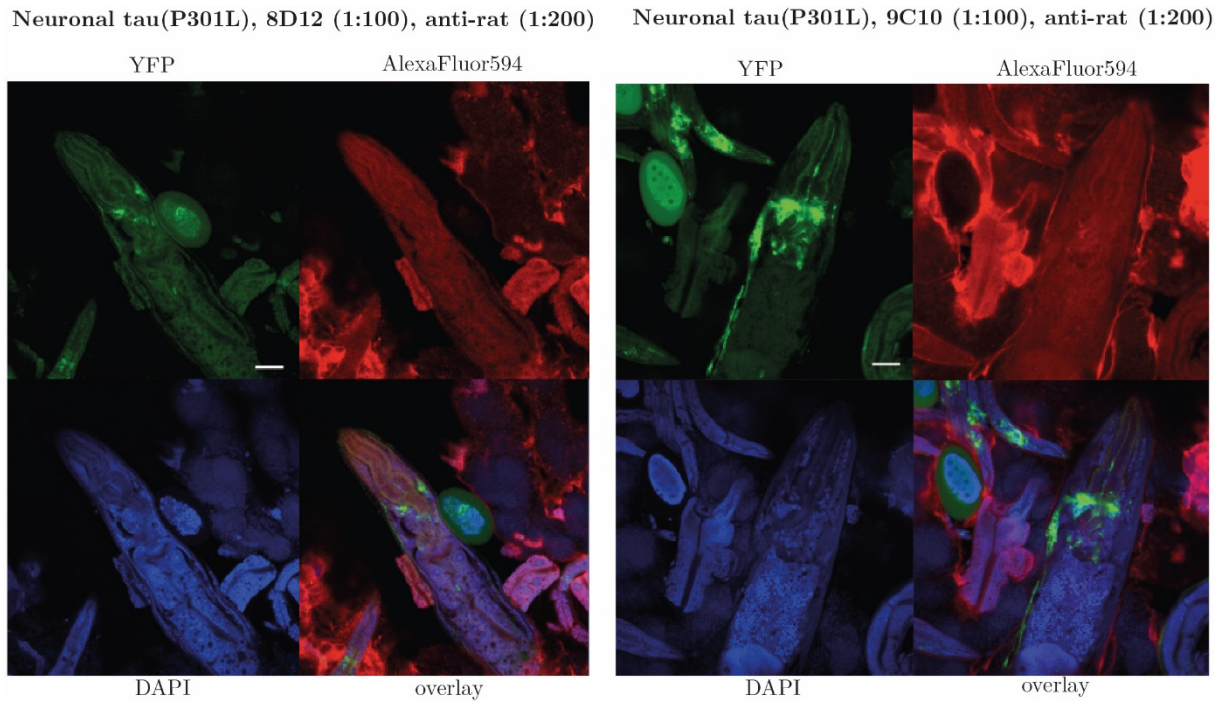
Figure 43: The human tau mutant P301L was exposed to DAPI staining (blue), showing staining of the nuclei. Further, YFP (green) was monitored under the fluorescence microscope, showing tau localization inside the animal. The primary antibodies 8D12 (left) and 9C10 (right) were applied, followed by the addition of a secondary antibody rat with AlexaFluor594 labeling (red). Finally, the images were merged (bottom right pictures) to check for tau detection by green and red overlay.

It was hypothesized that the tau antibodies were low in concentration and thus, buffered 1:1 dilutions of the ppp-tau antibodies were applied, which also did not lead to a positive detection. Since a proof of principle was still missing, the worms were lysed and the worm lysate was used for western blot detection with a pan-antibody (tau 46, SantaCruz Biotechnology), thereby resorting to a technique, which was previously successfully used to detect tau phosphorylated in PHF-1 (see section **4.6.3.4**). No detection was observed, which suggested the presence of low concentrations of tau. To address the issue of general low tau concentration, the model was changed to worms overexpressing the WT-tau YFP fusion and the P301L mutant tau YFP fusion in muscular cells instead of neuronal cells. Higher signals of YFP-tau fusion were visible by fluorescent microscopy, but a successful live-imaging with the ppp-tau antibodies was still not possible. Worms overexpressing tau in muscle cells were analyzed by western blot after lysis with the clones 15F1, 9C10 and 8D12 (**Table 13**), providing an adequate precedence of phospho-tau in the given model. In the western blot analysis, three markers were used. The intracellular component tubulin was monitored with a tubulin specific antibody, thus showing

a successful lysis of the animals. There, the observed intensity was identical for WT- and M-tau (tau P301L) in sample volumes of equal size. Moreover, pan-tau and GFP western blotting yielded detection of bands of equal height on the ablot indicating the presence of the tau-YFP fusion protein (**Table 13**). Then, M-tau samples were blotted and detected with the three ppp-tau antibodies 15F1, 8D12 and 9C10.

Table 13: Detected species are framed in red; protein marker for 100 kDa are labeled with blue arrows, WT = wiltdype, M = mutant tau P301L. From left to right: The tubulin western blot marks successful worm lysis; the phospho-unspecific antibody tau 46 targeting C-terminal tau showed the presence of tau on the blot (M_W calcd. for tau YFP fusion = 73 kDa; observed above 100 kDa due to low retardation of tau on SDS-PAGE;[123] the blot against GFP shows a detection as well, since tau is expressed as a YFP fusion protein (GFP antibody recognizes YFP); 15F1, 8D12 and 9C10 recognized phospho-tau from *C.elegans*.
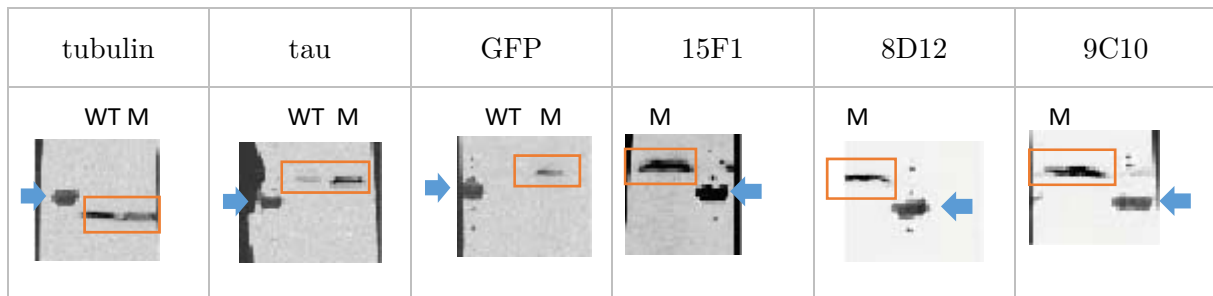
In summary, live-imaging of phospho-tau in *C.elegans* with ppp-tau antibodies was not successful, but the presence of correspondingly phosphorylated tau species was confirmed by western blot analysis of lysate of worms overexpressing tau in muscular cells. The unsuccessful detection of phospho-tau inside *C.elegans* animals could be traced back to a low overall concentration of the corresponding tau species or the low antibody concentration in cell supernatants. The application of purified and concentrated antibody needs to be investigated in future attempts toward the detection of PHF-1 phosphorylation of tau, since thus far only unpurified hybridoma cell supernatant was used. Furthermore, a protocol was applied to separate nuclear from cytoplasmatic fractions of worm lysates, which were then analyzed on western blots. This technique was previously applied to study the transcriptional regulation of *lin-42* in the larval epidermal seam cells (see section **7.4.4** for experimental details).[519] This separation protocol could be used for further investigations on the ability of particular ppp-tau clones, such as 8D12, to specifically bind nuclear tau, as was shown previously (see section

4.6.3.2). The preliminary results obtained by western blot experiments of the nuclear and the cytoplasmatic fractions were not conclusive, since the separation protocol was not quantitative and needs to undergo further elaboration in the future.

Responsibility assignment: The generation of the *C.elegans* species, the live-labeling and the fluorescence microscopy were carried out by Kristin Arnsburg under the supervision of Dr. Kirstein. The western blot experiments were carried out by Kristin Arnsburg and Oliver Reimann. The protocol to separate the cell nuclei from the cytoplasmatic fractions was performed by Manuel Iburg under the supervision of Dr. Kirstein.

4.6.3.7 Neuronal model of aging

To study molecular mechanisms of aging, neuronal models are widely used.[520] There are numerous studies performed on cultured human fibroblasts,[521] T lymphocytes,[522] and several other types of mammalian cells.[523, 524] In these models it was demonstrated that normal dividing cells have a finite proliferation capacity *in vitro*, whereas this phenomenon is interpreted as aging on molecular level and is further known under the term "replicative senescence".[525] There is precedence that accumulative damage in differentiated cells over lifetime leads to the gradual loss of function and increased probability of degeneration.[526, 527] The use of neuronal models of cell aging in vitro may produce valuable information for the changes of cellular and molecular levels that ultimately lead to neuronal degeneration of the senescent brain.

In this project, primary neuronal cultures from the neuronal cortex of rats were obtained and used to study age-related changes of tau phosphorylation with the new ppp-tau antibodies. The cultures were differing in age, ranging between 20 and 80 days. In a first experiment, lysed neuronal cells of different ages (20, 30, 40, 50 and 60 days) were wet-blotted and investigated by western blot with two ppp-tau clones with cytoplasmatic tau recognition (9C10 and 15F1) and two ppp-tau clones with nuclear recognition (8D12 and 18E5) of phospho-tau. All four clones exhibited strong tau recognition in previous immunofluorescence experiments (see section **4.6.3.2**). In addition, pan-tau antibody was applied for a comparison (**Figure 44**). A good detection was observed for the tested ppp-tau antibody clones, as well as for total tau. The results showed that total and phospho-tau both show a decay in concentration upon aging.

This downregulation of tau translation in this neuronal model was not found in other publications and needs to be further investigated in the future. In some cases, a second band was detected on the blots, which could be explained by the presence of truncated tau versions, other isoforms of tau or simply unspecific binding of the applied secondary antibody used in these western blot experiments to other protein species. Additionally, neuronal cells treated with spermidine were blotted and analyzed, since spermidine diet increased the life-span in several model animals for neurodegenerative diseases.[528] In this experimental set-up, no significant changes were observed for cell cultures that were pretreated with spermidine (lines labeled with Sper on top, **Figure 44**).
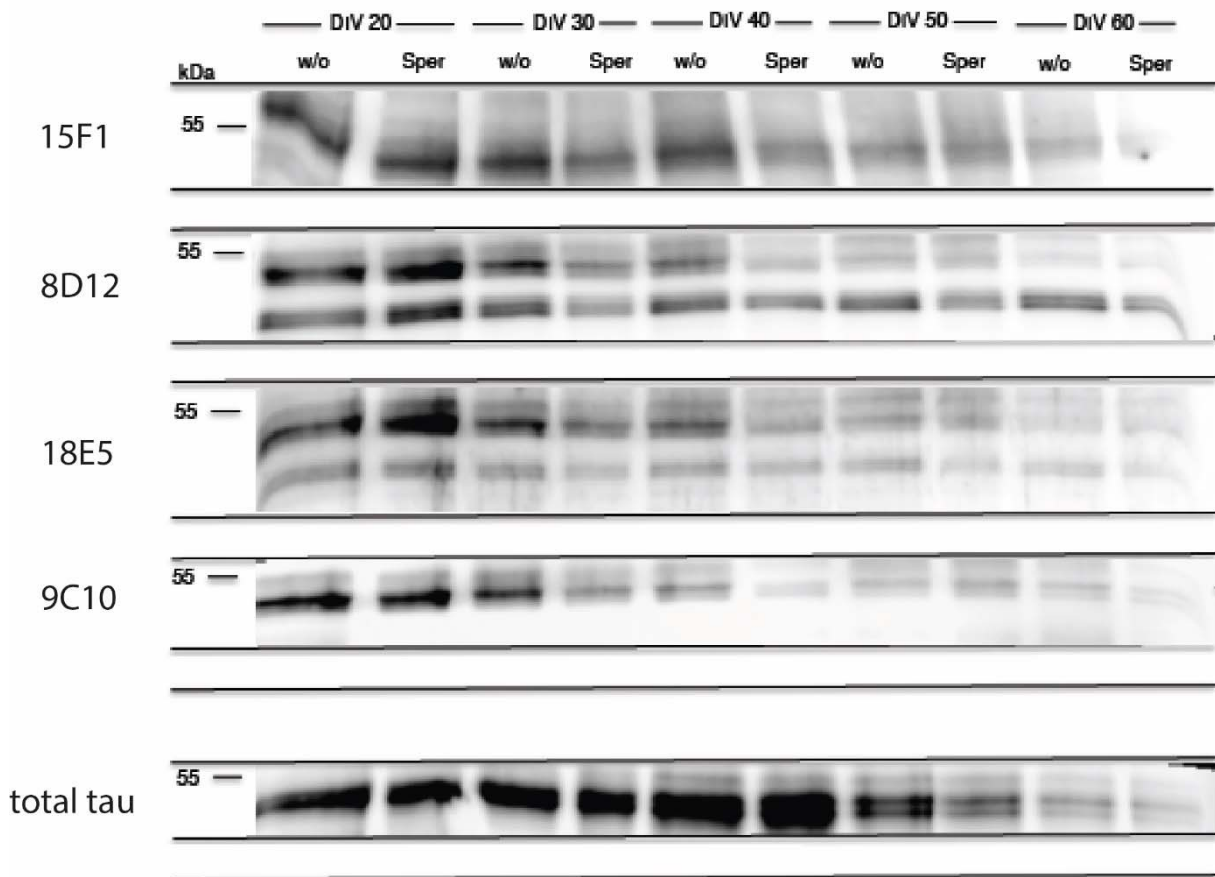
Figure 44: Blot of cell cultures of either 20, 30, 40, 50 or 60 days of age.

To obtain further insights on tau phosphorylation in this model of aging, immunocytochemistry (ICC) was carried out. In ICC, visualization and localization of specific proteins or antigens in cells is achieved by a primary antibody, binding the corresponding protein epitope. Furthermore, a fluorophore labeled secondary antibody that binds the primary antibody is

added, allowing visualization of the proteins under a fluorescence microscope. In each measurement, four different molecular markers were monitored in parallel. MAP2 is a general neuronal marker, rather specific for dendrites and well suited for mature neurons, whereas synaptophysin is a typical synapse marker. Additionally, the four clones 15F1, 9C10, 18E5 and 8D12 were tested and compared with a phospho-unspecific tau marker. The ppp-tau antibody clones that showed previously cytoplasmatic detection of phospho-tau (see section **4.6.3.2**), were shown to have very strong signals in young cultures of 20 days. As previously seen in western blots (**Figure 44**), phospho-tau levels were drastically decreasing over time and lastly completely vanishing, whereas only a slight decrease was observed for total tau. The signals obtained with 15F1 were of higher intensity than for 9C10, suggesting a higher abundance of the recognized species.
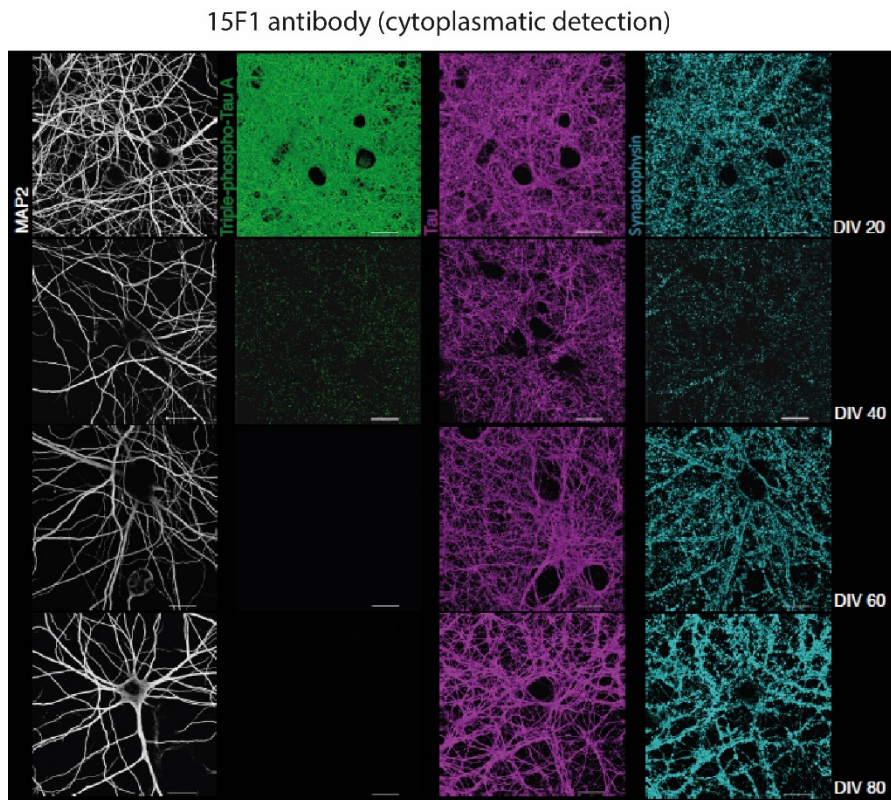
Figure 45: MAP2 marker on the left (white); 15F1 antibody clone (green); tau marker (pink) and synaptophysin (blue) in cell cultures of either 20, 40, 60 or 80 days of age.
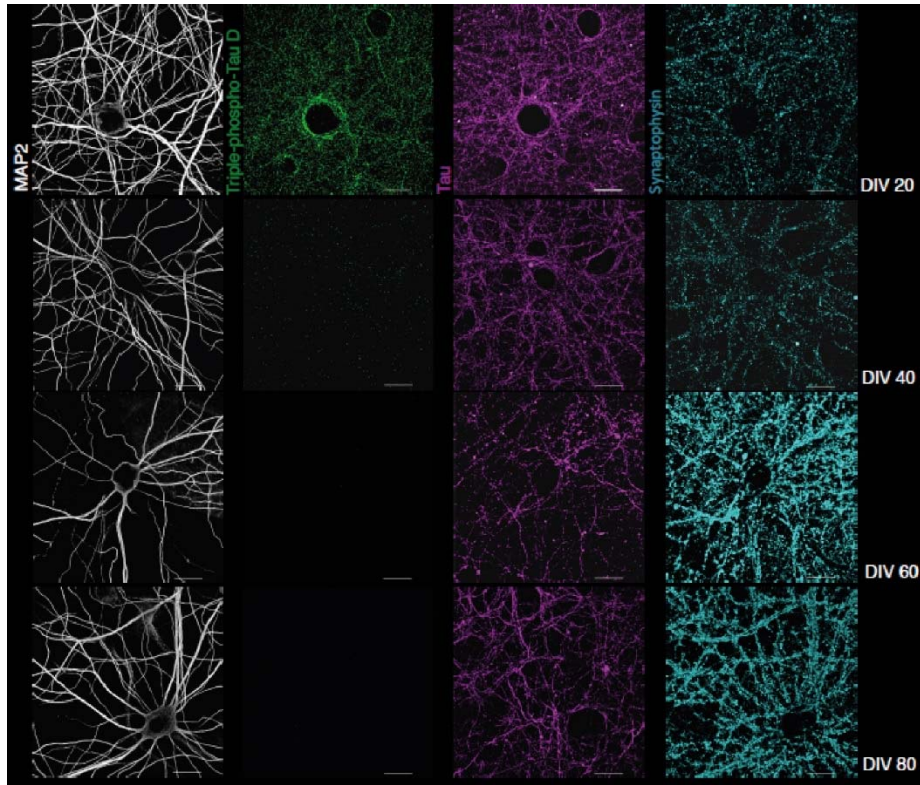
Figure 46: MAP2 marker on the left (white); 9C10 antibody clone (green); tau marker (pink) and synaptophysin (blue) in cell cultures of either 20, 40, 60 or 80 days of age.

The antibodies 9C10 and 15F1 were previously shown to bind tau species that have to be phosphorylated in position 396 (see section **4.6.3.3**). The antibodies 18E5 and 8D12 in contrast, were shown to have the Ser404 position as a crucial phosphorylation site. To check for differences in recognition by ICC, the same experiments were carried out with ppp-tau antibody clones that previously recognized tau in cell nuclei (see section **4.6.3.2**). The ppp-tau antibody 18E5 gave weak signals in ICC in 20 day old neuronal culture, which completely disappeared in measurements with older cultures (**Figure 47**). A different result was obtained for the 8D12 clone, which intensively recognized phospho-tau in 20 day old neuronal cells. The recognition of the 8D12 clone in the cytoplasm of the cells vanished upon application on older neurons, whereas only nuclear tau was recognized in cell cultures with an age of 80 days (**Figure 48**).

18E5 antibody (nuclear detection)
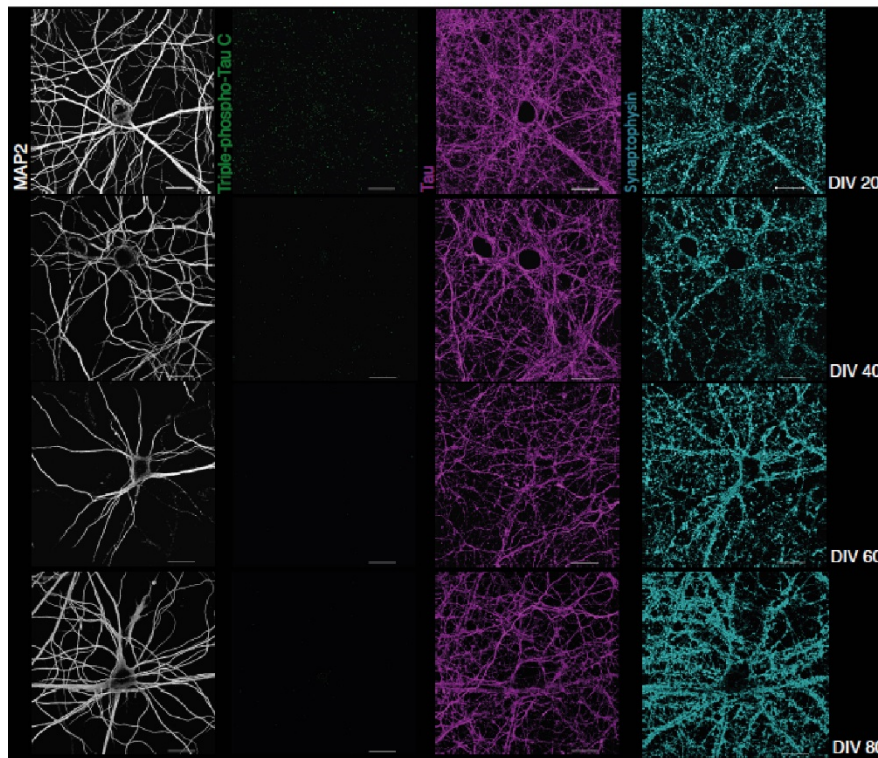
Figure 47: MAP2 marker on the left (white); 18E5 antibody clone (green); tau marker (pink) and synaptophysin (blue) in cell cultures of either 20, 40, 60 or 80 days of age.

8D12 antibody (nuclear detection)
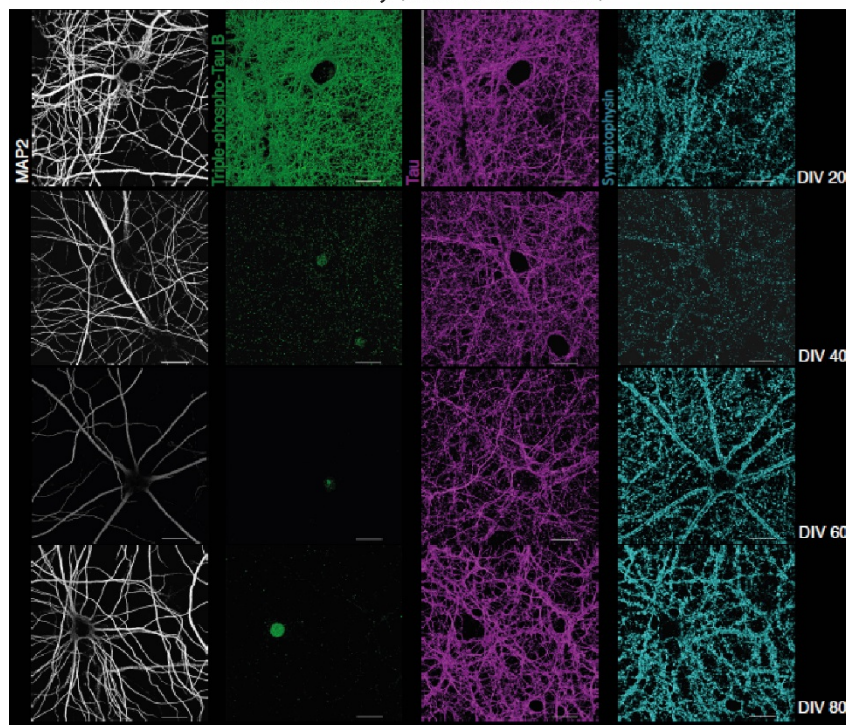
Figure 48: MAP2 marker on the left (white); 8D12 antibody clone (green); tau marker (pink) and synaptophysin (blue) in cell cultures of either 20, 40, 60 or 80 days of age.

The observation for clone 8D12 with its nuclear recognition could hint toward a change of function that phospho-tau undergoes in this neuronal model. The function of nuclear tau was previously discussed in section **2.2.4**. The local change of phospho-tau recognized by 8D12 could attribute to a conformational change of the tau molecule that is only recognized by 8D12. A concentration dependent effect could be another explanation. This could mean that tau delocalizes to the nucleus if only few tau is present, whereas this nuclear tau is only detected by 8D12. These observations cannot be traced back or linked to observations described in the literature by related experiments. Further experiments should involve the isolation of nuclear tau species from 80 days old cultures and their characterization to get a better understanding of these observations.

Responsibility assignment: The experiments were carried out by Julia Abele under the supervision of Prof. Dr. Daniela Dieterich from the Otto von Guericke University of Magdeburg.

4.6.3.8 Immunoprecipitation (IP) with the 15F1 clone and mass spectrometry of the pulled out fraction

Verification of signal specificity for antibodies in ELISA by immunoprecipitation experiments is a commonly applied methodology, which was also used for tau antibodies.[529] Immunoprecipitation describes a technique that uses antibodies to bind a specific antigen out of a complex solution. In a direct immunoprecipitation, the antibodies are immobilized on a solid-phase, such as superparamagnetic beads or on microscopic non-magnetic beads. These beads are often based on agarose. In the so-called indirect immunoprecipitation, free antibodies are added to a sample, which can bind their targets. After an adequate incubation time, paramagnetic beads coated with protein A/G are added to the mixture, leading to the immobilization of the antibody bound to the corresponding antigen. Washing steps remove other proteins that stick to the A/G protein beads and finally, the immobilized antibody and the corresponding antigen can be eluted either by low pH solutions or by boiling of the beads in SDS sample buffer followed by direct transfer to a SDS gel. After SDS-PAGE, the corresponding antigen band is excised and digested by trypsin.[530]

4. RESULTS & DISCUSSION

Tau and phospho-tau CSF levels increase in case of AD and thus contribute to a positive diagnosis of the disease in early stages (see section **2.2.9**). To ensure correct binding of the new ppp-tau antibody 15F1 to tau phosphorylated in PHF-1 in biological samples, an immunoprecipitation experiment from AD patients CSF was performed. Therefore, 450 µL CSF aliquots of AD patients were incubated with the 15F1 cell supernatant (10 µg/mL final concentration) that showed previously cytoplasmatic tau recognition (see sections **4.6.3.2**). Cytoplasmatic tau recognition was considered crucial due to a higher propensity to escape neuronal cells and localization in CSF by mechanisms previously described (section **2.2.5**, **Figure 8**). Immunoprecipitation was carried out according to the instructions of Pierce® Protein A/G Magnetic Beads (lot number 88802) (see experimental section). Proteins bound to A/G protein coated resin were eluted by heating at 95°C in SDS sample buffer and separated by SDS-PAGE. A band at approx. 55 kDa was observed, typical for tau (**Scheme 49**). Then, the band was excised and digested with trypsin,[530] which should yield peptide **29** that includes the complete PHF-1 epitope. In a following step, the samples were analyzed by mass-spectrometry, but tau peptide **29** was not identified, while other fragments of the tau protein were found. Instead, a weak signal was observed for the corresponding unphosphorylated peptide **29** (see section **7.4.5** for experimental details).
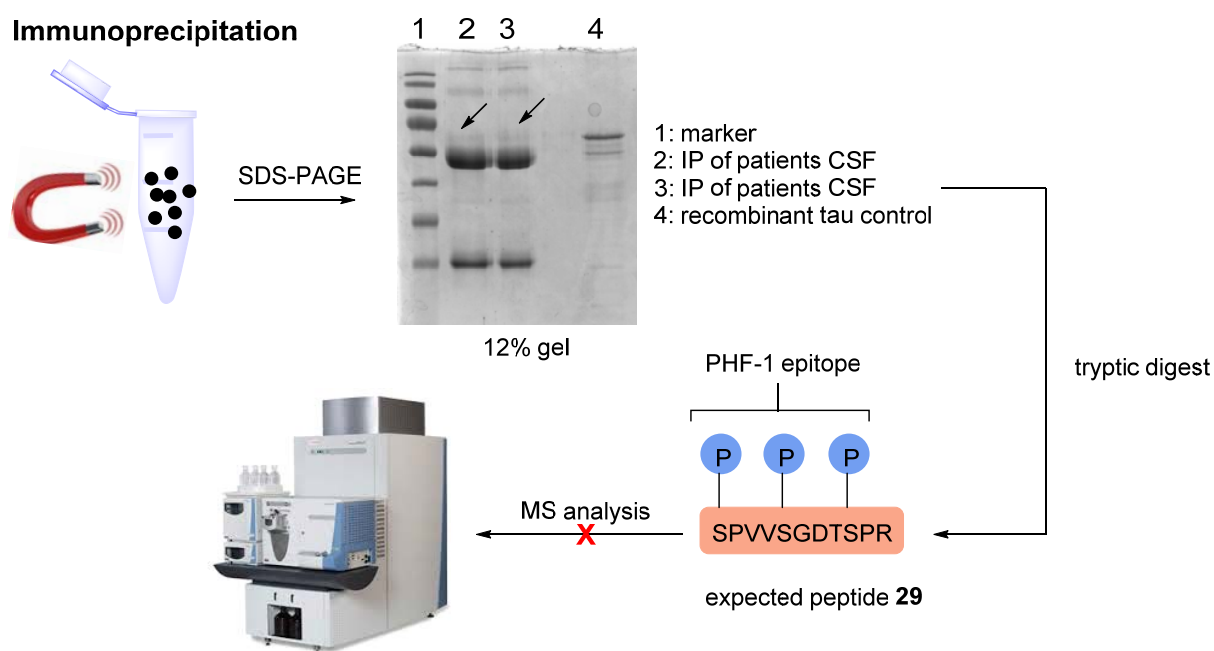
Scheme 49: Workflow of immunoprecipitation, protein isolation, tryptic digest and subsequent mass analysis of the corresponding peptide **29**, bearing the complete PHF-1 epitope.

It was assumed that the concentration of the highly phosphorylated peptide **29** was too low. This can implicate detection problems, which become more prevalent for highly phosphorylated peptides due to the high affinity of phosphate to metal ions.[531] It was reasoned that the phosphorylated tau peptide could bind in an IMAC-like fashion to components of the mass spectrometer, which in result hampers the detection.

In summary, the general protocol to detect antibody-bound tau was established, but the detection needs further improvements. An alternative protocol may be applied, in which the phosphates are eliminated by base, rendering dehydroalanines at these phospho-sites. These reactive alkenes can then further be functionalized by the addition of thiol reagents, which can react with the alkene in a thiol-ene type reaction. Such a protocol was previously established in the laboratory of Dr. Eberhardt Krause and is intended to be applied in the future.[532]

Responsibility assignment: The IP and the following tryptic digest was performed by Oliver Reimann under the supervision of Prof. Christian P. R. Hackenberger. Mass spectrometry experiments were conducted by Dr. Michael Schuemann and Dr. Eberhard Krause.

4.6.3.9 ELISA assays with the new antibodies

ELISA quantification of tau and phospho-tau levels in CSF is often used in clinics to diagnose AD and other tauopathies (see section **2.2.9**). It was thus an obvious task to check for the applicability of the new ppp-tau antibody clones in ELISA assays. A collaboration with Prof. Dr. Oliver Peters from the psychiatry faculty of the Charité was established, who provided CSF samples from AD patients that were used in ELISA assays.

In a first experiment, the identification of the most potent ppp-tau antibody clone for the detection of phospho-tau in CSF was aimed at. Therefore, the commercial tau ELISA-kit INNOTEST® hTau Ag (Fujirebio Europe) was applied, using the CSF probe of an AD patient in a Sandwich ELISA set-up (**Figure 49**, see section **7.4.6.1** for experimental details). According to the instructions from this kit, the plate was coated with one of the ppp-tau primary antibodies. Either undiluted cell supernatant or a 1:1 dilution in PBS buffer was applied. After washing of the wells with PBS buffer and blocking with 5% milk in PBS, CSF samples were

applied, followed by another wash. Hereinafter, two tau primary biotinylated antibodies BT2 (binds tau[190-195]) and HT7 (binds tau[160-164]) were applied to preclude interference of either HT7 or BT2 with the primary ppp-tau antibody. After extensive washing, HRP-conjugated streptavidin is added to each well, binding to biotinylated primary tau antibodies BT2 and HT7. Finally, 3,3',5,5'-tetramethylbenzidine (TMB) is added after extensive washing steps to create a color-reaction.
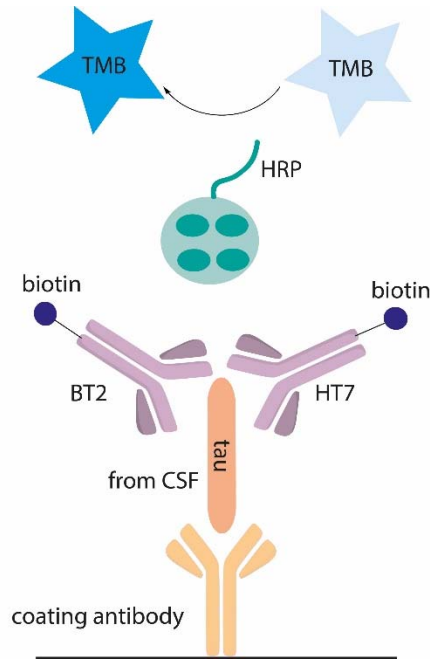
Figure 49: Sandwich ELISA to identify the most potent clone for CSF testing according to the INNOTEST® hTau Ag (Fujirebio Europe) kit.

For comparison, the antibodies AT8 (against pThr202 and 205) and PHF-1 (pSer396 and 404) were used in addition to primary antibodies for coating of the 96-well plates. The PHF-1 antibody was kindly provided by Prof. Peter Davies (Einstein College of Medicine, NY, USA). **Table 14** shows the tested antibodies and the dilutions they were applied in, whereas the results of the screening are summarized in **Figure 50**.

4. RESULTS & DISCUSSION

Table 14: Coated antibodies that were used in the experiment to identify the most potent clone.

	undiluted	1:1 diluted with PBS
A	AT8 (2µg/mL in PBS)	AT8 (2µg/mL in PBS)
B	PHF-1 (1:1000 in PBS)	PHF-1 (1:1000 in PBS)
C	8D12	8D12 (1:1 PBS)
D	15F1	15F1 (1:1 PBS)
E	6F11	6F11 (1:1 PBS)
F	9C10	9C10 (1:1 PBS)
G	7F2	7F2 (1:1 PBS)
H	18E5	18E5 (1:1 PBS)
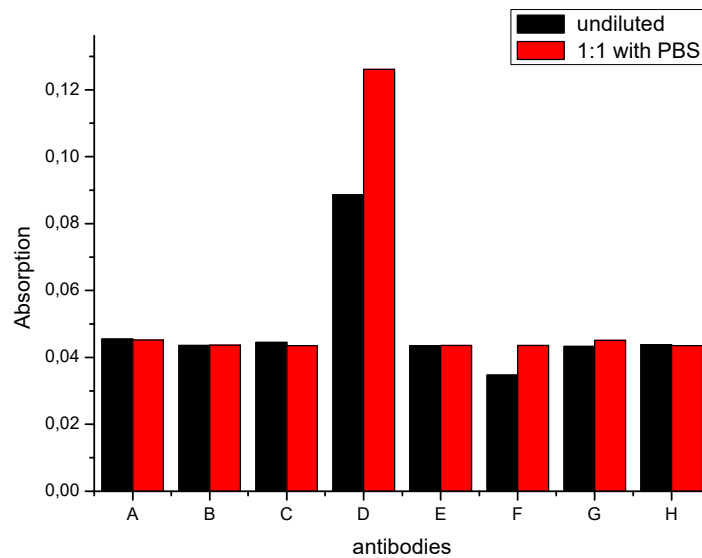
Figure 50: Absorption of the different antibody clones tested.

.

All antibodies showed a comparable binding of tau, except the 15F1 clone (D in **Figure 50**), which was thus selected for further experiments. Moreover, a more intensive detection was observed, when the cell-supernatant of the 15F1 clone (D) was diluted 1:1 in PBS, which might be attributed to better binding of the antibody to the plate in buffered solution. The 15F1 clone was also found to bind most efficiently, when CSF samples were applied in higher

concentration (see **Figure 80** in section **7.4.6.1**). After identifying the most potent clone 15F1, CSF material from a small cohort of seven different patients was analyzed in the same experimental set-up as shown in **Figure 49**. At first, total tau mirrors were measured for comparison, which showed that the patients had very different levels of total tau inside CSF (see section **7.4.6.2, Table 20**). Then, phospho-tau levels were measured and it was found that measured levels of phospho-tau were all comparable in all tested probes inside the cohort (see section **7.4.6.2**, **Table 21**). It was assumed that the phospho-tau assay as performed is not sensitive enough to distinguish between minor changes of phospho-tau levels. Therefore, two different experimental set-ups were tested (set-ups A and B shown in **Figure 51**). In both set-ups, secondary antibodies are applied, which can lead to signal enhancement due to binding of multiple copies of secondary antibodies (general procedure applied for sandwich ELISAs can be found in **7.4.6.3**).
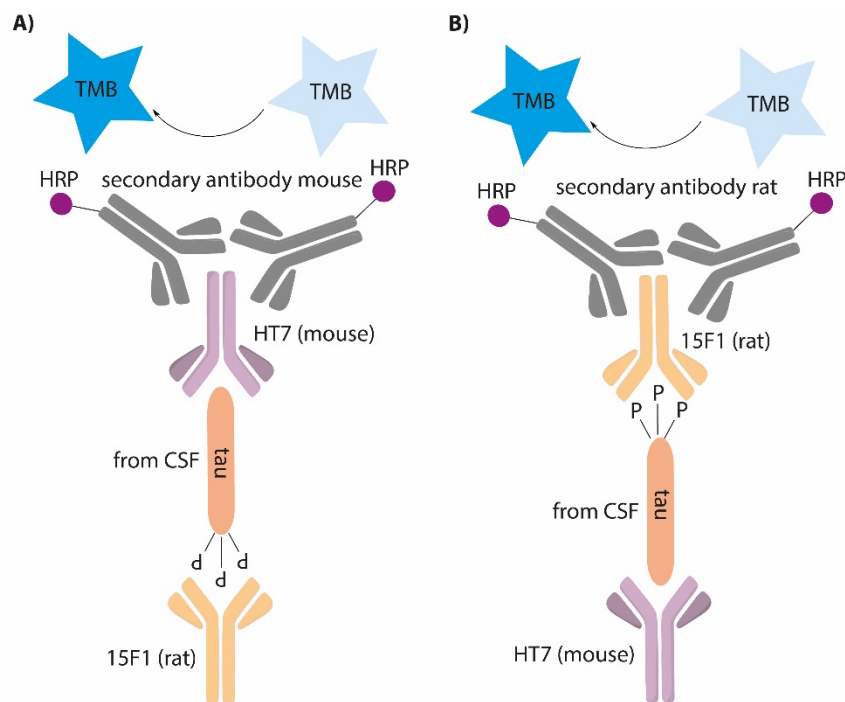
Figure 51: **A**) Sandwich ELISA, coating the plate with the 15F1 clone; **B**) sandwich ELISA, coating the plate with HT7 antibody.

Experiments carried out in set-ups described in **Figure 51** were also leading to similar results for CSF material of different patients. A negative control experiment, in which the secondly applied primary antibody (HT7 in setting A; 15F1 in setting B) was left out. There, a signal comparable to the in **Figure 51** depicted set-ups was detected, clearly pointing toward cross-

reactivity of the applied secondary antibodies to coated primary antibodies. Moreover, different phospho-tau levels were expected for the measured CSF probes, since in previous diagnostic assays, different total tau mirrors were measured (data shown in section **7.4.6.2**). In sandwich ELISA assays, cross-reactivities between the coating antibody and the later applied secondary antibodies can occur, falsifying the measured results. To check for potential cross-reactivity, western blot experiments were carried out (see section **7.4.6.4**). CSF of AD patients was blotted and detected by primary tau antibodies, before secondary antibodies were applied. In result, the detection of phospho-tau in CSF by western blot analysis using the 15F1 ppp-tau antibody was possible, but all tested secondary antibodies showed cross-reactivity between primary tau antibodies generated in different species (**Table 15**). In addition, all tested secondary antibodies except goat anti-rat (HRP) (ab6721) bound another species in western blot analysis, which could hint toward unspecific binding to abundant protein from CSF. The corresponding additional band appeared at around 30 kDa. Thus, a CSF probe was submitted to SDS-PAGE and the corresponding band at around 30 kDa was excised, digested with trypsin and analyzed by ESI-ToF mass analysis (see section **4.6.3.8**). The protein was identified as apoliprotein A-I with a nominal mass of 30759 Da.

Table 15: Results, showing that all tested secondary antibodies interacted with primary antibodies generated in different animal species. Not all primary antibodies were tested for each secondary antibody.

secondary antibody	primary antibodies recognized	No. of bands
goat anti-mouse (HRP) (ab97023)	Tau (rabbit, PA5-27287, Thermo Scientific), Tau 46 (SantaCruz Biotechnology)	2
mouse anti-rat (HRP) (212-036-168)	15F1 (rat); Tau (rabbit, PA5-27287, Thermo Scientific); Tau 46 (Santa Cruz Biotechnology)	2
Goat anti-rat (HRP) (112-035-003)	15F1 (rat); Tau (rabbit, PA5-27287, Thermo Scientific); Tau 46 (Santa Cruz Biotechnology)	2
goat anti-rabbit (HRP) (ab6721)	15F1 (rat); Tau (rabbit, PA5-27287, Thermo Scientific); PHF-1	1

In conclusion, no adequate system was identified that allowed for sandwich ELISA due to cross-reactivity, but the secondary antibody goat anti-rabbit (HRP) (ab6721) was found to selectively yield one proper band in western blot experiments using primary tau antibodies after blotting of CSF (**Figure 52**, see section **7.4.6.4** for experimental details on cross-reactivity study).
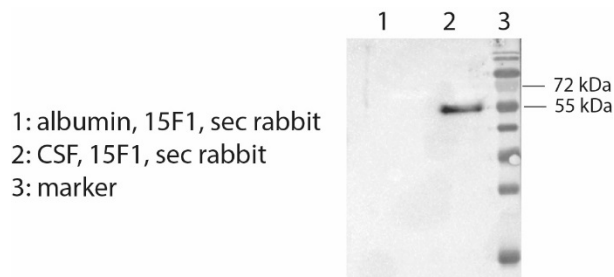
Figure 52: Functional secondary antibody goat anti-rabbit (HRP) (ab6721) reacting with 15F1 bound to phospho-tau in CSF and not to Albumin.

After precluding sandwich ELISA set-ups due to cross-reactivity of secondary antibodies, it was intended to apply an indirect ELISA, where tau from CSF samples is coated to the well-plate (**Figure 53**). After washing of the plate and blocking with 5% milk in PBS, 15F1 hybridoma cell-supernatant was applied. After another washing of the plate, HRP-labeled secondary antibody goat anti-rabbit was used and a coloration was provoked by the addition of TMB.
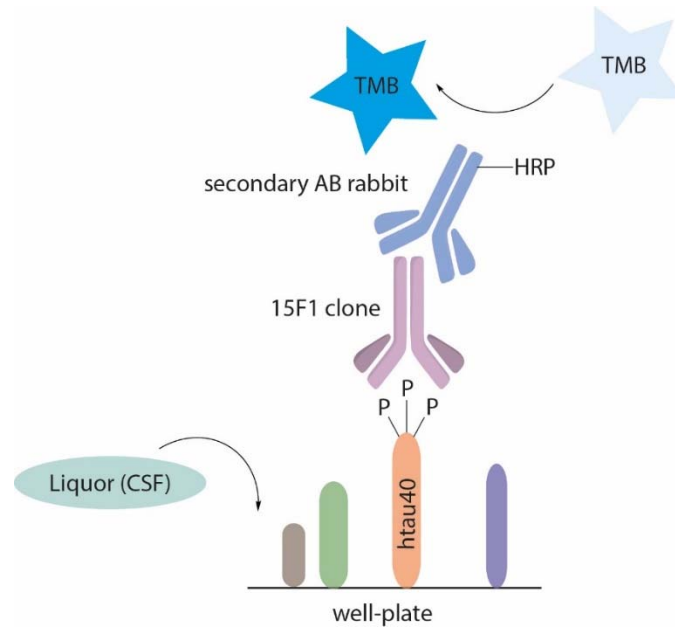
Figure 53: Indirect ELISA assay: Coating of the well-plate with CSF, detection with the 15F1 clone and the previously identified suitable secondary antibody goat anti-rabbit (HRP) (ab6721).

For the indirect ELISA set-up shown in **Figure 53**, triplicate measurements were conducted with CSF of four different patients with ppp-tau antibody 15F1 and the PHF-1 antibody. The CSF samples were used for well-plate coating in dilutions of either 1:2, 1:16 or 1:128 in carbonate buffer. After washing and blocking, either 15F1 or PHF-1 were applied in a 1:1 dilution with PBS containing 1% milk. After further washing steps, secondary antibody goat anti-rabbit was applied. After extensive washings, TMB was added to the plates and left for 45 min, until a coloration was visible. Additionally, two negative control experiments were carried out.

Negative control 1: In the first negative control (grey boxes in **Table 16**), CSF was coated onto the well-plates, but no primary antibodies (15F1 or PHF-1) were applied. Then, secondary HRP-conjugated antibody was used, followed by addition of the detection agent TMB.

4. RESULTS & DISCUSSION

Negative control 2: In the other control experiment (orange boxes in **Table 16**), no CSF was applied, followed by primary and secondary antibody.

Table 16: Scheme of coating of the 96-well plate with CSF diluted in carbonate buffer. Detection with 15F1 is marked in blue, the negative control sparing 15F1 is shown in grey, blanks are in dark orange and detections with the PHF-1 antibody are in yellow.

Pipettier-Schema:												
<>	1	2	3	4	5	6	7	8	9	10	11	12
A	Patient A (1:2)			Patient B (1:2)			Patient C (1:2)			Patient E (1:2)		
B	Patient A (1:16)			Patient B (1:16)			Patient C (1:16)			Patient E (1:16)		
C	Patient A (1:128)			Patient B (1:128)			Patient C (1:128)			Patient E (1:128)		
D	NC Patient A (1:16)			NC Patient B (1:16)			NC Patient C (1:16)			Patient E (1:16)		
E	Blank						Blank					
F	Patient A (1:2)			Patient B (1:2)			Patient C (1:2)			Patient E (1:2)		
G	Patient A (1:16)			Patient B (1:16)			Patient C (1:16)			Patient E (1:16)		
H	Patient A (1:128)			Patient B (1:128)			Patient C (1:128)			Patient E (1:128)		

15F1	
PHF-1	
Negative control	
Blank	

Table 17: Measured values of the triplicate measurements as seen in **Table 16**, showing negative control 1 results in red and negative control 2 results are shown in green.

Dual wave data (difference)					Temperature: 24 °C							
<>	1	2	3	4	5	6	7	8	9	10	11	12
A	0,0896	0,0897	0,0971	0,0879	0,0874	0,0826	0,0284	0,0269	0,0307	0,0824	0,0750	0,0835
B	0,1870	0,1740	0,1840	0,1040	0,1055	0,1117	0,0321	0,0335	0,0359	0,1230	0,1193	0,1158
C	0,1425	0,1249	0,1297	0,0286	0,0285	0,0281	0,0281	0,0310	0,0279	0,0593	0,0664	0,0782
D	0,1593	0,1454	0,1486	0,0955	0,1051	0,1108	0,0332	0,0319	0,0367	0,1130	0,1156	0,1223
E	0,0176	0,0185	0,0167	0,0164	0,0160	0,0182	0,0174	0,0186	0,0194	0,0178	0,0188	0,0216
F	0,0905	0,0793	0,0957	0,0860	0,0850	0,0911	0,0246	0,0318	0,0340	0,0844	0,0857	0,0803
G	0,1451	0,1642	0,1627	0,1045	0,1066	0,1146	0,0298	0,0319	0,0342	0,1175	0,1238	0,1269
H	0,1277	0,1160	0,1421	0,0269	0,0301	0,0251	0,0239	0,0299	0,0276	0,0659	0,0607	0,0510

The result obtained by **negative control 1** (**Table 17**, line D) showed that the envisioned measurement of phospho-tau by indirect ELISA did not work and had to be considered false, as the measured values with and without primary antibody were comparable.

In summary, an adequate primary and secondary antibody system was identified, which selectively leads to tau-only recognition (**Table 15**). Hereinafter, no set-up for a properly working ELISA assay was found. It may be possible to use the setting described in **Figure 49** with purified and concentrated 15F1 antibody, which possibly leads to a signal enhancement and finally allows for the detection of different phospho-tau levels in CSF.

Responsibility assignment: The ELISA assays shown were made by Oliver Reimann alone or in collaboration with either Dr. Schipke or Mrs. Kochnowsky. The project is supervised by Prof. Dr. Oliver Peters and Prof. Christian P. R. Hackenberger.

4.6.4 Summary and outlook

In summary, seven monoclonal antibody clones were generated in rats (section **4.6.3.1**) and evaluated by epitope mapping ELISA assays (section **4.6.3.3**) and by western blot analysis with semisynthetic tri-phosphorylated tau (section **4.6.3.4**). Moreover, it was shown by indirect immunofluorescence that some clones were able to detect tau inside the nuclei of cells, while others showed restricted recognition of cytoplasmatic tau species (section **4.6.3.2**). This observation was further confirmed in immunocytochemistry experiments that were conducted on a neuronal model of aging, where the clone 8D12 showed a cytoplasmatic tau recognition in neurons of 20 days of age, whereas in 80 days old neurons, merely nuclear tau was recognized (section **4.6.3.7**). To our knowledge, this is the first example of a phosphorylation dependent nuclear localization of tau.

It was further demonstrated that staining of neurofibrillary tangles and tau encapsulated in neuritic plaques in brain tissue derived from patients with AD works comparable to the established AT8 antibody, which is commonly used in the clinic (section **4.6.3.5**). The staining also worked for Pick bodies in brain tissue from patients that had suffered from Pick's disease.

Live-imaging of phospho-tau in *C.elegans* was so far not achieved, but western blot analysis of lysate from worms expressing human tau was achieved (section **4.6.3.6**). Purified antibody will be used in future experiments for tau detection in fixed animals upon immunohistochemistry and imaging via fluorescent microscopy.

In the future, the characterization of tau species bound by the generated clones in CSF samples is envisioned by immunoprecipitation, followed by mass spectrometry (section **4.6.3.8**). Additionally, the applicability of the antibody clone 15F1 for diagnostic ELISA for phospho-tau recognition is foreseen, applying purified and concentrated antibody. A proof of principle

of phospho-tau detection with the 15F1 antibody in CSF probes by western blot analysis was already achieved toward this goal (section **4.6.3.9**).

4.7 Cysteine-functional polymers via thiol-ene conjugation and subsequent NCL functionalization with peptides
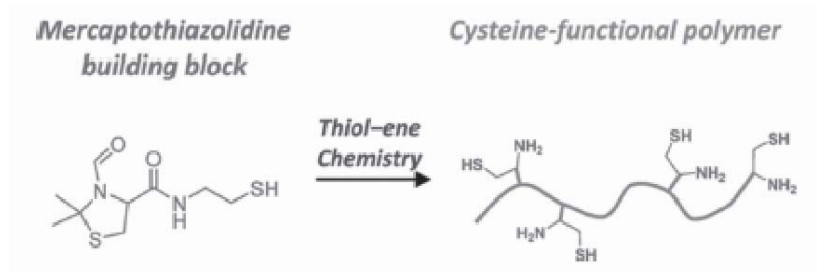
Figure 54: Table of contents, showing the generation of a cysteine-functional polymer by thiol-ene chemistry.

Abstract: A thiofunctional thiazolidine is introduced as a new low-molar-mass building block for the introduction of cysteine residues via a thiol-ene reaction. Allyl-functional polyglycidol (PG) is used as a model polymer to demonstrate polymer-analogue functionalization through reaction with the unsaturated side-chains. A modified trinitrobenzenesulfonic acid (TNBSA) assay is used for the redox-insensitive quantification and a precise final cysteine content can be predetermined at the polymerization stage. Native chemical ligation at cysteine-functional PG is performed as a model reaction for a chemoselective peptide modification of this polymer. The three-step synthesis of the thiofunctional thiazolidine reactant, together with the standard

4. RESULTS & DISCUSSION

thiol-ene coupling and the robust quantification assay, broadens the toolbox for thiol-ene chemistry and offers a generic and straightforward approach to cysteine-functional materials.

Summary of content: Conjugates of polymers and biomolecules are of great importance in the fields of medicine, biology and material science. In this work, an allyl-functional polyglycodol (PG) was used as a model polymer to demonstrate its functionalization by a mercaptothiazolidine building block, which allows for later conjugation to biomolecules such as peptides and proteins by NCL reactions.

The allyl-functional polymer was synthesized by statistical copolymerization with ethoxy ethyl glycidol ether (EEGE) with allyl glycidyl ether (AGE), as was published previously.[533] The 3-formyl-*N*-(2-mercaptoethyl)-2,2-dimethylthiazolidine-4-carboxamide (mercaptothiazolidine) compound was synthesized over three main steps and obtained by recrystallization. Cysteine functionalization was carried out by radical-initiated thiol-ene chemistry, whereas the radicals were formed by dimethoxyphenylacetophenone (DMPA) and UV-irradiation ($\lambda = 365$ nm), which yielded a complete conversion of the allyl-groups within 20 minutes, as determined by ^{1}H-NMR. The quantification of the successful thiol-ene conjugation was carried out by a trinitrobenzenesulfonic acid (TNBS) assay. Since TNBS can react with free thiols and free amines, the thiol residues were oxidized, which rendered them unreactive toward TNBS. The TNBS assay showed that an average of 4.2 amines were present on a polymer in average, whereas five were initially intended. With these results in hand, it was intended to address the Cys-like residues on the polymer by NCL. The PG polymer with 50 repeating units was bearing 4.2 Cys analogues was ligated with a model peptide sequence of the tau protein. Standard NCL conditions were used, whereas the MPAA thiol additive was used. Peptide-polymer ratios of 1:1, 3:1 and 5:1 were used in the NCL reaction to check for the possibility to tune the grade of functionalization through the addition of varying equivalents. Salts and NCL additives were then removed by dialysis and free unreacted peptide was removed from the functionalized polymers by reversed phase HPLC. Further MALDI-ToF characterization of the 1:1 functionalized polymer showed polymer with mono- and di-functionalization. For the constructs where higher ratios of peptide were used (3:1 and 5:1), higher degrees of functionalization were obtained, whereas mono- and di-functionalization was present in any

construct. A possible reason for this could be a saturation of the polymer (5 kDa) with the relatively long peptides (2 kDa). The polymer constructs were also examined by SDS-PAGE, which yielded very smeary bands due to the inhomogeneity of the polymer, but showed a trend toward higher masses upon higher degrees of functionalized by the peptide in constructs, in which higher ratios of peptide were used.

In summary, a protected thiofunctional mercaptothiazolidine building block was successfully used in thiol-ene functionalization of a polymer bearing allyl groups. Subsequent acidic hydrolysis yielded the free 1,2-aminothiol functionalities. The quantification of these residues was performed by oxidation of the Cys residues and subsequent TNBS assay. In a proof-of-principle reaction, the polymer was functionalized by NCL with a peptide derived from the tau protein in different ratios. The constructs were analyzed and demonstrated the possibility to address the 1,2-aminothiols by NCL. This new approach offers a new pathway for preparation of polymers and materials that allow in result for selective bioconjugation via NCL.

Outlook: Such constructs can help to solubilize otherwise insoluble peptides, may aid to control self-assembly and provide hydrophobic interactions for hydrogel formation. Additionally, this strategy can be applied to explore synthetic strategies for more efficient and versatile couplings.

Responsibility assignment: The work of generating the polymers, their functionalization with protected Cys-like compound and characterization was done by Matthias Kuhlmann under the supervision of Prof. Dr. Juergen Groll. The further functionalization of the polymer with peptide by NCL, the subsequent purification and characterization by MALDI-ToF was performed by Oliver Reimann under the supervision of Prof. Dr. Christian P. R. Hackenberger.

4.8 Poly(2-oxazoline)s used for Native Chemical Ligation

This chapter was published in the following journal:

Michael Schmitz, Matthias Kuhlmann, <u>Oliver Reimann</u>, Christian P. R. Hackenberger,

Jürgen Groll

"Side-Chain Cysteine-Functionalized Poly(2-oxazoline)s for Multiple Peptide Conjugation by

Native Chemical Ligation"

M. Schmitz, M. Kuhlmann, O. Reimann, C. P. Hackenberger, J. Groll, *Biomacromolecules*

2015.
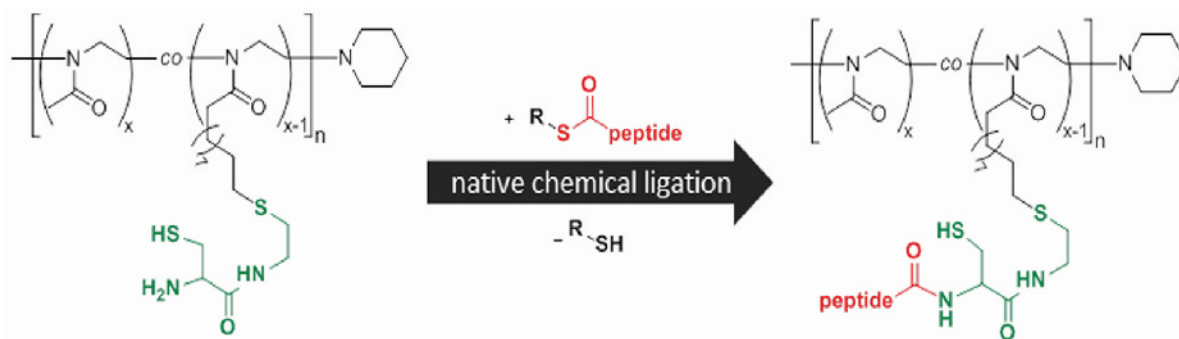
Figure 55: Cysteine-functionalized poly(2-oxazoline) used for NCL reaction.

Abstract: We prepared statistical copolymers composed of 2-methyl-2-oxazoline (MeOx) in combination with 2-butenyl-2-oxazoline (BuOx) or 2-decenyl-2-oxazoline (DecOx) as a basis for polymer analogous introduction of 1,2-aminothiol moieties at the side chain. MeOx provides hydrophilicity as well as cyto- and hemocompatibility, whereas the alkene groups of BuOx and DecOx serve for functionalization with a thiofunctional thiazolidine by UV-mediated thiol—ene reaction. After deprotection the cysteine content in functionalized poly(2-oxazoline) (POx) is quantified by NMR and a modified trinitrobenzenesulfonic acid assay. The luminescent cell

viability assay shows no negative influence of cysteine-functionalized POx (Cys-POx) concerning cell viability and cell number. Cys-POx was used for multiple chemically orthogonal couplings with thioester-terminated peptides through native chemical ligation (NCL), which was performed and confirmed by NMR and MALDI-ToF measurements.

Summary of content: In this work, an easy route to synthesize water-soluble side-chain functionalized poly(2-oxazoline) (Cys-POx) was elaborated that allowed for further functionalization by NCL. The polymer was generated by living cationic ring opening polymerization of 2-methyl-2-oxazoline (MeOx) and BuOx or DecOx. Further functionalization was achieved with 3-formyl-N-(2-mercaptoethyl)-2,2-dimethylthiazolidine-4-carboxamide (FTz4Cys, mercaptothiazolidine), which yields side-chain Cys-functionalization upon acidic treatment. The degree of functionalization was determined by statistical copolymerization of the monomers and was confirmed by NMR, GPC and a modified TNBSA assay, analogues as published previously and described in the previous chapter 4.7.[534] An average of 5.0 ± 0.6 adressable Cys-like groups was determined.

The modified POx polymers were cytocompatible, which was demonstrated by the "CellTiter-Glo" luminescent cell viability assay (LCV-assay). In this assay, the ATP production of the cells is monitored in order to determine their viability. Polymer constructs of different composition and degree of Cys-functionalization were tested. In addition, the concentrations of the tested constructs were also measured and ranged from 0.1 to 10 mg/mL, which in result showed that cell viability human fibroblasts wasn't compromised up to polymer concentrations of 1 mg/mL.

The accessability of the functionalized polymer was tested through the attachment of a short test-peptide with a Phe-Gly-Gly-Gly-Gly-SR sequence by NCL. We were able to correlate the NMR signals of the Phe amino acid from the peptide to the polymer side-chain, allowing us to show that with this short peptide, full-functionalization of the addressable Cys-functionalities was possible. In a next step, a biologically relevant peptide from the tau sequence (tau[390-410]) was attached to the Cys-groups. The peptide ratios were varied between 1:1, 3:1 and 6:1 (peptide to polymer). Excess salts were removed from the mixture after NCL by HPLC and the conjugated polymer constructs were analyzed by MALDI-ToF. Due to the dispersity of the

polymers, the MALDI-ToF spectra were yielding broad peaks, which, however, allowed us to see the different degrees of functionalization in a qualitative manner. Depending on the peptide ratio, the distribution of higher functionalized polymer varied as well and showed successful conjugation of up to seven peptides.

In summary, the successful synthesis of water-soluble Cys side-chain functionalized POx derivatives was demonstrated. These polymers beared reactive allyl-groups, which enabled thiol-ene reaction with mercaptothiazolidines. The polymer-bound Cys residues were generated upon acidic treatment of the mercaptothiazolidine groups, which were then addressable by NCL. These constructs were further shown to be non-toxic in a cell-viability assay up to concentrations of 1 mg/mL on fibroblast cells. The POx polymers thus proved to be a useful substitute of the often applied polyethylene glycol (PEG) polymer. The high addressability was demonstrated with a short test-peptide, which enabled a characterization by NMR. Moreover, a biologically relevant peptide from the tau sequence was attached, which yielded very heterogenous mixtures of polymers. However, a correlation between the applied equvalents of peptide and the grade of functionalization became obvious, which was characterized by MALDI-ToF.

Responsibility assignment: The generation of the polymer, its functionalization and characterization, including the cell viability test, were performed either by Michael Schmitz or by Matthias Kuhlmann, under the supervision of Prof. Dr. Juergen Groll. The peptide synthesis, the NCl reactions, HPLC purifications and characterization by MALDI-ToF of the polymer-peptide conjugates were performed by Oliver Reimann, under the supervision of Prof. Dr. Christian P. R. Hackenberger.

5. SUMMARY & OUTLOOK

In summary, new synthetic pathways were generated to obtain post-translationally modified tau proteins by EPL. Moreover, new purification protocols were established of these constructs that also allow for post-NCL or –EPL chemical processing. Additionally, new monoclonal antibody clones against phospho-tau were generated and characterized in divers experimental settings. At last, two different polymers were functionalized with peptides by NCL reactions, thus demonstrating the versatility of Cys-polymers for peptide conjugation.

Project 1 - A new synthetic route toward tri-phosphorylated C-terminal tau peptide by means of NCL[535]

Different pathways to obtain tri-phosphorylated C-terminal tau[390-441] peptides were established, generating substrates suitable for subsequent applications in EPL reactions. A ligation junction between Asn410 and Val411 was explored in the beginning. The N-terminal Val residue of the C-peptide was replaced by commercially available Pen, which can be converted to native Val after ligation by homogeneous radical initiated desulfurization. By testing this particular ligation, the formation of high amounts of by-products of either aspartimide-formation or hydrolysis of the thioester was observed, despite the presence of the highly activating thiol additive MPAA. This observation was surprising, since it was previously reported that ligations at Asn-Cys junctions can be carried out without the formation of considerable amounts of by-products.[267] When the ligation proceeds at Pen, the kinetics were rather slow compared to Cys ligations and required harsh reaction conditions, so that by-product formation was prevalent and another ligation site was investigated.

As a new ligation site, the junction between Leu425 and Ala426 was probed. The native Ala426 was replaced by Cys for the NCL step. This ligation site was then successfully applied during the synthesis of phosphorlylated C-terminal tau peptides and the Cys desulfurized to native Ala.

Project 2 – Development of a traceless linker for the affinity purification of ligation products[484]

A bifunctional traceless photocleavable linker was introduced into synthetic peptides on Lys side-chains, which allowed conjugation to biotin. The stability of this photocleavable biotin (PCB) group during SPPS conditions was demonstrated and the immobilization on streptavidin-coated agarose beads worked efficiently. Moreover, immobilized ligation products were cleaved in a traceless fashion by UV-light irradiation, generating native peptides. Desulfurization protocols are applied, when ligations are carried out at e.g. native Ala ligation sites or when other Cys surrogates are used. It was demonstrated that homogenous desulfurization was possible on PCB immobilized ligation products, as streptavidin does not contain any Cys residues that would compete with the desulfurization reaction. Thus, a new, facile and highly efficient protocol for the traceless purification and post ligation work-up of NCL products was developed with general applicability.

Since this bifunctional linker worked with high efficiency for purposes of purification, the incorporation of a linker-Lys conjugate by amber suppression was elaborated. Therefore, two synthetic pathways to generate Lys with the bifunctional photolinker (PC-Lys) were explored. After amber suppression and incorporation into the model protein GFP, the obtained protein product was analyzed by mass spectrometry. The efficiency of the incorporation needs to be further explored.

Project 3 – Semisynthesis of phosphorylated and *O*-GlcNAcylated tau proteins and their purification by a traceless affinity tag[536]

The generation of a homogeneously *O*-GlcNAcylated tau protein was demonstrated. Building upon a convenient synthetic access to Fmoc-Ser(β-D-GlcNAc(Ac)$_3$)-OH, *O*-GlcNAcylated tau peptides were produced by SPPS.

A sequential NCL/ EPL strategy and a desulfurization yielded the desired full-length homogeneously *O*-GlcNAcylated tau protein. Purification of the semisynthetic construct was

performed by means of the previously described PCB purification strategy, which was installed during SPPS in one of the synthetic fragments.

Moreover, the successful semisynthesis of a tri-phosphorylated tau version was demonstrated. However, the scaled semisynthesis of partially $^{13}C/^{15}N$-labeled tri-phosphorylated tau was not accomplished, mainly due to low expression yields of labeled proteins and the formation of insoluble amorphic tau aggregates, which were characterized by TEM. It was found in a systematic study that these aggregates are formed during EPL and thus significantly lower the semisynthesis yields.

Project 4 – Generation of antibodies targeted to tri-phosphorylated PHF-1 epitope of tau and assignment of the specificity of their binding

In collaboration with the group of Elisabeth Kremmer at the Helmholtz Center in Munich, seven monoclonal antibody clones were generated in rats by means of a peptide, comprising the tri-phosphorylated PHF-1 epitope. The specificities of the antibody clones were investigated by epitope mapping in ELISA format. Moreover, semisynthetic tri-phosphorylated full-length tau was used in western blot experiments to preclude any backbone interaction and thus ensure selectivity for the phosphorylated tau versions. In these experiments, it was shown that one clone was not functional, whereas the other six clones recognized selectively phospho-tau peptides and proteins. For each clone, crucial recognition sites were assigned. Moreover, no interaction with unphosphorylated tau was observed.

Project 5 – *In cellulo* and *in vivo* studies with the new antibodies and evaluation of the diagnostic potential

The binding of six functional ppp-tau antibody clones was tested in a cellular context. In result, three clones bound tau present in the cytoplasm of fibroblast cells, whereas other three clones bound tau strictly in the nuclei of the cells, thereby providing the first example of a visualization of a phosphorylation dependent nuclear localization of tau. This observation was strengthened in a completely different experimental setting, in which tau was visualized in

neuronal cells of different age. In these experiments, the 8D12 clone recognized tau in the cytoplasm of neurons of 20 days age, whereas in 80 days old neuronal cells, the same clone recognized only nuclear tau and the cytoplasmatic recognition vanished.

Further, the visualization of tau in *C.elegans* was intended. As live-imaging in these animals did not work, western blot experiments with worm lysates were carried out, where the tested ppp-tau antibody detected phospho-tau, which was expressed in muscular cells.

Further experiments with purified antibodies will show, if the visualization inside the animal will be possible. This would allow the delivery of a read-out for changes in tau phosphorylation and aggregation in these rapidly aging animals.

Moreover, it was demonstrated that phospho-tau derived from CSF of AD patients was recognized in western blot analysis, for which an adequate secondary antibody was identified. To test the diagnostic potential of the novel ppp-tau antibodies, the development of a straightforward ELISA assay for the quantification of phospho-tau in CSF from AD patients was explored. Several ELISA assay set-ups were tested, including sandwich and indirect ELISA. In result, none of the tried set-ups with cell-supernatants of antibodies worked to generate reproducible results. Future efforts will rely on the application of concentrated and purified antibody, possibly leading to an enhancement of detection.

Project 6 – Two different polymer backbones with Cys-functional groups modified by NCL[534, 537]

Allyl-functional polyglycidol (PG) and poly(2-oxazoline) (POx) were used as model polymers to demonstrate polymer-analogue functionalization. In a thiol-ene type reaction, mercaptothiazolidine was conjugated to allyl-groups, which yielded polymer-bound Cys residues in both cases upon acidic treatment. These Cys residues were then addressable by NCL with thioester peptides. It was demonstrated that the functionalization of the polymers worked in an equivalent dependent fashion. The number of peptide equivalents was decisive for the grade of functionalization of the polymers, as was shown by NMR and MALDI-ToF

5. SUMMARY & OUTLOOK

MS characterization of the polymer-peptide conjugates. These experiments can pave the way to polymer-peptide conjugation based hydrogel formation in future applications.

6. ZUSAMENFASSUNG & AUSBLICK

Zusammenfassend konnten neue Syntheserouten für die Herstellung von posttranslational modifizierten Tau Proteinen durch EPL etabliert und neuartige Reinigungsprotokolle dieser Konstrukte entwickelt werden, die auch chemische Bearbeitung nach der NCL oder EPL ermöglichen. Außerdem wurden neue monoklonale Antikörper Klone gegen phospho-Tau Spezies entwickelt und in ganz unterschiedlichen experimentellen Anordnungen charakterisiert. Zuletzt wurden zwei unterschiedliche Polymere mit Peptiden per NCL oder EPL funktionalisiert, wodurch die Einsetzbarkeit von Cys-Polymeren für Peptid-Konjugation demonstriert werden konnte.

Projekt 1 – Eine neue synthetische Route für die Herstellung von tri-phosphorylierten C-terminalen Tau Peptiden durch NCL[535]

Es wurden neue Synthese-Routen für die Herstellung von tri-phosphorylierten Tau Peptiden entwickelt. Die so generierten Peptide ließen sich für weitere Applikation in EPL Reaktionen nutzen. Zunächst wurde eine Ligationsstelle zwischen Asn410 und Val411 untersucht, wobei das N-terminale Val des C-Peptids durch ein kommerziell erhältliches Pen ersetzt wurde. Dieses kann nach der chemischen Ligation durch homogene Desulfurierung wieder in natives Val umgewandelt werden. Hier wurde jedoch die massive Bildung von Aspartimid beobachtet, die von einer Thioester-Hydrolyse begleitet wurde. Die Formation dieser beiden Nebenprodukte machte den Einsatz von einem vierfachen Überschuss an Thioester-Peptid gegenüber dem Cys Peptid notwendig, um das Cys Peptid zu über 90% in das Ligationsprodukt chemisch zu überführen. In einem zuvor publizierten Protokoll wurde jedoch die problemlose Ligation zwischen Asn und Cys Schnittstellen beschrieben, wenn das hoch aktivierende Thiol-Additiv MPAA genutzt wurde.[267]

Es wurde zudem festgestellt, dass die Reaktionskinetik mit Pen deutlich langsamer ist als mit Cys und zusätzlich einen leicht basischen pH von 8.0 - 8.5 erfordert, damit die NCL Reaktion stattfindet. Dadurch kam es jedoch zu der starken Ausbildung der Nebenreaktionen, die eine NCL an dieser Stelle ungünstig machte.

Als nächstes wurde eine die Ligationsstelle zwischen Leu425 und Ala426 erforscht, wobei das native Ala426 durch Cys ersetzt wurde. Dieses Cys kann nach der NCL Reaktion durch homogene Desulfurierung wieder in Ala umgewandelt werden. Schließlich zeigte sich, dass diese Ligationsstelle ausreichend gut funktionierte und das gewünschte Peptid ohne eine starke Hydrolyse des Thioesters lieferte.

Projekt 2 – Entwicklung eines spurlos-spaltbaren Linkers für die Affinitätsreinigung von Ligationsprodukten.[484]

Die Einführung eines bifunktionalen spurlos-spaltbaren Linkers in Peptiden an Festphase wurde erfolgreich etabliert und die anschließende Konjugation mit Biotin durchgeführt. Derartig konstruierte Peptide wurden an Streptavidin-beschichteter Agarose immobilisiert. So konnte gezeigt werden, dass Ligationsprodukte, die mit einem solchen Biotin-verbrückten Linker ausgestattet waren, problemlos aus komplexen Ligationsgemischen ohne die Anwendung einer HPLC isoliert werden konnten. Darüber hinaus wurde gezeigt, dass sich die immobilisierten Peptide unter homogenen Reaktionsbedingungen während ihrer Immobilisierung desulfurieren ließen. So wurde eine einfache Reaktionsabfolge entwickelt, die eine HPLC-freie Entschwefelung und Reinigung von Ligationsprodukten ermöglicht.

Auf Grund der erfolgreichen Anwendung dieses Systems zur Reinigung von Peptiden und Proteinen wurde ein Lys-Linker Konjugat synthetisiert und zum ortsspezifischen Einbau in GFP per Amber Stop-Codon Suppression genutzt. Der erfolgreiche Einbau der unnatürlichen Aminosäure konnte per Massenspektrometrie nachgewiesen werden, wobei der Grad des Einbaus noch weiter beleuchtet werden muss.

Projekt 3 – Semisynthese von phosphorylierten und *O*-GlcNAcylierten Tau Proteinen und ihrer Reinigung durch einen spurlos spaltbaren Affinitäts-Tag[536]

Die Herstellung von semisynthetischem Tau Protein, das homogen in der AD relevanten Position Ser400 durch *O*-GlcNAc modifiziert ist, wurde erfolgreich bewerkstelligt. Aufbauend auf einer effizienten Syntheseroute des Fmoc-Ser(β-D-GlcNAc(Ac)$_3$)-OH Bausteins wurde die

posttranslationale Modifikation während der SPPS in das Zielpeptid eingeführt. Eine sequenzielle Ligationsstrategie mit radikalischer Entschwefelung lieferte das gewünschte Produkt. Die Reinigung des semisynthetischen Konstruktes wurde durch die zuvor beschriebene photospaltbare Biotin-Gruppe bewerkstelligt, die ebenfalls während der SPPS in ein synthetisches Peptid eingebaut wurde.

Zudem wurde dreifach phosphoryliertes semisynthetisches Tau Protein erfolgreich hergestellt. Die skalierte Semisynthese von teilweise ^{15}N- oder ^{13}C/^{15}N-gelabelten tri-phosphorylierten Tau Protein konnte jedoch nicht bewerkstelligt werden. Dies lag zum einen an der niedrigen Expressionsrate von gelabeltem Protein und zum anderen an der Ausbildung unlöslicher amorpher Aggregate, die mittels TEM charakterisiert wurden. Diese Aggregate bildeten sich während der EPL und führten schließlich zu niedrigen Ausbeuten bei der Semisynthese von Tau und der sich anschließenden Aufarbeitung.

Projekt 4 – Herstellung von Antikörpern gegen das dreifach phosphorylierte PHF-1 Epitop des Tau Proteins und Zuweisung der Bindungsspezifitäten

Es wurde ein Peptid hergestellt, das drei Phosphorylierungen in PHF-1 (Ser396/400/404) aufwies und zur Herstellung von Antikörpern verwendet wurde (Kollaboration mit der Gruppe von Elisabeth Kremmer vom Helmholz Zentrum München). Es wurden sieben monoklonale Klone erhalten, die aus der Ratte gewonnen wurden. Die Spezifität dieser Antikörper wurde zunächst durch Epitopkartierung im ELISA Format bestimmt. Darüber hinaus wurde semisynthetisches tri-phosphoryliertes Tau für Western Blot Experimente genutzt. Sechs von sieben neuen ppp-Tau Antikörper Klonen erkannten lediglich homogen phosphoryliertes Tau, während ein Klon keinerlei Erkennung aufwies, was sich mit den Ergebnissen der Epitopkartierung deckte. Zudem konnten den einzelnen Klonen Phosphorylierungsmuster zugewiesen werden, die für die Bindung an das Antigen essentiell waren oder zu einer Stärkung oder Schwächung der Bindung führten.

Projekt 4 – Studien zu Tau *in cellulo* und *in vivo* durch die neuen Antikörper und Erforschung ihres diagnostischen Potentials

Im zellulären Kontext wurden Spezies untersucht, die durch die unterschiedlichen Antikörper gebunden wurden. So wurde durch indirekte Immunofluoreszenz beobachtet, dass drei Klone das Tau Protein im Zytoplasma erkannten, während drei andere Klone Tau lediglich im Nukleus der untersuchten Fibroblasten erkannten. Dies stellte das erste Beispiel für eine phosphorylierungs-abhängige Erkennung von nuklearem Tau dar. Diese Beobachtung wurde durch ein anderes Experiment untermauert, bei dem neuronale Zellen der Ratte unterschiedlichen Alters untersucht wurden. Der Klon 8D12, der auch in den vorigen Immunofluoreszenz Experimenten nukleares Tau detektierte, erkannte in 20 Tage alten neuronalen Zellen zytoplasmatisches Tau, während in 80 Tage alten Zellen nur nukleares Tau gebunden wurde.

Darüber hinaus wurden Versuche zur Visualisierung von Tau in *C.elegans* unternommen. Es konnte jedoch keine Detektion im Live-Imaging erreicht werden und so wurden Western Blot Experimente mit *C.elegans* Lysat durchgeführt. Die untersuchten Tiere exprimierten muskuläres Tau, wodurch phospho-Tau schließlich nachgewiesen werden konnte.

In weiteren Experimenten mit gereinigten und konzentrierten Antikörpern wird sich herausstellen, ob somit eine Visualisierung von phospho-Tau auch im Tier selbst möglich sein wird. Dieser Ansatz würde eine Methode liefern, um altersbedingte Veränderungen der Tau Phosphorylierung und Lokalisation in den Model-Tieren zu zeigen.

Es konnte ein System aus primären und sekundären Antikörpern gefunden werden, dass eine Detektion von phospho-Tau Spezies in CSF von AD Patienten durch Western Blot Analyse ermöglichte. Um das diagnostische Potential der neuen ppp-Tau Antikörper zu untersuchen wurde eine Anwendung in diagnostischen ELISA Assays von CSF vorgesehen, mit der phospho-Tau in CSF Proben von Alzheimer Patienten detektiert und quantifiziert werden kann. Es wurde jedoch keine reproduzierbare Detektion erzielt, was möglicherweise auf die Verwendung von ungereinigtem Myelomzell-Überstand zurückzuführen ist. Auch hier sind weitere Versuche mit gereinigten und konzentrierten Antikörpern vorgesehen.

Projekt 6 – Peptid-Funktionalisierung von zwei Polymeren per NCL[534, 537]

Allyl-funktionalisiertes Polyglycidol (PG) und Poly(2-oxazolin) (POx) wurden als Modell-Systeme genutzt, um eine Polymer-Peptid Konjugation zu demonstrieren. Die Verbindung Mercaptothiazolidin wurde über eine Thiol-ene Reaktion mit den Allyl-Gruppen verbrückt, die nach saurer Behandlung in Polymer-gebundenes Cys umgewandelt wurde. Die Cys-Gruppen wiederum waren nun zugänglich für weitere Funktionalisierung mit Thioester Peptiden durch NCL Reaktionen. So konnten demonstriert werden, dass sich der Grad der Funktionalisierung an den Polymeren durch die Anzahl der eingesetzten Equivalente an Peptid steuern ließ, was durch MALDI-ToF MS oder NMR nachgewiesen wurde. Diese Experimente könnten beispielsweise den Weg für die Herstellung von Hydrogelen ebnen.

7. EXPERIMENTAL PART

7.1 Exp: Materials and methods

Analytical HPLC was conducted on a Waters™ 600S controller system (Waters Corporation, Milford, Massachusetts, USA) with a 717 plus autosampler, 2 pumps 616 and a 2489 UV/Visible detector connected to a 3100 mass detector using a Kromasil C18 5 µm, 250 x 4.6 mm RP-HPLC-column with a flow rate of 1.0 mL/min. The following gradient of solvents was used if not stated otherwise: *Method A*: (A = H_2O + 0.1% TFA, B= MeCN + 0.1% TFA) 5 min at 10% B, 10 – 90% B from 5-36 min, 90% B from 36-45 min, 90-10% B in 45-50 min. HPLC chromatograms were recorded at 220 nm.

Analytical UPLC: UPLC-UV traces were obtained using a Waters H-class instrument, equipped with a Quaternary Solvent Manager, a Waters autosampler, a Waters TUV detector connected to a 3100 mass detector using an Acquity UPLC-BEH C18 1.7 µM 2.1 x 50 mm RP column with a flow rate of 0.6 mL/min. The following solvents and gradients were applied for all peptides if not further mentioned: *Method B*: (A = H_2O + 0.1% TFA, B= MeCN + 0.1% TFA) 5% B 0-5 min, 5-95% 5-15 min, 95% B 15-17 min. *Method C*: (A = H_2O + 0.1% TFA, B= MeCN + 0.1% TFA) 5-95% B 0-3 min, 95% B 3-5 min. UPLC-UV chromatograms were recorded at 220 nm.

Column chromatography was performed on silica gel (Acros Silica gel 60 Å, 0.035-0.070 mm).

Flourescence spectra were recorded using a FP-6500 fluorescence spectrometer (Jasco, Tokyo, Japan).

High resolution mass spectra (HRMS) were measured on an Aquity UPLC system and a LCT Premier™ (Waters Micromass, Milford, MA, USA) time-of-flight (TOF) mass spectrometer with electrospray ionization (ESI) using water and acetonitrile (10-90% gradient) with 0.1% formic acid as eluent. Alternatively, an Agilent 6210 ToF LC/MS system (Agilent Technologies, Santa Clara, CA, USA) with ESI source was used for mass detection of the peptides. H_2O and MeCN (both including 0.1% TFA) were used as eluents. The flow rate was 1.0 ml/min.

7. EXPERIMENTAL PART

MALDI-TOF MS anylsis was carried out AB SCIEX 5800 TOF/TOF System (Applied Biosystems) with nanoLC (Dionex) and robotic system for spotting (Probot, Dionex) and 4700 Proteomics Analyzer (Applied Biosystems).

NMR spectra were recorded on a Jeol ECX-400 400 MHz spectrometer (JEOL corporation, Akishima, Tokyo, Japan) or Bruker Ultrashield 300 MHz spectrometer (Bruker Corp. Billerica, Mass., USA) at ambient temperature in $CDCl_3$. The chemical shifts are reported in ppm, relative to the residual solvent peak.

Preparative HPLC was carried out on a JASCO LC-2000 Plus system (JASCO, Inc., Easton, Maryland, USA) using a reversed phase C18 column (Kromasil material) at a constant flow of 32 ml/min using water and acetonitrile with 0.1% TFA. This system was equipped with a Smartline Manager 5000 with interface module, two Smartline Pump 1000 HPLC pumps, a 6-port-3-channel injection valve with 1.0 mL loop, a UV detector (UV-2077) and a high pressure gradient mixer (All Knauer, Berlin, Germany). Purification was carried out after *Method D*: (A = H_2O + 0.1% TFA, B= MeCN + 0.1% TFA) 10% B 0-5 min, 10-70% B 5-70 min.

Reagents and solvents were, unless stated otherwise, commercially available as reagent grade and did not require further purification. All resins or Fmoc-protected amino acids were purchased from IRIS BioTech or Novabiochem.

Semi-preparative HPLC purification was carried out on a Dionex 580 HPLC system using a reversed phase Nucleodur C18 HTec column (10 x 250 mm) at a flow rate of 2 ml/min. Used was a gradient referred to as *Method D*: (A = H_2O + 0.1% TFA, B= MeCN + 0.1% TFA) 10% B 0-5 min, 10-70% B 5-70 min.

SPPS was carried out via standard Fmoc-based conditions (Fast-moc protocol with HOBt/HBTU conditions) on an Activo-P11 automated peptide synthesizer (Activotec) under Fmoc-based conditions and on a PTI peptide synthesizer, if not stated otherwise.

UV-irradiation was carried out with a LOT Hg (Xe) arc lamp (LOT-QuantumDesign GmbH, D-64293 Darmstadt, Germany) at 297 nm. Probes were positioned in 20 cm distance and irradiated, while stirring.

7.2 Experimental details on: Incorporation of the PCB-Lys into proteins by amber suppression

7.2.1 Exp: Synthesis of the PC-Lys building block by a solid phase approach

For the synthesis of compound PC-Lys **3**, Wang resin (0.22 mmol/g loading, IRIS Biotech) was used in 0.1 mmol scale. The resin was swollen in DMF/CH_2Cl_2 for 10 min, while shaking. Then, Fmoc-Lys(Alloc)-OH was added (5 mmol, 10 eq) together with HOBt and HBTU (10 eq each) in DMF. The reaction mixture was left over night shaking. Afterward, the excess reagents were filtrated off the resin. Then, the resin was washed 3 x with DMF, 3 x with CH_2Cl_2 and then again 3 x with DMF. Subsequently, the Alloc group was removed from the ε-amine of Lys by addition of $Pd(PPh_3)_4$ (12 mg, 0.01 mmol, 0.1 eq) and phenylsilane (300 µL, 2.4 mmol, 24 eq) in CH_2Cl_2 and shaking for 10 min. This deprotection step was repeated. The resin was extensively washed. Hereafter, the photolinker was introduced by addition of **2** (80 mg, 0.22 mmol, 2.2 eq) in 4 mL DMF with DIPEA (120 µL, 0.68 mmol, 6.8 eq). The mixture was shaken overnight and a test cleavage confirmed the coupling of **2** to the peptide. Then, the Fmoc-group was removed through treatment with 20% piperidine in DMF. After washing of the resin 5 x by DMF and 5 x CH_2Cl_2, the amino acid was cleaved from the resin by TFA/TIS/H_2O (95/2.5/2.5). Afterward, the amino acid was purified by preparative HPLC. The peptide was purified by C18 HPLC and analyzed by analytical UPLC. The desired peptide **3** was obtained with a yield of 32% (12 mg, 32 µmol); MS: m/z: 381.3 [M+H]$^+$; calcd. m/z: 381.2 [M+H]$^+$.
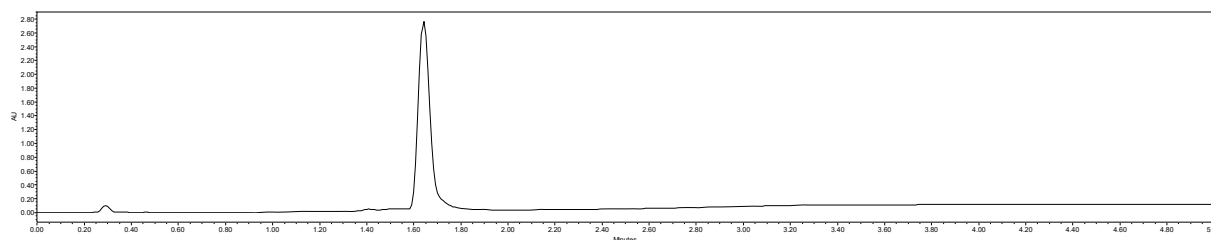

Figure 56: UPLC-UV trace of purified PC-Lys compound **3**, obtained by solid-phase approach.
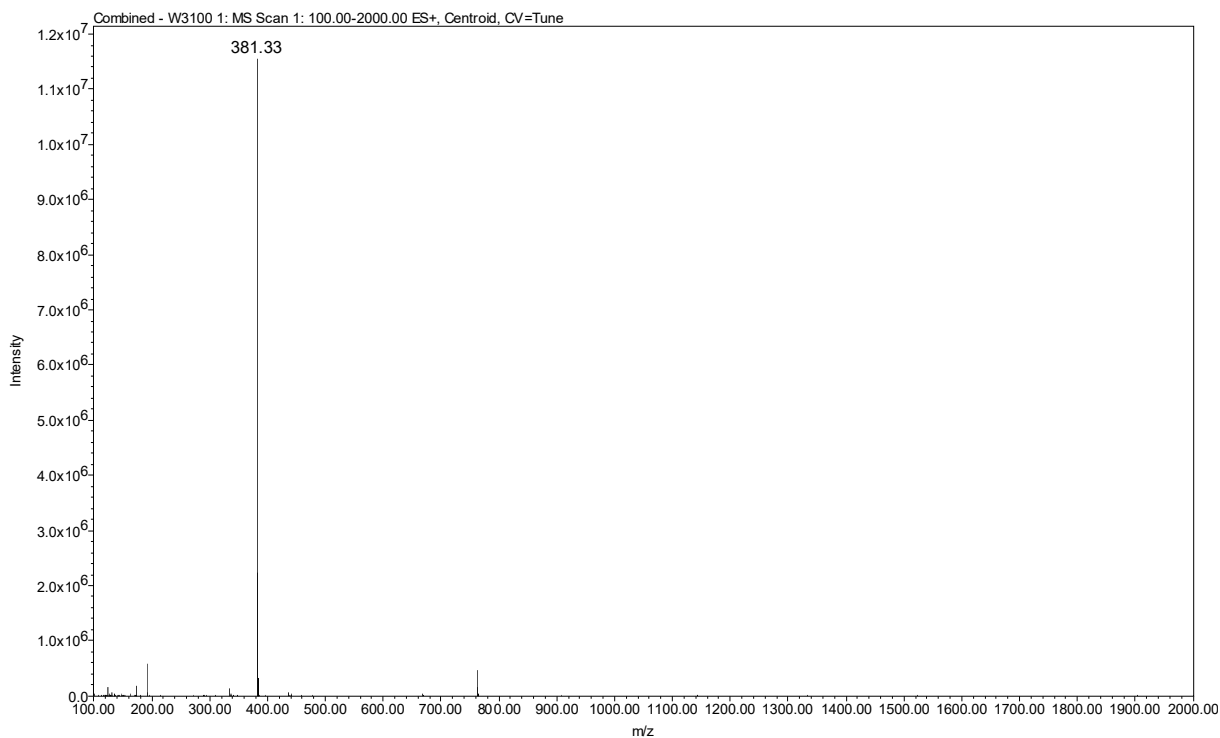
Figure 57: MS-spectrum of purified compound **3**, obtained by solid-phase approach.

7.2.2 Exp: Synthesis of the PC-Lys building block by in-solution approach

Compound **4** (450 mg, 1.8 mmol, 1.2 eq) was solubilized in 17 mL of buffer (10 mM NaHCO₃, pH 8.0). Separately, compound **2** (520 mg, 1.5 mmol, 1 eq) was dissolved in 670 µL aceton. The activated linker **2** crushed out of the aceton mixture, but the heterogeneous mixture was anyway added to the solubilized compound **4** and the mixture was stirred at 40°C for 16 h. Subsequently, the solvent was removed and the residual mixture was resolubilized in a solution of 20% TFA in CH₂Cl₂ (10 mL) and was stirred for 1 h at rt. The solvent was evaporated by nitrogen counter flow and *in vacuo* and the substance was then mixed with diethyl ether. This led to the precipitation of the desired product, while contaminants were removed with the ether phase. This step was repeated, the precipitate was air-dried and then resolubilized in water. After lyophylization, 260 mg (0.58 mmol, 39%) were isolated in high purity, as analyzed by analytical UPLC; MS: m/z: 381.3 [M+H]⁺; calcd. m/z: 381.2 [M+H]⁺.

¹H-NMR (300 MHz, D₂O): δ = 8.07 (d, J = 9.0 Hz, 1 H, CH), 7.73 (m, 2 H, CH), 7.62-7.45 (m, 1 H, CH), 6.20 (t, J = 6.0 Hz, 1 H, CH), 3.96 (t, J = 7.0 Hz, 1 H, CH), 3.71 (d, J = 6.5 Hz, 2 H, CH2), 3.05 (t, J = 7.5 Hz, 2 H, CH2), 2.01-1.76 (m, 2 H, CH2), 1.55-1.26 (m, 4 H, CH2) ppm.

¹³C-NMR (75 Mhz, D_2O): δ = 172.2, 156.9, 146.8, 134.4, 132.9, 129.5, 127.1, 124.9, 71.7, 53.6, 52.8, 39.7, 29.3, 28.1, 21.3 ppm.

HRMS: ($C_{15}H_{20}N_6O_6$) obs: 381.1510; calcd: 381.1517
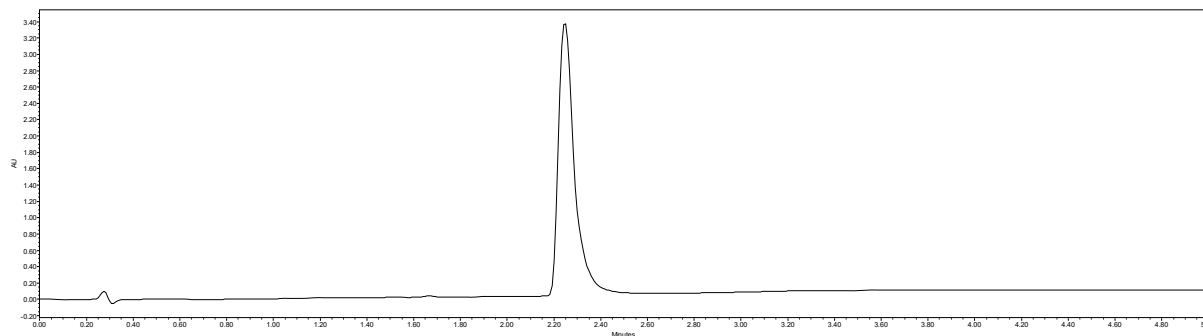
Figure 58: UPLC-UV trace of purified PC-Lys compound **3**, obtained by in-solution approach.
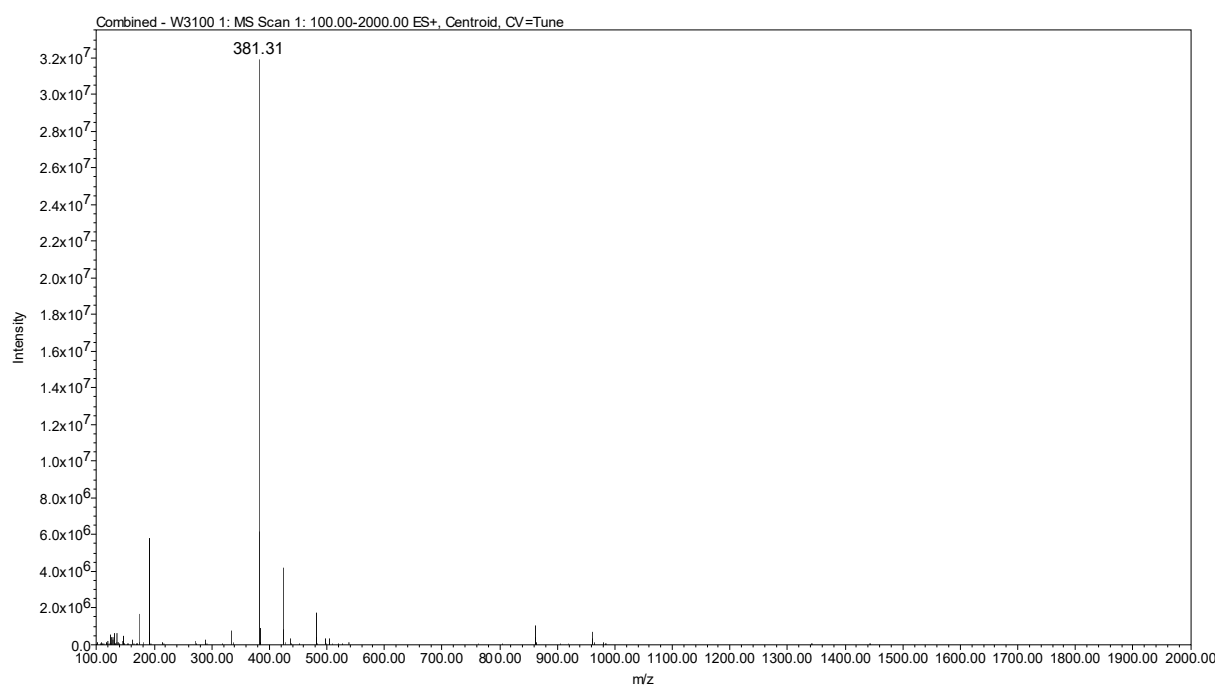
Figure 59: MS-spectrum of purified compound **3**, obtained by solution-phase approach.

MS Zoomed Spectrum
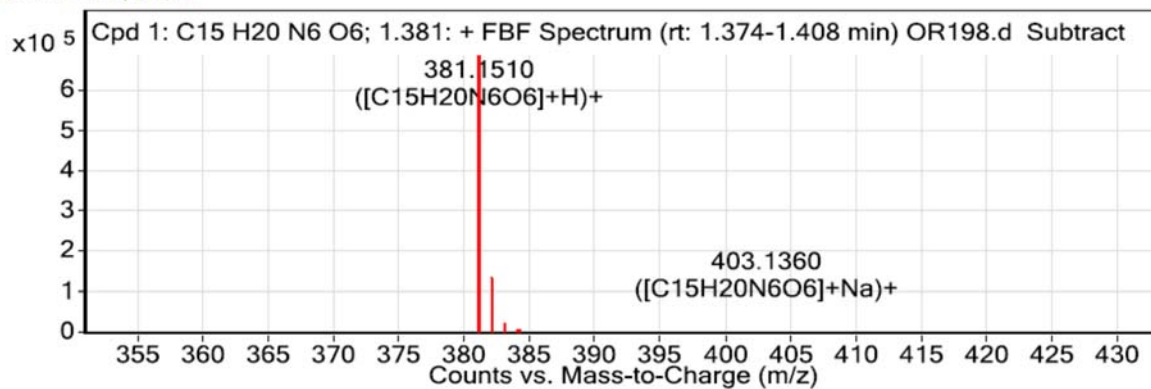
Figure 60: HRMS spectrum of compound **3**.
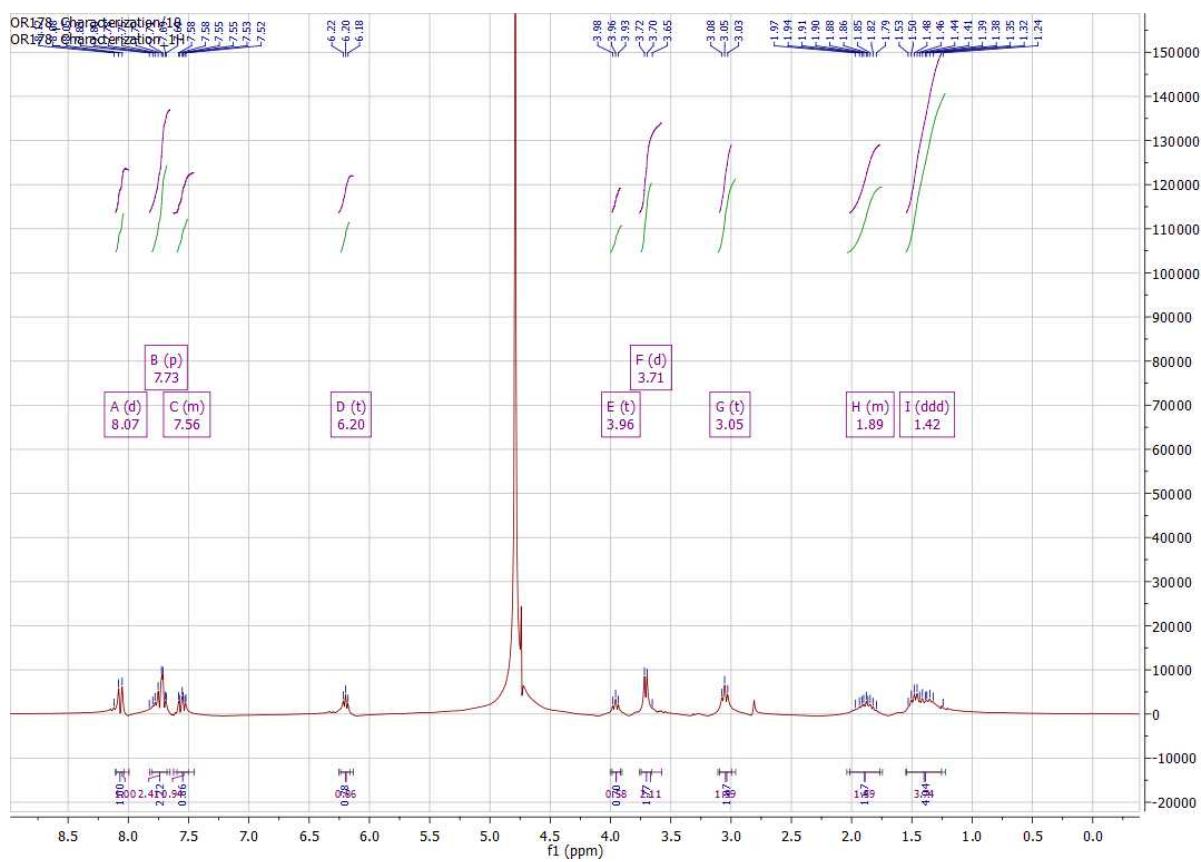
Figure 61: ¹H spectrum of compound **3**.
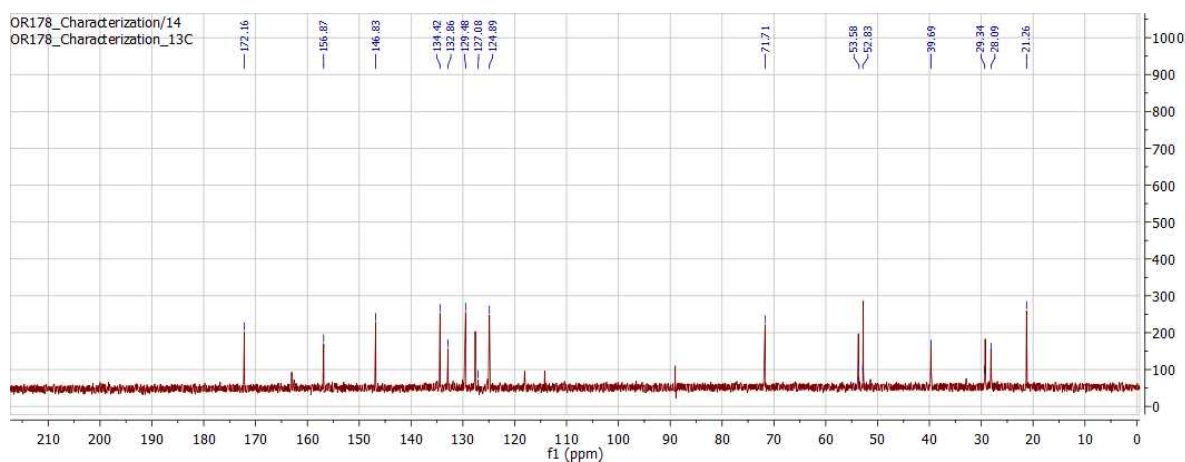
Figure 62: ^{13}C-NMR spectrum of the compound **3**.

7.2.3 Exp: Characterization of GFP containing the unnatural amino acid by mass spectrometry
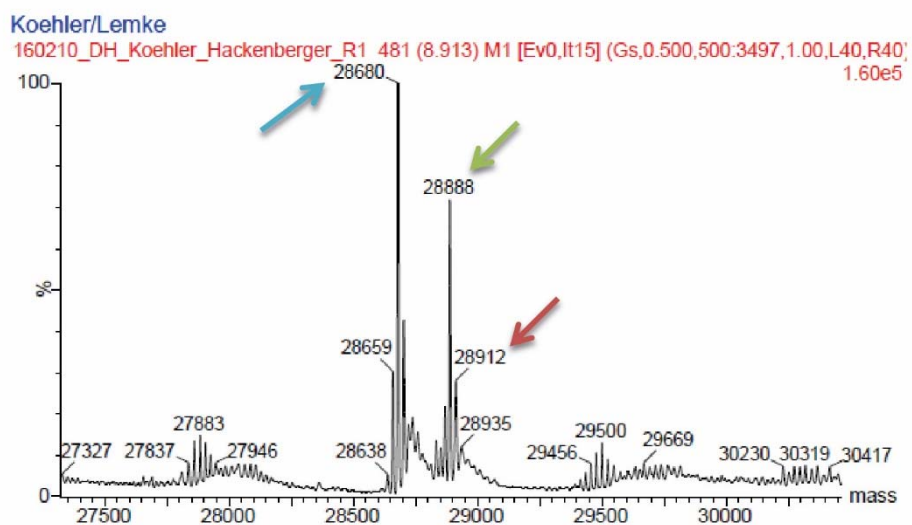
Figure 63: Measured Masses of the GFP construct after amber suppression. Mass of product (red arrow) MS: m/z: 28912 [M+H]$^+$; calcd. m/z: 28912 [M+H]$^+$; mass 2 (green arrow) MS: m/z: 2888; calcd. mass of protein with reduced azide m/z: 28886 [M+H]$^+$; mass 3 (blue arrow) MS: m/z: 28680; calcd. mass of protein with cleaved photolinker MS: m/z: 28676 [M+H]$^+$.

The protein was digested with trypsin and the peptides measured by ESI-ToF MS.

The sequence of the protein is the following:

Flag-tag

MSKGEELFTGVVPILVELDGDVNGHKFSVSGEGEGDATK(39)GKLTLKFICTTGKLPV

PWPTLVTTFSYGVQCFSRYPDHMKQHDFFKSAMPEGYVQERTIFFKDDGNYKTRAE

VKFEGDTLVNRIELKGIDFKEDGNILGHKLEYNYNSHNVYIMADKQKNGIKVNFKIRH

NIEDGSVQLADHYQQNTPIGDGPVLLPDNHYLSTQSALSKDPNEKRDHMVLLEFVTAA

GITHGMDELYK-His-tag

Therefore, the expected fragment was the following:
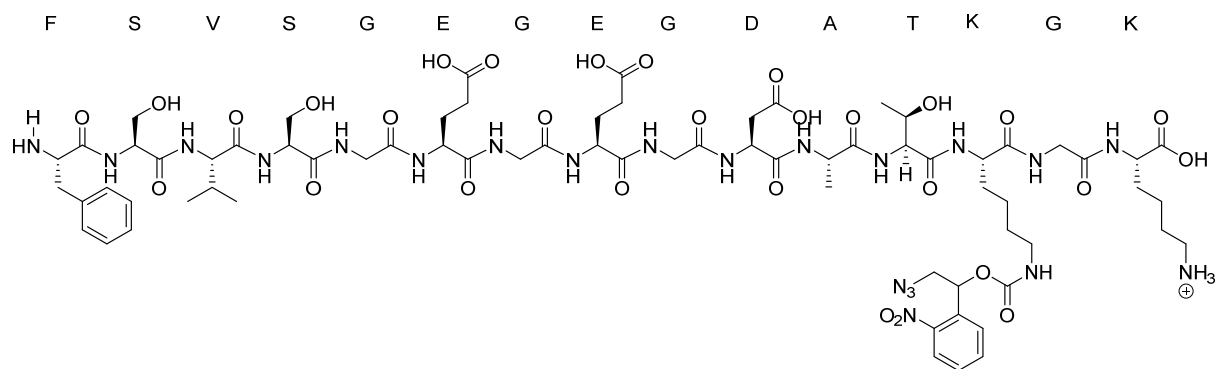
Figure 64: Peptide from modified GFP that results from trypsin digestion.

The peptide with the correct mass was identified: MS: m/z: 1701.7231 [M+H]$^+$, 851.8679 [M+2H]$^{2+}$; calcd. m/z: 1701.7213 [M+H]$^+$, m/z 851.3643 [M+2H]$^{2+}$. However, also strong signals of the corresponding peptide without the photolinker function were identified.
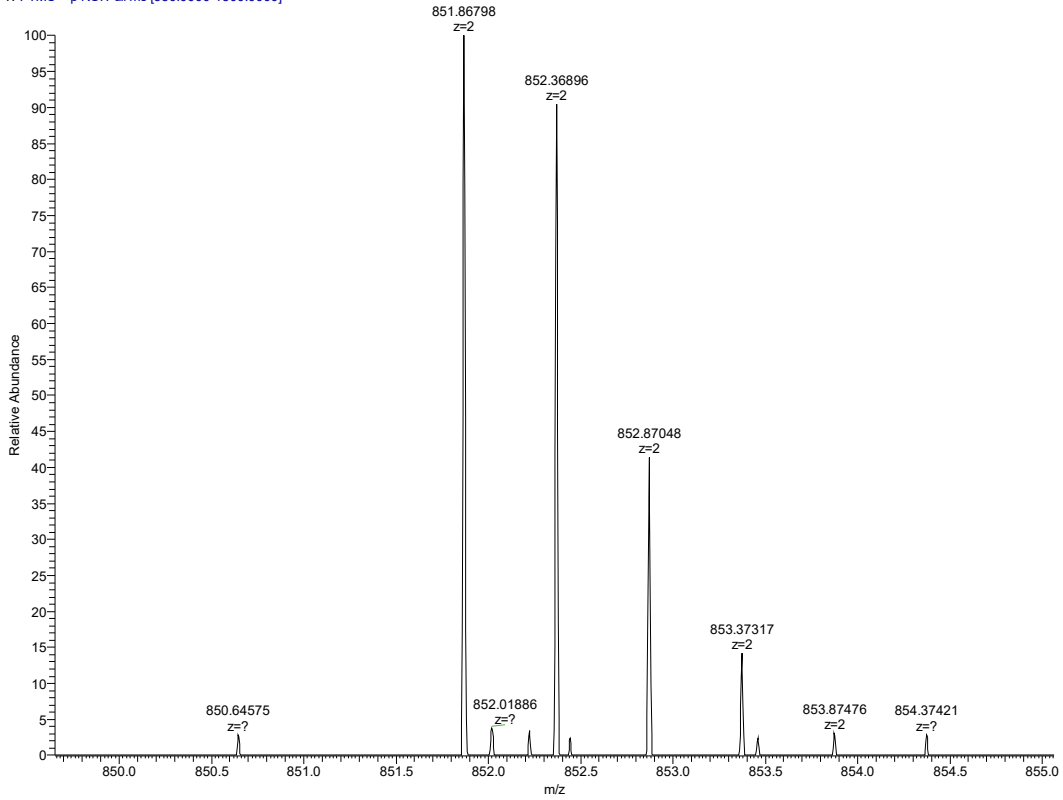
Figure 65: Mass spectrum of the correct peptide fragment from GFP containing the photolinker. MS: m/z: 851.8679 $[M+2H]^{2+}$; calcd. m/z 851.3643 $[M+2H]^{2+}$.

7.3 Experimental details on: Toward the semisynthesis of the tri-phosphorylated tau proteins and controls

7.3.1 Exp: Synthesis of the tri-phosphorylated N-peptide 5 for NCL

Peptide **5** was synthesized on Dawson Dbz NovaSyn TGR resin (subst: 0.24 mmol/g) applying an Alloc protection strategy.[538] The scale of the synthesis was 0.1 mmol. The resin was swollen in DMF/CH_2Cl_2 (1:1) for 30 min and subsequently treated with a solution of allyl chloroformate (50 eq) and DIPEA (2 eq) in CH_2Cl_2 for 12 h. Hereafter, Fmoc removal was accomplished by treating the resin with 20% piperidine in DMF for 20 min. Amino acid coupling was accomplished by using 10 eq of amino acid, 10 eq HCTU and 20 eq of DIPEA in DMF. Double coupling for 2 h each coupling step was conducted. All coupling steps were conducted manually. Occasionally, the Kaiser test was applied or a test cleavage was conducted. Asp^{402}-Thr^{403}, Leu^{408}-Ser^{409} and Gly^{415}-Ser^{416} junctions were introduced as pseudoprolines (Fmoc-Asp-Thr(ΨMe, Mepro)-OH, Fmoc-Leu-Ser(ΨMe,Mepro)-OH, Fmoc-Gly-Ser(ΨMe,Mepro)-OH). Phosphoserines (Fmoc-Ser(PO(OBzl)OH)-OH), pseudoprolines and the Thz-group were introduced by double couplings with 5 eq amino acid, 5 eq HCTU and 10 eq of DIPEA for 2 h.

On-resin Alloc removal and NCL precursor formation: The Alloc-protected resin was washed and swollen in CH_2Cl_2. Hereafter, a solution of Pd(PPh$_3$)$_4$ (0.35 eq with respect to the loading of the resin) and PhSiH$_3$ (20 eq with respect to initial loading of the resin) in CH_2Cl_2 were added to the resin and shaken for 10 min at ambient temperature. This step was then repeated. Hereafter, the resin was washed thoroughly with CH_2Cl_2 and a solution of *p*-nitrophenyl chloroformate (200 mg, 10 eq) in 4 mL CH_2Cl_2 was added. The mixture was allowed to shake o.n. and the activation step was repeated twice with 45 min reaction time each step. The resin was then washed intensively with CH_2Cl_2. Subsequently, a solution of 0.5 M DIPEA in DMF (2 mL) was added to the resin. The resin was left shaking in that mixture for 30 minutes at RT. This step was repeated in order to complete the cyclization.

Cleavage from the resin: The resin was washed with DMF, methanol and CH_2Cl_2 before it was dried in high vacuum. The cocktail used for peptide cleavage consisted of TFA/DTT/TIS/thioanisol (95/2/2/1). Cleavage was conducted for 3 h at rt, whereas 15 min before the end of the cleavage time, ethanedithiol (16.8 µL/ml cleavage cocktail; 0.2 mol/L) and trimethylsilyl bromide (13 µL/mL cleavage cocktail; 0.1 mol/L) were added to the mixture to reduce observed oxidation. Afterward, the TFA cocktail was nearly completely evaporated by nitrogen flow, followed by the addition of ice-cold diethyl ether. The precipitate was spun down and purified by preparative HPLC.

Peptide **5** was obtained with a yield of 4.4 mg (1 µmol, 1%); molar mass peptide = 4214.7 Da; LR-MS: m/z: 1406.8 $[M+3H]^{3+}$ (calcd. m/z: 1405.9).
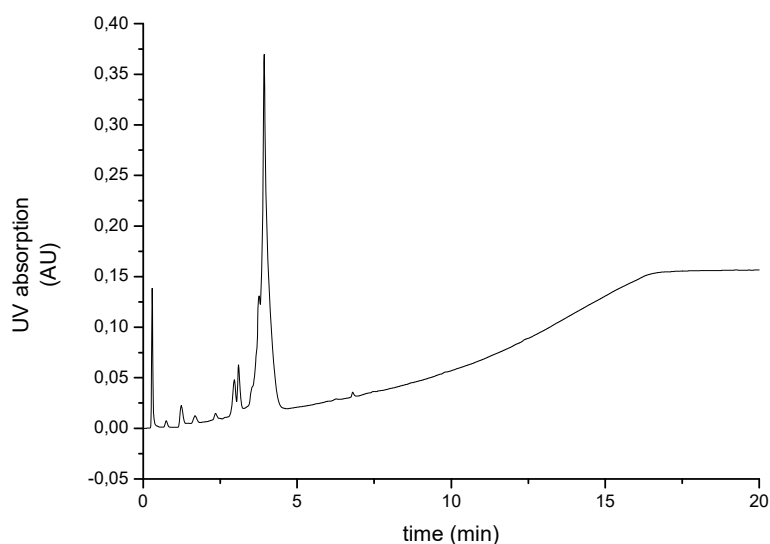
Figure 66: UPLC-UV trace of peptide **5**.
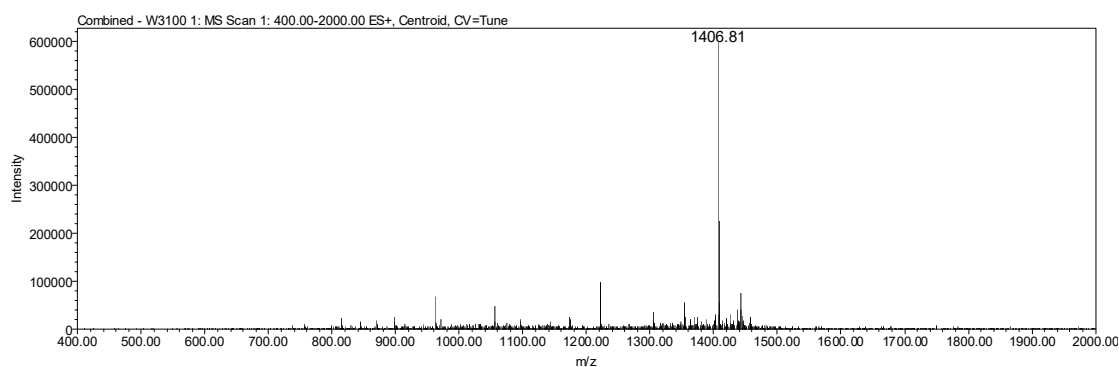
Figure 67: MS spectrum of peptide **5**.

7.3.2 Exp: One-pot native chemical ligation and desulfurization toward tri-phosphorylated tau peptide (7) using TFET as thiol additive

Peptide **6** (3.9 mg, 1.9 µmol, 2 eq) was dissolved in 382 µL ligation buffer (6 M Gn · HCl, 100 mM Na₂HPO₄, 50 mM TCEP, TFET 2% vol/vol, pH 7.6) to a final concentration of 5 mM. Subsequently, peptide **5** (4 mg, 0.95 µmol, 1 eq) was added to the solution and the mixture was flushed quickly with nitrogen gas. The closed reaction vessel was placed into a thermos-shaker and constantly shook at 100 rpm at 37°C for 90 min. The ligation was monitored by analytical HPLC and the end of the ligation was determined. Then, 500 µL EtSH in H₂O (2% vol/vol), 750 µL of a 250 mM TCEP in PBS solution (pH 7.4), 50 µL *t*-BuSH and 25 µL of a 0.1 mM solution of VA-044 radical initiator were added. The mixture was stirred at 37°C (waterbath) for 2.5 h, before direct purification was carried out by semi-preparative HPLC and peptide **7** was obtained with a yield of 10% (0.6 mg, about 0.1 µmol); molar mass peptide = 6044.7 Da; MS: m/z: 1513.25 [M+4H]$^{4+}$ (calcd. m/z: 1512.18).
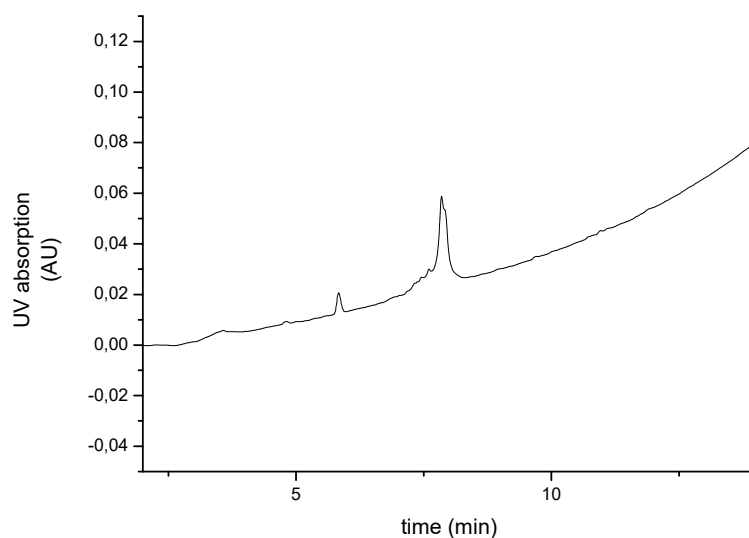
Figure 68: HPLC-UV trace of desulfurized ligation product **7**.

Combined - W3100 1: MS Scan 1: 400.00-2000.00 ES+, Centroid, CV=Tune
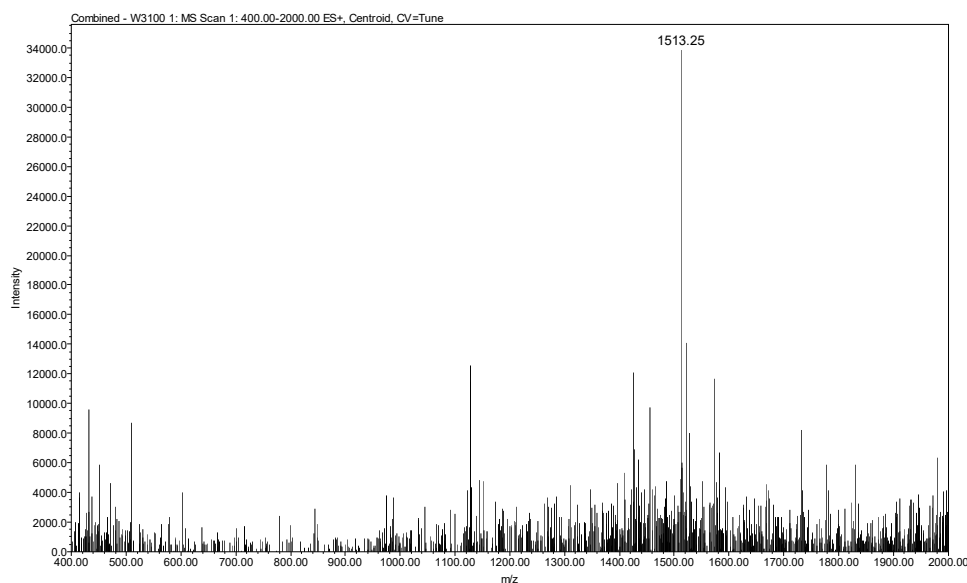
Figure 69: MS spectrum of peptide **7**.

7.3.3 Exp: Semisynthesis of unlabeled tri-phosphorylated tau (9)

The expression of tau[1-389]-intein-CBD (chitin binding domain) fusion protein and its loading on chitin resin was carried out as reported previously using a slightly different lysis buffer (20 mM Tris · HCl, 500 mM NaCl, 1 mM EDTA, 0.1% Triton X-100, 1 mM TCEP, complemented with 0.1 mM Na_3VO_4 as phosphatase inhibitor).[123] The expression volume was 700 mL, whereas the cell lysate was applied to 1.5 mL settled chitin resin. The chitin beads were washed 10 times with 5 mL equilibration buffer (20 mM Tris, pH 8.0, 500 mM NaCl, 1 mM EDTA, 0.1% Triton X-100, 1 mM TCEP) and then quickly flushed three times with cleavage buffer (20 mM Tris, pH 8.0, 500 mM NaCl, 1 mM EDTA, 0.1 mM TCEP, 200 mM MESNa). Peptide **7** (2 mg, 0.33 µmol) was prior to its use in EPL dissolved in a solution containing 0.2 M methoxyamine hydrochloride at pH 4 and mixed for 2 h at 37°C and subsequently lyophilized. The deprotected peptide was then re-dissolved in 2 mL EPL cleavage buffer and directly added to the chitin beads containing the immobilized protein tau[1-389]. The mixture was incubated for 2 d at ambient temperature and subsequently analyzed through SDS-PAGE (12% gel). The efficiency of the ligation was approx. 10% possibly due to a surplus of protein over peptide. In a following step, the ligation product **9** was purified as published previously by spin filtration and affinity purification on streptavidin coated agarose beads by means of PCB, generating a

50/50 mixture of ligation substrate and full-length tau ligation product (SDS-PAGE, see **Figure 23 B**). The sample was frozen and stored at -20°C until further use.

7.3.4 Exp: Characterization of semisynthetic protein 9

Mass spectrometry of 9: Super-DHB (Fluka) was dissolved in a 30:70 (v/v) mixture of acetonitrile and water containing 0.1% TFA to a final concentration of 50 mg/mL and used as matrix. The sample was prepared by precipitating a portion of the purified ligation mixture in ice-cold acetone. The pellet was dissolved in 1.5 µL H_2O containing 0.1% TFA and subsequently 1.5 µL Super-DHB was added, mixed carefully with the pipette and then applied on a MALDI target and dried at ambient temperature. Analysis of the samples was performed in the linear positive ion mode and for each spectrum 10000 consecutive laser shots were accumulated. The obtained data were analyzed Data Explorer software (Applied Biosystems). For all spectra baseline corrections was conducted and noise filter smooth applied using Gaussian Smooth.

Western blot against C-terminal tau protein: Proteins were separated by SDS-PAGE (4-20% Mini-Protein TGX precast gel, Bio-Rad) on a Bio-Rad Mini-Protean Tetra System and wet blotted onto a nitrocellulose membrane (0.2 µm, 300 mm x 3 m, 250 mA, 1 h). The membrane was blocked with Roti-Block (Carl Roth) over night at 4°C. The blot was incubated for 1 h with antibody Tau 46 (mouse monoclonal lgG1, Santa Cruz Biotechnology) (1:200) and carefully washed with PBS-T (0.1% TWEEN), followed by a 1 h incubation at RT with a secondary anti-mouse antibody (1:2000) (Thermo Scientific). The blot was again washed with PBS-T and PBS. Shortly before imaging, the blot was rinsed with WesternBright chemiluminescence solution (WesternBright ECL, advansta). Chemilumiscence detection was carried out on a fluorescence imager Lumi-Imager F1 (Boehringer Mannheim).

Western blot against biotin: Proteins were separated by SDS-PAGE (4-20% Mini-Protein TGX precast gel, Biorad) on a Bio-Rad Mini-Protean Tetra System and wet blotted onto a nitrocellulose membrane (0.2 µm, 300 mm x 3 m, 250 mA, 1h). The membrane was blocked with Roti-Block (Carl Roth) over night at 4°C. The blot was incubated for 1 h with streptavidin peroxidase conjugate (Merck Millipore, 500 U) (1:2000) at RT. After careful washing with PBS-T (0.1% TWEEN) the blot was rinsed with WesternBright chemiluminescence solution

(WesternBright ECL, Biozym Scientific). Chemilumiscence detection was carried out on a fluorescence imager Lumi-Imager F1 (Boehringer Mannheim).

7.3.5 Exp: Semisynthesis of unphosphorylated, partially ^{15}N-labeled tau (12)

About 3 mL of settled chitin beads containing the labeled tau-intein-CBD construct were washed 10 x with equilibration buffer (20 mM Tris, pH 8.0, 500 mM NaCl, 1 mM EDTA, 0.1% Triton X-100, 10 mM TCEP). Subsequently, the beads were quickly flushed one time with cleavage buffer (20 mM Tris, pH 8.0, 500 mM NaCl, 1 mM EDTA, 10 mM TCEP, 100 mM MBAA). Afterward, peptide **11** (4 mg, 630 nmol) was added to the chitin beads in 4 mL cleavage buffer. The mixture was protected from light and left gently rocking for 2 days at rt. The mixture was filtered and then concentrated in Amicon Ultra spin-filters (Ultracel-30K, 30 kDa cut-off). This procedure simultaneously allowed buffer exchange to streptavidin binding buffer (20 mM Tris · HCl, pH 7.0, 150 mM NaCl, 1 mM DTT) and removal of unligated peptide **11**. Subsequently, retained protein was applied in a volume of 2 mL streptavidin binding buffer to 1 mL precipitated streptavidin-coated agarose beads in a column (5 mL column volume) and incubated for 2 h at rt. In the next step, a stirring bar was added to the column and the beads were irradiated with UV light (297 nm wavelength) 3x for 10 min each from a distance of 20 cm. The buffer was filtered through the column and protein **12** was obtained with a yield approx. 1.5 mg, as determined by UV absorption (NanoDrop, ND-1000 spectrophotometer, Thermo Scientific), before the sample was frozen at -20°C until further use.

7.3.6 Exp: Characterization of semisynthetic unphosphorylated and ^{15}N-labeled tau (12)

Mass spectrometry of 12: Super-DHB (Fluka) was dissolved in a 30:70 (v/v) mixture of acetonitrile and water containing 0.1% TFA to a final concentration of 50 mg/mL and used as matrix. Samples were prepared by mixing 1 µL of the tau protein solution with 1 µL of water containing 0.1% TFA. Then 1 µL of matrix was added and carefully mixed by pipetting. From this mixture 1 µL was transferred to the MALDI sample plate and dried at ambient

temperature. Analysis of the samples was performed in the linear positive ion mode and 5000 consecutive laser shots were accumulated. The spectrum was analyzed with Data Explorer software (Applied Biosystems). For all spectra baseline corrections were conducted and noise filter smooth applied.

Western blot against C-terminal tau protein: Proteins were separated by SDS-PAGE (12%) on a Bio-Rad Mini-Protean Tetra System and wet blotted onto a nitrocellulose membrane (0.2 µm, 300 mm x 3 m, 250 mA, 1 h). The membrane was blocked with Roti-Block (Carl Roth) for 1 h at rt. The blot was incubated for 1 h with antibody Tau 46 (mouse monoclonal lgG1, Santa Cruz Biotechnology) (1:200) and carefully washed with PBS-T (0.1% TWEEN), followed by a 1 h incubation at rt with a secondary anti-mouse antibody (1:2000) (Thermo Scientific). The blot was again washed with PBS-T and PBS. Shortly before imaging, the blot was rinsed with WesternBright chemiluminescence solution (WesternBright ECL, advansta). Chemilumiscence detection was carried out on a fluorescence imager (ChemiDoc XRS system, Bio-Rad).

Western blot against biotin: Proteins were separated by SDS-PAGE (12%) on a Bio-Rad Mini-Protean Tetra System and wet blotted onto a nitrocellulose membrane (0.2 µm, 300 mm x 3 m, 250 mA, 1h). The membrane was blocked with Roti-Block (Carl Roth) for 1 h at RT. The blot was incubated for 1 h with streptavidin peroxidase conjugate (Merck Millipore, 500 U) (1:2000) at rt. After careful washing with PBS-T (0.1% TWEEN) the blot was rinsed with WesternBright chemiluminescence solution (WesternBright ECL, Biozym Scientific). Chemilumiscence detection was carried out on a fluorescence imager (ChemiDoc XRS system, Bio-Rad).

7.3.7 Exp: Expression of ^{15}N-labeled tau[1-389]-intein-GST fusion-protein

Cloning of the tau[1-389]-intein-GST construct: The cloning of the tau-intein-GST construct was conducted in the lab of Smet-Nocca as published.[536]

Bacterial culture: The recombinant T7 expression pET21a plasmid containing the tau[1-389]-intein-GST gene was transformed into competent *E. coli* BL21(DE3) strains. A

small-scale bacterial culture of 20 mL containing ampicillin (100 µg/mL) was started by taking colonies from the selection plate. The bacteria were grown over night to reach saturation corresponding to an O.D. measured at 600 nm. Then, 10 mL of this preculture were centrifuged at 1200 rpm at 4°C for 15 min, the supernatant was decanted and the cell pellets were resuspended in 10 mL of M9 medium. One liter of M9 medium was reconstituted by addition of the supplements and isotopes as follows : 20 mL/L of a glucose solution (20%), 1 g/L of $^{15}NH_4Cl$, ^{15}N Isogro® (yeast extract, Sigma), 1 mM of $MgCl_2$, 100 µM of $CaCl_2$, 10 mL of MEM vitamins (Sigma) and 100 µg/mL of ampicillin. The preculture was then added to 1 L of M9 medium and incubated at 37°C and 160 rpm. At an O_D of 1.03, induction was conducted by the addition of isopropyl β-D-1-thiogalactopyranoside (IPTG) to a final concentration of 500 µM. The mixture was left shaking at 160 rpm o.n. at 37°C and was then centrifuged at 6000 g for 35 min at 4°C. The supernatant was decanted and the cell pellets were resuspended in PBS buffer (containing 5% glycerol, 10 mM EDTA, 0.5% Triton-X 100). The samples were then frozen until further use at -20°C.

Purification of ^{15}N-labeled protein: The purification was carried out according to a protocol previously published by us.[536]

7.3.8 Exp: Synthesis of tau[390-441] (15)

The synthesis of peptide **15** was carried out on H-Leu-HMPB NovaPEG resin (0.54 g/mol loading) in a 0.05 mmol scale. The synthesis was conducted automatically on the PTI peptide synthesizer using standard Fast-moc conditions. Amino acids and coupling reagents were supplied in a fivefold excess. Double coupling was applied and pseudoprolines VS, LS, GS and AT were introduced as described by Broncel *et al.*[123] The peptide was cleaved off the resin by the addition of TFA/TIS/H_2O (95/2.5/2.5 vol/vol) within 3 h. The TFA volume was reduced by nitrogen flow and then the peptide was precipitated by excess ice-cold diethylether. The precipitate was air dried and then dissolved in H_2O and acetonitrile and subjected to HPLC purification. Peptide **15** was obtained with a yield of 4 mg (0.75 µmol, 2%); molar mass peptide = 5358 Da; LR-MS: m/z: 1341.4 [M+4H]$^{4+}$ (calcd. m/z: 1341.2).
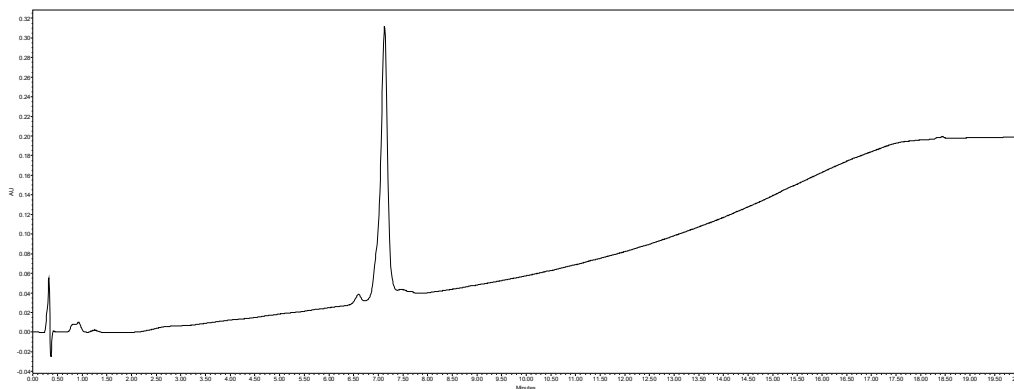
Figure 70: HPLC-UV trace of peptide **15**.
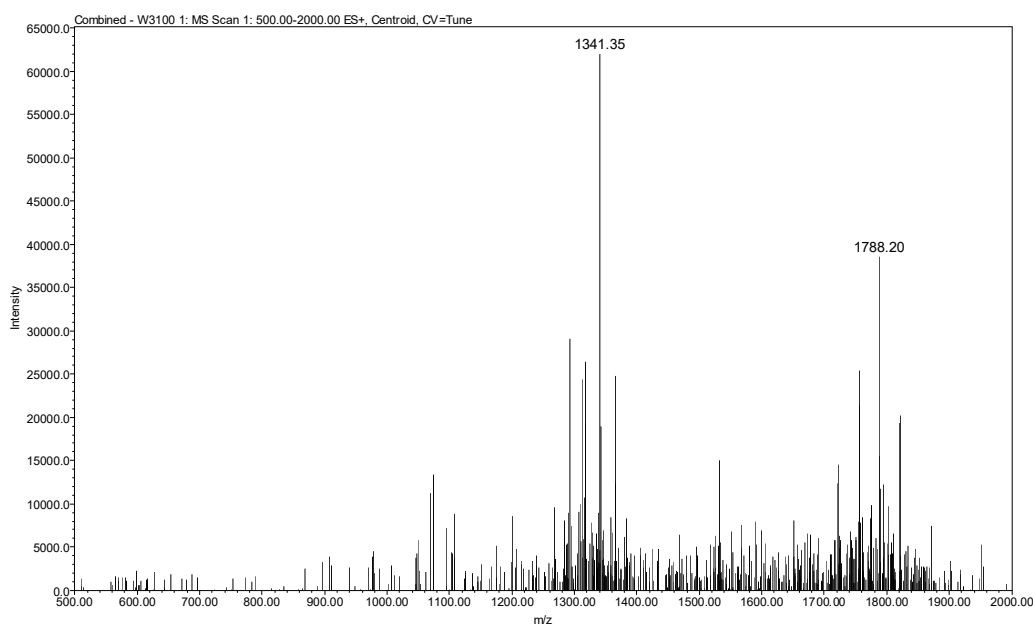
Figure 71: Mass spectrum of peptide **15**; m/z: 1341.4 [M+4H]$^{4+}$ (calcd. m/z: 1341.2).

7.3.9 Exp: EPL with unbiotinylated peptide 15 and subsequent HPLC purification

The glutathione beads with the immobilized tau[1-389]-intein-GST fusion-protein (section **7.3.7**) were equilibrated with equilibration buffer (20 mM Tris HCl pH 8.0, 500 mM NaCl, 1 mM EDTA, 0.1% Triton X100, 0.1 mM TCEP) 10 times with the double volume of the beads. Hereinafter, the beads were quickly flushed once with cleavage buffer (20 mM Tris HCl pH 7.3, 500 mM NaCl, 1mM EDTA, 0.1 mM TCEP, 150 mM MMBA). Then, peptide **15** (4 mg, 0.75 µmol) was added in 3 mL of cleavage buffer and the EPL was allowed to proceed for 48 h at rt. The product was eluted from the column and the beads were subsequently washed with 2

mL of cleavage buffer, yielding a total elution volume of 5 mL. Dialysis (12-15 kDa M_W-cut-off) was performed and those 5 mL were administered on a preparative HPLC with a C4 column (C4 BEH, Waters) and purified at a flow-rate of 7 mL/min. The product was lyophilized and then dissolved in 1 mL. Subsequently, purification was carried out on a C18 semi-preparative HPLC. Two fractions were obtained, both containing the desired product and contaminants, thus making the determination of the yield impossible.

7.3.10 Exp: EPL of 7 and 16 toward double-labeled tri-phosphorlylated tau (17)

About 3 mL of settled glutathion beads containing the labeled tau-intein-GST construct were washed 10 x with equilibration buffer (20 mM Tris, pH 7.3, 500 mM NaCl, 1 mM EDTA, 0.1% Triton X-100, 10 mM TCEP). Subsequently, the beads were quickly flushed once with cleavage buffer (20 mM Tris, pH 7.3, 500 mM NaCl, 1 mM EDTA, 10 mM TCEP, 100 mM MBAA). Afterward, peptide **7** (1.9 mg, 0.31 µmol) was added to the glutathion beads in 4 mL cleavage buffer. The mixture was protected from light and left gently rocking for 70 h at rt. The reaction did not lead to the formation of the desired product **17**. The ligation was heated to 37°C for 3 h more and then again investigated by SDS-PAGE. No formation of ligation product was observed.

7.3.11 Exp: Experiments on tau aggregation during EPL

The proteins WT-tau, tau(Ala390Cys) and albumin (each 0.1 mg) were dissolved in 100 µL of EPL buffer (20 mM Tris HCl pH 8.0, 500 mM NaCl, 1 mM EDTA, 0.1% Triton-X 100, 0.1 mM TCEP, 200 mM MESNa), yielding a protein concentration of about 20 µM, which is approx. expected in EPL reactions. The incubation was either carried out at rt or at 4°C for 72 h, before the samples were frozen and then measured by TEM.

The positive control for tau aggregation was achieved by dissolving 0.1 mg recombinant WT tau in PBS-buffer with pH 7.4, a protein concentration of 50 µM and a heparin concentration

of 12.5 µM. The samples were incubated at 50°C for 14 days, whereas DTT aliquots to a final concentration of 1 mM were added over the first 5 days.[487]

Afterward, all probes were dialyzed against 50 mM ammonium bicarbonate buffer (pH 7.8) (7 kDa cut-off) for 48 h, before they were finally analyzed by TEM.

7.4 Experimental details on: New antibodies against the tri-phosphorylated PHF-1 epitope of tau

7.4.1 Exp: Antibody generation

Synthesis of peptide 18

The peptide **18** was synthesized on NovaPEG HMPB resin (0.64 mmol/g) in a 0.1 mmol scale. The synthesis was conducted on the Activotec peptide synthesizer per single coupling with 10 eq of amino acids, HOBt, HBTU and DIPEA until residue Pro405. From there on the synthesis was continued manually. The three phospho-serines were attached to the peptide by a double coupling strategy applying 5 eq of amino acid, HATU, HOAt, and DIPEA for 2 h each coupling step. The peptide was cleaved from the resin by treatment with a TFA/H_2O/TIS (95:2.5:2.5 v/v) mixture for 3 h. The peptide was purified by preparative HPLC and isolated with a yield of 8% (2.2 mg, 0.8 µmol, approx. 1%); molar mass peptide = 2801.1 Da; MS: m/z: 1401.7 $[M+2H]^{2+}$ (calcd. m/z: 1401.6); 935.0 $[M+3H]^{3+}$ (calcd. m/z: 934.7).
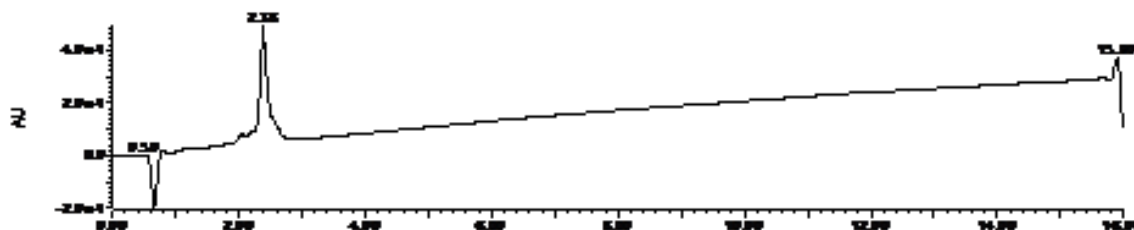
Figure 72: HPLC-UV trace of purified peptide **18**.
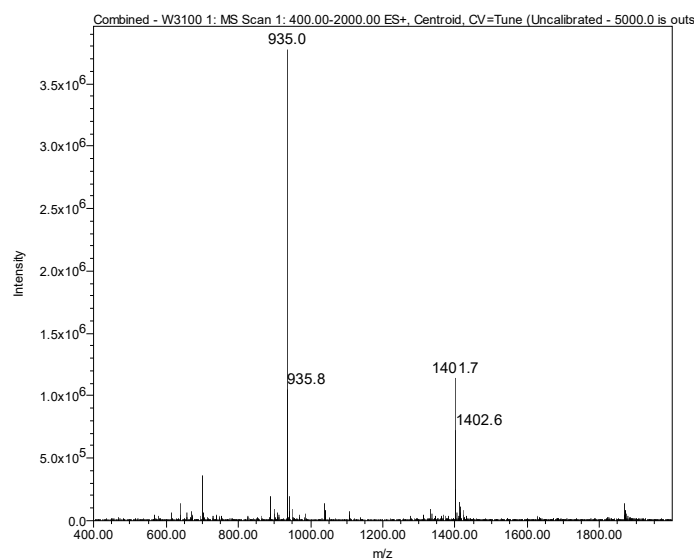
Figure 73: Mass spectrum of purified peptide **18**.

360

7.4.2 Exp: Epitope mapping

Synthesis of peptides 27 and 28

peptide **27**: biotin-spacer-EIVYKSPVVGlcNAcSGDTpSPRHLSNHH

peptide **28**: biotin-spacer-EIVYKpSPVVGlcNAcSGDTpSPRHLSNHH
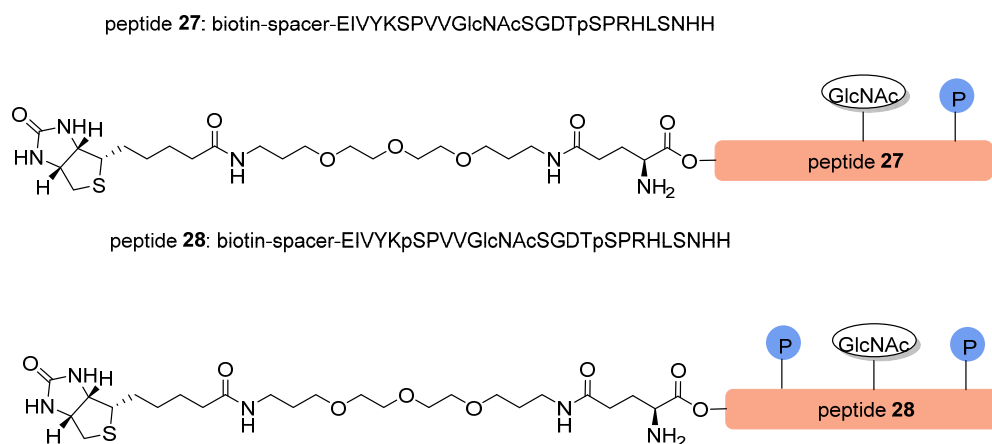
Figure 74: Sequence of peptides **27** and **28**.

The peptides were synthesized on Fmoc-Rink-Amid resin (0.14 mmol/g) on a 0.033 mmol scale. The synthesis was carried out manually by using 10 eq of amino acids, HOBt, HBTU and DIPEA in DMF for 1 h. It was capped after each second coupling with 10% v/v DIPEA and 10% v/v acetic anhydride in DMF for 20 min. The phospho-serines were double coupled with 5 eq amino acid, HATU, HOBt and DIPEA in DMF for 3 h. The Fmoc-Ser(β-D-GlcNAc(Ac)3)-OH compound was obtained as described in another publication by us.[536] The glycosylated serine was coupled with 2.5 eq amino acid, HATU, HOBt and DIPEA over night. The amino acids Val399, Val398 and Pro397 were attached by double coupling with 10 eq amino acid, HATU, HOBt and DIPEA ind DMF for 2 h. Biotin-PEG-Gln was coupled with 2.5 eq of the amino acid, HATU, HOBt and DIPEA in DMF over night. The peptide was cleaved with 4 ml solution of TFA/H$_2$O/TIS (95/2.5/2.5 v/v) at 37 °C in 4 h. The deacetylation of the sugar was performed with NaOMe in MeOH at pH 10 in 4 h. The peptides were purified by preparative HPLC and isolated with a yield of 4% (4.4 mg, 1.4 µmol) for peptide **28** and 4% for peptide **27** (4.6 mg, 1.5 µmol); molar mass peptide **28** = 3249.51 Da; MS: m/z: 1626.48 [M+2H]$^{2+}$ (calcd. m/z: 1625.76); 1084.63 [M+3H]$^{3+}$ (calcd. m/z: 1084.17); molar mass peptide **27** = 3169.55 Da; MS: m/z: 1586.24 [M+2H]$^{2+}$ (calcd. m/z: 1585.78); 1058.04 [M+3H]$^{3+}$ (calcd. m/z: 1057.52).
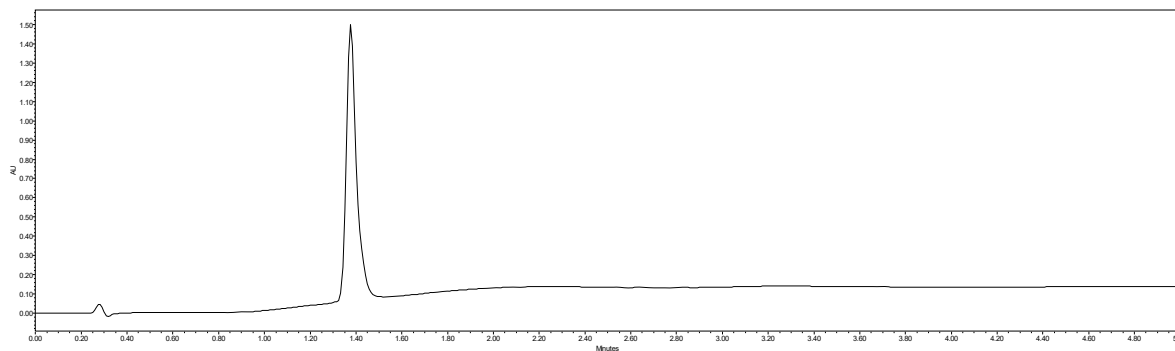
Figure 75: HPLC-UV trace of purified peptide **27**.
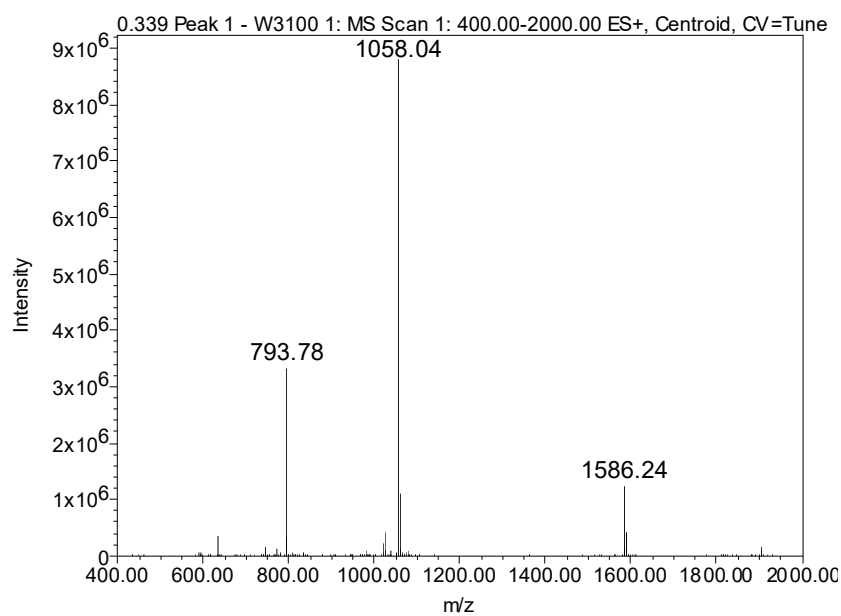
Figure 76: Mass spectrum of purified peptide **27**: m/z: 1586.24 $[M+2H]^{2+}$ (calcd. m/z: 1585.78); 1058.04 $[M+3H]^{3+}$ (calcd. m/z: 1057.52).
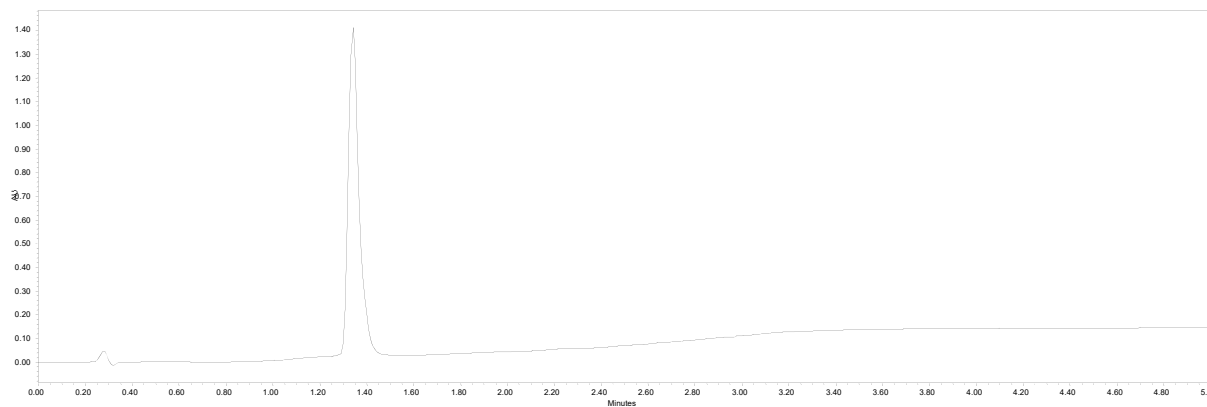
Figure 77: HPLC-UV trace of peptide **28**.

3.036 Peak 1 - W3100 1: MS Scan 1: 400.00-2000.00 ES+, Centroid, CV=Tune
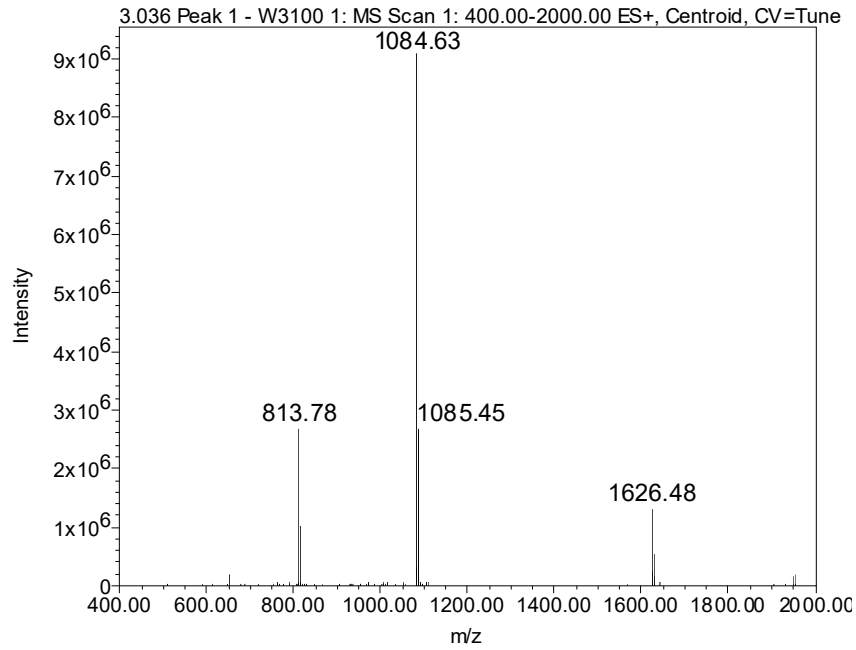
Figure 78: Mass spectrum of purified peptide **28**: m/z: 1626.48 [M+2H]$^{2+}$ (calcd. m/z: 1625.76); 1084.63 [M+3H]$^{3+}$ (calcd. m/z: 1084.17).

General ELISA protocol for epitope mapping (AG Kremmer)

Materials:

- 96-well plate

- wash buffer: PBS

- fetal calf serum (FCS) in PBS (2%)

- carbonate buffer (0.2 M)

- handwasher for ELISA plates

- multi-channel pipette

- biotinylated antigen

- primary antibody cell supernatant

- peroxidase-conjugated secondary antibody

- detection substrate TMB (3,3′,5,5′-tetramethylbenzidine) 1:10 in VE water diluted

Protocol:

- coating of the plate wells with streptavidin in carbonate buffer

- blocking with FCS (2%) in PBS

- incubation with antigen in PBS containing FCS (2%) (50 µL per well) for 10 min

363

- remove liquid and tapping of the plate onto a tower of paper towels

- wash with PBS once, remove liquid and tap again on paper towels

- 30 – 50 µL of cell supernatant of the primary antibodies to test were pipetted into each well

- incubation for 30 min on a rocker at rt

- remove liquid, tap on paper towels, wash once with PBS and tap again on paper towels

- addition of 50 µL of the milk powder solution containing the secondary antibody in the corresponding dilution and incubate for 20 min on a rocker

- remove liquid, tap plate on paper towels and wash with PBS 5 times, then tap again on paper towels

- add 50 µL of detection substrate TMB, wait for the color reaction to happen, stop the reaction by the addition of 1 N H_2SO_4

- measure immediately at 450 nm on an adequate plate reader

7.4.3 Exp: Evaluation of antibody clones by semisynthetic tri-phosphorylated tau proteins by western blot experiments

Western blots: Proteins were separated by SDS-PAGE (12% Mini-Protein TGX precast gel, Biorad) on a Bio-Rad Mini-Protean Tetra System and wet blotted onto a nitrocellulose membrane (0.2 µm, 300 mm x 3 m, 250 mA, 1h). Hereafter, the membranes were rinsed with Ponceau staining solution and initial Ponceau staining was recorded. Then, the membranes were washed with water until the Ponceau staining had vanished and the blots were blocked for 20 min at RT with TBS-T containing 3% milk powder. The blots were washed four times with TBS-T and then the antibodies (cell-supernatants) were applied in a 1:4 dilution in TBS-T and incubation was allowed to proceed over night at 4°C on a rocker. The membrane was then washed 3 times with TBS-T. The secondary antibody rat (anti-rat IgG AP conjugate, Promega) was applied in TBS-T containing 2.5% milk powder (weight/vol) in a 1:2500 dilution. The blot was then incubated for 90 min at RT and subsequently washed three times with TBS-T and once with TBS and then dried at ambient temperature. The dried blots were rinsed with a solution of 5-bromo-4-chloro-3'-indolyphosphate *p*-toluidine salt (BCIP) and nitro-blue

tetrazolium chloride (NBT) (premixed, Sigma Aldrich) to show colored bands after approx. 5 min. Pictures were taken on a Bio-Rad ChemiDoc system.

7.4.4 Exp: PHF-1 phosphorylation on tau in the *C.elegans* model

Worm strains used in this study

Neuronal human tau strains were derived from the lab of prof. Morimoto from the Northwestern university (USA) and were labeled as follows:

- AM355 (F35B3.3p::YFP::hTau40_wt)
- AM361 (F35B3.3p::YFP::hTau40_P301L)

DNA vectors for muscular strains were obtained by the Kirstein lab and transformed into *C.elegans.* The vectors had the following labeling:

- pPD30.38_YFP.hTau40_wt (unc-54p::YFP::hTauwt)
- pPD30.38_YFP_hTau40_P301L (unc-54p::YFP::hTau40_P301L)

Preparation of nuclear and cytoplasmatic extracts of *C.elegans* (Manuel Iburg)

The worm pellet (50 µL) was washed with M9 buffer and 100 µL of solution 1 (**Table 18**) were added. After freezing the pellet with liquid nitrogen, the sample was homogenized (4 times) and then, 100 µL of solution 2 were added, followed by a 22 min incubation on ice. The probe is centrifuged 30 min at 13400 g and subsequently, the supernatant is removed and frozen for further analysis (cytosolic fraction). The pellet was washed with 150 µL of solution 3 and was incubated for 30 min on ice. Then, centrifugation was carried out at 16100 g for 30 min. The supernatant is frozen with liquid nitrogen and frozen at -80°C for further use (nuclear fraction).

Table 18: Solutions used for preparation of nuclear and cytoplasmatic extracts.

Solution 1	Solution 2	Solution 3
50 mM Tris HCl (pH 7.5)	50 mM Tris HCl (pH 7.5)	50 mM Tris HCl (pH 7.5)
10 mM potassium acetate	100 mM potassium acetate	400 mM potassium acetate
5 mM DTT	5 mM DTT	2 mM Mg-acetate
	2 mM Mg-acetate	

7.4.5 Exp: Immunoprecipitation (IP) with the 15F1 clone and mass spectrometry of the pulled-out fraction

Immunoprecipitation (IP)

For the IP, 450 µL of the CSF of an AD patient were taken and incubated with 1 mL of cell-supernatant of 15F1, which should correspond to approx. 10 µg of antibody. The incubation was left for 1 h at ambient temperature on a rocker. Then, 25 µL of magnetic bead slurry (Pierce protein A/G magnetic beads) were added in a separate 2 mL vial and washed with 175 µL of wash buffer (Tris buffered saline containing 0.05% Tween-20 and 0.5 M NaCl). The liquid was removed and subsequently, the washing was repeated with 1 mL wash buffer. A final quick wash with VE-water rendered the beads ready for the pull-out. The cell-supernatant CSF mixture was added to the magnetic beads, followed by a 1 h incubation time. Afterward, the supernatant was removed and saved for further analysis. The beads were washed twice with wash buffer (500 µL) and once with quickly washed VE-water. Then, 50 µL of 4 x SDS Laemmli buffer were added and the beads were heated at 97°C for 15 min. Then, the whole probe was put in two different bands on a 12% SDS-PAGE gel and SDS-PAGE was carried out. The corresponding bands were excised and exposed to tryptic digest, as published.[530] Mass spectrometry was performed on a Dionex Ultimate 3000 NCS-3500RS Nano system, equipped with a PikoTip 75µm*250 mm analytical column (Christian Sommer AG Selbach MDC). The MS method applied was Orbitrap Fusion (Thermo Scientific) with the corresponding Tune

Software 2.0.1258.15. The peptide SPVVSGDTSPR containing the PHF-1 epitope was found only in unphosphorylated state.
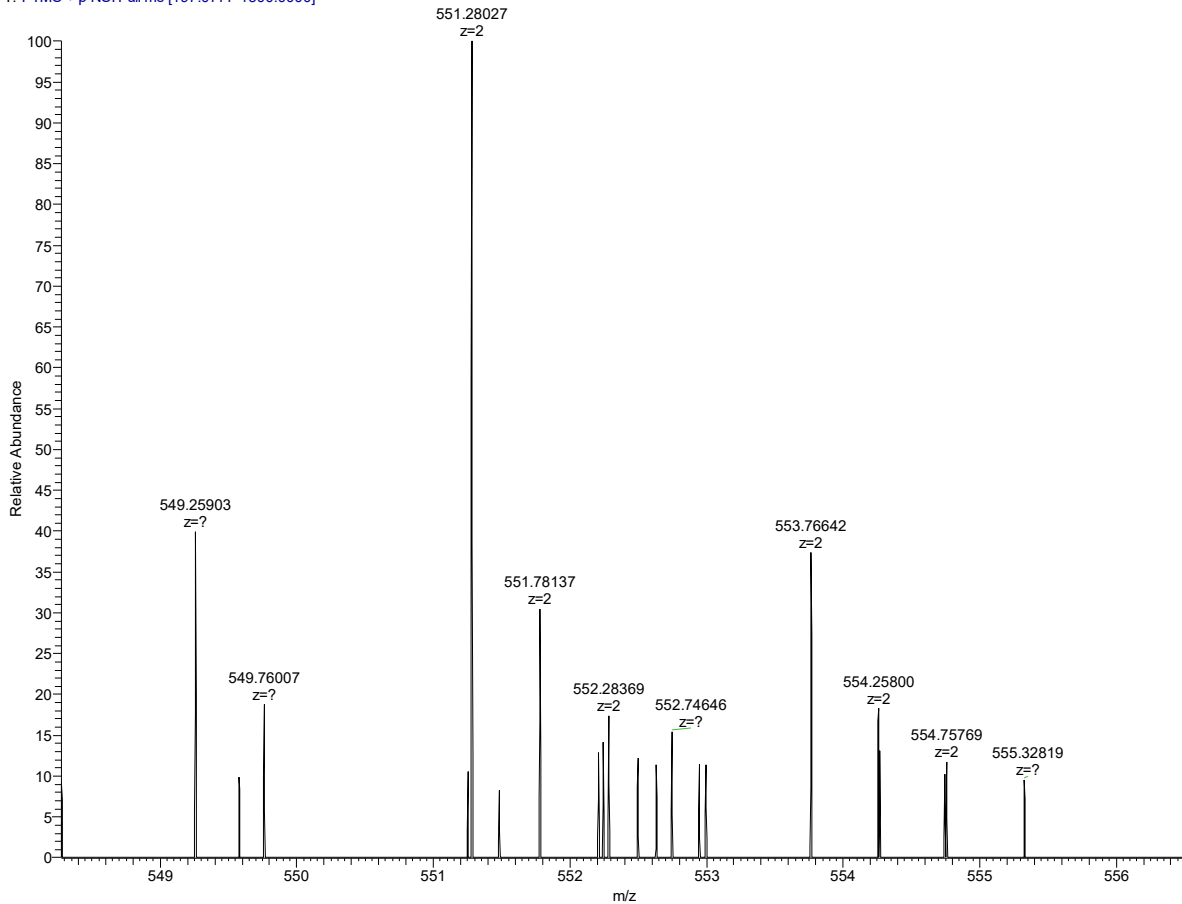
Figure 79: Mass spectrum of the identified unphosphorylated peptide tau[396-406] (SPVVSGDTSPR); M_W obs: m/z: 551.2803 [M+2H]$^{2+}$; M_W calcd: m/z: 551.2803 [M+2H]$^{2+}$.

7.4.6 Exp: ELISA assays with the new antibodies

7.4.6.1 Identification of the most potent clone (according to setting shown in Figure 50)

A 96-well microtiter plate (microtiter plate, immunograde, Brandt) was coated with 50 µL of antibody. The generated clones were either used directly as cell-supernatant (approx. 10 µg/mL) or in a 1:1 dilution with PBS o.n. at 4°C. Then, the liquid was removed from the wells and the plate was tapped on a paper towel tower. Then, the wells were washed three times with PBS and then blocked for 30 min on a rocker with 300 µL of PBS containing 1% milk.

The plate was washed three times with PBS and subsequently, 37 µL of a solution of HT7 and BT2 antibody in PBS buffer (conjugate 1 from INNOTEST hTau Ag kit) were mixed with 12 µL of CSF of an AD patient were mixed and pipetted into the corresponding wells. The plate was left standing at rt for 6 h and then further o.n. at 4°C. Then, the plate was thoroughly washed six time with PBS and in between always tapped on paper towels. Then 50 µL of conjugate 2, containing an HRP-streptavidin conjugate, were added and the plate was left slightly rocking for 30 min at rt. The plate was washed 5 times with PBS and then, 50 µL of the TMB substrate from the kit were added. The plate was left in the dark standing for about 30 min, before 50 µL of 2N H_2SO_4 were added to stop the enzymatic reaction of the TMB conversion.

Table 19: Measured absorbance of the identification of the most potent clone experiment.

clone [X]	undiluted	1:1 diluted with PBS
A	0.0455	0.0452
B	0.0436	0.0437
C	0.0445	0.0435
D	0.0886	0.1261
E	0.0435	0.0436
F	0.0437	0.0436
G	0.0433	0.0451
H	0.0438	0.0435

A second attempt to find the most potent clone was carried out with CSF, which was fivefold concentrated. The experimental setting remained the same to the above described, whereas the primary ppp-tau antibody was used as pure cell-supernatant without further dilution. The results are shown in **Figure 80**.
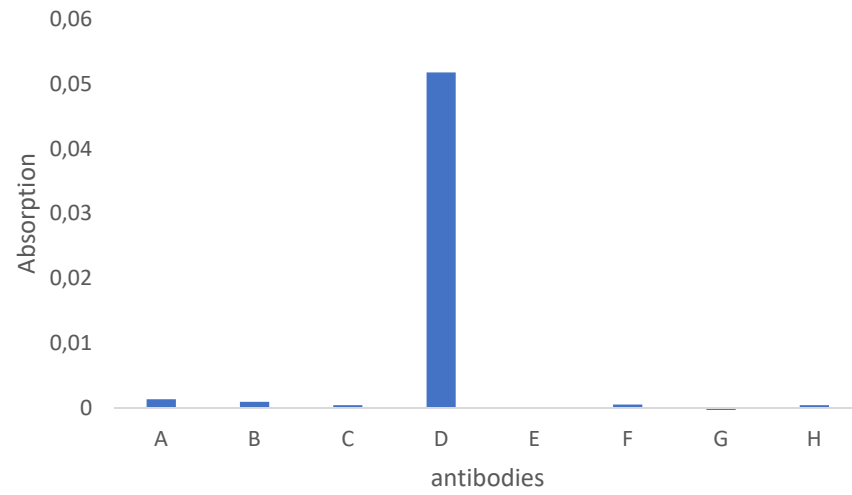
Figure 80: Determination of the most potent clone with fivefold concentrated CSF probe.

7.4.6.2 Measurement of total tau content by ELISA assays of a small cohort with the INNOTEST hTau Ag kit and comparison to phospho-tau levels detected with the 15F1 antibody

The procedure of the measurements was carried out as described in section **7.4.6.2**.

Table 20: Total tau measurement of a small CSF cohort of seven people by the INNOTEST hTau Ag kit. Probes with a critical amount of total tau are shown in red.

tTau (pg/ml)	initials (first name, last name)
98	W.A.
255	W.Z.
670	H.W.
310	D.Z.
584	J.N.
444	H.C.
489	H.M.

Table 21: Phospho-tau determination in ELISA assays by the 15F1 antibody.

Absorbance (450 nm)	initials (first name, last name)
0.0467	W.A.
0.05	W.Z.
0.0662	H.W.
0.0587	D.Z.
0.0643	J.N.
0.0388	H.C.
0.0617	H.M.

7.4.6.3 General Protocol for ELISA assays shown in Figure 51

General protocol applied for sandwich ELISA assays shown in Figure 51:

- coating with 100 µL antibody and incubation for 1 h

- wash 3x with PBS

- blocking with 5% milk in PBS (300 µL)

- wash 3x with PBS

- load CSF (50 µL) in PBS containing 1% milk (50 µL) and incubate for 1 h at rt

- wash 3x with PBS

- load new primary antibody (100 µL) and incubate for 1 h at ambient temperature

- wash 3 x with PBS

- load secondary antibody in PBS containing 1% milk (100 µL) and incubate for 30 min at ambient temperature

- wash 5x with PBS

- add 100 µL TMB and incubate for 30-45 min, then stop reaction by the addition of 50 µL of 1 N H_2SO_4

7.4.6.4 Cross-reactivity study

General protocol for western blot analysis of CSF with different primary and secondary antibodies:

- defreeze aliquot of CSF, mix 15 µL with 7.5 µL SDS Laemmli buffer (4x)

- prepare negative control samples with albumin in the same way

- heat samples at 97°C for 5 min

- apply to 12% gel and run SDS-PAGE (Bio-Rad Mini Protean Tetra system)

- wet blot onto a nitro cellulose membrane (0.2 µm, 300 mm x 3 m, 250 mA, 1 h)

- block membrane with 5% milk in PBS at rt for 1 h

- wash blot 3 x 10 min with PBS

- apply primary antibody in adequate dilution in PBS (1% milk) (15F1 and PHF-1 cell supernatants were diluted 1:10)

- wash blot 3 x with PBS

- incubate secondary antibody in adequate dilution (as stated by provider) in PBS (1% milk)

- wash 6 x with PBS

- rinse blot with WesternBright chemiluminescence solution (WesternBright ECL, advansta)

- incubate for 2 min and detect chmiluminescence on fluorescence imager

Results on secondary antibody goat anti-mouse (HRP) (ab97023)

Table 22: Western blot results for goat anti-mouse (HRP) (ab97023). A band at 55 kDa was found where tau was expected, whereas an additional band at 26 kDa was observed.

No.	probe	primary AB	secondary AB	blot
1	CSF	Tau 46 (mouse monoclonal IgG1, SantaCruz Biotechnology) in 1:200 dilution	goat anti-mouse (HRP) (ab97023) in 1:3000 dilution	55 kDa 26 kDa
2	CSF	Tau (rabbit polyclonal IgG, PA5-27287, Thermo Scientific)	goat anti-mouse (HRP) (ab97023) in 1:3000 dilution	55 kDa 26 kDa

Results on secondary antibody mouse anti-rat (HRP) (212-036-168)

Table 23: Western blot results for mouse anti-rat (HRP) (212-036-168). In blot 3, only unspecific binding to albumin was recognized. In blot No. 4 and 5, tau is recognized in addition to prevalent detection of a band at 26 kDa.

No.	probe	primary AB	secondary AB	blot
3	CSF	Tau 46 (mouse monoclonal IgG1, SantaCruz Biotechnology) in 1:200 dilution	mouse anti-rat (HRP) (212-036-168) in 1:5000 dilution	60 kDa
4	CSF	15F1 antibody in a 1:10 dilution	mouse anti-rat (HRP) (212-036-168) in 1:5000 dilution	55 kDa 26 kDa
5	CSF	Tau (rabbit polyclonal IgG, PA5-27287, Thermo Scientific)	mouse anti-rat (HRP) (212-036-168) in 1:5000 dilution	55 kDa 26 kDa

Results on secondary antibody goat anti-rat (HRP) (112-035-003)
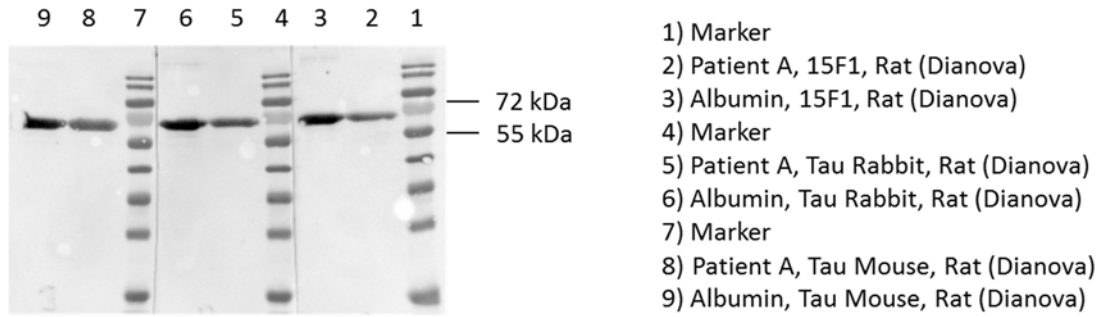
Figure 81: Western blots generated with the secondary antibody goat anti-rat (HRP) (112-035-003). No tau specific regonition was observed and instead, unspecific binding to albumin either purely blotted or present in CSF was recognized.

Results on secondary antibody goat anti-rabbit (HRP) (ab6721)

No.	probe	primary AB	secondary AB	blot
6	CSF	Tau (rabbit polyclonal IgG, PA5-27287, Thermo Scientific)	goat anti-rabbit (HRP) (ab6721) in 1:3000 dilution	55 kDa
7	CSF	15F1 antibody in a 1:10 dilution	goat anti-rabbit (HRP) (ab6721) in 1:3000 dilution	55 kDa
8	CSF	PHF-1 antibody in a 1:10 dilution	goat anti-rabbit (HRP) (ab6721) in 1:3000 dilution	55 kDa

8. REFERENCES

[1]   G. P. Morris, I. A. Clark, B. Vissel, *Acta Neuropathol. Commun.* **2014**, *2*, 135.

[2]   M. E. Murray, V. J. Lowe, N. R. Graff-Radford, A. M. Liesinger, A. Cannon, S. A. Przybelski, B. Rawal, J. E. Parisi, R. C. Petersen, K. Kantarci, O. A. Ross, R. Duara, D. S. Knopman, C. R. Jack, Jr., D. W. Dickson, *Brain* **2015**, *138*, 1370-1381.

[3]   I. Grundke-Iqbal, K. Iqbal, Y. C. Tung, M. Quinlan, H. M. Wisniewski, L. I. Binder, *Proc. Natl. Acad. Sci. U S A,* **1986**, *83*, 4913-4917.

[4]   M. Morris, G. M. Knudsen, S. Maeda, J. C. Trinidad, A. Ioanoviciu, A. L. Burlingame, L. Mucke, *Nat. Neurosci.* **2015**, *18*, 1183-1189.

[5]   A. D. Alonso, T. Zaidi, M. Novak, I. Grundke-Iqbal, K. Iqbal, *Proc. Natl. Acad. Sci. U S A,* **2001**, *98*, 6923-6928.

[6]   E. T. Lund, R. McKenna, D. B. Evans, S. K. Sharma, W. R. Mathews, *J. Neurochem.* **2001**, *76*, 1221-1232.

[7]   A. Abraha, N. Ghoshal, T. C. Gamblin, V. Cryns, R. W. Berry, J. Kuret, L. I. Binder, *J. Cell. Sci.* **2000**, *113 Pt 21*, 3737-3745.

[8]   C. P. Hackenberger, D. Schwarzer, *Angew. Chem. Int. Ed. Engl.* **2008**, *47*, 10030-10074.

[9]   http://www.alz.co.uk/research/WorldAlzheimerReport2015.pdf, Access date: February 1st, 2016

[10]   http://www.who.int/mediacentre/news/releases/2015/action-on-dementia/en/, Access date: 17th of May, 2016

[11]   http://www.phrma.org/sites/default/files/pdf/alzheimersetbacksreportfinal912.pdf, Access date: February 3rd, 2016

[12]   M. Hay, D. W. Thomas, J. L. Craighead, C. Economides, J. Rosenthal, *Nat. Biotechnol.* **2014**, *32*, 40-51.

[13]   http://www.alz.org/research/science/alzheimers_disease_treatments.asp, Access date: February 1st, 2016

[14]   S. Salomone, F. Caraci, G. M. Leggio, J. Fedotova, F. Drago, *Br. J. Clin. Pharmacol.* **2012**, *73*, 504-517.

[15]   R. J. Castellani, G. Perry, *Arch. Med. Res.* **2012**, *43*, 694-698.

[16]   H. Geerts, P. Roberts, A. Spiros, R. Carr, *Front. Pharmacol.* **2013**, *4*.

[17]   A. Alzheimer, *Allgemeine Zeitschrift fur Psychiatrie und Psychisch-gerichtliche Medizin,* **1907**, *64*, 146-148.

[18]   A. Alzheimer, R. A. Stelzmann, H. N. Schnitzlein, F. R. Murtagh, *Clin. Anat.* **1995**, *8*, 429-431.

[19]   G. G. Glenner, C. W. Wong, *Biochem. Biophys. Res. Commun.* **1984**, *120*, 885-890.

[20]   C. L. Masters, G. Simms, N. A. Weinman, G. Multhaup, B. L. McDonald, K. Beyreuther, *Proc. Natl. Acad. Sci. U S A,* **1985**, *82*, 4245-4249.

[21]   M. Goedert, C. M. Wischik, R. A. Crowther, J. E. Walker, A. Klug, *Proc. Natl. Acad. Sci. U S A,* **1988**, *85*, 4051-4055.

[22]   Y. Ihara, N. Nukina, R. Miura, M. Ogawara, *J. Biochem.* **1986**, *99*, 1807-1810.

[23]   J. M. Rozemuller, P. Eikelenboom, F. C. Stam, *Virchows Arch. B Cell. Pathol. Incl. Mol. Pathol.* **1986**, *51*, 247-254.

[24]   T. Wyss-Coray, *Nat. Med.* **2006**, *12*, 1005-1015.

8. REFERENCES

[25] D. Pratico, *Trends Pharmacol. Sci.* **2008**, *29*, 609-615.

[26] P. L. McGeer, J. Rogers, E. G. McGeer, *J. Alzheimers Dis.* **2006**, *9*, 271-276.

[27] F. M. LaFerla, K. N. Green, S. Oddo, *Nat. Rev. Neurosci.* **2007**, *8*, 499-509.

[28] J. T. Jarrett, E. P. Berger, P. T. Lansbury, Jr., *Biochemistry,* **1993**, *32*, 4693-4697.

[29] S. G. Younkin, *J. Physiol. Paris,* **1998**, *92*, 289-292.

[30] M. P. Murphy, H. LeVine, 3rd, *J. Alzheimers Dis.* **2010**, *19*, 311-323.

[31] V. L. Villemagne, K. E. Pike, G. Chetelat, K. A. Ellis, R. S. Mulligan, P. Bourgeat, U. Ackermann, G. Jones, C. Szoeke, O. Salvado, R. Martins, G. O'Keefe, C. A. Mathis, W. E. Klunk, D. Ames, C. L. Masters, C. C. Rowe, *Ann. Neurol.* **2011**, *69*, 181-192.

[32] C. Holmes, D. Boche, D. Wilkinson, G. Yadegarfar, V. Hopkins, A. Bayer, R. W. Jones, R. Bullock, S. Love, J. W. Neal, E. Zotova, J. A. Nicoll, *Lancet,* **2008**, *372*, 216-223.

[33] J. A. Hardy, G. A. Higgins, *Science,* **1992**, *256*, 184-185.

[34] C. A. Lemere, E. Masliah, *Nat. Rev. Neurol.* **2010**, *6*, 108-119.

[35] W. L. Klein, *Neurochem. Int.* **2002**, *41*, 345-352.

[36] D. J. Selkoe, *Science,* **2002**, *298*, 789-791.

[37] F. Hefti, W. F. Goure, J. Jerecic, K. S. Iverson, P. A. Walicke, G. A. Krafft, *Trends Pharmacol. Sci.* **2013**, *34*, 261-266.

[38] W. I. Rosenblum, *Neurobiol. Aging,* **2014**, *35*, 969-974.

[39] http://www.alzforum.org/therapeutics/solanezumab, Access date: February, 7th, 2016

[40] M. D. Weingarten, A. H. Lockwood, S. Y. Hwo, M. W. Kirschner, *Proc. Natl. Acad. Sci. U S A,* **1975**, *72*, 1858-1862.

[41] M. L. Garcia, D. W. Cleveland, *Curr. Opin. Cell. Biol.* **2001**, *13*, 41-48.

[42] L. Cassimeris, C. Spittle, *Int. Rev. Cytol.* **2001**, *210*, 163-226.

[43] M. Kidd, *Nature,* **1963**, *197*, 192-193.

[44] V. M. Lee, M. Goedert, J. Q. Trojanowski, *Annu. Rev. Neurosci.* **2001**, *24*, 1121-1159.

[45] A. Andreadis, *Prog. Mol. Subcell. Biol.* **2006**, *44*, 89-107.

[46] P. LoPresti, S. Szuchet, S. C. Papasozomenos, R. P. Zinkowski, L. I. Binder, *Proc. Natl. Acad. Sci. U S A,* **1995**, *92*, 10369-10373.

[47] Y. Wang, E. Mandelkow, *Nat. Rev. Neurosci.* **2016**, *17*, 22-35.

[48] G. Lee, N. Cowan, M. Kirschner, *Science,* **1988**, *239*, 285-288.

[49] S. Kar, J. Fan, M. J. Smith, M. Goedert, L. A. Amos, *EMBO J.* **2003**, *22*, 70-77.

[50] R. A. Santarella, G. Skiniotis, K. N. Goldie, P. Tittmann, H. Gross, E. M. Mandelkow, E. Mandelkow, A. Hoenger, *J. Mol. Biol.* **2004**, *339*, 539-553.

[51] N. Gustke, B. Trinczek, J. Biernat, E. M. Mandelkow, E. Mandelkow, *Biochemistry,* **1994**, *33*, 9511-9522.

[52] Y. S. Jho, E. B. Zhulina, M. W. Kim, P. A. Pincus, *Biophys. J.* **2010**, *99*, 2387-2397.

[53] S. Wegmann, I. D. Medalsy, E. Mandelkow, D. J. Muller, *Proc. Natl. Acad. Sci. U S A,* **2013**, *110*, E313-321.

[54] M. Morris, S. Maeda, K. Vossel, L. Mucke, *Neuron,* **2011**, *70*, 410-426.

[55] M. Goedert, R. Jakes, *EMBO J.* **1990**, *9*, 4225-4230.

8. REFERENCES

[56]   J. Chen, Y. Kanai, N. J. Cowan, N. Hirokawa, *Nature,* **1992**, *360*, 674-677.

[57]   T. F. Frappier, I. S. Georgieff, K. Brown, M. L. Shelanski, *J. Neurochem.* **1994**, *63*, 2288-2294.

[58]   C. Liu, J. Gotz, *PLoS One,* **2013**, *8*, e84849.

[59]   G. Lee, S. T. Newman, D. L. Gard, H. Band, G. Panchamoorthy, *J. Cell. Sci.* **1998**, *111 (Pt 21)*, 3167-3177.

[60]   S. Jeganathan, M. von Bergen, H. Brutlach, H. J. Steinhoff, E. Mandelkow, *Biochemistry,* **2006**, *45*, 2283-2293.

[61]   L. S. Yang, H. Ksiezak-Reding, *Eur. J. Biochem.* **1995**, *233*, 9-17.

[62]   A. Kenessey, P. Nacharaju, L. W. Ko, S. H. Yen, *J. Neurochem.* **1997**, *69*, 2026-2038.

[63]   N. Canu, L. Dus, C. Barbato, M. T. Ciotti, C. Brancolini, A. M. Rinaldi, M. Novak, A. Cattaneo, A. Bradbury, P. Calissano, *J. Neurosci.* **1998**, *18*, 7061-7074.

[64]   C. M. Wischik, M. Novak, H. C. Thogersen, P. C. Edwards, M. J. Runswick, R. Jakes, J. E. Walker, C. Milstein, M. Roth, A. Klug, *Proc. Natl. Acad. Sci. U S A,* **1988**, *85*, 4506-4510.

[65]   S. C. Feinstein, L. Wilson, *Biochim. Biophys. Acta,* **2005**, *1739*, 268-279.

[66]   E. M. Mandelkow, E. Mandelkow, *Cold Spring Harb. Perspect. Med.* **2012**, *2*, a006247.

[67]   H. Kadavath, R. V. Hofele, J. Biernat, S. Kumar, K. Tepper, H. Urlaub, E. Mandelkow, M. Zweckstetter, *Proc. Natl. Acad. Sci. U S A,* **2015**, *112*, 7501-7506.

[68]   K. Stamer, R. Vogel, E. Thies, E. Mandelkow, E. M. Mandelkow, *J. Cell. Biol.* **2002**, *156*, 1051-1063.

[69]   A. Yuan, A. Kumar, C. Peterhoff, K. Duff, R. A. Nixon, *J. Neurosci.* **2008**, *28*, 1682-1687.

[70]   A. Caceres, K. S. Kosik, *Nature,* **1990**, *343*, 461-463.

[71]   J. Knops, K. S. Kosik, G. Lee, J. D. Pardee, L. Cohen-Gould, L. McConlogue, *J. Cell. Biol.* **1991**, *114*, 725-733.

[72]   M. DiTella, F. Feiguin, G. Morfini, A. Caceres, *Cell. Motil. Cytoskeleton,* **1994**, *29*, 117-130.

[73]   M. M. Black, T. Slaughter, S. Moshiach, M. Obrocka, I. Fischer, *J. Neurosci.* **1996**, *16*, 3601-3619.

[74]   U. Preuss, F. Doring, S. Illenberger, E. M. Mandelkow, *Mol. Biol. Cell.* **1995**, *6*, 1397-1410.

[75]   M. Arrasate, M. Perez, J. Avila, *Neurochem. Res.* **2000**, *25*, 43-50.

[76]   L. Buee, T. Bussiere, V. Buee-Scherrer, A. Delacourte, P. R. Hof, *Brain Res. Brain Res. Rev.* **2000**, *33*, 95-130.

[77]   A. M. Pooler, A. Usardi, C. J. Evans, K. L. Philpott, W. Noble, D. P. Hanger, *Neurobiol. Aging.* **2012**, *33*, 431 e427-438.

[78]   T. Kawarabayashi, M. Shoji, L. H. Younkin, L. Wen-Lang, D. W. Dickson, T. Murakami, E. Matsubara, K. Abe, K. H. Ashe, S. G. Younkin, *J. Neurosci.* **2004**, *24*, 3801-3809.

[79]   R. Williamson, A. Usardi, D. P. Hanger, B. H. Anderton, *FASEB J.* **2008**, *22*, 1552-1559.

[80]   N. Sahara, M. Murayama, M. Higuchi, T. Suhara, A. Takashima, *Front. Neurol.* **2014**, *5*, 26.

[81]   G. Lee, *Biochim. Biophys. Acta,* **2005**, *1739*, 323-330.

[82]   L. M. Ittner, Y. D. Ke, F. Delerue, M. Bi, A. Gladbach, J. van Eersel, H. Wolfing, B. C. Chieng, M. J. Christie, I. A. Napier, A. Eckert, M. Staufenbiel, E. Hardeman, J. Gotz, *Cell,* **2010**, *142*, 387-397.

8. REFERENCES

[83] B. R. Hoover, M. N. Reed, J. Su, R. D. Penrod, L. A. Kotilinek, M. K. Grant, R. Pitstick, G. A. Carlson, L. M. Lanier, L. L. Yuan, K. H. Ashe, D. Liao, *Neuron,* **2010**, *68*, 1067-1081.

[84] M. Bukar Maina, Y. K. Al-Hilaly, L. C. Serpell, *Biomolecules,* **2016**, *6*.

[85] J. Metuzals, Y. Robitaille, S. Houghton, S. Gauthier, R. Leblanc, *J. Neurocytol.* **1988**, *17*, 827-833.

[86] P. A. Loomis, T. H. Howard, R. P. Castleberry, L. I. Binder, *Proc. Natl. Acad. Sci. U S A,* **1990**, *87*, 8422-8426.

[87] J. A. Greenwood, G. V. Johnson, *Exp. Cell Res.* **1995**, *220*, 332-337.

[88] V. C. Thurston, R. P. Zinkowski, L. I. Binder, *Chromosoma,* **1996**, *105*, 20-30.

[89] Y. Wang, P. A. Loomis, R. P. Zinkowski, L. I. Binder, *J. Cell. Biol.* **1993**, *121*, 257-267.

[90] T. B. Shea, C. M. Cressman, *Int. J. Dev. Neurosci.* **1998**, *16*, 41-48.

[91] R. M. Brady, R. P. Zinkowski, L. I. Binder, *Neurobiol. Aging,* **1995**, *16*, 479-486.

[92] M. P. Lambert, S. Sabo, C. Zhang, S. A. Enam, W. L. Klein, *Neurobiol. Aging,* **1995**, *16*, 583-589.

[93] J. Lu, J. Miao, T. Su, Y. Liu, R. He, *Biochim. Biophys. Acta,* **2013**, *1830*, 4102-4116.

[94] Y. Lu, H. J. He, J. Zhou, J. Y. Miao, J. Lu, Y. G. He, R. Pan, Y. Wei, Y. Liu, R. Q. He, *J. Alzheimers Dis.* **2013**, *37*, 551-563.

[95] Q. Hua, R. Q. He, N. Haque, M. H. Qu, A. del Carmen Alonso, I. Grundke-Iqbal, K. Iqbal, *Cell. Mol. Life. Sci.* **2003**, *60*, 413-421.

[96] Y. Wei, M. H. Qu, X. S. Wang, L. Chen, D. L. Wang, Y. Liu, Q. Hua, R. Q. He, *PLoS One,* **2008**, *3*, e2600.

[97] S. Camero, M. J. Benitez, A. Barrantes, J. M. Ayuso, R. Cuadros, J. Avila, J. S. Jimenez, *J Alzheimers Dis.* **2014**, *39*, 649-660.

[98] Q. Hua, R. Q. He, *Chin. Sci. Bull.* **2000**, *45*, 999-1002.

[99] W. J. Welch, J. R. Feramisco, *J. Biol. Chem.* **1984**, *259*, 4501-4513.

[100] S. Mondragon-Rodriguez, G. Perry, X. W. Zhu, P. I. Moreira, M. C. Acevedo-Aquino, S. Williams, *Oxid. Med. Cell. Longev.* **2013**.

[101] G. Alvarez, J. Aldudo, M. Alonso, S. Santana, F. Valdivieso, *J. Neurosci. Res.* **2012**, *90*, 1020-1029.

[102] V. Padmaraju, S. S. Indi, K. S. Rao, *Neurochem. Int.* **2010**, *57*, 51-57.

[103] K. Hernandez-Ortega, P. Garcia-Esparcia, L. Gil, J. J. Lucas, I. Ferrer, *Brain Pathol.* **2015**.

[104] K. Kanemaru, K. Takio, R. Miura, K. Titani, Y. Ihara, *J. Neurochem.* **1992**, *58*, 1667-1675.

[105] E. Kopke, Y. C. Tung, S. Shaikh, A. C. Alonso, K. Iqbal, I. Grundke-Iqbal, *J. Biol. Chem.* **1993**, *268*, 24374-24384.

[106] D. P. Hanger, B. H. Anderton, W. Noble, *Trends Mol. Med.* **2009**, *15*, 112-119.

[107] N. Shahani, R. Brandt, *Cell. Mol. Life Sci.* **2002**, *59*, 1668-1680.

[108] E. Planel, T. Miyasaka, T. Launey, D. H. Chui, K. Tanemura, S. Sato, O. Murayama, K. Ishiguro, Y. Tatebayashi, A. Takashima, *J. Neurosci.* **2004**, *24*, 2401-2411.

[109] T. Arendt, J. Stieler, A. M. Strijkstra, R. A. Hut, J. Rudiger, E. A. Van der Zee, T. Harkany, M. Holzer, W. Hartig, *J. Neurosci.* **2003**, *23*, 6972-6981.

8. REFERENCES

[110] E. Planel, K. E. Richter, C. E. Nolan, J. E. Finley, L. Liu, Y. Wen, P. Krishnamurthy, M. Herman, L. Wang, J. B. Schachter, R. B. Nelson, L. F. Lau, K. E. Duff, *J. Neurosci.* **2007**, *27*, 3090-3097.

[111] P. J. Lu, G. Wulf, X. Z. Zhou, P. Davies, K. P. Lu, *Nature,* **1999**, *399*, 784-788.

[112] E. Thies, E. M. Mandelkow, *J. Neurosci.* **2007**, *27*, 2896-2907.

[113] H. Zempel, E. Thies, E. Mandelkow, E. M. Mandelkow, *J. Neurosci.* **2010**, *30*, 11938-11950.

[114] A. L. Guillozet-Bongaarts, M. E. Cahill, V. L. Cryns, M. R. Reynolds, R. W. Berry, L. I. Binder, *J. Neurochem.* **2006**, *97*, 1005-1014.

[115] L. M. Ittner, Y. D. Ke, J. Gotz, *J. Biol. Chem.* **2009**, *284*, 20909-20916.

[116] S. Barghorn, Q. Zheng-Fischhofer, M. Ackmann, J. Biernat, M. von Bergen, E. M. Mandelkow, E. Mandelkow, *Biochemistry,* **2000**, *39*, 11714-11721.

[117] M. Hong, V. Zhukareva, V. Vogelsberg-Ragaglia, Z. Wszolek, L. Reed, B. I. Miller, D. H. Geschwind, T. D. Bird, D. McKeel, A. Goate, J. C. Morris, K. C. Wilhelmsen, G. D. Schellenberg, J. Q. Trojanowski, V. M. Lee, *Science,* **1998**, *282*, 1914-1917.

[118] I. Khlistunova, J. Biernat, Y. Wang, M. Pickhardt, M. von Bergen, Z. Gazova, E. Mandelkow, E. M. Mandelkow, *J. Biol. Chem.* **2006**, *281*, 1205-1214.

[119] T. Kampers, P. Friedhoff, J. Biernat, E. M. Mandelkow, E. Mandelkow, *FEBS Lett.* **1996**, *399*, 344-349.

[120] M. Goedert, R. Jakes, M. G. Spillantini, M. Hasegawa, M. J. Smith, R. A. Crowther, *Nature,* **1996**, *383*, 550-553.

[121] H. Wille, G. Drewes, J. Biernat, E. M. Mandelkow, E. Mandelkow, *J. Cell. Biol.* **1992**, *118*, 573-584.

[122] E. Braak, H. Braak, E. M. Mandelkow, *Acta Neuropathol.* **1994**, *87*, 554-567.

[123] M. Broncel, E. Krause, D. Schwarzer, C. P. Hackenberger, *Chem. Eur. J.* **2012**, *18*, 2488-2492.

[124] A. Schneider, J. Biernat, M. von Bergen, E. Mandelkow, E. M. Mandelkow, *Biochemistry,* **1999**, *38*, 3549-3558.

[125] K. Tepper, J. Biernat, S. Kumar, S. Wegmann, T. Timm, S. Hubschmann, L. Redecke, E. M. Mandelkow, D. J. Muller, E. Mandelkow, *J. Biol. Chem.* **2014**, *289*, 34389-34407.

[126] Y. Wang, E. Mandelkow, *Biochem. Soc. Trans.* **2012**, *40*, 644-652.

[127] A. de Calignon, L. M. Fox, R. Pitstick, G. A. Carlson, B. J. Bacskai, T. L. Spires-Jones, B. T. Hyman, *Nature,* **2010**, *464*, 1201-1204.

[128] Z. Zhang, M. Song, X. Liu, S. S. Kang, I. S. Kwon, D. M. Duong, N. T. Seyfried, W. T. Hu, Z. Liu, J. Z. Wang, L. Cheng, Y. E. Sun, S. P. Yu, A. I. Levey, K. Ye, *Nat. Med.* **2014**, *20*, 1254-1262.

[129] M. von Bergen, P. Friedhoff, J. Biernat, J. Heberle, E. M. Mandelkow, E. Mandelkow, *Proc. Natl. Acad. Sci. U S A,* **2000**, *97*, 5129-5134.

[130] Y. P. Wang, J. Biernat, M. Pickhardt, E. Mandelkow, E. M. Mandelkow, *Proc. Natl. Acad. Sci. U S A,* **2007**, *104*, 10252-10257.

[131] F. Clavaguera, J. Hench, I. Lavenir, G. Schweighauser, S. Frank, M. Goedert, M. Tolnay, *Acta Neuropathol.* **2014**, *127*, 299-301.

[132] D. W. Sanders, S. K. Kaufman, S. L. DeVos, A. M. Sharma, H. Mirbaha, A. Li, S. J. Barker, A. C. Foley, J. R. Thorpe, L. C. Serpell, T. M. Miller, L. T. Grinberg, W. W. Seeley, M. I. Diamond, *Neuron,* **2014**, *82*, 1271-1288.

[133] B. B. Holmes, M. I. Diamond, *J. Biol. Chem.* **2014**, *289*, 19855-19861.

8. REFERENCES

[134] V. Zhukareva, V. Vogelsberg-Ragaglia, V. M. Van Deerlin, J. Bruce, T. Shuck, M. Grossman, C. M. Clark, S. E. Arnold, E. Masliah, D. Galasko, J. Q. Trojanowski, V. M. Lee, *Ann. Neurol.* **2001**, *49*, 165-175.

[135] T. Gomez-Isla, R. Hollister, H. West, S. Mui, J. H. Growdon, R. C. Petersen, J. E. Parisi, B. T. Hyman, *Ann. Neurol.* **1997**, *41*, 17-24.

[136] R. Morsch, W. Simon, P. D. Coleman, *J. Neuropath. Exp. Neurol.* **1999**, *58*, 188-197.

[137] A. D. Alonso, B. Li, I. Grundke-Iqbal, K. Iqbal, *Proc. Natl. Acad. Sci. U S A,* **2006**, *103*, 8864-8869.

[138] C. A. Lasagna-Reeves, D. L. Castillo-Carranza, U. Sengupta, J. Sarmiento, J. Troncoso, G. R. Jackson, R. Kayed, *Faseb J.* **2012**, *26*, 1946-1959.

[139] H. Tian, E. Davidowitz, P. Lopez, S. Emadi, J. Moe, M. Sierks, *Int. J. Cell Biol.* **2013**, *2013*, 9.

[140] K. Flach, I. Hilbrich, A. Schiffmann, U. Gartner, M. Kruger, M. Leonhardt, H. Waschipky, L. Wick, T. Arendt, M. Holzer, *J. Biol. Chem.* **2012**, *287*, 43223-43233.

[141] P. Rizzu, J. C. Van Swieten, M. Joosse, M. Hasegawa, M. Stevens, A. Tibben, M. F. Niermeijer, M. Hillebrand, R. Ravid, B. A. Oostra, M. Goedert, C. M. van Duijn, P. Heutink, *Am. J. Hum. Genet.* **1999**, *64*, 414-421.

[142] M. M. Mocanu, A. Nissen, K. Eckermann, I. Khlistunova, J. Biernat, D. Drexler, O. Petrova, K. Schonig, H. Bujard, E. Mandelkow, L. Zhou, G. Rune, E. M. Mandelkow, *J. Neurosci.* **2008**, *28*, 737-748.

[143] K. Eckermann, M. M. Mocanu, I. Khlistunova, J. Biernat, A. Nissen, A. Hofmann, K. Schonig, H. Bujard, A. Haemisch, E. Mandelkow, L. Zhou, G. Rune, E. M. Mandelkow, *J. Biol. Chem.* **2007**, *282*, 31755-31765.

[144] H. C. Tai, B. Y. Wang, A. Serrano-Pozo, M. P. Frosch, T. L. Spires-Jones, B. T. Hyman, *Acta Neuropathol. Commun.* **2014**, *2*, 146.

[145] H. Zempel, J. Luedtke, Y. Kumar, J. Biernat, H. Dawson, E. Mandelkow, E. M. Mandelkow, *EMBO J.* **2013**, *32*, 2920-2937.

[146] T. A. Fulga, I. Elson-Schwab, V. Khurana, M. L. Steinhilb, T. L. Spires, B. T. Hyman, M. B. Feany, *Nat. Cell Biol.* **2007**, *9*, 139-U117.

[147] C. R. Torres, G. W. Hart, *J. Biol. Chem.* **1984**, *259*, 3308-3317.

[148] K. Vosseller, J. C. Trinidad, R. J. Chalkley, C. G. Specht, A. Thalhammer, A. J. Lynn, J. O. Snedecor, S. Guan, K. F. Medzihradszky, D. A. Maltby, R. Schoepfer, A. L. Burlingame, *Mol. Cell Proteomics,* **2006**, *5*, 923-934.

[149] J. C. Trinidad, D. T. Barkan, B. F. Gulledge, A. Thalhammer, A. Sali, R. Schoepfer, A. L. Burlingame, *Mol. Cell Proteomics,* **2012**, *11*, 215-229.

[150] Y. V. Skorobogatko, J. Deuso, J. Adolf-Bryfogle, M. G. Nowak, Y. Gong, C. F. Lippa, K. Vosseller, *Amino Acids,* **2011**, *40*, 765-779.

[151] L. K. Kreppel, M. A. Blomberg, G. W. Hart, *J. Biol. Chem.* **1997**, *272*, 9308-9315.

[152] W. A. Lubas, D. W. Frank, M. Krause, J. A. Hanover, *J. Biol. Chem.* **1997**, *272*, 9316-9324.

[153] C. F. Chou, A. J. Smith, M. B. Omary, *J. Biol. Chem.* **1992**, *267*, 3901-3906.

[154] E. P. Roquemore, M. R. Chevrier, R. J. Cotter, G. W. Hart, *Biochemistry,* **1996**, *35*, 3578-3586.

[155] Y. Gao, L. Wells, F. I. Comer, G. J. Parker, G. W. Hart, *J. Biol. Chem.* **2001**, *276*, 9838-9845.

[156] Y. Zhu, X. Shan, S. A. Yuzwa, D. J. Vocadlo, *J. Biol. Chem.* **2014**, *289*, 34472-34481.

[157] R. Okuyama, S. Marshall, *J. Neurochem.* **2003**, *86*, 1271-1280.

8. REFERENCES

[158] X. Li, F. Lu, J. Z. Wang, C. X. Gong, *Eur. J. Neurosci.* **2006**, *23*, 2078-2086.

[159] S. Marshall, V. Bacote, R. R. Traxinger, *J. Biol. Chem.* **1991**, *266*, 4706-4712.

[160] C. S. Arnold, G. V. Johnson, R. N. Cole, D. L. Dong, M. Lee, G. W. Hart, *J. Biol. Chem.* **1996**, *271*, 28741-28744.

[161] F. Liu, K. Iqbal, I. Grundke-Iqbal, G. W. Hart, C. X. Gong, *Proc. Natl. Acad. Sci. U S A,* **2004**, *101*, 10804-10809.

[162] S. A. Yuzwa, M. S. Macauley, J. E. Heinonen, X. Shan, R. J. Dennis, Y. He, G. E. Whitworth, K. A. Stubbs, E. J. McEachern, G. J. Davies, D. J. Vocadlo, *Nat. Chem. Biol.* **2008**, *4*, 483-490.

[163] D. L. Graham, A. J. Gray, J. A. Joyce, D. Yu, J. O'Moore, G. A. Carlson, M. S. Shearman, T. L. Dellovade, H. Hering, *Neuropharmacol.* **2014**, *79*, 307-313.

[164] S. A. Yuzwa, X. Shan, M. S. Macauley, T. Clark, Y. Skorobogatko, K. Vosseller, D. J. Vocadlo, *Nat. Chem. Biol.* **2012**, *8*, 393-399.

[165] S. A. Yuzwa, A. K. Yadav, Y. Skorobogatko, T. Clark, K. Vosseller, D. J. Vocadlo, *Amino Acids,* **2011**, *40*, 857-868.

[166] Z. Wang, N. D. Udeshi, M. O'Malley, J. Shabanowitz, D. F. Hunt, G. W. Hart, *Mol. Cell Proteomics,* **2010**, *9*, 153-160.

[167] C. Smet-Nocca, M. Broncel, J. M. Wieruszeski, C. Tokarski, X. Hanoulle, A. Leroy, I. Landrieu, C. Rolando, G. Lippens, C. P. Hackenberger, *Mol. Biosyst.* **2011**, *7*, 1420-1429.

[168] L. Amniai, P. Barbier, A. Sillen, J. M. Wieruszeski, V. Peyrot, G. Lippens, I. Landrieu, *FASEB J.* **2009**, *23*, 1146-1152.

[169] I. Landrieu, L. Lacosse, A. Leroy, J. M. Wieruszeski, X. Trivelli, A. Sillen, N. Sibille, H. Schwalbe, K. Saxena, T. Langer, G. Lippens, *J. Am. Chem. Soc.* **2006**, *128*, 3575-3583.

[170] I. Landrieu, A. Leroy, C. Smet-Nocca, I. Huvent, L. Amniai, M. Hamdane, N. Sibille, L. Buee, J. M. Wieruszeski, G. Lippens, *Biochem. Soc. Trans.* **2010**, *38*, 1006-1011.

[171] A. Leroy, I. Landrieu, I. Huvent, D. Legrand, B. Codeville, J. M. Wieruszeski, G. Lippens, *J Biol. Chem.* **2010**, *285*, 33435-33444.

[172] K. S. Kosik, H. Shimura, *Biochim. Biophys. Acta,* **2005**, *1739*, 298-310.

[173] M. Morishima-Kawashima, M. Hasegawa, K. Takio, M. Suzuki, H. Yoshida, K. Titani, Y. Ihara, *J. Biol. Chem.* **1995**, *270*, 823-829.

[174] M. Morishima-Kawashima, M. Hasegawa, K. Takio, M. Suzuki, H. Yoshida, A. Watanabe, K. Titani, Y. Ihara, *Neurobiol. Aging,* **1995**, *16*, 365-371; discussion 371-380.

[175] N. Sergeant, A. Delacourte, L. Buee, *Biochim. Biophys. Acta,* **2005**, *1739*, 179-197.

[176] W. H. Stoothoff, G. V. Johnson, *Biochim. Biophys. Acta,* **2005**, *1739*, 280-297.

[177] E. Masliah, A. Sisk, M. Mallory, D. Games, *J. Neuropathol. Exp. Neurol.* **2001**, *60*, 357-368.

[178] S. W. Scheff, D. A. Price, F. A. Schmitt, S. T. DeKosky, E. J. Mufson, *Neurology,* **2007**, *68*, 1501-1508.

[179] S. W. Scheff, D. A. Price, F. A. Schmitt, E. J. Mufson, *Neurobiol. Aging,* **2006**, *27*, 1372-1384.

[180] J. Gotz, F. Chen, J. van Dorpe, R. M. Nitsch, *Science,* **2001**, *293*, 1491-1495.

[181] J. Lewis, D. W. Dickson, W. L. Lin, L. Chisholm, A. Corral, G. Jones, S. H. Yen, N. Sahara, L. Skipper, D. Yager, C. Eckman, J. Hardy, M. Hutton, E. McGowan, *Science,* **2001**, *293*, 1487-1491.

[182] E. D. Roberson, K. Scearce-Levie, J. J. Palop, F. Yan, I. H. Cheng, T. Wu, H. Gerstein, G. Q. Yu, L. Mucke, *Science,* **2007**, *316*, 750-754.

8. REFERENCES

[183] M. A. Chabrier, D. Cheng, N. A. Castello, K. N. Green, F. M. LaFerla, *Neurobiol. Dis.* **2014**, *64*, 107-117.

[184] R. M. Nisbet, J. C. Polanco, L. M. Ittner, J. Gotz, *Acta Neuropathol.* **2015**, *129*, 207-220.

[185] L. M. Ittner, J. Gotz, *Nat. Rev. Neurosci.* **2011**, *12*, 65-72.

[186] G. Mairet-Coello, J. Courchet, S. Pieraut, V. Courchet, A. Maximov, F. Polleux, *Neuron,* **2013**, *78*, 94-108.

[187] F. Grueninger, B. Bohrmann, C. Czech, T. M. Ballard, J. R. Frey, C. Weidensteiner, M. von Kienlin, L. Ozmen, *Neurobiol. Dis.* **2010**, *37*, 294-306.

[188] W. Yu, J. Polepalli, D. Wagh, J. Rajadas, R. Malenka, B. Lu, *Hum. Mol. Genet.* **2012**, *21*, 1384-1390.

[189] G. S. Bloom, *JAMA Neurol.* **2014**, *71*, 505-508.

[190] L. S. Schneider, F. Mangialasche, N. Andreasen, H. Feldman, E. Giacobini, R. Jones, V. Mantua, P. Mecocci, L. Pani, B. Winblad, M. Kivipelto, *J. Intern. Med.* **2014**, *275*, 251-283.

[191] T. Gomez-Isla, J. L. Price, D. W. McKeel, Jr., J. C. Morris, J. H. Growdon, B. T. Hyman, *J Neurosci.* **1996**, *16*, 4491-4500.

[192] J. L. Price, A. I. Ko, M. J. Wade, S. K. Tsou, D. W. McKeel, J. C. Morris, *Arch. Neurol.* **2001**, *58*, 1395-1402.

[193] R. A. Sperling, D. M. Rentz, K. A. Johnson, J. Karlawish, M. Donohue, D. P. Salmon, P. Aisen, *Sci. Trans. Med.* **2014**, *6*.

[194] R. J. Bateman, P. S. Aisen, B. De Strooper, N. C. Fox, C. A. Lemere, J. M. Ringman, S. Salloway, R. A. Sperling, M. Windisch, C. Xiong, *Alzheimers Res. Ther.* **2011**, *3*, 1.

[195] E. M. Reiman, J. B. Langbaum, A. S. Fleisher, R. J. Caselli, K. Chen, N. Ayutyanont, Y. T. Quiroz, K. S. Kosik, F. Lopera, P. N. Tariot, *J. Alzheimers Dis.* **2011**, *26 Suppl 3*, 321-329.

[196] C. Humpel, *Trends Biotechnol.* **2011**, *29*, 26-32.

[197] K. Blennow, *J. Intern. Med.* **2004**, *256*, 224-234.

[198] K. Blennow, *Expert. Rev. Mol. Diagn.* **2005**, *5*, 661-672.

[199] J. Marksteiner, H. Hinterhuber, C. Humpel, *Drugs Today (Barc),* **2007**, *43*, 423-431.

[200] K. Blennow, H. Hampel, M. Weiner, H. Zetterberg, *Nat. Rev. Neurol.* **2010**, *6*, 131-144.

[201] H. Hampel, R. Frank, K. Broich, S. J. Teipel, R. G. Katz, J. Hardy, K. Herholz, A. L. Bokde, F. Jessen, Y. C. Hoessler, W. R. Sanhai, H. Zetterberg, J. Woodcock, K. Blennow, *Nat. Rev. Drug Discov.* **2010**, *9*, 560-574.

[202] A. K. Desai, G. T. Grossberg, *Neurology,* **2005**, *64*, S34-39.

[203] M. Sjogren, N. Andreasen, K. Blennow, *Clin. Chim. Acta,* **2003**, *332*, 1-10.

[204] H. Zetterberg, L. O. Wahlund, K. Blennow, *Neurosci. Lett.* **2003**, *352*, 67-69.

[205] M. Sjogren, H. Vanderstichele, H. Agren, O. Zachrisson, M. Edsbagge, C. Wikkelso, I. Skoog, A. Wallin, L. O. Wahlund, J. Marcusson, K. Nagga, N. Andreasen, P. Davidsson, E. Vanmechelen, K. Blennow, *Clin. Chem.* **2001**, *47*, 1776-1781.

[206] H. Zetterberg, K. Blennow, E. Hanse, *Exp. Gerontol.* **2010**, *45*, 23-29.

[207] A. Cedazo-Minguez, B. Winblad, *Exp. Gerontol.* **2010**, *45*, 5-14.

[208] H. Hampel, K. Blennow, L. M. Shaw, Y. C. Hoessler, H. Zetterberg, J. Q. Trojanowski, *Exp. Gerontol.* **2010**, *45*, 30-40.

[209] I. Blasko, W. Lederer, H. Oberbauer, T. Walch, G. Kemmler, H. Hinterhuber, J. Marksteiner, C. Humpel, *Dement. Geriatr. Cogn. Disord.* **2006**, *21*, 9-15.

8. REFERENCES

[210] L. Olson, C. Humpel, *Exp. Gerontol.* **2010**, *45*, 41-46.

[211] C. Hock, K. Heese, F. Muller-Spahn, P. Huber, W. Riesen, R. M. Nitsch, U. Otten, *Neurology,* **2000**, *54*, 2009-2011.

[212] P. Lewczuk, J. Kornhuber, H. Vanderstichele, E. Vanmechelen, H. Esselmann, M. Bibl, S. Wolf, M. Otto, U. Reulbach, H. Kolsch, F. Jessen, J. Schroder, P. Schonknecht, H. Hampel, O. Peters, E. Weimer, R. Perneczky, H. Jahn, C. Luckhaus, U. Lamla, T. Supprian, J. M. Maler, J. Wiltfang, *Neurobiol. Aging,* **2008**, *29*, 812-818.

[213] K. Hochgrafe, A. Sydow, D. Matenia, D. Cadinu, S. Konen, O. Petrova, M. Pickhardt, P. Goll, F. Morellini, E. Mandelkow, E. M. Mandelkow, *Acta Neuropathol. Commun.* **2015**, *3*, 25.

[214] Q. Zhou, M. Wang, Y. Du, W. Zhang, M. Bai, Z. Zhang, Z. Li, J. Miao, *Ann. Neurol.* **2015**, *77*, 637-654.

[215] A. Camins, E. Verdaguer, J. Folch, A. M. Canudas, M. Pallas, *Drug News Perspect,* **2006**, *19*, 453-460.

[216] A. V. de la Torre, F. Junyent, J. Folch, C. Pelegri, J. Vilaplana, C. Auladell, C. Beas-Zarate, M. Pallas, E. Verdaguer, A. Camins, *Pharmacol. Res.* **2012**, *65*, 66-73.

[217] G. U. Hoglinger, H. J. Huppertz, S. Wagenpfeil, M. V. Andres, V. Belloch, T. Leon, T. Del Ser, T. M. Investigators, *Mov. Disord.* **2014**, *29*, 479-487.

[218] S. Lovestone, M. Boada, B. Dubois, M. Hull, J. O. Rinne, H. J. Huppertz, M. Calero, M. V. Andres, B. Gomez-Carrillo, T. Leon, T. del Ser, A. investigators, *J. Alzheimers Dis.* **2015**, *45*, 75-88.

[219] N. M. Corcoran, D. Martin, B. Hutter-Paier, M. Windisch, T. Nguyen, L. Nheu, L. E. Sundstrom, A. J. Costello, C. M. Hovens, *J. Clin. Neurosci.* **2010**, *17*, 1025-1033.

[220] T. C. Baddeley, J. McCaffrey, J. M. Storey, J. K. Cheung, V. Melis, D. Horsley, C. R. Harrington, C. M. Wischik, *J. Pharmacol. Exp. Ther.* **2015**, *352*, 110-118.

[221] S. A. Sievers, J. Karanicolas, H. W. Chang, A. Zhao, L. Jiang, O. Zirafi, J. T. Stevens, J. Munch, D. Baker, D. Eisenberg, *Nature,* **2011**, *475*, 96-100.

[222] A. L. Boxer, A. E. Lang, M. Grossman, D. S. Knopman, B. L. Miller, L. S. Schneider, R. S. Doody, A. Lees, L. I. Golbe, D. R. Williams, J. C. Corvol, A. Ludolph, D. Burn, S. Lorenzl, I. Litvan, E. D. Roberson, G. U. Hoglinger, M. Koestler, C. R. Jack, Jr., V. Van Deerlin, C. Randolph, I. V. Lobach, H. W. Heuer, I. Gozes, L. Parker, S. Whitaker, J. Hirman, A. J. Stewart, M. Gold, B. H. Morimoto, A. L. Investigators, *Lancet Neurol.* **2014**, *13*, 676-685.

[223] K. R. Brunden, B. Zhang, J. Carroll, Y. Yao, J. S. Potuzak, A. M. Hogan, M. Iba, M. J. James, S. X. Xie, C. Ballatore, A. B. Smith, 3rd, V. M. Lee, J. Q. Trojanowski, *J. Neurosci.* **2010**, *30*, 13861-13866.

[224] T. Wisniewski, F. Goni, *Neuron,* **2015**, *85*, 1162-1176.

[225] E. M. Sigurdsson, *Neurodegener. Dis.* **2014**, *13*, 103-106.

[226] A. A. Asuni, A. Boutajangout, D. Quartermain, E. M. Sigurdsson, *J. Neurosci.* **2007**, *27*, 9115-9129.

[227] E. E. Congdon, J. P. Gu, H. B. R. Sait, E. M. Sigurdsson, *J. Biol. Chem.* **2013**, *288*, 35452-35465.

[228] L. Collin, B. Bohrmann, U. Gopfert, K. Oroszlan-Szovik, L. Ozmen, F. Gruninger, *Brain,* **2014**, *137*, 2834-2846.

[229] Y. C. Liou, A. Sun, A. Ryo, X. Z. Zhou, Z. X. Yu, H. K. Huang, T. Uchida, R. Bronson, G. Bing, X. Li, T. Hunter, K. P. Lu, *Nature,* **2003**, *424*, 556-561.

[230] A. Kondo, K. Shahpasand, R. Mannix, J. Qiu, J. Moncaster, C. H. Chen, Y. Yao, Y. M. Lin, J. A. Driver, Y. Sun, S. Wei, M. L. Luo, O. Albayram, P. Huang, A. Rotenberg, A. Ryo, L. E.

8. REFERENCES

Goldstein, A. Pascual-Leone, A. C. McKee, W. Meehan, X. Z. Zhou, K. P. Lu, *Nature,* **2015**, *523*, 431-436.

[231] C. d'Abramo, C. M. Acker, H. T. Jimenez, P. Davies, *PLoS One,* **2013**, *8*, e62402.

[232] K. Yanamandra, N. Kfoury, H. Jiang, T. E. Mahan, S. M. Ma, S. E. Maloney, D. F. Wozniak, M. I. Diamond, D. M. Holtzman, *Neuron,* **2013**, *80*, Cp4-Cp4.

[233] F. H. Crick, *Symp. Soc. Exp. Biol.* **1958**, *12*, 138-163.

[234] R. J. Sims, 3rd, D. Reinberg, *Nat. Rev. Mol. Cell Biol.* **2008**, *9*, 815-820.

[235] D. P. Gamblin, S. I. van Kasteren, J. M. Chalker, B. G. Davis, *FEBS J.* **2008**, *275*, 1949-1959.

[236] L. R. Malins, R. J. Payne, *Curr. Opin. Chem. Biol.* **2014**, *22*, 70-78.

[237] V. R. Pattabiraman, J. W. Bode, *Nature,* **2011**, *480*, 471-479.

[238] R. B. Merrifield, *J. Am. Chem. Soc.* **1963**, *85*, 2149-&.

[239] R. B. Merrifield, *Angew. Chem. Int. Ed.* **1985**, *24*, 799-810.

[240] J. M. Palomo, *Rsc Advances* **2014**, *4*, 32658-32672.

[241] M. Schnolzer, P. Alewood, A. Jones, D. Alewood, S. B. Kent, *Int. J. Pept. Protein. Res.* **1992**, *40*, 180-193.

[242] L. A. Carpino, G. Y. Han, *J. Am. Chem. Soc* **1970**, *92*, 5748-&.

[243] E. Kaiser, Colescot.Rl, Bossinge.Cd, P. I. Cook, *Anal. Biochem.* **1970**, *34*, 595-&.

[244] Y. Garcia-Ramos, M. Paradis-Bas, J. Tulla-Puche, F. Albericio, *J. Pept. Sci.* **2010**, *16*, 675-678.

[245] S. L. Pedersen, A. P. Tofteng, L. Malik, K. J. Jensen, *Chem. Soc. Rev.* **2012**, *41*, 1826-1844.

[246] P. Beltrao, P. Bork, N. J. Krogan, V. van Noort, *Mol. Sys. Biol.* **2013**, *9*.

[247] M. Broncel, J. A. Falenski, S. C. Wagner, C. P. Hackenberger, B. Koksch, *Chem. Eur. J.* **2010**, *16*, 7881-7888.

[248] J. Bertran-Vicente, R. A. Serwa, M. Schumann, P. Schmieder, E. Krause, C. P. Hackenberger, *J. Am. Chem. Soc.* **2014**, *136*, 13622-13628.

[249] J. M. Kee, T. W. Muir, *Acs Chem. Biol.* **2012**, *7*, 44-51.

[250] N. Gaidzik, U. Westerlind, H. Kunz, *Chem. Soc. Rev.* **2013**, *42*, 4421-4442.

[251] T. Buskas, S. Ingale, G. J. Boons, *Glycobiology,* **2006**, *16*, 113R-136R.

[252] M. C. Galan, P. Dumy, O. Renaudet, *Chem. Soc. Rev.* **2013**, *42*, 4599-4612.

[253] P. Wang, B. Aussedat, Y. Vohra, S. J. Danishefsky, *Angew. Chem. Int. Ed.* **2012**, *51*, 11571-11575.

[254] V. Ullmann, M. Radisch, I. Boos, J. Freund, C. Pohner, S. Schwarzinger, C. Unverzagt, *Angew. Chem. Int. Ed.* **2012**, *51*, 11566-11570.

[255] P. E. Dawson, T. W. Muir, I. Clark-Lewis, S. B. Kent, *Science,* **1994**, *266*, 776-779.

[256] G. S. Beligere, P. E. Dawson, *J. Am. Chem. Soc.* **2000**, *122*, 12079-12082.

[257] J. W. Blankenship, P. E. Dawson, *J. Mol. Biol.* **2003**, *327*, 537-548.

[258] W. Y. Lu, M. A. Starovasnik, J. J. Dwyer, A. A. Kossiakoff, S. B. H. Kent, W. Y. Lu, *Biochemistry,* **2000**, *39*, 3575-3584.

[259] J. Wilken, D. Hoover, D. A. Thompson, P. N. Barlow, H. McSparron, L. Picard, A. Wlodawer, J. Lubkowski, S. B. H. Kent, *Chemistry & Biology,* **1999**, *6*, 43-51.

8. REFERENCES

[260] K. Tripsianes, N. K. Chu, A. Friberg, M. Sattler, C. F. W. Becker, *Acs Chem. Biol.* **2014**, *9*, 347-352.

[261] C. Haase, O. Seitz, *Angew. Chem. Int. Ed.* **2008**, *47*, 1553-1556.

[262] F. Nagaike, Y. Onuma, C. Kanazawa, H. Hojo, A. Ueki, Y. Nakahara, Y. Nakahara, *Org. Lett.* **2006**, *8*, 4465-4468.

[263] T. M. Hackeng, J. H. Griffin, P. E. Dawson, *Proc. Natl. Acad. Sci. U S A,* **1999**, *96*, 10068-10073.

[264] J. A. Camarero, T. W. Muir, in *Curr. Protoc. Protein Sci.* John Wiley & Sons, Inc., **2001**.

[265] M. Villain, H. Gaertner, P. Botti, *Eur. J. Org. Chem.* **2003**, 3267-3272.

[266] E. C. B. Johnson, S. B. H. Kent, *J. Am. Chem. Soc.* **2006**, *128*, 6640-6646.

[267] B. B. Dang, T. Kubota, K. Mandal, F. Bezanilla, S. B. H. Kent, *J. Am. Chem. Soc.* **2013**, *135*, 11911-11919.

[268] J. A. Camarero, A. R. Mitchell, *Protein Pept. Lett.* **2005**, *12*, 723-728.

[269] R. Ingenito, E. Bianchi, D. Fattori, A. Pessi, *J. Am. Chem. Soc.* **1999**, *121*, 11369-11374.

[270] Y. He, J. P. Wilkins, L. L. Kiessling, *Org. Lett.* **2006**, *8*, 2483-2485.

[271] B. J. Backes, A. A. Virgilio, J. A. Ellman, *J. Am. Chem. Soc.* **1996**, *118*, 3055-3056.

[272] B. J. Backes, D. R. Dragoli, J. A. Ellman, *J. Org. Chem.* **1999**, *64*, 5472-5478.

[273] Y. Shin, K. A. Winans, B. J. Backes, S. B. H. Kent, J. A. Ellman, C. R. Bertozzi, *J. Am. Chem. Soc.* **1999**, *121*, 11684-11689.

[274] A. R. Mezo, R. P. Cheng, B. Imperiali, *J. Am. Chem. Soc.* **2001**, *123*, 3885-3891.

[275] S. Futaki, K. Sogawa, J. Maruyama, T. Asahara, M. Niwa, H. Hojo, *Tetrahedron Lett.* **1997**, *38*, 6237-6240.

[276] C. P. Hackenberger, *Org. Biomol. Chem.* **2006**, *4*, 2291-2295.

[277] Y. Kajihara, A. Yoshihara, K. Hirano, N. Yamamoto, *Carbohydr. Res.* **2006**, *341*, 1333-1340.

[278] P. Botti, M. Villain, S. Manganiello, H. Gaertner, *Org. Lett.* **2004**, *6*, 4861-4864.

[279] J. D. Warren, J. S. Miller, S. J. Keding, S. J. Danishefsky, *J. Am. Chem. Soc.* **2004**, *126*, 6576-6578.

[280] J. B. Blanco-Canosa, P. E. Dawson, *Angew. Chem. Int. Ed.* **2008**, *47*, 6851-6855.

[281] R. Sola, P. Saguer, M. L. David, R. Pascal, *Chem. Commun.* **1993**, 1786-1788.

[282] R. Pascal, D. Chauvey, R. Sola, *Tetrahedron Lett.* **1994**, *35*, 6291-6294.

[283] H. P. Hemantha, S. N. Bavikar, Y. Herman-Bachinsky, N. Haj-Yahya, S. Bondalapati, A. Ciechanover, A. Brik, *J. Am. Chem. Soc.* **2014**, *136*, 2665-2673.

[284] J. B. Blanco-Canosa, B. Nardone, F. Albericio, P. E. Dawson, *J. Am. Chem. Soc.* **2015**, *137*, 7197-7209.

[285] G. M. Fang, Y. M. Li, F. Shen, Y. C. Huang, J. B. Li, Y. Lin, H. K. Cui, L. Liu, *Angew. Chem. Int. Ed.* **2011**, *50*, 7645-7649.

[286] J. S. Zheng, S. Tang, Y. K. Qi, Z. P. Wang, L. Liu, *Nat. Prot.* **2013**, *8*, 2483-2495.

[287] G. M. Fang, J. X. Wang, L. Liu, *Angew. Chem. Int. Ed.* **2012**, *51*, 10347-10350.

[288] D. Bang, B. L. Pentelute, S. B. H. Kent, *Angew. Chem. Int. Ed.* **2006**, *45*, 3985-3988.

[289] D. Bang, S. B. Kent, *Angew. Chem. Int. Ed.* **2004**, *43*, 2534-2538.

[290] N. Ollivier, J. Dheur, R. Mhidia, A. Blanpain, O. Melnyk, *Org. Lett.* **2010**, *12*, 5238-5241.

8. REFERENCES

[291]   L. Raibaut, N. Ollivier, O. Melnyk, *Chem. Soc. Rev.* **2012**, *41*, 7001-7015.

[292]   A. Dirksen, P. E. Dawson, *Curr. Opin. Chem. Biol.* **2008**, *12*, 760-766.

[293]   L. E. Canne, S. J. Bark, S. B. H. Kent, *J. Am. Chem. Soc.* **1996**, *118*, 5891-5896.

[294]   P. Botti, M. R. Carrasco, S. B. H. Kent, *Tetrahedron Lett.* **2001**, *42*, 1831-1833.

[295]   T. Kawakami, S. Aimoto, *Tetrahedron Lett.* **2003**, *44*, 6059-6061.

[296]   C. Marinzi, J. Offer, R. Longhi, P. E. Dawson, *Bioorg. Med. Chem.* **2004**, *12*, 2749-2757.

[297]   S. F. Loibl, Z. Harpaz, O. Seitz, *Angew. Chem. Int. Ed.* **2015**, *54*, 15055-15059.

[298]   C. P. R. Hackenberger, D. Schwarzer, *Angew. Chem.* **2008**, *120*, 10182-10228.

[299]   L. Z. Yan, P. E. Dawson, *J. Am. Chem. Soc.* **2001**, *123*, 526-533.

[300]   Q. Wan, S. J. Danishefsky, *Angew. Chem.* **2007**, *119*, 9408-9412.

[301]   Y. Tian, L. Wang, J. Shi, H. Z. Yu, *Chin. J. Chem. Phys.* **2015**, *28*, 269-276.

[302]   D. Crich, A. Banerjee, *J. Am. Chem. Soc.* **2007**, *129*, 10064-+.

[303]   S. Y. Shang, Z. P. Tan, S. J. Danishefsky, *Proc. Natl. Acad. Sci. U S A,* **2011**, *108*, 5986-5989.

[304]   L. R. Malins, K. M. Cergol, R. J. Payne, *Chembiochem,* **2013**, *14*, 559-563.

[305]   M. Hejjaoui, M. Haj-Yahya, K. S. A. Kumar, A. Brik, H. A. Lashuel, *Angew. Chem. Int. Ed.* **2011**, *50*, 405-409.

[306]   B. L. Pentelute, S. B. H. Kent, *Org. Lett.* **2007**, *9*, 687-690.

[307]   N. Metanis, E. Keinan, P. E. Dawson, *Angew. Chem. Int. Ed.* **2010**, *49*, 7049-7053.

[308]   S. D. Townsend, Z. P. Tan, S. W. Dong, S. Y. Shang, J. A. Brailsford, S. J. Danishefsky, *J. Am. Chem. Soc.* **2012**, *134*, 3912-3916.

[309]   L. R. Malins, R. J. Payne, *Org. Lett.* **2012**, *14*, 3142-3145.

[310]   L. R. Malins, N. J. Mitchell, S. McGowan, R. J. Payne, *Angew. Chem. Int. Ed.* **2015**, *54*, 12716-12721.

[311]   N. J. Mitchell, L. R. Malins, X. Liu, R. E. Thompson, B. Chan, L. Radom, R. J. Payne, *J. Am. Chem. Soc.* **2015**, *137*, 14011-14014.

[312]   E. C. Johnson, S. B. Kent, *J. Am. Chem. Soc.* **2006**, *128*, 6640-6646.

[313]   K. M. Cergol, R. E. Thompson, L. R. Malins, P. Turner, R. J. Payne, *Org. Lett.* **2014**, *16*, 290-293.

[314]   T. Moyal, H. P. Hemantha, P. Siman, M. Refua, A. Brik, *Chem. Sci.* **2013**, *4*, 2496-2501.

[315]   R. E. Thompson, X. Y. Liu, N. Alonso-Garcia, P. J. B. Pereira, K. A. Jolliffe, R. J. Payne, *J. Am. Chem. Soc.* **2014**, *136*, 8161-8164.

[316]   M. Jbara, M. Seenaiah, A. Brik, *Chem. Commun.* **2014**, *50*, 12534-12537.

[317]   T. W. Muir, D. Sondhi, P. A. Cole, *Proc. Natl. Acad. Sci. U S A,* **1998**, *95*, 6705-6710.

[318]   T. W. Muir, *Ann. Rev. Biochem.* **2003**, *72*, 249-289.

[319]   R. David, M. P. O. Richter, A. G. Beck-Sickinger, *Eur. J. Biochem.* **2004**, *271*, 663-677.

[320]   S. R. Chong, F. B. Mersha, D. G. Comb, M. E. Scott, D. Landry, L. M. Vence, F. B. Perler, J. Benner, R. B. Kucera, C. A. Hirvonen, J. J. Pelletier, H. Paulus, M. Q. Xu, *Gene,* **1997**, *192*, 271-281.

[321]   N. H. Shah, T. W. Muir, *Chem. Sci.* **2014**, *5*, 446-461.

[322]   J. X. Shi, T. W. Muir, *J. Am. Chem. Soc.* **2005**, *127*, 6198-6206.

8. REFERENCES

[323] H. D. Mootz, *Chembiochem,* **2009**, *10*, 2579-2589.

[324] A. J. Stevens, Z. Z. Brown, N. H. Shah, G. Sekar, D. Cowburn, T. W. Muir, *J. Am. Chem. Soc.* **2016**, *138*, 2162-2165.

[325] J. Kang, N. L. Reynolds, C. Tyrrell, J. R. Dorin, D. Macmillan, *Org. & Biomol. Chem.* **2009**, *7*, 4918-4923.

[326] J. Masania, J. J. Li, S. J. Smerdon, D. Macmillan, *Org. & Biomol. Chem.* **2010**, *8*, 5113-5119.

[327] S. van Kasteren, *Biochem. Soc. Trans.* **2012**, *40*, 929-944.

[328] M. K. Tarrant, P. A. Cole, *Ann. Rev. Biochem.* **2009**, *78*, 797-825.

[329] L. S. Zhang, J. P. Tam, *Tetrahedron Lett.* **1997**, *38*, 3-6.

[330] C. F. Liu, J. P. Tam, *Proc. Natl. Acad. Sci. U S A,* **1994**, *91*, 6584-6588.

[331] Y. F. Zhang, C. Xu, H. Y. Lam, C. L. Lee, X. C. Li, *Proc. Natl. Acad. Sci. U S A,* **2013**, *110*, 6657-6662.

[332] C. T. T. Wong, T. Li, H. Y. Lam, Y. Zhang, X. LI, *Front. Chem.* **2014**, *2*.

[333] J. W. Bode, R. M. Fox, K. D. Baucom, *Angew. Chem. Int. Ed.* **2006**, *45*, 1248-1252.

[334] V. R. Pattabiraman, A. O. Ogunkoya, J. W. Bode, *Angew. Chem. Int. Ed.* **2012**, *51*, 5114-5118.

[335] B. L. Nilsson, L. L. Kiessling, R. T. Raines, *Org. Lett.* **2000**, *2*, 1939-1941.

[336] E. Saxon, J. I. Armstrong, C. R. Bertozzi, *Org. Lett.* **2000**, *2*, 2141-2143.

[337] M. B. Soellner, A. Tam, R. T. Raines, *J. Org. Chem.* **2006**, *71*, 9824-9830.

[338] A. Tam, M. B. Soellner, R. T. Raines, *J. Am. Chem. Soc.* **2007**, *129*, 11421-11430.

[339] R. Kleineweischede, C. P. Hackenberger, *Angew. Chem. Int. Ed. Engl.* **2008**, *47*, 5984-5988.

[340] B. L. Nilsson, R. J. Hondal, M. B. Soellner, R. T. Raines, *J. Am. Chem. Soc.* **2003**, *125*, 5268-5269.

[341] J. Kalia, N. L. Abbott, R. T. Raines, *Bioconjugate Chem.,* **2007**, *18*, 1064-1069.

[342] M. Mühlberg, Ph.D. thesis, Freie Universitaet Berlin **2014**.

[343] G. H. Hakimelahi, G. Just, *Tetrahedron Lett.* **1980**, *21*, 2119-2122.

[344] T. Rosen, I. M. Lico, D. T. W. Chu, *J. Org. Chem.* **1988**, *53*, 1580-1582.

[345] N. Shangguan, S. Katukojvala, R. Greenburg, L. J. Williams, *J. Am. Chem. Soc.* **2003**, *125*, 7754-7755.

[346] R. Merkx, M. J. van Haren, D. T. S. Rijkers, R. M. J. Liskamp, *J. Org. Chem.* **2007**, *72*, 4574-4577.

[347] X. H. Zhang, F. P. Li, X. W. Lu, C. F. Liu, *Bioconjugate Chem.* **2009**, *20*, 197-200.

[348] V. W. Wittmann, O. Keiper, J. Mannuthodikayil, *J. Pep. Sci.* **2010**, *16*, 91-91.

[349] R. Raz, J. Rademann, *Org. Lett.* **2012**, *14*, 5038-5041.

[350] J. M. Xie, P. G. Schultz, *Nat. Rev. Mol. Cell Biol.* **2006**, *7*, 775-782.

[351] J. M. Xie, P. G. Schultz, *Methods,* **2005**, *36*, 227-238.

[352] L. Davis, J. W. Chin, *Nat. Rev. Mol. Cell Biol.* **2012**, *13*, 168-182.

[353] J. W. Chin, T. A. Cropp, J. C. Anderson, M. Mukherji, Z. W. Zhang, P. G. Schultz, *Science,* **2003**, *301*, 964-967.

8. REFERENCES

[354] N. Wu, A. Deiters, T. A. Cropp, D. King, P. G. Schultz, *J. Am. Chem. Soc.* **2004**, *126*, 14306-14307.

[355] S. M. Hancock, R. Uprety, A. Deiters, J. W. Chin, *J. Am. Chem. Soc.* **2010**, *132*, 14819-14824.

[356] T. Mukai, T. Kobayashi, N. Hino, T. Yanagisawa, K. Sakamoto, S. Yokoyama, *Biochem. Biophys. Res. Commun.* **2008**, *371*, 818-822.

[357] H. Neumann, S. Y. Peak-Chew, J. W. Chin, *Nat. Chem. Biol.* **2008**, *4*, 232-234.

[358] S. Greiss, J. W. Chin, *J. Am. Chem. Soc.* **2011**, *133*, 14196-14199.

[359] H. Neumann, J. L. Hazen, J. Weinstein, R. A. Mehl, J. W. Chin, *J. Am. Chem. Soc.* **2008**, *130*, 4028-4033.

[360] C. C. Liu, P. G. Schultz, *Nat. Biotechnol.* **2006**, *24*, 1436-1440.

[361] H. S. Park, M. J. Hohn, T. Umehara, L. T. Guo, E. M. Osborne, J. Benner, C. J. Noren, J. Rinehart, D. Soll, *Science,* **2011**, *333*, 1151-1154.

[362] H. W. Ai, J. W. Lee, P. G. Schultz, *Chem. Commun.* **2010**, *46*, 5506-5508.

[363] D. Groff, P. R. Chen, F. B. Peters, P. G. Schultz, *Chembiochem,* **2010**, *11*, 1066-1068.

[364] S. Lee, S. Oh, A. Yang, J. Kim, D. Soll, D. Lee, H. S. Park, *Angew. Chem. Int. Ed.* **2013**, *52*, 5771-5775.

[365] H. Neumann, K. Wang, L. Davis, M. Garcia-Alai, J. W. Chin, *Nature,* **2010**, *464*, 441-444.

[366] D. Schumacher, C. P. R. Hackenberger, *Curr. Op. Chem. Biol.* **2014**, *22*, 62-69.

[367] D. Agrawal, C. P. R. Hackenberger, in *Chem. Org.-Hybrids*, John Wiley & Sons, Inc., **2014**, pp. 299-348.

[368] D. Bohme, A. G. Beck-Sickinger, *J. Pept. Sci.* **2015**, *21*, 186-200.

[369] K. Chen, X. Y. Chen, *Curr. Top. Med. Chem.* **2010**, *10*, 1227-1236.

[370] M. L. Metzker, *Genome Res.* **2005**, *15*, 1767-1776.

[371] B. F. Cravatt, A. T. Wright, J. W. Kozarich, *Annu. Rev. Biochem.* **2008**, *77*, 383-414.

[372] G. C. Rudolf, W. Heydenreuter, S. A. Sieber, *Curr. Opin. Chem. Biol.* **2013**, *17*, 110-117.

[373] C. L. Young, Z. T. Britton, A. S. Robinson, *Biotechnol. J.* **2012**, *7*, 620-634.

[374] S. Graslund, P. Nordlund, J. Weigelt, J. Bray, B. M. Hallberg, O. Gileadi, S. Knapp, U. Oppermann, C. Arrowsmith, R. Hui, J. Ming, S. Dhe-Paganon, H. W. Park, A. Savchenko, A. Yee, A. Edwards, R. Vincentelli, C. Cambillau, R. Kim, S. H. Kim, Z. Rao, Y. Shi, T. C. Terwilliger, C. Y. Kim, L. W. Hung, G. S. Waldo, Y. Peleg, S. Albeck, T. Unger, O. Dym, J. Prilusky, J. L. Sussman, R. C. Stevens, S. A. Lesley, I. A. Wilson, A. Joachimiak, F. Collart, I. Dementieva, M. I. Donnelly, W. H. Eschenfeldt, Y. Kim, L. Stols, R. Wu, M. Zhou, S. K. Burley, J. S. Emtage, J. M. Sauder, D. Thompson, K. Bain, J. Luz, T. Gheyi, F. Zhang, S. Atwell, S. C. Almo, J. B. Bonanno, A. Fiser, S. Swaminathan, F. W. Studier, M. R. Chance, A. Sali, T. B. Acton, R. Xiao, L. Zhao, L. C. Ma, J. F. Hunt, L. Tong, K. Cunningham, M. Inouye, S. Anderson, H. Janjua, R. Shastry, C. K. Ho, D. Y. Wang, H. Wang, M. Jiang, G. T. Montelione, D. I. Stuart, R. J. Owens, S. Daenke, A. Schutz, U. Heinemann, S. Yokoyama, K. Bussow, K. C. Gunsalus, S. G. Consortium, A. F. Macromol, B. S. G. Ctr, C. S. G. Consortium, I. C. S. Function, I. S. P. Ctr, J. C. S. Genomics, M. C. S. Genomics, N. Y. S. G. R. Ctr, N. S. G. Consortium, O. P. P. Facility, P. S. P. Facility, M. D. C. M. Med, R. S. G. Proteomics, S. Complexes, *Nat. Methods,* **2008**, *5*, 135-146.

[375] X. Chen, J. L. Zaro, W. C. Shen, *Adv. Drug Deliv. Rev.* **2013**, *65*, 1357-1369.

[376] J. Arnau, C. Lauritzen, G. E. Petersen, J. Pedersen, *Protein Expr. Purif.* **2006**, *48*, 1-13.

[377] F. Guillier, D. Orain, M. Bradley, *Chem. Rev.* **2000**, *100*, 3859.

8. REFERENCES

[378] G. A. Truran, K. S. Aiken, T. R. Fleming, P. J. Webb, J. H. Markgraf, *J. Chem. Edu.* **2002**, *79*, 85-86.

[379] G. A. Lemieux, C. R. Bertozzi, *Trends Biotechnol.* **1998**, *16*, 506-513.

[380] G. Leriche, L. Chisholm, A. Wagner, *Bioorg. Med. Chem.* **2012**, *20*, 571-582.

[381] G. C. Rudolf, W. Heydenreuter, S. A. Sieber, *Curr. Opin. Chem. Biol.* **2013**, *17*, 110-117.

[382] G. Leriche, L. Chisholm, A. Wagner, *Biorg. Med. Chem.* **2012**, *20*, 571-582.

[383] R. Axen, J. Porath, S. Ernback, *Nature,* **1967**, *214*, 1302-&.

[384] X. Zhao, G. Li, S. Liang, *J. Anal. Methods Chem.* **2013**, *2013*, 581093.

[385] J. J. Lichty, J. L. Malecki, H. D. Agnew, D. J. Michelson-Horowitz, S. Tan, *Protein Expr. Purif.* **2005**, *41*, 98-105.

[386] D. F. Westra, G. W. Welling, D. G. Koedijk, A. J. Scheffer, T. H. The, S. Welling-Wester, *J Chromatogr. B Biomed. Sci. Appl.* **2001**, *760*, 129-136.

[387] K. R. Andersen, N. C. Leksa, T. U. Schwartz, *Proteins,* **2013**, *81*, 1857-1861.

[388] D. M. Charbonneau, F. Meddeb-Mouelhi, M. Beauregard, *Protein Pept. Lett.* **2012**, *19*, 264-269.

[389] K. Terpe, *Appl. Microbiol. Biotechnol.* **2003**, *60*, 523-533.

[390] N. Hage, J. G. Renshaw, G. S. Winkler, P. Gellert, S. Stolnik, F. H. Falcone, *Protein. Expr. Purif.* **2015**, *106*, 25-30.

[391] H. M. Sassenfeld, S. J. Brewer, *Bio-Technology* **1984**, *2*, 76-81.

[392] D. W. Wood, *Curr. Opin. Struct. Biol.* **2014**, *26*, 54-61.

[393] S. Chong, F. B. Mersha, D. G. Comb, M. E. Scott, D. Landry, L. M. Vence, F. B. Perler, J. Benner, R. B. Kucera, C. A. Hirvonen, J. J. Pelletier, H. Paulus, M. Q. Xu, *Gene,* **1997**, *192*, 271-281.

[394] D. Guillen, S. Moreno-Mendieta, P. Aguilera, S. Sanchez, A. Farres, R. Rodriguez-Sanoja, *Appl. Microbiol. Biotechnol.* **2013**, *97*, 4141-4148.

[395] E. Ong, N. R. Gilkes, R. C. Miller, Jr., A. J. Warren, D. G. Kilburn, *Enzyme Microb. Technol.* **1991**, *13*, 59-65.

[396] M. R. Banki, T. U. Gerngross, D. W. Wood, *Protein Sci.* **2005**, *14*, 1387-1395.

[397] J. N. Rybak, S. B. Scheurer, D. Neri, G. Elia, *Proteomics* **2004**, *4*, 2296-2299.

[398] N. M. Green, *Adv. Protein Chem.* **1975**, *29*, 85-133.

[399] E. Morag, E. A. Bayer, M. Wilchek, *Anal. Biochem.* **1996**, *243*, 257-263.

[400] S. M. Ellerbroek, Y. I. Wu, C. M. Overall, M. S. Stack, *J. Biol. Chem.* **2001**, *276*, 24833-24842.

[401] T. G. Schmidt, J. Koepke, R. Frank, A. Skerra, *J. Mol. Biol.* **1996**, *255*, 753-766.

[402] S. Voss, A. Skerra, *Protein Eng.* **1997**, *10*, 975-982.

[403] I. P. Korndorfer, A. Skerra, *Protein Sci.* **2002**, *11*, 883-893.

[404] M. R. Junttila, S. Saarinen, T. Schmidt, J. Kast, J. Westermarck, *Proteomics,* **2005**, *5*, 1199-1203.

[405] R. E. Stofko-Hahn, D. W. Carr, J. D. Scott, *FEBS Lett.* **1992**, *302*, 274-278.

[406] S. Honey, B. L. Schneider, D. M. Schieltz, J. R. Yates, B. Futcher, *Nucleic Acids Res.* **2001**, *29*, E24.

[407] T. Asai, L. A. Wims, S. L. Morrison, *J. Immunol. Methods,* **2005**, *299*, 63-76.

8. REFERENCES

[408] J. Zhang, L. Ma, S. Q. Zhang, *Protein Expr. Purif.* **2014**, *95*, 177-181.

[409] D. W. Urry, *Prog. Biophys. Mol. Bio.* **1992**, *57*, 23-57.

[410] Y. Kim, P. Ganesan, H. Ihee, *Protein Sci.* **2013**, *22*, 1109-1117.

[411] W. B. Asher, K. L. Bren, *Protein Sci.* **2010**, *19*, 1830-1839.

[412] J. M. Moon, G. Y. Kim, H. Rhim, *Biotechnol. Lett.* **2012**, *34*, 1841-1846.

[413] M. C. Hillman, L. S. Yang, S. X. Sun, J. L. Duke, K. T. O'Neil, J. E. Kochie, A. Karjoo, P. Nath, L. A. Breth, K. Murphy, O. H. Ross, U. C. Burn, G. F. Hollis, R. Wynn, *Protein Expr. Purif.* **2001**, *23*, 359-368.

[414] L. Schembri, R. Dalibart, F. Tomasello, P. Legembre, F. Ichas, F. De Giorgi, *Nat. Methods* **2007**, *4*, 107-108.

[415] L. C. Leong, *Mol. Biotechnol.* **1999**, *12*, 269-274.

[416] S. Costa, A. Almeida, A. Castro, L. Domingues, *Front. Microbiol.* **2014**, *5*, 63.

[417] J. M. Vergis, M. C. Wiener, *Protein Expr. Purif.* **2011**, *78*, 139-142.

[418] Y. Li, *Biotechnol. Lett.* **2011**, *33*, 869-881.

[419] D. S. Waugh, *Protein Expr. Purif.* **2011**, *80*, 283-293.

[420] R. J. Jenny, K. G. Mann, R. L. Lundblad, *Protein Expr. Purif.* **2003**, *31*, 1-11.

[421] J. Arnau, C. Lauritzen, G. E. Petersen, J. Pedersen, *Protein Expr. Purif.* **2006**, *48*, 1-13.

[422] F. B. Perler, E. O. Davis, G. E. Dean, F. S. Gimble, W. E. Jack, N. Neff, C. J. Noren, J. Thorner, M. Belfort, *Nucleic Acids Res.* **1994**, *22*, 1125-1127.

[423] S. Chong, Y. Shao, H. Paulus, J. Benner, F. B. Perler, M. Q. Xu, *J. Biol. Chem.* **1996**, *271*, 22159-22168.

[424] B. A. Fong, W. Y. Wu, D. W. Wood, *Trends Biotechnol.* **2010**, *28*, 272-279.

[425] T. H. Truong, F. J. Garcia, Y. H. Seo, K. S. Carroll, *Bioorg. Med. Chem. Lett.* **2011**, *21*, 5015-5020.

[426] R. Ramos, S. Moreira, A. Rodrigues, M. Gama, L. Domingues, *Biotechnol. Prog.* **2013**, *29*, 17-22.

[427] A. H. Gemeay, *Dyes and Pigments,* **2002**, *54*, 201-212.

[428] J. Szychowski, A. Mahdavi, J. J. Hodas, J. D. Bagert, J. T. Ngo, P. Landgraf, D. C. Dieterich, E. M. Schuman, D. A. Tirrell, *J. Am. Chem. Soc.* **2010**, *132*, 18351-18360.

[429] M. A. Nessen, G. Kramer, J. Back, J. M. Baskin, L. E. Smeenk, L. J. de Koning, J. H. van Maarseveen, L. de Jong, C. R. Bertozzi, H. Hiemstra, C. G. de Koster, *J. Proteome Res.* **2009**, *8*, 3702-3711.

[430] Y. Yang, H. Hahne, B. Kuster, S. H. Verhelst, *Mol. Cell Proteomics,* **2013**, *12*, 237-244.

[431] C. G. Bochet, *J. Chem. Soc. Perkin Tran. 1* **2002**, 125-142.

[432] V. N. R. Pillai, *Synthesis-Stuttgart* **1980**, 1-26.

[433] Patchorn.A, B. Amit, R. B. Woodward, *J. Am. Chem. Soc.* **1970**, *92*, 6333-&.

[434] K. Gordon, S. Balasubramanian, *J. Chem. Technol. Biotechnol.* **1999**, *74*, 835-851.

[435] B. J. Backes, J. A. Ellman, *Curr. Opin. Chem. Biol.* **1997**, *1*, 86-93.

[436] P. Lloydwilliams, F. Albericio, E. Giralt, *Tetrahedron,* **1993**, *49*, 11065-11133.

[437] J. Olejnik, S. Sonar, E. Krzymanskaolejnik, K. J. Rothschild, *Proc. Natl. Acad. Sci. U S A,* **1995**, *92*, 7590-7594.

8. REFERENCES

[438] T. Q. Zheng, H. Jiang, P. Wu, *Bioconjugate Chem.* **2013**, *24*, 859-864.

[439] P. V. Chang, X. Chen, C. Smyrniotis, A. Xenakis, T. Hu, C. R. Bertozzi, P. Wu, *Angew. Chem. Int. Ed.* **2009**, *48*, 4030-4033.

[440] V. V. Rostovtsev, L. G. Green, V. V. Fokin, K. B. Sharpless, *Angew. Chem. Int. Ed.* **2002**, *41*, 2596-2599.

[441] C. W. Tornoe, C. Christensen, M. Meldal, *J. Org. Chem.* **2002**, *67*, 3057-3064.

[442] W. Wang, S. Hong, A. Tran, H. Jiang, R. Triano, Y. Liu, X. Chen, P. Wu, *Chem. Asian J.* **2011**, *6*, 2796-2802.

[443] D. J. O'Shannessy, R. H. Quarles, *J. Immunol. Methods,* **1987**, *99*, 153-161.

[444] M. Muhlberg, M. G. Hoesl, C. Kuehne, J. Dernedde, N. Budisa, C. P. R. Hackenberger, *Beilstein J. Org. Chem.* **2015**, *11*, 784-791.

[445] S. Ng, M. R. Jafari, R. Derda, *Chem. Biol.* **2012**, *7*, 123-138.

[446] Y. Zeng, T. N. C. Ramya, A. Dirksen, P. E. Dawson, J. C. Paulson, *Nat. Methosts* **2009**, *6*, 207-209.

[447] E. Klement, Z. Lipinszki, Z. Kupihar, A. Udvardy, K. F. Medzihradszky, *J. Proteome Res.* **2010**, *9*, 2200-2206.

[448] A. Maurer, C. Zeyher, B. Amin, H. Kalbacher, *J. Proteome Res.* **2013**, *12*, 199-207.

[449] T. Saku, H. Sakai, Y. Shibata, Y. Kato, K. Yamamoto, *J. Biochem.* **1991**, *110*, 956-964.

[450] K. Mori, H. Shimizu, A. Konno, T. Iwanaga, *Arch. Histol. Cytol.* **2002**, *65*, 359-368.

[451] Y. Yasuda, T. Kageyama, A. Akamine, M. Shibata, E. Kominami, Y. Uchiyama, K. Yamamoto, *J. Biochem.* **1999**, *125*, 1137-1143.

[452] S. B. Athauda, K. Takahashi, *Protein Pept. Lett.* **2002**, *9*, 15-22.

[453] N. Zaidi, T. Herrmann, W. Voelter, H. Kalbacher, *Biochem. Biophys. Res. Commun.* **2007**, *360*, 51-55.

[454] E. Weerapana, C. Wang, G. M. Simon, F. Richter, S. Khare, M. B. Dillon, D. A. Bachovchin, K. Mowen, D. Baker, B. F. Cravatt, *Nature,* **2010**, *468*, 790-795.

[455] Y. Qian, J. Martell, N. J. Pace, T. E. Ballard, D. S. Johnson, E. Weerapana, *Chembiochem,* **2013**, *14*, 1410-1414.

[456] M. Fonovic, S. H. Verhelst, M. T. Sorum, M. Bogyo, *Mol. Cell Proteomics,* **2007**, *6*, 1761-1770.

[457] S. H. Verhelst, M. Fonovic, M. Bogyo, *Angew. Chem. Int. Ed.* **2007**, *46*, 1284-1286.

[458] K. J. Rangan, Y. Y. Yang, G. Charron, H. C. Hang, *J. Am. Chem. Soc.* **2010**, *132*, 10628-10629.

[459] J. S. Yount, B. Moltedo, Y. Y. Yang, G. Charron, T. M. Moran, C. B. Lopez, H. C. Hang, *Nat. Chem. Biol.* **2010**, *6*, 610-614.

[460] Y. Y. Yang, J. M. Ascano, H. C. Hang, *J. Am. Chem. Soc.* **2010**, *132*, 3640-3641.

[461] M. Grammel, M. M. Zhang, H. C. Hang, *Angew. Chem. Int. Ed.* **2010**, *49*, 5970-5974.

[462] J. K. Bocker, K. Friedel, J. C. Matern, A. L. Bachmann, H. D. Mootz, *Angew. Chem. Int. Ed.* **2015**, *54*, 2116-2120.

[463] S. Batjargal, C. R. Walters, E. J. Petersson, *J. Am. Chem. Soc.* **2015**, *137*, 1734-1737.

[464] R. Warden-Rothman, I. Caturegli, V. Popik, A. Tsourkas, *Anal. Chem.* **2013**, *85*, 11090-11097.

[465] H. Y. Mao, S. A. Hart, A. Schink, B. A. Pollok, *J. Am. Chem. Soc.* **2004**, *126*, 2670-2671.

8. REFERENCES

[466] J. J. Bellucci, M. Amiram, J. Bhattacharyya, D. McCafferty, A. Chilkoti, *Angew. Chem. Int. Ed.* **2013**, *52*, 3703-3708.

[467] Y. Yang, S. H. Verhelst, *Chem. Commun.* **2013**, *49*, 5366-5368.

[468] J. Yamamoto, M. Denda, N. Maeda, M. Kita, C. Komiya, T. Tanaka, W. Nomura, H. Tamamura, Y. Sato, A. Yamauchi, A. Shigenaga, A. Otaka, *Org. Biomol. Chem.* **2014**, *12*, 3821-3826.

[469] L. Xing, W. Xu, B. Zhou, Y. Chen, Z. Lin, *Protein Expr. Purif.* **2013**, *88*, 248-253.

[470] L. A. Bobek, H. Tsai, M. J. Levine, *Crit. Rev. Oral Biol. Med.* **1993**, *4*, 581-590.

[471] J. Driscoll, Y. Zuo, T. Xu, J. R. Choi, R. F. Troxler, F. G. Oppenheim, *J. Dent. Res.* **1995**, *74*, 1837-1844.

[472] H. Tsai, P. A. Raj, L. A. Bobek, *Infect. Immun.* **1996**, *64*, 5000-5007.

[473] J. Driscoll, C. Duan, Y. Zuo, T. Xu, R. Troxler, F. G. Oppenheim, *Gene,* **1996**, *177*, 29-34.

[474] Y. Zuo, T. Xu, R. F. Troxler, J. Li, J. Driscoll, F. G. Oppenheim, *Gene,* **1995**, *161*, 87-91.

[475] A. M. Yang, Y. P. Li, S. Pantoom, G. Triola, Y. W. Wu, *Chembiochem,* **2013**, *14*, 1296-1300.

[476] C. F. Portal, J. M. Seifert, C. Buehler, N. C. Meisner-Kober, M. Auer, *Bioconjugate Chem.* **2014**, *25*, 1213-1222.

[477] I. W. Hamley, *Biomacromolecules,* **2014**, *15*, 1543-1559.

[478] C. Stutz, A. Meszynska, J. F. Lutz, H. G. Borner, *Acs Macro. Lett.* **2013**, *2*, 641-644.

[479] A. Conway, T. Vazin, D. P. Spelke, N. A. Rode, K. E. Healy, R. S. Kane, D. V. Schaffer, *Nat. Nanotechnol.* **2013**, *8*, 831-838.

[480] E. A. Lemke, D. Summerer, B. H. Geierstanger, S. M. Brittain, P. G. Schultz, *Nat. Chem. Biol.* **2007**, *3*, 769-772.

[481] D. S. Lawrence, *Curr. Opin. Chem. Biol.* **2005**, *9*, 570-575.

[482] P. R. Chen, D. Groff, J. T. Guo, W. J. Ou, S. Cellitti, B. H. Geierstanger, P. G. Schultz, *Angew. Chem. Int. Ed.* **2009**, *48*, 4052-4055.

[483] H. Edwards, P. Schimmel, *Mol. Cell. Biol.* **1990**, *10*, 1633-1641.

[484] O. Reimann, C. Smet-Nocca, C. P. Hackenberger, *Angew. Chem. Int. Ed. Engl.* **2015**, *54*, 306-310.

[485] I. Landrieu, L. Lacosse, A. Leroy, J. M. Wieruszeski, X. Trivelli, A. Sillen, N. Sibille, H. Schwalbe, K. Saxena, T. Langer, G. Lippens, *J. Am. Chem. Soc.* **2006**, *128*, 3575-3583.

[486] A. Reif, S. Siebenhaar, A. Troster, M. Schmalzlein, C. Lechner, P. Velisetty, K. Gottwald, C. Pohner, I. Boos, V. Schubert, S. Rose-John, C. Unverzagt, *Angew. Chem. Int. Ed.* **2014**, *53*, 12125-12131.

[487] M. von Bergen, S. Barghorn, J. Biernat, E. M. Mandelkow, E. Mandelkow, *Biochim. Biophy. Acta,* **2005**, *1739*, 158-166.

[488] N. Sibille, A. Sillen, A. Leroy, J. M. Wieruszeski, B. Mulloy, I. Landrieu, G. Lippens, *Biochemistry,* **2006**, *45*, 12560-12572.

[489] B. Bulic, M. Pickhardt, E. M. Mandelkow, E. Mandelkow, *Neuropharmacol.* **2010**, *59*, 276-289.

[490] E. Gatta, T. Lefebvre, S. Gaetani, M. Dos Santos, J. Marrocco, A. M. Mir, T. Cassano, S. Maccari, F. Nicoletti, J. Mairesse, *Pharmacol. Res.* **2016**, *105*, 186-197.

[491] S. Jeganathan, A. Hascher, S. Chinnathambi, J. Biernat, E. M. Mandelkow, E. Mandelkow, *J. Biol. Chem.* **2008**, *283*, 32066-32076.

8. REFERENCES

[492] G. T. Bramblett, M. Goedert, R. Jakes, S. E. Merrick, J. Q. Trojanowski, V. M. Y. Lee, *Neuron,* **1993**, *10*, 1089-1099.

[493] J. S. Song, S. D. Yang, *J. Protein Chem.* **1995**, *14*, 95-105.

[494] J. Z. Wang, Q. L. Wu, A. Smith, I. Grundke-Iqbal, K. Iqbal, *Febs Lett.* **1998**, *436*, 28-34.

[495] J. Z. Wang, C. X. Gong, T. Zaidi, I. Grundkeiqbal, K. Iqbal, *J. Biol. Chem.* **1995**, *270*, 4854-4860.

[496] J. Z. Wang, I. GrundkeIqbal, K. Iqbal, *Mol. Brain Res.* **1996**, *38*, 200-208.

[497] E. Maverakis, K. Kim, M. Shimoda, M. E. Gershwin, F. Patel, R. Wilken, S. Raychaudhuri, L. R. Ruhaak, C. B. Lebrilla, *J. Autoimmun.* **2015**, *57*, 1-13.

[498] S. P. C. Cole, B. G. Campling, T. Atlaw, D. Kozbor, J. C. Roder, *Mol. Cell. Biochem.* **1984**, *62*, 109-120.

[499] K. Blennow, A. Wallin, H. Agren, C. Spenger, J. Siegfried, E. Vanmechelen, *Mol. Chem. Neuropathol.* **1995**, *26*, 231-245.

[500] E. Vanmechelen, H. Vanderstichele, P. Davidsson, E. Van Kerschaver, B. Van Der Perre, M. Sjogren, N. Andreasen, K. Blennow, *Neurosci. Lett.* **2000**, *285*, 49-52.

[501] K. Ishiguro, H. Ohno, H. Arai, H. Yamaguchi, K. Urakami, J. M. Park, K. Sato, H. Kohno, K. Imahori, *Neurosci. Lett.* **1999**, *270*, 91-94.

[502] R. Kohnken, K. Buerger, R. Zinkowski, C. Miller, D. Kerkman, J. DeBernardis, J. F. Shen, H. J. Moller, P. Davies, H. Hampel, *Neurosci. Lett.* **2000**, *287*, 187-190.

[503] Y. Y. Hu, S. S. He, X. C. Wang, Q. H. Duan, I. Grundke-Iqbal, K. Iqbal, J. Z. Wang, *Am. J. Pathol.* **2002**, *160*, 1269-1278.

[504] D. A. Loeffler, L. M. Smith, A. C. Klaver, S. Martic, *Exp. Gerontol.* **2015**, *67*, 15-18.

[505] F. Liu, K. Iqbal, I. Grundke-Iqbal, C. X. Gong, *Febs Lett.* **2002**, *530*, 209-214.

[506] T. Umeda, H. Eguchi, Y. Kunori, Y. Matsumoto, T. Taniguchi, H. Mori, T. Tomiyama, *Ann. Clin. Trans. Neurol.* **2015**, *2*, 241-255.

[507] S. G. Greenberg, P. Davies, J. D. Schein, L. I. Binder, *J. Biol. Chem.* **1992**, *267*, 564-569.

[508] G. Drewes, B. Lichtenberg-Kraag, F. Doring, E. M. Mandelkow, J. Biernat, J. Goris, M. Doree, E. Mandelkow, *EMBO J.* **1992**, *11*, 2131-2138.

[509] A. Boutajangout, J. Ingadottir, P. Davies, E. M. Sigurdsson, *J. Neurochem.* **2011**, *118*, 658-667.

[510] A. A. Asuni, A. Boutajangout, D. Quartermain, E. M. Sigurdsson, *J. Neurosci.* **2007**, *27*, 9115-9129.

[511] C. Bauer, K. Gobel, N. Nagaraj, C. Colantuoni, M. X. Wang, U. Muller, E. Kremmer, A. Rottach, H. Leonhardt, *J. Biol. Chem.* **2015**, *290*, 4801-4812.

[512] A. Sultan, F. Nesslany, M. Violet, S. Begard, A. Loyens, S. Talahari, Z. Mansuroglu, D. Marzin, N. Sergeant, S. Humez, M. Colin, E. Bonnefoy, L. Buee, M. C. Galas, *J. Biol. Chem.* **2011**, *286*, 4566-4575.

[513] Q. Hua, R. Q. He, *Protein Pept. Lett.* **2002**, *9*, 349-357.

[514] K. Paholikova, B. Salingova, A. Opattova, R. Skrabana, P. Majerova, N. Zilka, B. Kovacech, M. Zilkova, P. Barath, M. Novak, *J. Alzheimers Dis.* **2015**, *43*, 915-926.

[515] J. A. Lewis, J. T. Fleming, *Methods Cell Biol.* **1995**, *48*, 3-29.

[516] R. Brandt, A. Gergou, I. Wacker, T. Fath, H. Hutter, *Neurobiol. Aging,* **2009**, *30*, 22-33.

[517] R. Brandt, M. Hundelt, N. Shahani, *Mol. Basis Dis.* **2005**, *1739*, 331-354.

8. REFERENCES

[518] B. C. Kraemer, B. Zhang, J. B. Leverenz, J. H. Thomas, J. Q. Trojanowski, G. D. Schellenberg, *Proc. Natl. Acad. Sci. U S A,* **2003**, *100*, 9980-9985.

[519] T. James, Virginia Ph.D. thesis at Polytechnic Institute and State University **2012**.

[520] M. V. Aksenova, M. Y. Aksenov, W. R. Markesbery, D. A. Butterfield, *J. Neurosci. Res.* **1999**, *58*, 308-317.

[521] C. Wistrom, B. Villeponteau, *Exp. Gerontol.* **1990**, *25*, 97-105.

[522] G. Pawelec, A. Rehbein, K. Haehnel, A. Merl, M. Adibzadeh, *Immunol. Rev.* **1997**, *160*, 31-42.

[523] C. A. Peterson, J. *Gerontol. A Biol. Sci. Med. Sci.* **1995**, *50*, 142-144.

[524] H. G. Augustinvoss, A. K. Voss, B. U. Pauli, *J. Cell. Physiol.* **1993**, *157*, 279-288.

[525] L. Hayflick, *Keio J. Med.* **1998**, *47*, 174-182.

[526] H. Rubin, *Mech. Ageing Dev.* **1997**, *98*, 1-35.

[527] D. A. Drachman, *Ann. Neurol.* **1997**, *42*, 819-828.

[528] N. Minois, D. Carmona-Gutierrez, F. Madeo, *Aging-US,* **2011**, *3*, 716-732.

[529] J. E. Meredith, S. Sankaranarayanan, V. Guss, A. J. Lanzetti, F. Berisha, R. J. Neely, J. R. Slemmon, E. Portelius, H. Zetterberg, K. Blennow, H. Soares, M. Ahlijanian, C. F. Albright, *Plos One,* **2013**, *8*.

[530] A. Shevchenko, H. Tomas, J. Havlis, J. V. Olsen, M. Mann, *Nat. Prot.* **2006**, *1*, 2856-2860.

[531] M. R. Larsen, T. E. Thingholm, O. N. Jensen, P. Roepstorff, T. J. D. Jorgensen, *Mol. Cell. Proteom.* **2005**, *4*, 873-886.

[532] C. Klemm, S. Schroder, M. Gluckmann, M. Beyermann, E. Krause, *Rapid Commun. Mass Spectrom.* **2004**, *18*, 2697-2705.

[533] B. Schulte, A. Walther, H. Keul, M. Möller, *Macromolecules,* **2014**, *47*, 1633-1645.

[534] M. Schmitz, M. Kuhlmann, O. Reimann, C. P. Hackenberger, J. Groll, *Biomacromolecules,* **2015**.

[535] O. Reimann, M. Glanz, C. P. Hackenberger, *Bioorg. Med. Chem.* **2015**, *23*, 2890-2894.

[536] S. Schwagerus, O. Reimann, C. Despres, C. Smet-Nocca, C. P. R. Hackenberger, *J. Pept. Sci.* **2016**, *22*, 327-333.

[537] M. Kuhlmann, O. Reimann, C. P. Hackenberger, J. Groll, *Macromol. Rapid Commun.* **2015**, *36*, 472-476.

[538] H. P. Hemantha, S. N. Bavikar, Y. Herman-Bachinsky, N. Haj-Yahya, S. Bondalapati, A. Ciechanover, A. Brik, *J. Am. Chem. Soc.* **2014**, *136*, 2665-2673.

9. CURRICULUM VITAE

For reasons of data protection, the curriculum vitae is not published in the electronic version.

9. CURRICULUM VITAE

9. CURRICULUM VITAE